

UNCLASSIFIED

AD NUMBER

AD142023

LIMITATION CHANGES

TO:

Approved for public release; distribution is unlimited. Document partially illegible.

FROM:

Distribution authorized to U.S. Gov't. agencies and their contractors; Specific Authority; 30 JUN 1961. Other requests shall be referred to Air Force Wright Air Development Center, Wright-Patterson AFB, OH 45433. Document partially illegible.

AUTHORITY

afwal ltr 21 Feb 1986

THIS PAGE IS UNCLASSIFIED

UNCLASSIFIED

AD NUMBER

AD142023

CLASSIFICATION CHANGES

TO: UNCLASSIFIED

FROM: CONFIDENTIAL

LIMITATION CHANGES

TO:
Distribution authorized to U.S. Gov't. agencies and their contractors; Specific Authority; 30 JUN 1961. Other requests shall be referred to Air Force Wright Air Development Center, Wright-Patterson AFB, OH 45433. Document partially illegible.

FROM:

Code 9: DTIC Classified Users Only. Controlling DoD Organization: Air Force Wright Air Development Center, Wright-Patterson AFB, OH 45433. JUN 1957. Document partially illegible.

AUTHORITY

arl, w-p afb ltr dtd 30 Jun 1961 arl, w-p afb ltr dtd 30 Jun 1961

UNCLASSIFIED

AD 142 023

*Reproduced
by the*

ARMED SERVICES TECHNICAL INFORMATION AGENCY
ARLINGTON HALL STATION
ARLINGTON 12, VIRGINIA



CLASSIFICATION CHANGED
TO *UNCLASSIFIED*
FROM *CONFIDENTIAL*
PER AUTHORITY LISTED IN
ASTIA TAB NO. *U61-3-5*
DATE *1 SEPT 61*

UNCLASSIFIED

NOTICE: When government or other drawings, specifications or other data are used for any purpose other than in connection with a definitely related government procurement operation, the U. S. Government thereby incurs no responsibility, nor any obligation whatsoever; and the fact that the Government may have formulated, furnished, or in any way supplied the said drawings, specifications, or other data is not to be regarded by implication or otherwise as in any manner licensing the holder or any other person or corporation, or conveying any rights or permission to manufacture, use or sell any patented invention that may in any way be related thereto.

AD No. 142023

ASTIA FILE COPY

WADC TECHNICAL REPORT 56-589
ASTIA Document Number AD 142023

7
(Unclassified Title)

AERODYNAMIC CRITERIA FOR OPTIMUM
DESIGN OF MIXED-FLOW INJECTORS

J. L. DRISCOLL

ALLIANCE MANUFACTURING COMPANY OF ARIZONA

FOC

JUNE 1957

WRIGHT AIR DEVELOPMENT CENTER

WADC-56-589

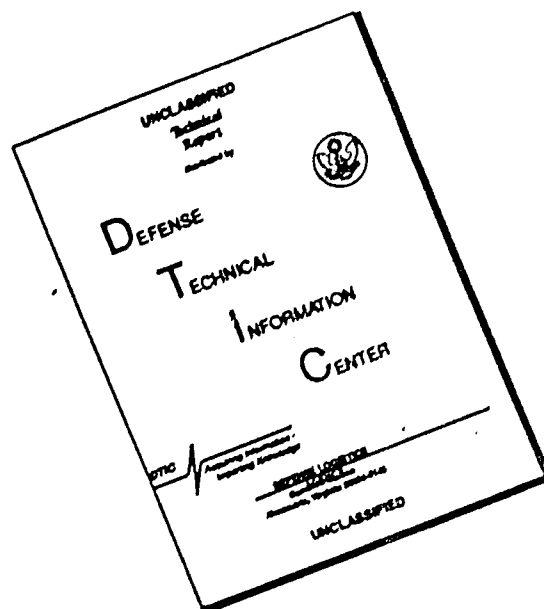
JAN 9 1958

5742-572

This document is the property of the United States Government. It is furnished for the duration of the contract and shall be returned when no longer required, or upon recall by ASTIA to the following address:
Armed Services Technical Information Agency, Arlington Hall Station,
Arlington 12, Virginia

NOTICE: THIS DOCUMENT CONTAINS INFORMATION AFFECTING THE NATIONAL DEFENSE OF THE UNITED STATES WITHIN THE MEANING OF THE ESPIONAGE LAWS, TITLE 18, U.S.C., SECTIONS 793 and 794. THE TRANSMISSION OR THE REVELATION OF ITS CONTENTS IN ANY MANNER TO AN UNAUTHORIZED PERSON IS PROHIBITED BY LAW.

DISCLAIMER NOTICE



THIS DOCUMENT IS BEST QUALITY AVAILABLE. THE COPY FURNISHED TO DTIC CONTAINED A SIGNIFICANT NUMBER OF PAGES WHICH DO NOT REPRODUCE LEGIBLY.

~~CONFIDENTIAL~~

WADC TECHNICAL REPORT 56-589
ASTIA Document Number AD 142023

(Unclassified Title)

AERODYNAMIC CRITERIA FOR OPTIMUM
DESIGN OF MIXED-FLOW IMPELLERS

J. L. Dussourd

AiResearch Manufacturing Company of Arizona

June 1957

Aeronautical Research Laboratory
Contract No. AF 33(616)-2940
Project 3066, Task 70155

Wright Air Development Center
Air Research and Development Command
United States Air Force
Wright-Patterson Air Force Base, Ohio

~~CONFIDENTIAL~~

576P-572

ation,
ECTING THE
E MEANING
793 and 794.
ENTS IN
BITED BY LAW.

FOREWORD

This report was prepared by Jules Dussourd of the AiResearch Manufacturing Company of Arizona, Phoenix, Arizona, and notes a portion of the work done under Air Force Contract AF33(616)-2940, "Research on Mixed-Flow Compressors for Small Turbomachinery Application," Project Number 3066, "Gas Turbine Technology," Task Number 70155, "Three-Dimensional Flow Effects in Turbomachines," with S. Hasinger, Fluid Dynamics Research Branch, Aeronautical Research Laboratory, WADC, as Task Scientist. The work was carried out under the direction of F. Dallanbach, Chief Aerodynamicist, AiResearch Manufacturing Company of Arizona.

This document is classified CONFIDENTIAL in view of the like classification of portions of the referenced material.

CONFIDENTIAL

ABSTRACT

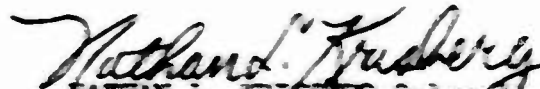
The main objective of this study is to establish theoretically and experimentally basic design criteria for mixed-flow impellers with transonic inlet, which impellers are suitable for small turbo-machinery compressors of 5:1 pressure ratio. In the present phase of the work the significant parameters have been identified as exit cone angle, over-all blade loading, and blade loading distribution (where the blade loading is expressed as relative velocities on pressure and suction sides of blade). A series of 10 designs has been made all for the same inlet and outlet conditions and with each of the above parameters systematically varied. In later phases experimental investigation will be made of the most significant impellers.

A certain amount of work has been initiated to study the transonic flow phenomena in a compressor cascade. Some qualitative and quantitative results have been obtained.

PUBLICATION REVIEW

The publication of this report does not constitute approval by the Air Force of the findings or conclusions contained herein. It is published only for the exchange and stimulation of ideas.

FOR THE COMMANDER:


NATHAN L. KRISBERG, Colonel, USAF
Chief, Aeronautical Research Laboratory
Directorate of Laboratories

CONFIDENTIAL

CONFIDENTIAL

TABLE OF CONTENTS

	PAGE
INTRODUCTION	
Section I STUDY OF VARIABLES AND DESIGN CRITERIA	1
A. Discussion of Design Variables	1
B. Selection of Design Variables	2
1. Over-all Blade Loading	2
2. Distribution of Blade Loading	4
3. Impeller Exit Cone Angle	5
Section II GENERAL IMPELLER DESIGN PROCEDURE	6
A. One-Dimensional Aspects of Design and Determination of External Geometry of Impeller	8
1. Impeller Blade Angle at Exit	10
2. Impeller Tip Speed	10
3. Impeller Mean Exit Diameter	12
4. Inducer Tip Diameter	13
5. Inducer Hub Diameter	13
6. Impeller Exit Width	13
7. Impeller Exit Cone Angle and Impeller Over-all Length . .	14

CONFIDENTIAL

	PAGE	
B.	Three-Dimensional Aspects of Design Procedure and Determination of Impeller Internal Geometry.....	14
	Basic Design Procedure.....	15
	(a) Calculation of the Meridional Flow in the Impeller.....	15
	(b) Blade-to-Blade Solution.....	18
	(c) Inlet Design.....	20
2.	Flow Analysis by Numerical Procedures	21
C.	Summary of Design Procedure.....	22
Section III	DESIGN OF IMPELLERS.....	24
A.	Basic Design Feature Common to all Configurations....	24
	i. Velocity Triangles.....	24
	2. Exit Cone Angle.....	25
	3. Diameter Ratios.....	26
	4. Inlet Arrangement.....	26
B.	Internal Aerodynamic Design of Impellers.....	27
C.	Geometry of Impellers.....	28
D.	Impeller Aerodynamic Characteristics.....	29
	1. Impeller Series I.....	29
	2. Impeller Series II.....	29
	3. Impeller Series IV.....	30

CONFIDENTIAL

	PAGE
E. Impeller Structural Considerations.....	30
1. Centrifugal Stresses.....	30
2. Critical Speeds.....	31
3. Impeller Thrust.....	31
Section IV STUDY OF TRANSONIC INDUCER.....	32
A. Review of Previous Work.....	32
B. General Procedure.....	33
C. Extent of Work Completed.....	34
D. Significant Qualitative Results.....	35
E. Method of Analysis of the Two-Dimensional Supersonic Flow.....	36
F. Calculated Flow Pattern.....	38
G. Process of Diffusion in Transonic Impeller.....	40
SUMMARY.....	41
NOMENCLATURE.....	132
BIBLIOGRAPHY.....	136
APPENDIX A, DERIVATION OF RELATIONS CONTROLLING THE IMPELLER EXTERNAL OVER-ALL GEOMETRY.....	142
APPENDIX B, EQUATIONS FOR THE AXI-SYMMETRIC FLOW IN IMPELLER PASSAGES, EQUATIONS FOR DESIGN PROCEDURE.....	150

CONFIDENTIAL

	PAGE
APPENDIX C. EQUATIONS FOR THE AXI-SYMMETRIC FLOW IN IMPELLER PASSAGES. EQUATIONS FOR THE NUMERICAL SOLUTION OF THE DIRECT PROBLEM.....	157
APPENDIX D. EQUATIONS FOR THE CORRECTION FROM THE TWO-DIMENSIONAL TO THE AXI-SYMMETRIC FLOW UPSTREAM OF THE IMPELLER.....	163
APPENDIX E. BLADE TO BLADE SOLUTION.....	165

CONFIDENTIAL

LIST OF ILLUSTRATIONS

FIGURE		PAGE
1	Effect of Impeller Deceleration Ratio Upon Impeller and Compressor Efficiency	42
2	Optimum Tip Flow Angle for Minimum Relative Velocity	43
3	Impeller Inducer-to-Tip Diameter Ratio	44
4	Variation of Flow Coefficient for High Pressure Ratio Impellers	45
5	Measured Flow Coefficient in Typical Radial Inlet Flow Passage of Compressor	46
6	Deviation of Flow Direction from Blade Direction at Impeller Exit	47
7	Zones of Significance As Applied to the Numerical Solution of Flow in Impeller Passages	48
8	Inlet and Exit Mean Velocity Triangles	49
9	Relative Mach Number Along Impeller Leading Edge	50
10	Absolute Mach Number Along Impeller Leading Edge	51
11	Shape of Leading Edges - Theoretically Calculated Shape and First Design Shape	52
12	Impeller Series I	53

CONFIDENTIAL

FIGURE	TITLE	PAGE
13	Impeller Series II	54
14	Impeller Series IV	55
15	Impeller I, Blade Angular Coordinates	56
16	Impeller IA, Blade Angular Coordinates	57
17	Impeller IAA, Blade Angular Coordinates	58
18	Impeller IB, Blade Angular Coordinates	59
19	Impeller II, Blade Angular Coordinates	60
20	Impeller IIA, Blade Angular Coordinates	61
21	Impeller IIB, Blade Angular Coordinates	62
22	Impeller IV, Blade Angular Coordinates	63
23	Impeller IVA, Blade Angular Coordinates	64
24	Impeller IVB, Blade Angular Coordinates	65
25	Impeller I, Relative Velocity Distribution, Blade and Flow Angle at the Shroud Streamsurface	66
26	Impeller I, Relative Velocity Distribution at the Mean Streamsurface	67
27	Impeller I, Relative Velocity Distribution, Blade and Flow Angle at the Hub Streamsurface	68
28	Pressure Distribution Along Shroud and Hub for Impeller I	69

CONFIDENTIAL

FIGURE	TITLE	PAGE
29	Impeller IA, Relative Velocity Distribution, Blade and Flow Angle at the Shroud Streamsurface	70
30	Impeller IA, Relative Velocity Distribution at the Mean Streamsurface	71
31	Impeller IA, Relative Velocity Distribution, Blade and Flow Angle at the Hub Streamsurface	72
32	Pressure Distribution Along Shroud and Hub for Impeller IA	73
33	Impeller IAA, Relative Velocity Distribution, Blade and Flow Angle at the Shroud Streamsurface	74
34	Impeller IAA, Relative Velocity Distribution at the Mean Streamsurface	75
35	Impeller IAA, Relative Velocity Distribution, Blade and Flow Angle at the Hub Streamsurface	76
36	Pressure Distribution Along Shroud and Hub for Impeller IAA	77
37	Impeller IB, Relative Velocity Distribution, Blade and Flow Angle at the Shroud Streamsurface	78
38	Impeller IB, Relative Velocity Distribution, at the Mean Streamsurface	79
39	Impeller IB, Relative Velocity Distribution, Blade and Flow Angle at the Hub Streamsurface	80

CONFIDENTIAL

FIGURE	TITLE	PAGE
40	Pressure Distribution Along Shroud and Hub for Impeller IB	81
41	Impeller II Relative Velocity Distribution, Blade and Flow Angle at the Shroud Streamsurface	82
42	Impeller II, Relative Velocity Distribution at the Mean Streamsurface	83
43	Impeller II, Relative Velocity Distribution, Blade and Flow Angle at the Hub Streamsurface	84
44	Pressure Distribution Along Shroud and Hub for Impeller II	85
45	Impeller IIA, Relative Velocity Distribution, Blade and Flow Angle at the Shroud Streamsurface	86
46	Impeller IIA, Relative Velocity Distribution at the Mean Streamsurface	87
47	Impeller IIA, Relative Velocity Distribution, Blade and Flow Angle at the Hub Streamsurface	88
48	Pressure Distribution Along Shroud and Hub for Impeller IIA	89
49	Impeller IIB, Relative Velocity Distribution, Blade and Flow Angle at the Shroud Streamsurface	90
50	Impeller IIB, Relative Velocity Distribution at the Mean Streamsurface	91

CONFIDENTIAL

FIGURE	TITLE	PAGE
51	Impeller IIB, Relative Velocity Distribution, Blade and Flow Angle at the Hub Streamsurface	92
52	Pressure Distribution Along Shroud and Hub for Impeller IIB	93
53	Impeller IV, Relative Velocity Distribution, Blade and Flow Angle at the Shroud Streamsurface	94
54	Impeller IV, Relative Velocity Distribution at the Mean Streamsurface	95
55	Impeller IV, Relative Velocity Distribution, Blade and Flow Angle at the Hub Streamsurface	96
56	Pressure Distribution Along Shroud and Hub for Impeller IV	97
57	Impeller IVA, Relative Velocity Distribution, Blade and Flow Angle at the Shroud Streamsurface	98
58	Impeller IVA, Relative Velocity Distribution at the Mean Streamsurface	99
59	Impeller IVA, Relative Velocity Distribution, Blade and Flow Angle at the Hub Streamsurface	100
60	Pressure Distribution Along Shroud and Hub for Impeller IVA	101

CONFIDENTIAL

FIGURE	TITLE	PAGE
61	Impeller IVB, Relative Velocity Distribution, Blade and Flow Angle at the Shroud Streamsurface	102
62	Impeller IVB, Relative Velocity Distribution at the Mean Streamsurface	103
63	Impeller IVB, Relative Velocity Distribution, Blade and Flow Angle at the Hub Streamsurface	104 104
64	Pressure Distribution Along Shroud and Hub for Impeller IVB	105
65	Design of Impeller with 30° Cone Angle	106
66	Calculated Blade Stresses in Impeller I	107
67	Hub Stresses at Critical Section of Impeller I	108
68	Calculated Blade Stresses in Impeller II	109
69	Hub Stresses at Critical Section of Impeller II	110
70	Two-Dimensional Transonic Flow Near the Inlet of a Compressor Cascade	111
71	Two-Dimensional Supersonic Flow at Inducer Inlet, Impeller I, r/r shroud = 1.0	112
72	Shroud Pressure Distribution in Transonic Impeller	113
73	Comparison of Velocity Gradients in Two-Dimensional and Three-Dimensional inlets (Incompressible Irrotational Flow)	114
74	Fluid Element Between Two Blades for the Calculation of the Blade Loading	115

CONFIDENTIAL

LIST OF TABLES

TABLE		PAGE
I	Aerodynamic Features, Mixed-Flow Impellers	116 116
II	Impeller Design Conditions	118
III	Inlet Coordinates	119
IV	Impeller Series I, Hub and Shroud Coordinates	121
V	Impeller Series II, Hub and Shroud Coordinates	123
VI	Impeller I, Blade Coordinates	125
VII	Impeller IB, Blade Coordinates	127
VIII	Impeller II, Blade Coordinates	129
IX	Leading Edges for Impellers I, IB, II	131

CONFIDENTIAL

INTRODUCTION

As compared to the work on axial machinery, very little basic experimental work has been done on mixed and radial type compressors, particularly for high speed, high pressure ratio machines. This is due, primarily, to the fact that axial compressors have exhibited greater promise for application to aircraft propulsion. Other factors are: (1) the relative compactness of the radial machine in which the internal aerodynamic processes are more difficult to dissociate than in the multistage axial machines; (2) the aerodynamic complexity of the radial machine and the greater number of interacting variables which enormously complicate systematic investigations similar to those achieved on stationary cascades; (3) the nature of the internal flow in which centrifugal and Coriolis effects play major roles both on the main flow and the boundary layer, thus rendering theoretical computations difficult and stationary testing useless.

While the axial compressor remains unchallenged for turbomachine applications requiring medium to large through flows with minimum over-all diameter, the mixed and radial compressors are first choices for a great many other specific applications. This choice may be dictated by considerations of specific speed, limited axial length, ruggedness, simplicity, or the need of operating in a dusty environment. Such specific applications are innumerable, embracing the fields of aircraft accessories, auxiliary power plants, small aircraft engines, ground equipment, etc. In brief, turbomachines of small to medium power outputs, where the over-all diameter is not a limiting factor, fall into this category. The need for applied research aimed at providing an increased understanding of the flow phenomena in mixed and radial compressors is obvious, if smaller, lighter, and more dependable equipment is desired. Such research must be aimed at providing missing design information and improving the performance from the standpoints of efficiency, width of the operating range, attainable pressure levels and through flow capacities. The need for this work is made more imperative by the inherent complexity of the flow phenomena. In addition, progress made and the techniques developed in connection with axial machines are available and will be of great value toward improving our understanding of the radial machine.

To this date, test work on mixed and radial flow machines to investigate experimentally the effect of changes of geometry has been done mainly by NACA. The information, however, was not obtained for the specific purpose of establishing design criteria. The original intention was either to investigate simple and inexpensive modifications in the hope of achieving some performance improvement, or to alter a region of the impeller where some design uncertainty existed until the optimum shape was arrived at experimentally.

CONFIDENTIAL

In references (36) and (37), the amount of deceleration in the impeller was reduced successively in two ways; first, by thickening the blades, and second, by narrowing the exit width. While measurements taken inside the impeller show an increase in efficiency, this improvement is not reflected in the over-all performance of the compressor because of extraneous effects such as changes in the thickness of the blade wake and changes in leakage. These results, coupled with the fact that the test impeller was run at very low tip speeds, detract considerably from the usefulness of the basic information for design purposes.

In references (2) to (7), experimental study was made of two families of impellers. The two families differ in that the flow area is controlled in one case by the meridional shape and in the other by the blade thickness variation. Similar blade loadings were aimed at but were not achieved. Within each family, variation of the tip exit width was introduced to change the amount of deceleration in the impeller. The test results clearly brought out the superiority of the thin-bladed impeller, although one can only guess at the causes. Difficulty also exists in evaluating the effect of changing tip width, which is not clearly brought out by test, probably due to simultaneous changes in the diffuser performance.

The effect of blade loading was investigated in references (21), (22), and other reports yet to be published. Preliminary information available at this date seems to indicate that better performance will be achieved with a lightly loaded inducer.

It is seen that there is only meager systematic investigation of the basic parameters in the field of radial or mixed-flow compressors. Without this information, basic design criteria cannot be set and fundamental improvements in compressor performance are left to chance. It is the prime objective of the present program to isolate a few more basic and significant variables in order to investigate them singly, to evaluate their effects upon the impeller performance, and ultimately to set up basic criteria for the design of high performance compressors.

CONFIDENTIAL

I

STUDY OF VARIABLES AND DESIGN CRITERIA

The first objective of the present research program is to select among all the variables entering the design of an impeller those which, first, are universal enough to be used for any impeller design, and second, are of greatest significance in their effect upon the impeller performance. The second objective of this program is to investigate theoretically and experimentally these effects to establish basic design criteria.

A. Discussion of Design Variables

Within the framework of externally imposed impeller design features, based on non-aerodynamic requirements or on aerodynamic considerations the effects of which are thought to be well understood, there remains a considerable amount of design freedom, particularly in the internal shape of the impeller. Those aerodynamic features which are believed to be understood become part of the regular design procedure. They are fully described in Section II, General Impeller Design Procedure. The remaining aerodynamic features required to complete the design are, for the most part, established from experience and judgement. As will be explained they consist mainly of the choice of the meridional contour, the number, shape, and thickness of the blades, the distribution and amount of incidence, and the length of the flow passages. It is among these variables that selection of the most significant quantities must be made in the present study. Only a few of these variables can be considered separately, if the total number of variations is to be kept within reason. These few will be called primary variables. The question then arises as to what constant value to assign to the so-called secondary variables. One approach is that the secondary variables be optimized within the design. Each design would then, in itself, be an optimum configuration for the particular variation chosen. The problem ultimately would then be reduced to the finding of the best of several optimized impellers or, figuratively speaking, finding the highest peak among several peaked curves. However, it is quite apparent that, if such an approach were rigidly followed, a good impeller would undoubtedly be produced but it would be virtually impossible to isolate the separate effects of the primary variables because of variation in the secondary variables. Another approach would be

CONFIDENTIAL

CONFIDENTIAL

to keep the secondary variables unchanged. This has the disadvantage of not being able to produce an optimum impeller, because the ultimate optimum combination of primary variables would not be achieved with the optimum combination of secondary variables (which have remained unchanged). It appears then, that a compromise approach becomes necessary. Optimization of each primary variable should be carried out only so far as variation of the secondary variables is not required. Each primary design variation must be so made that all secondary variables can remain unchanged and yet make up a near optimum design. If this compromise is practical, it will have the advantage of isolating the significant variables and still produce a near optimum impeller.

B. Selection of Design Variables

It was quite apparent from the start that the choice of the design variation should be limited to variables internal to the impeller rather than to variable relationships between the impeller and its external surroundings, such as mean line velocity triangles, impeller cone angle, inlet geometry, and the like. This will be done consistently in this work, except as is otherwise specified in the original research contract.

1. Over-all Blade Loading

One of the most fundamental quantities entering the design of the compressor in general is the over-all blade loading. This criteria is, at the present time, missing in centrifugal impellers and is left to the experience of the designer. What is needed is the counterpart of such axial compressor design quantities as the diffusion factor or the product of solidity times lift coefficient. This need is particularly important in view of the fact that the radial nature of the flow may permit the achievement of quite high loading, if advantage is taken of potential boundary layer control by centrifugal action.

CONFIDENTIAL

CONFIDENTIAL

Achievement of variable over-all blade loading can be done either by changing the number of blades or by changing the impeller flow length, each affecting directly the blade solidity. Changing of the number of blades is not altogether satisfactory in view of the fact that in high specific speed machines an upper limit to the number of blades is soon reached because of restrictions imposed by cutter size requirements in machining the blades in the hub region. A more flexible solution is to vary the over-all blade loading by combining changes in the number of blades together with changes in blade chord, i.e., changes in impeller length. It is difficult to predict which of the two effects is best from the standpoint of efficiency. Wall friction is about the same for both. The extent of the secondary flow in both cases is controlled by the pressure gradients in the boundary layer, the magnitude and direction of which is affected by many considerations besides passage length and number of blades. In favor of the impeller with many blades, and a short passage is the fact that secondary flow accumulations are quickly discharged through the exit, but this action is somewhat offset by the fact that greater design flexibility exists with longer passage and fewer blades. Again, in favor of the former, is the lighter weight of the impeller.

It appears then that an impeller with lightly loaded blades will have a general appearance of being longer and will offer greater design flexibility than its stubbier counterpart with heavily loaded blades. It must here be brought out that the success or failure of either type will have profound implication upon the form of the best design philosophy. The former approach (lightly loaded blades and long passages) is based upon a design philosophy in which large frictional effects are tolerated but where boundary layer build-ups are minimized. The latter (heavily loaded blades and short passages) is based on the idea that some flow separation is anticipated but, because of the shortness of the impeller and the shape of the meridional section, stagnating fluid will be discharged before it can build up in one area and disrupt the over-all flow pattern.

CONFIDENTIAL

CONFIDENTIAL

2. Distribution of Blade Loading

Just as important as the amount of over-all loading is the distribution of that loading between inducer end and wheel outlet end. A heavily loaded inducer is attractive in that considerable work is done where the boundary layer is new and little developed. However, it is felt that because of the high sensitivity of the flow in a transonic inducer the above achievement is difficult. A heavily loaded wheel portion suffers from accumulated boundary layer and from developed secondary flow, but may be successful if full advantage is taken of the centrifugation of the boundary layer.

Variation in blade loading distribution along the impeller can be achieved by changing the meridional shape or by adjusting the blade thickness or blade camber. Of these, blade thickness changes are not satisfactory, since an appreciable fraction of the flow relative to the blade is supersonic. In order to minimize blade losses, it is necessary to keep the blades as thin as feasible. Changing the meridional contour to achieve changes in loading is subject to two difficulties. First, any desired loading cannot be so attained, if blade camber, inlet, and exit conditions are fixed. Such contour changes are much more suitable as a tool for making refinements of a local nature rather than basic changes for the whole impeller. Second, changes in meridional contour almost always entail changes both at shroud and hub. This causes loading readjustments between hub and shroud, changes in channel aspect ratio, etc., with the net result that the effect of loading distribution between inlet and exit cannot be isolated. A more direct approach then is to achieve the desired effect by changing the shape of the blade camber line only. Loading is very sensitive to this latter variable and no other extraneous effect is introduced.

CONFIDENTIAL

3. Impeller Exit Cone Angle

Investigation of the effect of varying the exit cone angle was specifically requested in the original problem statement for this program. Even though exit cone angle is an external impeller variable, its main effect is that of varying the impeller length. As such, it may be considered as an additional variation under part (1) above. In addition, it is anticipated that a redistribution of blade loading between shroud and hub will take place. The hub loading in the inducer will be even lower in the case of the 30-degree impeller than for the 60-degree exit case, first, because of the lesser fluid deceleration there and second, because turning of the blade at the hub (with radial blade elements) will be less severe than for a 60-degree case with the same blade shape at the shroud.

At the present time, it would be extremely hazardous to attempt to make predictions of the efficiency potentialities of the 30-degree impeller as compared to the 60-degree type. It may be said, however, that a good part of the answer may be known when the results of part (1) above are available.

It must be kept in mind that an impeller with a 30-degree cone angle will require a different diffuser. As such, the potentialities of the compressor must not be confused with the potentialities of the impeller. In addition, the impeller with a low exit cone angle will almost necessarily be a heavier piece of machinery.

CONFIDENTIAL

II

GENERAL IMPELLER DESIGN PROCEDURE

Contrary to the aerodynamic design information available for axial-flow compressors, no generally accepted procedure, backed by extensive and detailed test information, exists for radial or mixed-flow machines. Partly because of the complex nature of the flow process inside such impellers and because of the large number of possible geometrical parameters, no known systematic testing of impellers or impeller components has been undertaken. Whatever information is available on such things as details of the internal flow patterns or the effect of some particular geometrical variation is restricted either to liquid pumps or to low speed centrifugal compressors, (ref. 35.37.) Design of the higher speed compressors is based mainly on theoretical considerations combined with whatever information can be borrowed from the work done with axial compressors and with centrifugal compressors handling incompressible or nearly incompressible fluids. In short, experimentally determined design criteria are not available to supplement theory in those areas where the theory is insufficiently developed to supply the information.

Among the many such design criteria may be listed: (1) the best loading distribution between inducer and radial portion of impeller, (2) a means of predicting and controlling the behavior of the boundary layer, (3) an optimum combination of blade turning and meridional deceleration, (4) the effects on the loading distribution between hub and shroud, (5) which loading (hub, shroud or 50 per cent streamline) must be controlled most carefully in that it bears greatest influence on the over-all performance of the compressor, (6) a quantitative understanding of the sources of losses, their magnitude and distribution, (7) the effect of impeller geometry on the shape of the exit velocity profile, etc. In the absence of such general information, other criteria must be devised. Some are based on a meager understanding of the internal flow behavior from theoretical considerations and others are based on judgement and experience.

CONFIDENTIAL

CONFIDENTIAL

It is generally felt that a good design must not only be such that all calculated flow quantities vary in a manner acceptable to theory but also that the design as a whole must be appealing to the experienced eye. This restriction rules out oddities in design such as startling wall contour shapes, waving flow passages etc. It is also felt that the greater care in design must be given to the shroud rather than to the hub. This is supported not only by the fact that the larger fraction of the total flow is subjected to the shroud conditions, but also because relative velocities there are higher. Low Mach number flows have the ability to adjust themselves comparatively easily to geometrical variations, whereas high Mach number flows are extremely sensitive to such changes. In addition, losses incurred in high velocity flow are usually large.

At this time, indications are that the variation of suction and pressure side relative velocities is a good index of the quality of a design. Difficulties arise only when the criteria of rate of deceleration and amount and distribution of loading are needed. In the absence of such specific data, we must satisfy ourselves with the following rules:

- (1) All flow passage areas must exhibit smooth and gradual variations.
- (2) All velocities and pressures along streamlines must change in a smooth continuous way, with avoidance of high localized gradients.
- (3) Avoidance of all unnecessary accelerations or decelerations. If an over-all deceleration process is desired, for example, the intermediate process must be decelerating everywhere, except for unavoidable exceptions where accelerations must be kept at a minimum.
- (4) Relative velocities must be kept comfortably positive everywhere in order to avoid dead fluid areas or back flow.
- (5) Impeller blade loading must be uniformly distributed, with the loading limit on the inducer not greatly exceeding that attainable in a corresponding axial cascade.

CONFIDENTIAL

- (6) Large decelerations in regions of anticipated thick boundary layers must be avoided. Reference (1) provides information on boundary layer growth against adverse pressure gradients.
- (7) A certain amount of control of secondary flow can be had by designing in such a way that the radial pressure gradients in the main flow will tend to neutralize the centrifugal pressure gradients set up on the blades in the boundary layer.

In transonic flow, it is felt that most of the difficulty experienced is due to our inability to describe the flow with sufficient accuracy. Transonic flow is extremely sensitive to area changes. Design procedures which predict the flow passage areas with sufficient accuracy for low subsonic velocities become inadequate at high Mach numbers because approximations are no longer tolerable without great sacrifices in efficiency. With the development of more exact design procedures it is reasonable to expect that the efficiency of high flow, high pressure ratio machines can be made as high as their more conservative relatives.

A. One-Dimensional Aspects of Design and Determination of External Geometry of Impeller

It is intended in this section to present the procedure by which the basic external dimensions of an impeller are established. While the procedure is based on concepts which are generally accepted, a good many different approaches exist. The present one (considered here) has the advantage of reducing and grouping several steps of the procedure into a simpler form which is applicable to any radial or mixed-flow impeller.

The usual requirements of a compressor are that it be capable of handling a specified mass rate of flow against a specified pressure ratio. This information together with some knowledge of the particular application of the unit establish almost completely the one-dimensional over-all features of the compressor. A small amount of freedom, however, is left to the designer. It is one of the purposes of the present research program to single out these degrees of freedom with the intention of establishing criteria leading to optimum designs.

CONFIDENTIAL

CONFIDENTIAL

It is necessary to differentiate between impeller external and internal geometry. In the external geometry there are included all quantities and dimensions which are independent of the details of the flow pattern inside the impeller passages. The external geometry can, in general, be established by one-dimensional study of the inlet and exit conditions. It involves the following quantities:

- Impeller blade angle at the exit
- Impeller tip speed
- Impeller mean exit diameter
- Inducer tip diameter
- Inducer hub diameter
- Impeller exit width
- Impeller (approximate) over-all length
- Impeller exit cone angle

On the other hand, the internal geometry of the impeller can only be arrived at by detailed two- and three-dimensional analysis of the internal flow. The internal geometry is completely defined by the following quantities.

- Exact shape of hub and shroud contour
- Blade camber distribution
- Number of blades
- Blade thickness distribution.

The details of the analysis of the internal flow will be the subject of the next chapter.

CONFIDENTIAL

As a rule, it is not possible to solve directly for each external quantity in succession. The procedure is rather one of successive approximations to be repeated until all conditions are met and all the various physical quantities are consistent throughout.

Two of the above listed internal quantities are, at the present time, without benefit of specific design criteria and are left to the designers experience: they are impeller length, and impeller exit cone angle. As previously mentioned, these quantities have been selected as two of the primary variables to be studied in the present program. It is believed that all other external physical quantities are fixed by specific design criteria. A discussion of these criteria will now be undertaken; taken together they make up the design procedure followed by AiResearch for the impeller external features.

(1) Impeller blade angle at exit.

In reference (1) a generalized study was undertaken to optimize the geometry of radial impellers. The results are applicable to impellers with slightly mixed-flow as well. The study indicates that, for the type of impellers here considered, the effect of blade exit angle on over-all compressor efficiency is slight provided the blades are nearly radial. In addition, the impeller with nearly radial blades was found to be optimum in efficiency for the range of pressure ratios, here considered.

A further consideration entering into the selection of blade exit angle is that of stress. High tip speed dictates the choice of blades consisting of radial elements. In strongly mixed-flow impellers backward-bent blades can be had with radial elements but for impellers which are only slightly mixed-flow (nearly radial) the amount of backward curvature possible is diminishingly small.

(2) Impeller tip speed.

CONFIDENTIAL

The selection of the impeller tip speed depends on the choice of the mean inlet and exit velocity triangles. These triangles, in turn, must satisfy the requirement of impeller work input. While the amount of work input is primarily dictated by the required pressure ratio, it also involves consideration of the extent and distribution of the losses in the compressor. The assignment of numerical values to these losses must obviously be based on experience and available test results. This circumstance holds equally true for several other factors required to complete the velocity triangles. They are:

- (1) Amount of impeller slip (ref. 1, 8, 9, 10, 11)
- (2) The radial velocity gradients anticipated along the inducer leading edge.
- (3) Maximum permissible relative flow deceleration in the impeller, expressed either in the form of a diffusion factor, or more commonly, as a deceleration ratio, (ref. 10, 11)

Figure 1 summarizes some of the results of ref (1). As might be anticipated, the impeller efficiency is strongly affected by the amount of wheel reaction, i. e., high values of the deceleration ratio W_2/W_1 produce high impeller efficiencies. Less obvious, however, are the indications that the compressor efficiency also improves for decreasing wheel reaction. This trend is, in general, also supported by a study of a large number of compressors in actual operation. It is obvious, moreover, that a limit of efficiency must soon be reached, since for zero reaction, the compressor efficiency will be below that of an overloaded diffuser. Furthermore, it is clear that the over-all size of the unit must also increase, if a reasonable diffusion rate is to be maintained. The optimum amount of impeller reaction is a design variable of great importance and could well form the subject of an independent, extensive research program. Information on the effects of specific speed and compressibility for an optimum degree of reaction are absolutely needed. In the absence of such data, one usually adopts a compromise value of impeller reaction at from 55 to 60 per cent, (a value above 50 per cent being selected in view of the fact that boundary layer conditions are felt to be more favorable in the impeller than in the diffuser). In practice most of these

CONFIDENTIAL

CONFIDENTIAL

factors require re-evaluation as the design progresses and more of the impeller geometry becomes known. These modifications can usually best be accommodated by slightly changing the exit blade angle.

(3) Impeller Mean Exit Diameter.

Since the compressor flow and total head are prescribed, selection of the impeller mean exit diameter establishes the impeller specific speed (equation A - 5), which, in turn, very closely sets most of the remaining impeller external dimensions. Selection of the impeller diameter is often made by considerations other than purely aerodynamic ones: (1) since the selection determines the physical speed, it must be so made as to provide favorable matching between turbine and compressor. In a complete unit design, therefore, the selection of impeller diameter is invariably tied to the turbine design. Obviously, for the purpose of the present program, a somewhat greater degree of freedom is permissible, since the turbine matching requirement is reduced to the requirement of tailoring the compressor to fit an already existing convenient driving unit. (2) A further consideration is that of physical size and weight.

Small envelope dimensions together with lightweight impose conditions of high rpm and high absolute and relative flow Mach numbers, i.e., a critical design. These requirements taken together completely define the impeller tip diameter.

(4) Inducer Tip Diameter.

A convenient expression for the ratio of inducer tip diameter to mean exit tip diameter can be deduced by making use of the concept of specific speed and by designing for a minimum inducer tip relative Mach number. Combination of expressions A-1 and A-5 for specific speed yields the following convenient expression

$$\frac{1}{6.69} \left[\frac{U}{\sqrt{\theta_{01}}} \frac{Kf}{\frac{W_c \sqrt{\theta_{01}}}{\delta_{01}}} \frac{1}{\tan \beta_s} \right]^{1/2} D_{\text{inches}} = \sqrt{\frac{D}{d_s}}$$

CONFIDENTIAL

which is derived in Appendix A-1-d. In this relationship, everything is known, except the value of β_g . This angle must be varied to achieve the optimum condition of minimum inducer tip relative Mach number. This optimization was carried out in Appendix A-1-b, in which it is shown that the optimum angle is a function of mean inlet Mach number only (see Figure 2). Thus, for incompressible flow, the angle for minimum relative velocity is 54.8 degrees. For a mean inlet Mach number of 0.5, this angle is 58.5 degrees. Combining these conditions with equation II-1-1 above yields the relationship illustrated on Figure 3. From this figure, the desired inducer diameter may be obtained from the known values of compressor flow, tip speed, and exit diameter, and from estimates of inlet mean Mach number, inlet velocity gradient, and inducer hub-tip ratio. The possible error introduced by misjudgement of these various estimates is small, first because the inducer diameter is a weak function of these variables and second, because near the optimum point, small variations in inducer diameter result in insignificant changes in inducer tip relative Mach number.

(5) Inducer Hub Diameter.

From considerations of unit size and weight, it is obvious that small inducer hub diameters are desirable in order to increase the gulp capacity of the unit. Restrictions are introduced by the stress limitations at the blade roots and by cutter limitations in machining the blades. These considerations, taken together for the chosen number of blades, determine the minimum possible hub diameter. At this stage of the design, the choice of the number of blades may or may not be final, however, the initial choice is nevertheless accurate enough for the purpose of finding the hub diameter.

(6) Impeller Exit Width.

The width of the impeller at the exit must be such that continuity is satisfied (at the design mass flow) for the desired exit velocity triangles. For computation of continuity, the state of the fluid at the impeller outlet is required. Appendix A derives expressions for the pressure and density variation inside an impeller as a function of the local velocity triangle and a polytropic exponent n . This procedure obviously assumes homogeneous distribution of the irreversibilities. Appendix A also gives a relationship between the exponent n and impeller efficiency.

CONFIDENTIAL

CONFIDENTIAL

An increase in the exit width by a certain amount, in the form of a viscous clogging coefficient ϵ , has been used to accommodate the boundary layer displacement thickness. More recent work has demonstrated that (1) the introduction of such an independent viscous factor introduces a redundancy in the design and cannot be justified theoretically, (2) test data indicates that the theoretically correct value of ϵ is close to 1.0. Inasmuch as the present design was made to incorporate a variation of flow factor as given in Figure 4, it is felt that perhaps slightly excessive flow deceleration is built into the impeller and that the exit width is too large. A more elaborate treatment on the subject of flow factors is developed in Appendix A. The analysis indicates that for a reasonably good exit profile, a coefficient of the order of 0.96 is sufficient for computing the impeller exit width.

(7) Impeller exit cone angle and impeller over-all length.

As mentioned earlier, the effects of these variables on impeller performance are not known and one to be investigated as part of this program. The effects of these variables on the theoretical quality of the design are, however, understood to some extent. Thus, for example, favorable shroud velocity distribution can be achieved only if the design employs gentle shroud curvatures. For impellers with a high ratio of inducer to tip diameter (say above 0.5) gentle shroud curvature can be achieved only in an impeller of the mixed-flow type. An approximate guide for shroud curvature is that the mean shroud radius of curvature in the meridional view should be equal to about 1.25 times the length of the inducer blade. This rule, in general, results in reasonable velocity gradients. It also fixes the impeller length. Whether this approach can be proved best experimentally remains, however, to be demonstrated.

B. Three-Dimensional Aspects of Design Procedure and Determination of Impeller Internal Geometry

Once the external dimensions of the impeller have been established, use is made of a combination of direct and indirect procedures for the calculation of the internal impeller geometry, i.e., the meridional contour and the number and shape of the blades. The best meridional shape is established indirectly, in that successive modifications are made until all velocities have the desired variation and all shapes, contours, and area variations have the desired degree of smoothness. For each such meridional shape, the blade camber and blade thickness are prescribed by a direct method of solution.

CONFIDENTIAL

AIResearch is presently engaged in a program of confirming and improving its compressor design procedures. The original procedure is based on the use of hand computers and is well adapted for design purposes. Necessarily involved are a number of simplifying assumptions to keep the computing time within reason. An improvement of the design procedures presently in progress involves the carrying out on high speed computers of more exact analyses of the impeller internal flow for comparison with the approximate solution and with test data. If these computations are successful, it would be extremely desirable to apply this procedure to some impellers of the present program. Below, follows a description of the original design procedure and of the more exact method subsequently developed.

1. Basic Design Procedure

(a) Calculation of the Meridional Flow in the Impeller.

The basic working approach of the design procedure involves the analysis of the flow through the inlet and through the impeller annulus as inviscid, irrotational, quasi-compressible, and quasi-three dimensional flow. Corrections are made, either concurrently or subsequently, for a more accurate description of the real flow. The corrections allow for viscous effects, blade clogging effects, the three-dimensional nature of the flow, and for vorticity effects as introduced by the nonuniformity of the work addition in the impeller.

The inviscid, irrotational, quasi-compressible, and quasi-three dimensional flow is taken as an approximate flow picture showing all the main properties of the final flow. This flow description is used as a basic tool for the study of the characteristics of various designs. As such it may be defined as that flow which has the same velocity gradients along a potential line from hub to shroud as the two-dimensional, incompressible, inviscid and irrotational flow, but in which satisfaction of continuity is achieved by using the three-dimensional area with the correct densities corresponding to the calculated velocities.

CONFIDENTIAL

CONFIDENTIAL

The two-dimensional, incompressible, inviscid and irrotational velocity gradients are obtained by making an analog field plot of the meridional shape under study. This meridional shape includes both the impeller and the inlet portions. The analog field plot consists of an electrical analog cut from Teledeltos conductive paper in the trial meridional shape. The equipment and the procedures used are those of ref. 18. For the present application, a plot of potential lines rather than streamlines is of greater convenience. The plot is made by imposing a fixed potential across two estimated conductive potential lines, one for the upstream boundary and the other for the downstream boundary. Between these boundary potential lines, additional equipotential lines are found. For incompressible flow and along a given potential line, their spacing Δm is inversely proportional to the local velocity

$$c_m = \frac{K}{\Delta m}$$

The value of K can be obtained by satisfying continuity, as

$$\epsilon \int_{\text{shroud}}^{\text{hub}} g \rho (2\pi r - Z r_r) \frac{K d\eta}{\Delta m} = W_c$$

In this relationship, the quantity ϵ is introduced as a viscous flow factor and $Z r_r$ represents the blade blockage area. Both these quantities can be prescribed with fair accuracy.

The flow coefficient ϵ has been computed experimentally at the impeller inlet and exit. At the impeller inlet, definition of the term ϵ is similar to that used in a plain nozzle. Experimental values are shown on Figure 5 for an actual compressor inlet. At the impeller exit, ϵ is defined as shown in Appendix A-2B. A good exit profile yields 97 per cent, a poor one 92 per cent. Between the inlet and exit, linear or near-linear variation is assumed.

CONFIDENTIAL

For all high performance and high Mach number compressors, the blades are designed as thin as possible. Manufacturing considerations establish the minimum blade thickness at the shroud while stress and vibration considerations establish the required blade taper.

The density in the above equation must be converged upon by iteration. As a first trial, one-dimensional isentropic densities can be used for the inlet portion upstream of the impeller; inside the impeller, equation A-8 is used in conjunction with an assumed variation of w (in general, the ultimate desired variation is satisfactory). Later, as the design becomes more firmly established, densities and velocities will be recomputed until satisfactory accuracy is obtained.

The flow picture thus found is used as a preliminary criterion of design. With some experience in the interpretation of velocity distribution some modifications can be anticipated, discrimination can be made between basically good and bad designs and, finally, a preliminary selection can be made of a promising design.

As indicated earlier, the meridional flow field obtained thus far is an approximate one. Corrections must be made for the three-dimensional nature of the flow and for the effect of nonuniform work addition. Several approximate corrections for the former effect are available; one such correction is given in ref. (1). This correction has the disadvantage of being able to correct the wall velocities only. A more preferred correction is given in Appendix C. Here it is demonstrated that the three-dimensional incompressible flow pattern may be deduced from the two-dimensional incompressible pattern by taking the velocity gradient along any potential line of the three-dimensional flow to be $3/4$ of the corresponding gradient of the two-dimensional flow. In practice, this correction is not large and its effect on velocity gradients along a streamline is negligible. Care must be taken, however, to apply this correction in the region immediately upstream of the impeller leading edge. The correction will always be such as to increase the flow incidence near the shroud by an amount which cannot be neglected.

CONFIDENTIAL

CONFIDENTIAL

A second correction must be made for the effect of non-uniform work addition along the blade span. This correction is made simultaneously with re-satisfaction of radial equilibrium in the meridional plane. This correction is necessary because of the streamline distortion resulting (1) from the introduction of the three-dimensional correction and (2) from the effect of variable blade blockage from hub to shroud.

The equations of Appendix B express the condition of radial equilibrium for the case of transfer of mechanical energy to or from an incompressible fluid. Their solution requires the knowledge of the shape of the blade mean camber line. This solution will be discussed in part (b) below. The solution of these equations also requires the knowledge of the slope and radii of curvature of the meridional streamlines. This information must be obtained by an iterative process in which successive streamline plots are made and streamline slopes and curvatures obtained for substitution in the equations. From experience, it has been found that five or more iterations are necessary for convergence.

(b) Blade-to-Blade Solution

All calculations up to this point have been carried out under the assumption that the flow is symmetrical about the axis of rotation i. e., that flow corresponding to an infinite number of blades. Reference 19 indicates that this flow is representative of the mean flow between blades for an impeller with a finite number of blades. A separate procedure is required to calculate the blade loading of an impeller with a finite number of blades. This blade loading is used as the basic criterion of impeller design. Appendix D gives equations both for the direct and the inverse problem. The direct solution expresses the blade loading of a given impeller operating with given inlet and exit conditions. The inverse solution enables one to calculate the blade shape required to produce a given desired loading.

CONFIDENTIAL

CONFIDENTIAL

The blade-to-blade solution must be carried out prior to the corrections for vorticity and it usually must be repeated afterward. Fortunately, small changes in the blade shape have but little effects upon the vorticity correction, so that repetition of this lengthy correction calculation is seldom warranted. Final results are usually presented as relative velocities (mean pressure, and suction side) along the hub, shroud, and 50 per cent streamlines.

This procedure for the blade-to-blade solution is based on channel theory and is, therefore, unreliable in the regions near the leading and the trailing edges. Near the leading edges, a separate more detailed procedure is involved. Near the trailing edges, corrections have to be introduced to account for the impeller slip. The flow angles obtained differ from the corresponding blade angles principally because of the rotational nature of the relative flow and because of the boundary layer thickness on the blade suction side. Figure 6 is a summary of the theoretical work done at NACA for inviscid flow between rotating radial blades (ref. 17). It represents the theoretical deviation of the average flow from the blade. This information coupled with an additional boundary layer deviation can be used to find the blade shape required to produce a given flow angle distribution. The total deviation at the trailing edge is known (from slip factor considerations) and using the appropriate curve of Figure 6, the deviation due to the boundary layer can be obtained by difference. The deviation due to boundary layer is assumed to decrease linearly from exit to inlet.

The inducer portion very near the leading edges must be designed separately to establish (1) the shape of the leading edge, (2) the blade angle variation immediately downstream just inside the impeller. The procedure is one of successive approximations in which blade cylindrical developments at various radii must be matched together aerodynamically and structurally. The aerodynamic requirements prescribe the variation in incidence along the blade (± 3 degrees in the supersonic zone and ± 7 degrees in the low subsonic zone) according to the data of references 25 to 33. The

CONFIDENTIAL

CONFIDENTIAL

requirements also limit the amount of initial deceleration as the flow enters the cascade. In subsonic cascades, a ratio of cascade-throat area to upstream relative flow area of about 1.08 is usually found best. In transonic cascades such a ratio is not definitely established, but is believed to be somewhat lower. The structural requirements call for radial blade elements and a prescribed blade taper. In general, all these conditions tend to overdefine the design of the blade leading edges, in which case the best compromise must be sought.

A new approach to the design of the inducer in the regions of supersonic flow is made possible from the present study of transonic inducers. The results are incomplete in that only the two-dimensional problem has been worked out numerically. Nevertheless, considering this restriction, the study provides means for finding the optimum operating incidence for a given supersonic inducer. Conversely the blade shape required to best meet fixed upstream conditions can be calculated. Also, some indication of the possibility of boundary layer separation as a result of shock interaction could conceivably be deduced, although the task would be laborious and the results of doubtful validity.

(c) Inlet Design

The description of the flow in the inlet is obtained in a manner identical to that described earlier for the impeller. Starting from the inviscid, irrotational, quasi-three dimensional, quasi-compressible flow, corrections are introduced (1) for the boundary displacement thickness by a flow factor varying linearly from 1.0 outside to 0.95 at the start of the impeller, and (2) for the three-dimensionality of the flow as previously described. With high meridional Mach numbers, the transverse gradients in velocity are corrected for compressibility by using the Karman Tsien relation referred to the one-dimensional Mach number. This correction is made with some reservation, however, insofar as there is some doubt of its validity for certain applications.

CONFIDENTIAL

CONFIDENTIAL

Finally, graphical matching between the streamlines in the inlet and those in the impeller must be made. A good inlet is considered to be one in which the flow is accelerating everywhere and in which leading edge velocity gradients are held down as much as is compatible with the over-all geometrical requirements.

2. Flow Analysis by Numerical Procedures

This problem consists of making an analysis of the flow with given geometry by direct solution of the basic equations of fluid flow. Reference 52 combines the basic equations of fluid flow into a convenient form as given as C-1 in Appendix C. For the problem at hand, equation C-1 may be simplified to equation C-7 which is valid for compressible, isentropic flow through an impeller with radial elements. Equation C-1 may be simplified further to equation C-3 in the inlet portions.

The solution presently under way attempts to solve equations C-3 and C-7 by relaxation techniques on high speed computers. The basic equations are expressed in finite differences and solved by being applied to a grid of about 600 points in the impeller passage. In order to permit computation within the capacity of the IBM 650 machine, a procedure of dual iteration is used. For each sequence of iteration (intended to satisfy the stream function) the density is maintained at the value calculated from the previously computed velocities. With new values of the stream function, new densities are obtained, and so on.

Unusual difficulty is introduced at the impeller leading and trailing edges because discontinuities exist there both in the direction of the flow and in the form of the governing equations. This condition necessitates division of the impeller as pictured on Figure 7, each section to be studied separately. Equation C-3 for compressible, irrotational flow is solved in region AA'B'B and the results are considered valid in the region AA'C'C. Equation C-7 for compressible rotational polytropic flow in the blade passages is solved in the region CC'T'T. The boundary conditions along CC' are known from the above calculations. The variation of flow direction between CC' and LL' is arbitrarily prescribed a priori. Likewise the boundary conditions at TT' are arbitrarily prescribed. The results are considered valid in the region BB'D'D.

CONFIDENTIAL

Region CC'B'B is then investigated. The boundary conditions are known but the problem is one in which the condition along LL' must be studied by successive approximations until both sides of LL' show continuity in flow velocity (including direction).

A like situation exists at the trailing edge where the two regions EE'T'T and TT'D'D must be matched.

As described, it is obvious that this complete solution is an undertaking of considerable magnitude, and is too time consuming for design purposes.

C. SUMMARY OF DESIGN PROCEDURE

For clarity, the over-all design procedure may be summarized as follows in the order in which it must be carried out.

1. Impeller External Geometry

(a) Establishment of exit velocity triangle. This is based on:

(1) Selected exit blade angle, as established by desired compressor characteristics.

(2) Selected impeller degree of reaction.

(3) Estimated slip factor.

(b) Selection of mean exit diameter. This depends upon the compressor application, the matching of the turbine and compressor, the over-all limitation in size, weight etc.

(c) Proportioning of the impeller is made by using specific speed and minimum inlet relative Mach number considerations to find the hub/tip ratio.

CONFIDENTIAL

CONFIDENTIAL

(d) Minimum inducer hub diameter follows from cutter clearance requirements for the estimated number of blades.

(e) With the foregoing established the exit width is that required to pass the mass flow.

2. Impeller Internal Geometry

(a) Field plot studies are made of a series of potentially promising meridional shapes. For each shape, the velocities are calculated from the streamline or potential line pattern and are subsequently corrected for

(1) Compressibility: outside the impeller, one-dimensional compressibility corrections; inside the impeller, densities are calculated from a desired variation in relative velocities.

(2) Blade and viscous clogging effects.

(3) Three-dimensionality.

(4) Effects of nonuniform work addition. At this stage, this correction must be estimated and its value recalculated later.

(b) The shape of the blade is calculated by a direct method to provide the desired loading at the shroud.

(c) In the process of the design, undesirable features of certain meridional shapes may become apparent. These shapes are eliminated. More refined analyses are made of the remaining shapes. They include: two-dimensional density corrections in the inlet, final calculated impeller densities, and vorticity effects.

(d) Careful design of leading edges.

(e) The entire design should then be exactly analyzed by the numerical method.

CONFIDENTIAL

III

DESIGN OF IMPELLERS

As concluded in the preceding section, Impeller Design Procedure, a sufficient number of impellers should be designed to investigate the effects of three primary variables; namely, the impeller length, the blade loading distribution, and the exit cone angle. A total of ten impellers have been designed. They are subdivided into three classes, I, II, and IV, including three or four impellers each. Classes I and II feature impellers with 60-degree exit cone angle, the former involving comparatively long impellers with lighter blade loading, the latter shorter impellers with greater blade loading. Class IV features impellers with 30-degree exit cone angle and lighter loadings. Each class includes at least one impeller with the higher loading at the inducer and designated by the letter "A"; one impeller nominally with uniform loading, without letter designation; and one impeller with the higher loading displaced toward the discharge and designated by the letter "B". The main over-all features of each impeller are tabulated in Table I.

A summary of the design conditions, assumptions, and objectives is given in Table II.

A. Basic Design Features Common to All Configurations

Inasmuch as the present program is concerned with the optimization of the impeller internal geometry, it is essential that all impellers be subjected to identical inlet and exit conditions.

(1) Velocity Triangles

The mean or one-dimensional inlet and exit velocity triangles are all identical. Because of the nature of the loading distribution, however, small variations are present at shroud and hub.

CONFIDENTIAL

The mean inlet and exit triangles are shown on Figure 8. In accordance with the criteria formulated under Section II, the exit blade angle is very nearly radial. The exit Mach number is slightly supersonic, but may easily be reduced to a safe value for eventual matching with a vaned diffuser. The slip factor was estimated to be 0.81.

The mean inlet diagram corresponds to the local velocity triangle at the 50 per cent streamline. This designation indicates that over 50 per cent of the inlet flow is supersonic. A typical inlet relative Mach number variation with radius is as shown in Figure 9, while Figure 10 shows a similar variation in inlet absolute Mach number.

A relative mean deceleration ratio $\frac{w_2}{w_1} = 0.625$ was selected. This represents a considerable amount of deceleration, especially in view of the fact that the deceleration ratio at the shroud will be considerably lower and still lower along the blade suction surface. In view of the design philosophy outlined in Section II, however, a value of reaction slightly above 50 per cent is desirable, and the present reaction is 59 per cent. It is felt, furthermore, that, if at a later date it becomes apparent that excessive deceleration is present, this variable may be investigated by successive decreases of the exit width. This procedure thus considers eventual matching of this impeller with a diffuser.

(2) Exit Cone Angle

For impeller Classes I and II, a 60-degree exit cone angle was selected. This angle is felt to be best for the present specific speed. The effect of smaller angles upon performance cannot be fully evaluated beforehand but will be investigated through impeller Series IV. A smaller angle will, however, obviously result in a heavier wheel.

CONFIDENTIAL

CONFIDENTIAL

(3) Diameter Ratios

As dictated by the consideration of specific speed, the ratio of inducer tip diameter to mean impeller tip diameter is 0.713 for all impellers. The inducer hub/tip diameter ratio was designed as low as compatible with blade root thickness and cutter dimensions: it is 0.322.

The impeller exit hub/tip diameter ratio is set by the desired distribution of work between the hub and shroud. Because of the loss distribution inside the impeller (the majority of which is estimated to be at the shroud because of supersonic relative speeds), high ratios of deceleration, blade leakage effect, and accumulation of secondary flow, more work must be done by the impeller along the blade tip, if a uniform distribution of total pressure is to be achieved at the exit. This work increase at the tip was set at three per cent more than the mean and at the root three per cent less than the mean which brought about a hub/tip ratio at the exit of 0.94, this ratio being the same for all impellers.

(4) Inlet Arrangement

The shape of the inlet duct to the impeller has been selected as one turning the flow from a radial direction. Some controversy exists as to the relative merits of designing for axial or radial inflow. Clearly, an axial inlet is superior from the standpoint of standardization and mechanical simplicity. On the other hand, the radial inlet is more representative of the majority of small gas turbine installations. Furthermore, mixed-flow compressors require a straddle-bearing arrangement; an axial inlet would lose part of its advantage of simplicity in that it would have to be a structural element and provide front bearing space and support. It thus appears justified to use a radial inlet for the present research program.

CONFIDENTIAL

B. Internal Aerodynamic Design of Impellers

In accordance with the conclusions of Section I, the problem at hand is to produce for each class of impeller a series of designs which will permit variation of the distribution of blade loading by varying only one physical variable (meridional shape or blade camber) and, yet, will be near optimum throughout. From a study made to investigate which of the two to vary it was found most desirable to hold the meridional shape constant and change the blade camber distribution. For each impeller class, four to five meridional shapes were studied until one was found optimum with a blade shape producing uniform loading while near optimum for other loading distributions. This shape was retained for the final design and subjected to the more refined design procedure for each particular desired blade loading. The details of the procedure are fully described in Section II.

Some additional work was expended upon the design of the impeller leading edges. Since transonic impellers have the undesirable characteristic of being capable of operation only in a very narrow flow range, a more refined design approach must be made at the inlet, if design flow is to be met. This is particularly so, since there has been evidence that the present design procedure tends to overestimate the inlet shroud velocities somewhat. Among other things, a study was made to investigate the effect of successive readjustments of the streamline radii in the meridional plane, since this is not always done in the basic design procedure. The resultant shroud velocities were found to be reduced by as much as 10 per cent, compared to the originally calculated values.

From these results, it was felt necessary to undertake a more exact solution of inlet flow. This effort involves the numerical solution of the equations of motion on an IBM 650 high speed computer. This work is being done in two phases, in increasing degrees of difficulty. The first phase treats of the three-dimensional, irrotational flow in the inlet and impeller passage without blades. This work is complete. The second phase treats of the same problem but for compressible flow. Contrary to what was originally expected, the second of these phases has not yet progressed far enough for results to be incorporated herein. While these results are not as

CONFIDENTIAL

yet complete, they afford some information in the form of predicted velocity upstream of the leading edge. The combined effect of the iteration of the streamlines and the more exact solution of the three dimensional flow indicates a shroud meridional velocity about 10 per cent lower than originally calculated. The net result is that a forward extension of the leading edge is required for the design flow to meet the blades at the correct incidence. The design incidence was allowed to vary from 3 degrees at the shroud to 5 degrees at the relative sonic point to 7 degrees at the hub. This incidence variation is the same for all impellers. This effect, together with the variation of inducer blade loading among impellers, causes small differences in the amounts of inducer extension forward of the original position. Figure 11 illustrates typical shapes of leading edges.

It must be emphasized that these modifications will not detract from the objectives of the original designs. True, the reported velocities may differ by as much as 10 per cent from those calculated by the more exact solution, but the gradients and, above all, the loading of each impeller relative to any other will be unchanged.

More will be said about this flow analysis in the final report when all results are available. In the meanwhile, Appendix C summarizes the method of attack and produces the pertinent equations.

C. Geometry of Impellers

Description of the geometry of the impellers involves blade coordinates and meridional shape coordinates. Both are presented in accurate tabular and graphical forms against the axial coordinate Z. A "smoothing out" of the tabulated coordinates is necessary before machining of impellers can be started. That is, the coordinates must be refined to a point where the first and second derivatives are smooth and continuous functions. Only the coordinates for Impellers I, IB, and II, which are to be fabricated first have been so smoothed out. The meridional coordinates of the inlet and Impeller Series I and II are tabulated on Tables III through V. Drawings of the meridional shapes are seen as Figures 12 to 14. Tabulation of "smoothed out" blade coordinates are given in Tables VI through VIII and plots for the blade angular coordinates of all impellers are shown on Figures 15 through 24.

CONFIDENTIAL

CONFIDENTIAL

D. Impeller Aerodynamic Characteristics

Figures 25 through 64 picture the impeller characteristics for all designs. They are presented in the form of blade loading curves expressed as relative velocities and in terms of mean pressure along the shroud and along the hub. All curves are typical of impellers with radial blade elements. Since the entire blade shape is fixed when the blade contour is prescribed, say at the shroud, there is not the freedom to control the loading both at the shroud and hub. The desired loading is built in at the shroud, since this region is the most influential. Appreciable hub loading in the inducer cannot be achieved without overloading the shroud.

(1) Impeller Series I

Of all three meridional configurations that of Impeller Series I proved, during design, to be the most tractable. It was found that the desired loadings could be achieved comparatively easily. It is felt that this design is the most conservative and the one best suited to the design specific speed.

(2) Impeller Series II

With this series, the impeller design is short and crowded together resulting in a certain lack of freedom and flexibility. The displayed loadings were obtained only at the expense of designing with thinner blades. They are so thin, in fact, that serious machining problems are anticipated. All data given herein are for the design with thin blades, but the possibility remains that a slight increase in thickness may have to be allowed, if difficulties are encountered in fabrication. This impeller was designed with 18 blades instead of 17 for Impeller Series I because of the somewhat higher blade loadings.

CONFIDENTIAL

(3) Impeller Series IV

Changing from 60 to 30 degrees exit cone angle was originally expected to bring about a shift in the loading distribution relationship between shroud and hub. This shift proved to be small and essentially equivalent hub loadings were achieved. The 30-degree exit angle, however, is too low for this specific speed. This was apparent in that it was found difficult to arrive at a good meridional shape. An axially short design called for a certain amount of canting at the discharge as shown in Figure 65. This canting produced velocity gradients in the exit region, tending to unload the blade tip and causing turbining. In order to avoid this condition, a longer impeller was needed which is undesirable from a weight standpoint. However, with a longer impeller loadings are lower permitting one less blade than the Series I impeller.

A common inlet passage matches all configurations and is designed to provide accelerating flow in all regions.

E. Impeller Structural Considerations

(1) Centrifugal Stresses

Analysis of the stress level in the blades and in the hub were made for a steel wheel operating at 10 per cent overspeed. The calculated stresses are those due to rotation alone and include neither vibratory nor thermal stresses. These latter stresses must be kept in mind even though their magnitude cannot readily be calculated. The calculated blade stress for Impeller I is shown on Figure 66. The maximum is above 75,000 psi and occurs at the root at $Z = 0.6$. The critical hub stress condition is shown on Figure 67. At the center of the hub the maximum stress is 84,000 psi.

The corresponding data for Impeller Series II is indicated on Figure 68 and 69. Similarly the maximum stresses are, respectively, 86,000 and 87,000 psi.

CONFIDENTIAL

CONFIDENTIAL

Other impellers of the I and II Series show appreciable differences in their relative chord length of the blades, thus exhibiting differences in hub stresses. The maximum stress point, however, is in the aft portion of the impeller where the blades are of nearly equal length. It may then be stated with confidence that no higher maximum stresses will be found in the other impellers.

No stress analysis has yet been made for Impeller IV. Most likely it will be of the same order of magnitude or lower.

(2) Critical Speeds

Calculations were made for the impeller critical speeds for the configuration of one rear (at impeller exit) journal bearing and a ball bearing in the front. In view of the great rigidity of the impeller and short stub shafts, the calculated critical speed depends largely upon the estimated rigidity of the journal bearings. With the best available estimate the first critical mode was found to be 10,400 rpm and the second mode 96,000 rpm. If the rigidity were ten times higher than the original estimate, the first mode would only be 27,500 rpm. It appears then that operating speed is sufficiently far away from any critical speed.

(3) Impeller Thrust

At standard conditions, calculations indicate an impeller thrust of 1033 lb. This will require the use of tandem bearings at the front of the impeller.

CONFIDENTIAL

IV

STUDY OF TRANSONIC INDUCER

One of the most convenient characteristics of low Mach number fluid flow (both incompressible and compressible) rests in its ability to conform to less than optimum geometrical configurations. Such flows will tolerate a comparatively wide variation in incidence upstream of a cascade with only slight effects on efficiency. This is not the case in a transonic inducer. Angles and effective flow variations must be met exactly, or sizeable penalty in efficiency will be incurred. As a result, conventional design methods are no longer adequate; more exact approaches for predicting flow behavior must be devised. In high specific speed machines such as axial compressors, it is quite evident that losses in the inlet will have a large effect on the over-all efficiency, since the inlet relative dynamic head is a large fraction of the total head of the compressor. In lower specific speed units, tests at AiResearch on high Mach number machines of radial and mixed-flow types have shown that unsatisfactory distribution of incidence along the leading edge is apt to disrupt completely the flow inside the impeller as evidenced by the distorted shape of the velocity profile out of the impeller. It is, therefore, of utmost importance that work be done toward improving the general understanding of the flow phenomena in a transonic cascade. Only then will it become possible to design blading such that diffusion takes place without separation or such that shock patterns can be accommodated without extraneous losses.

A. Review of Previous Work

Up to this time (as indicated by available publications) the work done toward providing this information may be subdivided as follows:

1. Mathematical formulation of the basic equations describing the fluid motion between blades of an impeller with a finite number of blades have been made. Reference 43 deals independently with two relative stream surfaces, one radial and the other tangential upstream of the impeller. Solution (leading to a description of the flow) requires a lengthy iterative procedure until the basic equations are everywhere satisfied for both surfaces. No complete solution is known to have been carried out.

CONFIDENTIAL

2. For the two-dimensional case, several qualitative or quantitative solutions have been worked out, mainly by graphical methods and for supersonic Mach numbers of the order of 20. References 37 and 44 are typical.

3. Considerable experimental work has been done (as in references 44 and 45) on supersonic cascades by observation of the flow with optical means. On rotating cascades, successful Schlieren pictures have been taken by NACA for a compressor rotor with supersonic flow at the tip.

The problem at hand differs from other similar ones treated in the literature in that (1) the blade solidity is high compared to that of a system of axial vanes, (2) the relative Mach number range up and down the leading edge is large, from low supersonic at shroud to low subsonic at hub, and (3) the supersonic tip Mach number is lower, closer to 1.0, in general, than in other cascades so investigated.

B. General Procedure

The following general procedure here prescribed involves a back-and-forth iterative procedure on two families of surfaces one of them being a series of surfaces of revolution, on which the blade-to-blade flow must be satisfied, the other being a series of surfaces generated by a radial element in the fluid moving parallel to the blade camber surface on which radial equilibrium must be satisfied. The blade-to-blade flow is to be solved at four different radii, two radii where the relative flow is supersonic and two where it is subsonic. In the supersonic region, graphical solution will be used by an adaptation of the conventional field solution while in the subsonic region an analog field plotter will be used and the results subsequently corrected for compressibility and three-dimensional effects. Radial equilibrium is to be satisfied at three angular positions, blade suction, and pressure sides, and mid-channel. The procedure is similar to that used in the solution of the flow equations for the axi-symmetric condition. Its objective is to find the radial variation in the thickness of the stream sheets adjacent to the four selected surfaces of revolution. This thickness is expected to vary in the tangential as well as in the axial-radial direction.

CONFIDENTIAL

CONFIDENTIAL

The iterative procedure consists of recalculating the blade-to-blade flow allowing for the thickness variation in the third dimension and then repeating the radial flow equilibrium calculation to obtain new stream sheet thickness variation. Repetition of this procedure must be continued until convergence is met everywhere.

Boundary conditions for upstream and downstream are established by an independent design analysis. Upstream in the inlet axi-symmetrical flow applies while downstream the blade-to-blade flow is computed by channel theory. The downstream boundary must be taken only where the relative flow is subsonic, since the channel flow analysis does not distinguish between subsonic and supersonic flows.

C. Extent of Work Completed

The original general approach to this part of the over-all program was to carry on this inducer work simultaneously with the impeller design study but on a lower priority basis. As work progressed, it soon became apparent that the inducer work was a problem requiring a formidable effort to bring it to completion. It also became obvious that only an enormously simplified version of the above procedure would have usefulness, if it were to be incorporated as part of the design procedure. It was therefore decided to carry this work only as far as time would allow and, rather than attempt to reach a complete detailed numerical solution, look for possible features useful for design and for a better general understanding of the phenomenon.

The initial assumption for the first attempt at the blade-to-blade solution was taken as a constant stream sheet thickness. Even this two-dimensional solution requires a compound iterative procedure in the supersonic zone. It was carried out for one stream surface only, the one at the shroud. As anticipated, with the imposed condition of two-dimensionality, it was not possible to satisfy the downstream conditions completely, that is, the three-dimensional effects must be sizeable. In spite of this result, some understanding was gained as to the general nature of the flow pattern. Means of computing the optimum blade incidences have been found, and some insight has been gained about the relationships existing between blade shapes and the form of the shock patterns.

CONFIDENTIAL

CONFIDENTIAL

D. Significant Qualitative Results

Two possible basic shock configurations were found to exist; one is represented by a line such as LCR on Figure 70 (curved-oblique shock configuration), the other by a line such as LCR' (curved-normal shock configuration). Both the shape of the shock (whether normal or oblique) and its location upstream of the leading edge can be calculated. The shape and location of the shock are functions of the blade shape, the upstream flow Mach number and direction, and the downstream conditions.

1. The shape and location of the left-hand branch of the shock, for a given cascade under given upstream conditions, is entirely determined by the requirement of periodicity upstream of the blades. The calculation can be made independent of the downstream conditions and independent of the shape of the right-hand branch.

2. The shape of the right-hand branch is a function of the downstream conditions and requires the solution of the entire flow field.

3. Optimum incidence or optimum blade shape may be defined as that which will produce at R or R' a pressure rise least likely to bring about boundary layer separation. Calculations show the reflected curved-oblique configuration to be more desirable than the normal shock configuration. For a rigorous application of this criterion, a complete solution of the flow is required. With lower downstream pressures, the curved-oblique shock will exist. As the back pressure is raised, the shock will jump into the normal position. When this takes place, breakdown of the flow and collapse of impeller performance is likely to take place. The design, then, should be made for a curved-oblique shock pattern.

CONFIDENTIAL

4. To the two possible shock configurations, there corresponds two separate mechanisms by which the flow becomes subsonic for an inviscid fluid. When the shock is curved-normal, such as LCR', everything downstream becomes and remains subsonic. When the shock is curved-oblique, such as LCR, the transition from super to subsonic takes place in steps as sketched on Figure 70, subsonic flow gradually filling the channel.

It is possible to shape the blades in such a way as to promote the desirable curved-oblique configuration. For this configuration, the blade curvature must be such that the oblique shock can be reflected. Insufficient curvature will result in too low a Mach number at R to permit reflection and the shock will jump out to a position such as CR'. Excessive curvature will slow down the deceleration process and result in an extensive zone of supersonic flow between the blades.

E. Method of Analysis of the Two-Dimensional Supersonic Flow

The procedure of analysis outlined below is applicable to the two-dimensional inviscid flow on a cylindrical surface of large radius. The analysis is based on the assumption that a system of detached shocks is present in front of the cascade. Only this flow pattern is logical for flows at low supersonic Mach numbers. Furthermore such a pattern has been confirmed experimentally by optical observation. The shape of each detached shock differs from that of the more familiar variety existing ahead of a single airfoil because of the presence of adjacent blades and because the downstream conditions may be varied independently of the upstream conditions. It is necessary to distinguish between the center portion, the right and left branches of the shock. Their shapes are governed by separate considerations.

CONFIDENTIAL

1. For a given geometry and upstream condition, the shape of the left branch LC on Figure 70, and its position ahead of the leading edge, is dictated purely by requirements of periodicity. Thus, at point P, the Mach number must go through a discontinuity from the value it has along wave W_1 to the value it must have along wave W_2 (which must be the same as W_2'). If the local Mach numbers were known, the direction of the shock at P (or any other such point) would also be known.

Assignment of the numerical values of Mach numbers at various points must be made by successive approximations. Assignment of a Mach number to a point such as Q, permits the drawing of all expansion waves W_0, W_1 , etc. over the entire field, each labelled with its particular Mach number. At all points such as P, little elements of shocks can be drawn as explained above. If the center portion of the shock location is selected, the entire left branch can be sketched in. One particular Mach line will never intersect any shock. The stream velocity and direction along this line must be equal to the stream Mach number and direction far upstream. If the Mach number condition is not met, another Mach number value is assigned at point Q. If the directional requirement is not met, the position of the shock center portion is moved a little upstream or downstream relative to the blade leading edge. Thus, satisfaction of the blade geometry and the upstream conditions fix the shape and location of the left branch of the shock.

2. The shape of the shock right-hand branch (branch CR) must be such as to satisfy the downstream conditions previously established by channel theory analysis. The problem is one of calculating a flow satisfying given boundary conditions.

For purposes of engineering computations, it is perhaps best as an initial working procedure to analyze the flow by graphical means rather than attempt, from the start, to set up a complete mathematical solution. The merits of this approach were quite evident in the calculation of the flow on both sides of the shock left branch where a solution could be converged upon comparatively rapidly. The flow on the right side is mixed subsonic and supersonic. The supersonic regions will be handled by the conventional field method of shocks and characteristic lines of finite strength. The subsonic regions will be handled by plots of streamlines such that continuity and radial equilibrium are satisfied.

CONFIDENTIAL

CONFIDENTIAL

Solution of the pattern involves a method of successive approximations with adjustment of the sonic point S and the sonic line SN. Adjustment of SN (or MM') is required to satisfy the basic flow equations. Changing the location of S must be made until the desired downstream subsonic channel conditions are met. For a given selection of point S and line SN, the entire region SRN can be computed in the conventional way in terms of the properties within finite patches, between shocks and Mach lines. The flow picture in the subsonic region is necessarily less precise in that the streamline shape must be calculated and plotted point by point. The reflected shock RN must terminate as a normal shock at N, since the local Mach number will be near 1.0. Region MM'T is computed in a similar manner. Whether another oblique reflection takes place or whether the supersonic flow finally ends in a normal shock depends on the downstream condition. At the point where the flow is subsonic, the velocities on both the suction and pressure sides of the blade must check those calculated by channel theory. If this is not realized, a fresh start is made for the position of points.

3. Little concern need be had about the shock center region. Its position forward of the leading edge follows automatically from part (1) above. The limits of the subsonic zone and the shock direction at points C behind the shock follows from parts (1) and (2). The exact shape of that portion of the shock has little effect on the over-all flow picture.

F. Calculated Flow Pattern

Study of the blade loading within the impeller as calculated by the method of Section II indicates that the flow remains supersonic on the blade suction side for a considerable distance. Thus, if downstream conditions are to be met, a system of curved-oblique shocks must be present. Figure 71 pictures such a flow, as far as it was calculated, and is the result of a series of iterations. The flow was not carried all the way downstream when it became apparent that continuity could not be satisfied in the subsonic zone, if the requirements of two-dimensionality alone are adhered to. This indicates that:

CONFIDENTIAL

CONFIDENTIAL

1. A two-dimensional flow is not possible with the imposed upstream and downstream conditions.
2. A two-dimensional solution exists, but it does not satisfy the downstream conditions. Such a solution requires a frontal normal shock such as CR' on Figure 70. This solution is of little interest here.
3. An illustrative two-dimensional flow may be conceived in which its upstream and downstream conditions are met approximately but in which the pressure side boundary is so modified as to permit satisfaction of continuity. The flow pattern of Figure 71 conforms to this description. The following interesting points were encountered:
 - (a) The shock location satisfying both upstream Mach number and direction is one which has its center portion very near the blade leading edge.
 - (b) Because of the multiple shocks and expansions upstream of the leading edges, the Mach number immediately upstream of the center portion of the shock is considerably higher than in the undisturbed stream (1.50 compared to 1.32).
 - (c) The possibility of the right-hand shock branch being of the curved oblique form but becoming normal at the section surface of the adjacent blade was investigated and found impossible.
 - (d) For regular shock reflection on the blade suction surface, the local incoming Mach number must be above 1.9. Lower local Mach numbers will cause the shock pattern to alter itself to the curved normal configuration.
 - (e) Regardless of the position of the sonic point s and the shape of the streamline sd , continuity cannot be satisfied between streamlines $OO-c$ and $OO-d$. This points to the extreme significance of the three-dimensional effects.

CONFIDENTIAL

CONFIDENTIAL

G. Process of Diffusion in Transonic Impeller

At this time, it is of great interest to compare the qualitative results of the foregoing analysis with some observed behavior of AiResearch transonic impellers. Figure 72 shows an approximate sketch of experimental shroud pressure data for a typical set of runs of a transonic radial impeller. Of particular interest is the fact that at high mass flows, extremely low pressures are reached, indicating very high local Mach numbers. The humps on the curve indicate the presence of several successive shocks, separated by re-expansions. As the mass flow is reduced, the downstream expansions disappear first, in a noticeable step-wise fashion until the inlet expansion ceases to be present. At this point, it is found that violent and unannounced impeller surge takes place.

From the theoretical work of this section some insight can be gained as to the nature of the phenomena taking place in a transonic impeller operated at constant speed with the mass flow gradually reduced. Study of Figure 70 suggests that, as the back pressure goes up, shock MU jumps from the oblique to the normal position and all points R, N, T, M, etc. become compressed a little towards the upstream direction. With further pressure increase shock NT, in turn, becomes normal. This accounts for the observed step-wise change in pressure, which progresses from downstream to upstream. Finally, the Mach number at R is no longer high enough to permit a reflected oblique shock at R, and shock CR itself becomes normal. It may well be that the presence of a strong normal shock at the inlet causes widespread boundary layer separation there. The resulting sudden drop in impeller efficiency would bring about impeller surge.

It is clear that the above described process may be quite efficient up to the instant when boundary layer separation occurs. In order to retard this occurrence, the blade design must be such that either the oblique shock pattern can be maintained as long as possible or efficient operation can be had with a normal shock at the inlet. In view of the past lack of success of the so-called shock-in-rotor type of compressor, the former alternative seems to be preferable.

CONFIDENTIAL

CONFIDENTIAL

SUMMARY

The basic objective of the present work is to formulate basic criteria for the design of centrifugal and mixed-flow impellers. These criteria must be general in nature and must be so selected as to supply design information in the specific areas where, presently, the design is left to judgement and to the experience of the designer. A second objective is to improve the understanding of the internal aerodynamics so as to advance the state of the art of high performance compressor design.

A study to allow selection of the quantities to be investigated, indicated that the over-all blade loading, the distribution of blade loading, and the exit cone angle, are most significant quantities in that their effect on compressor performance is large and is not well understood. In order to investigate these effects experimentally, ten impellers were designed. Two series of three and four impellers, respectively, were designed to investigate the effect of impeller length on performance and simultaneously that of over-all blade loading. A third series of three impellers was made to study the effect of exit cone angle. Within each series, the maximum blade loading of each impeller is varied from inducer to exit. Each impeller was so designed as to isolate, as completely as possible, the effect of the primary variable under study. The characteristics of each impeller are fully described in this report as well as the design procedure used to compute these characteristics.

Future work will involve fabrication and testing of the three most promising impellers as an initial step towards attaining the desired objectives.

CONFIDENTIAL

CONFIDENTIAL

DATA FROM REFERENCE I

$$\frac{g \Delta H_{12}}{a_0^2} = 1.81$$

RADIAL BLADES
INDUCER TO EXIT DIAMETER RATIO : 0.715

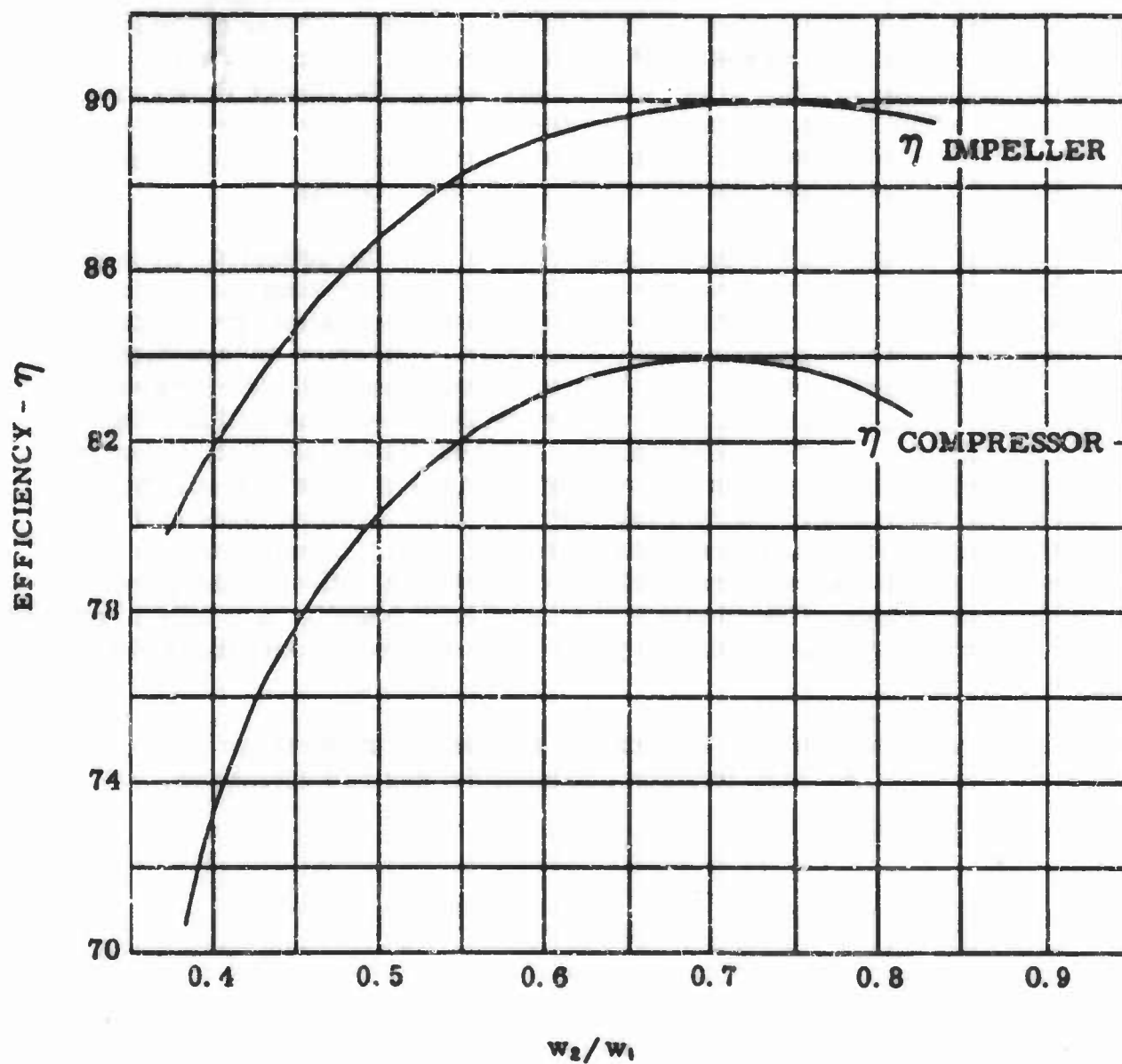


Figure 1

EFFECT OF IMPELLER DECELERATION RATIO UPON
IMPELLER AND COMPRESSOR EFFICIENCY

CONFIDENTIAL

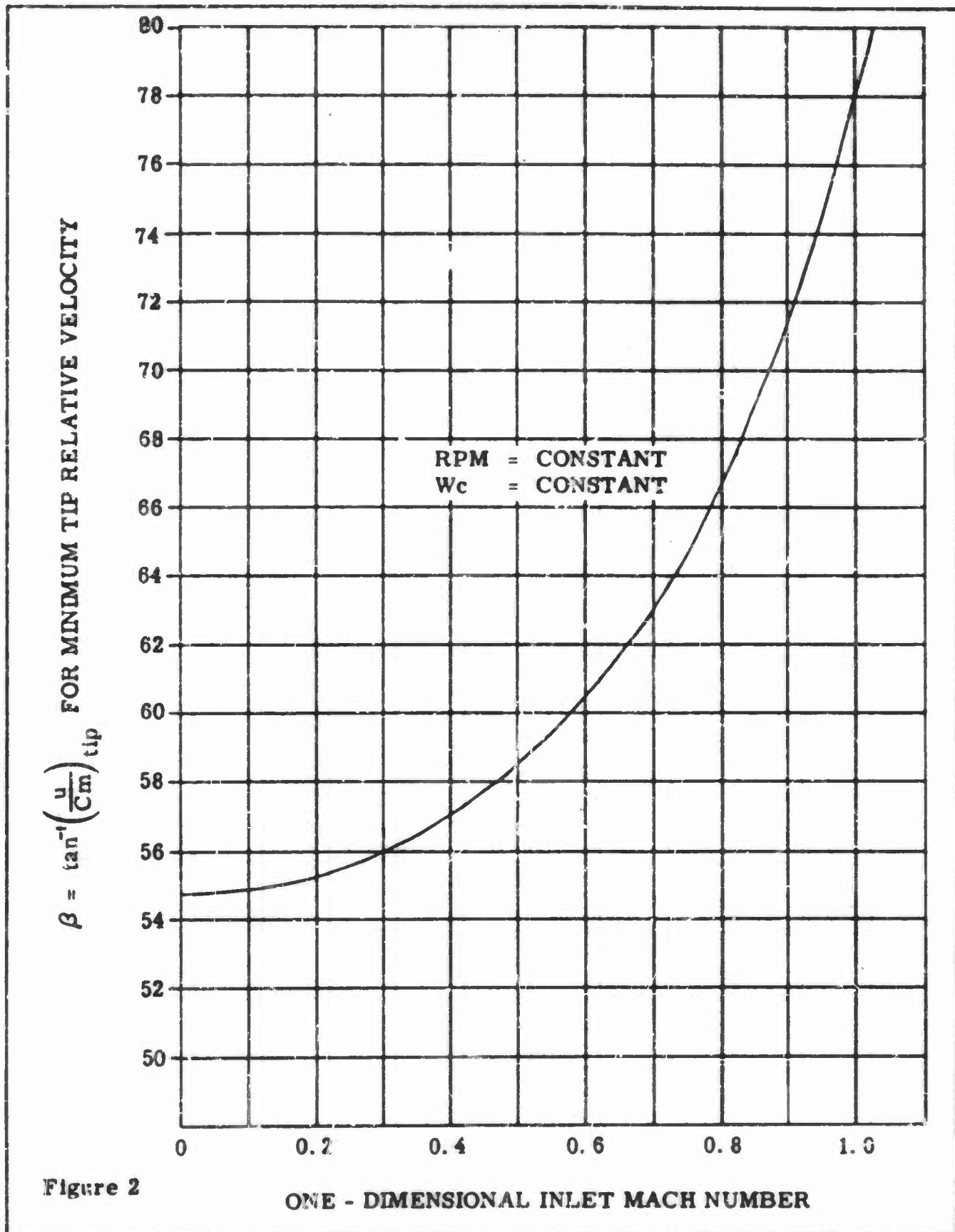


Figure 2

OPTIMUM TIP FLOW ANGLE FOR MINIMUM RELATIVE VELOCITY

CONFIDENTIAL

CONFIDENTIAL

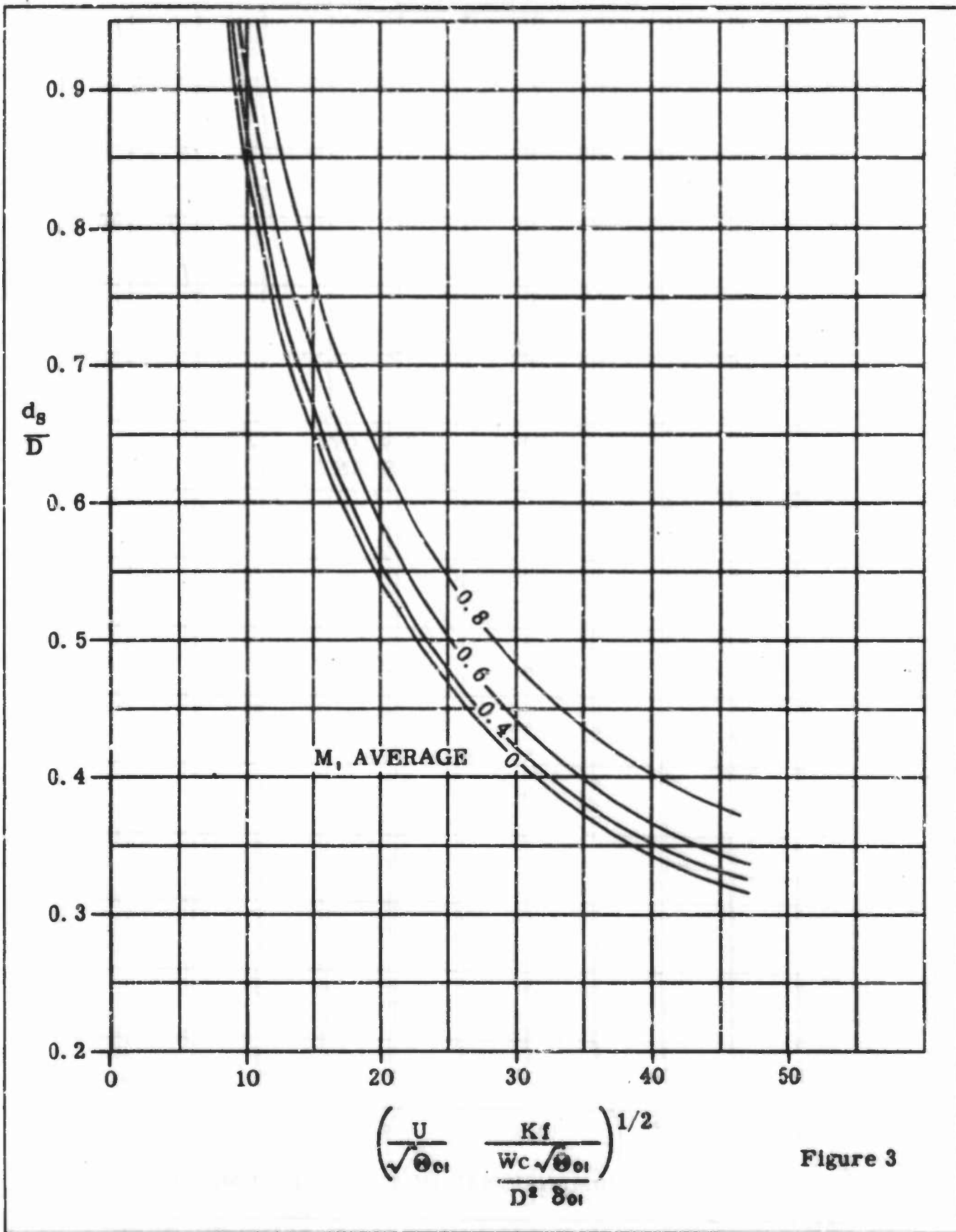


Figure 3

IMPELLER INDUCER TO TIP DIAMETER RATIO

CONFIDENTIAL

CONFIDENTIAL

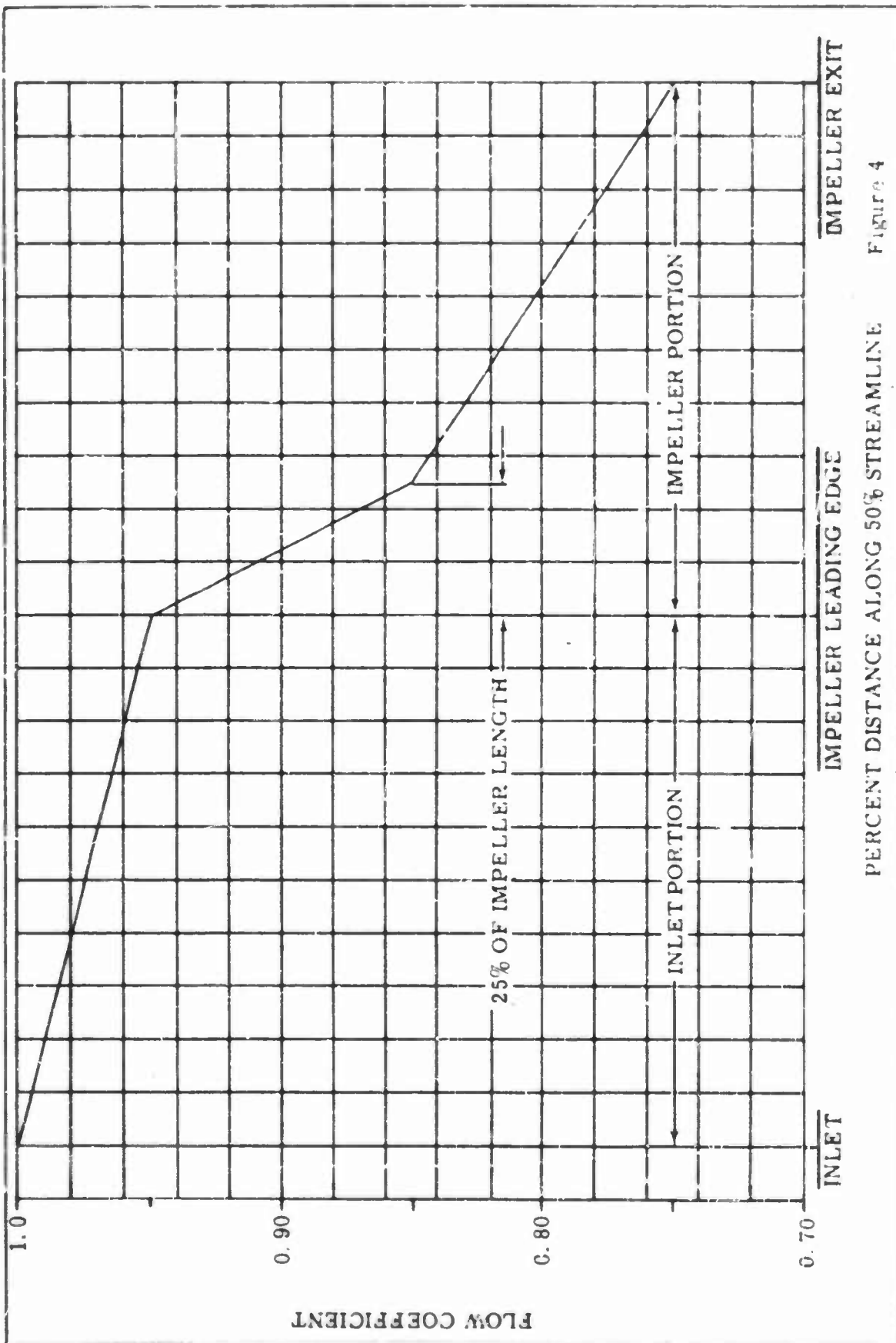


FIGURE 4
PERCENT DISTANCE ALONG 50% STREAMLINE

VARIATION OF FLOW COEFFICIENT FOR HIGH PRESSURE RATIO IMPELLERS

CONFIDENTIAL

CONFIDENTIAL

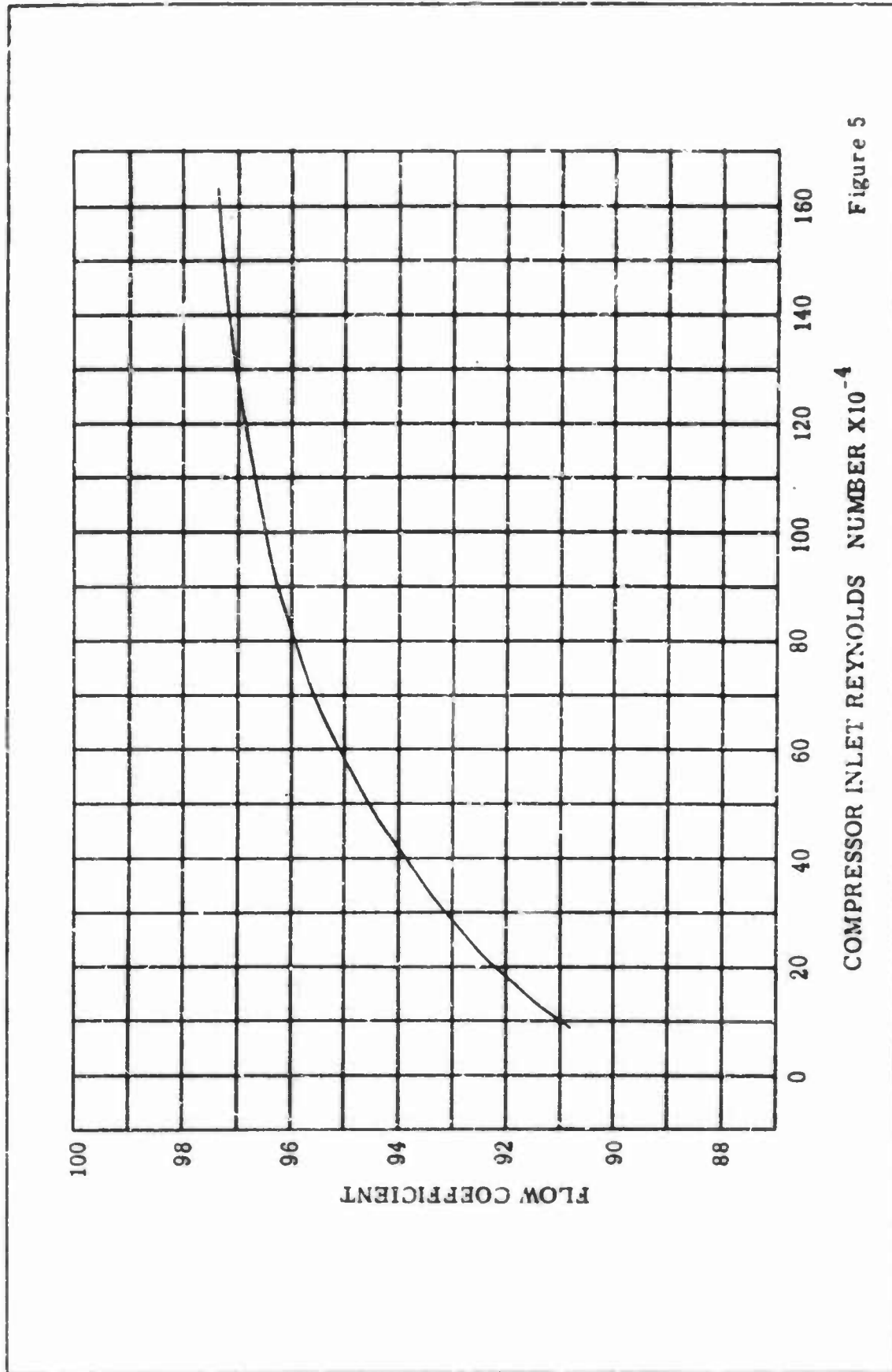


Figure 5
COMPRESSOR INLET REYNOLDS NUMBER $\times 10^{-4}$

MEASURED FLOW COEFFICIENT IN TYPICAL RADIAL INLET FLOW PASSAGE OF COMPRESSOR

CONFIDENTIAL

CONFIDENTIAL

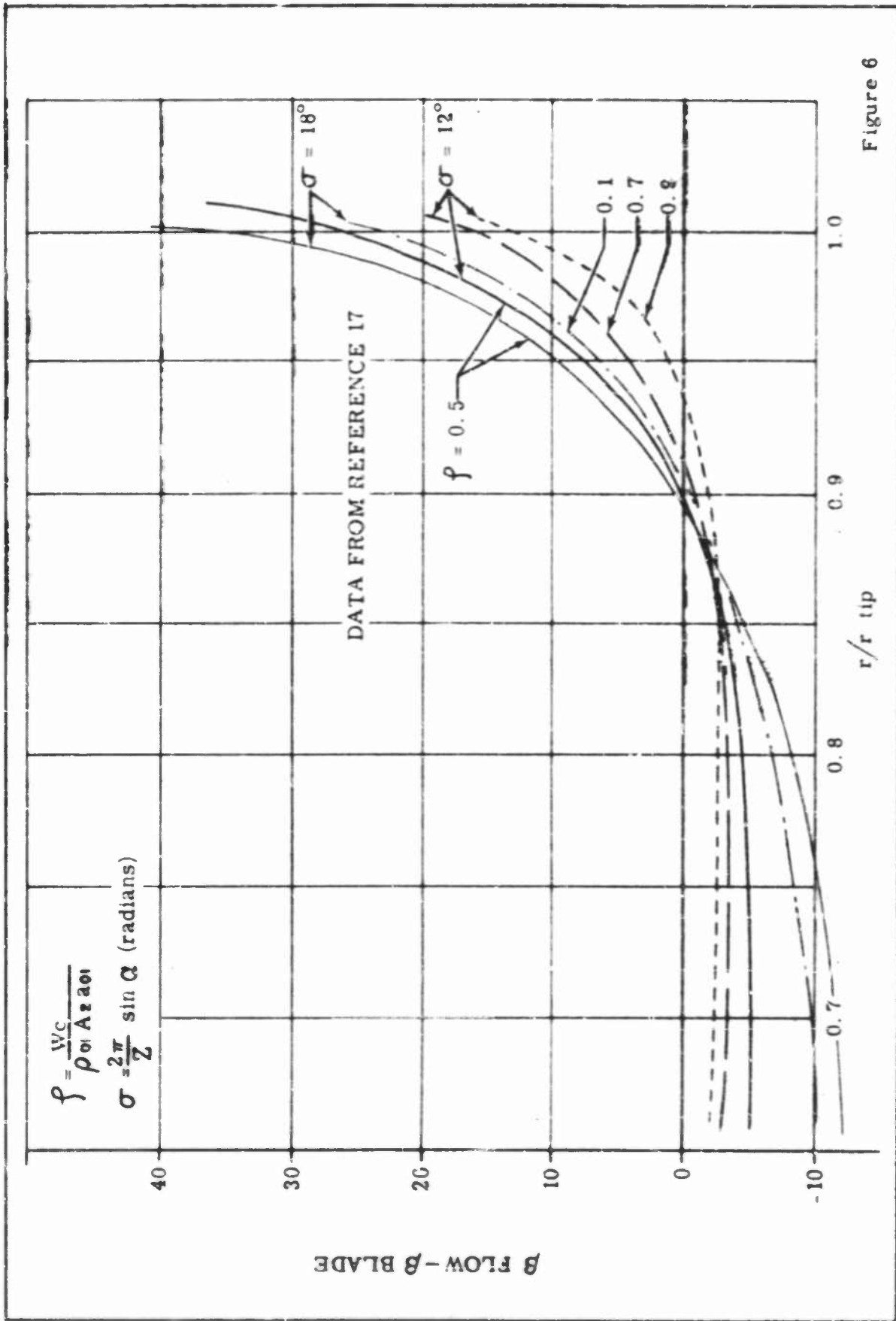


Figure 6

DEVIATION OF FLOW DIRECTION FROM BLADE DIRECTION AT IMPELLER EXIT

CONFIDENTIAL

CONFIDENTIAL

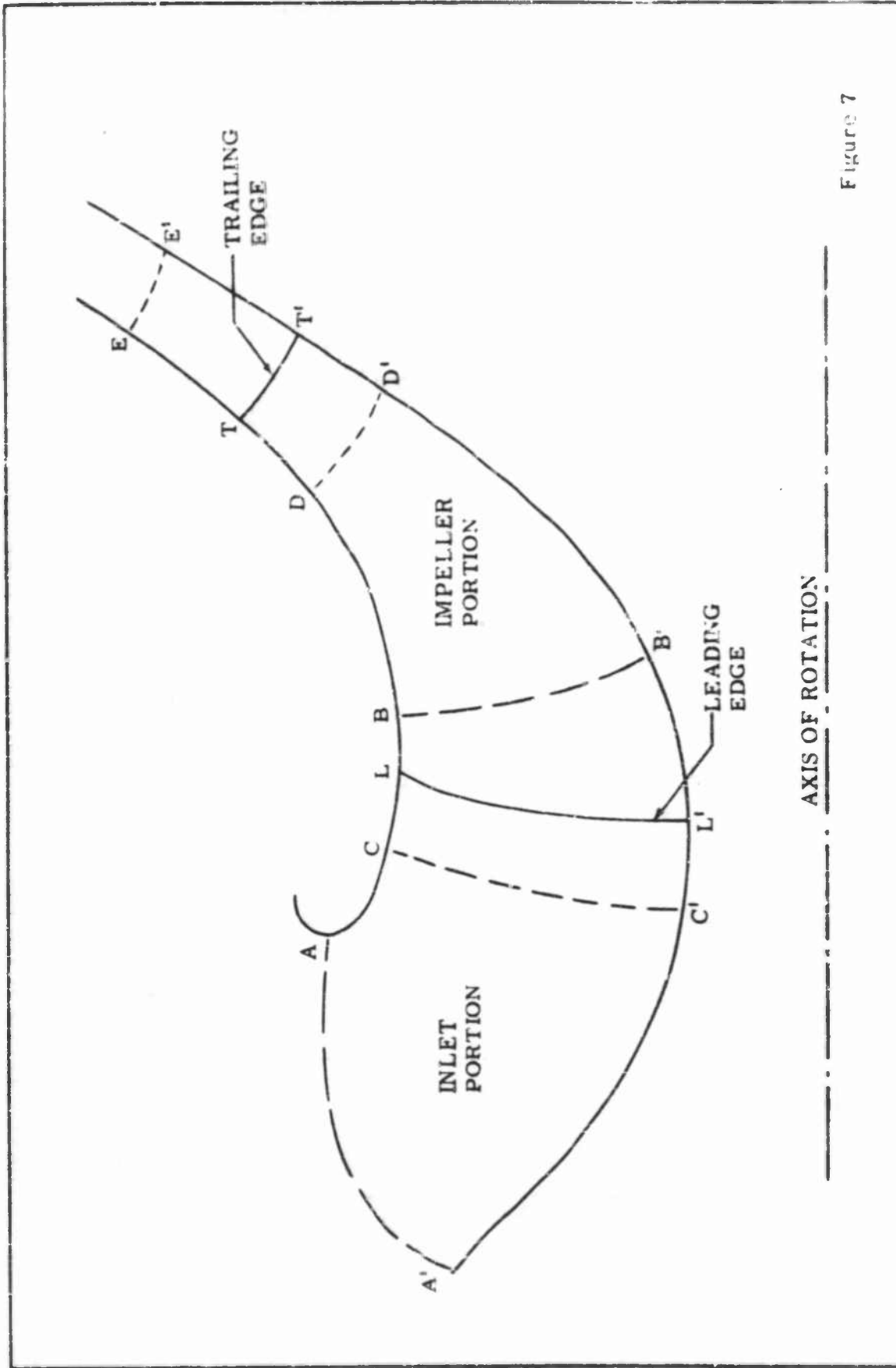
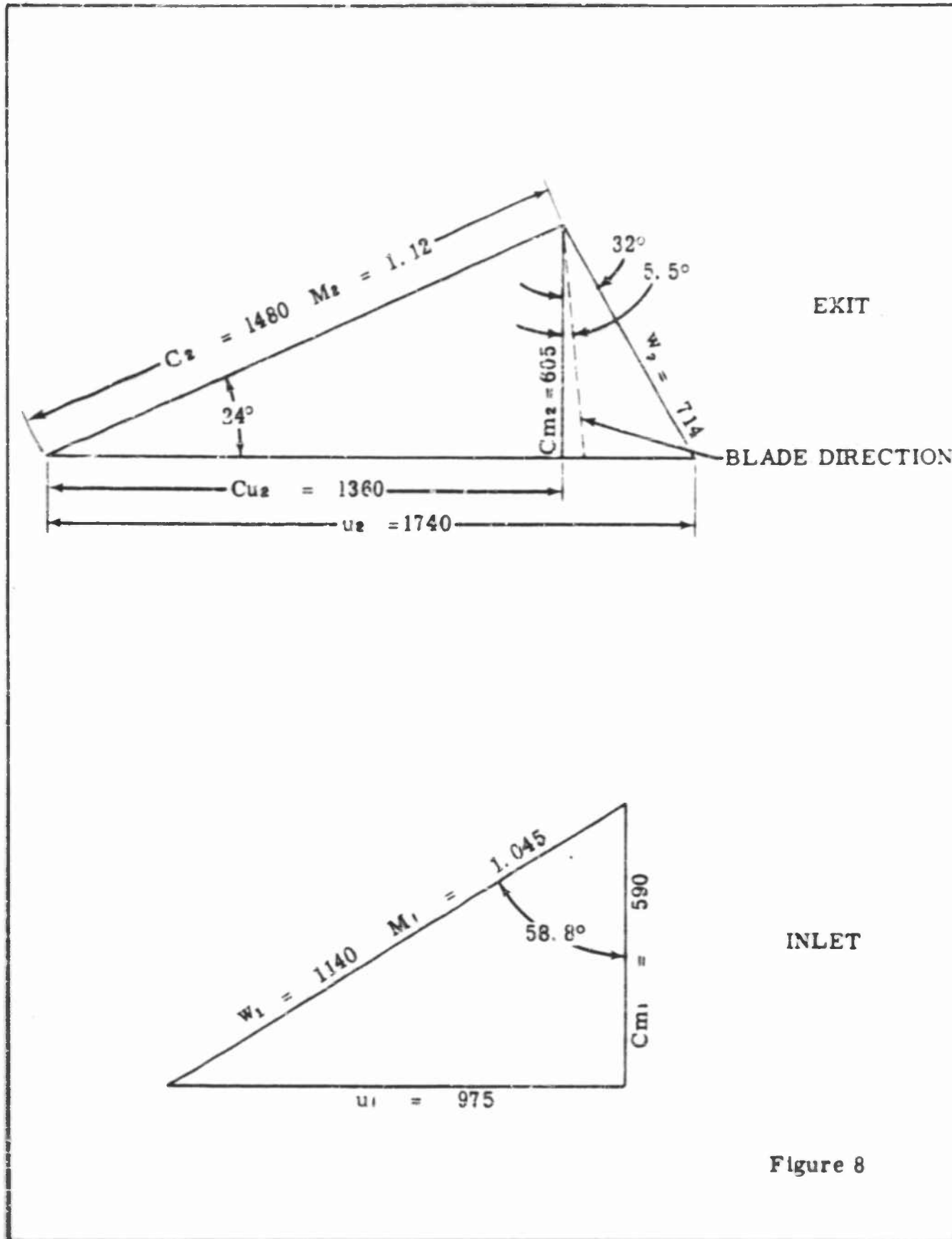


Figure 7

ZONES OF SIGNIFICANCE AS APPLIED TO THE NUMERICAL SOLUTION OF FLOW IN IMPELLER PASSAGES

CONFIDENTIAL

CONFIDENTIAL



INLET AND EXIT MEAN VELOCITY TRIANGLES

CONFIDENTIAL

CONFIDENTIAL

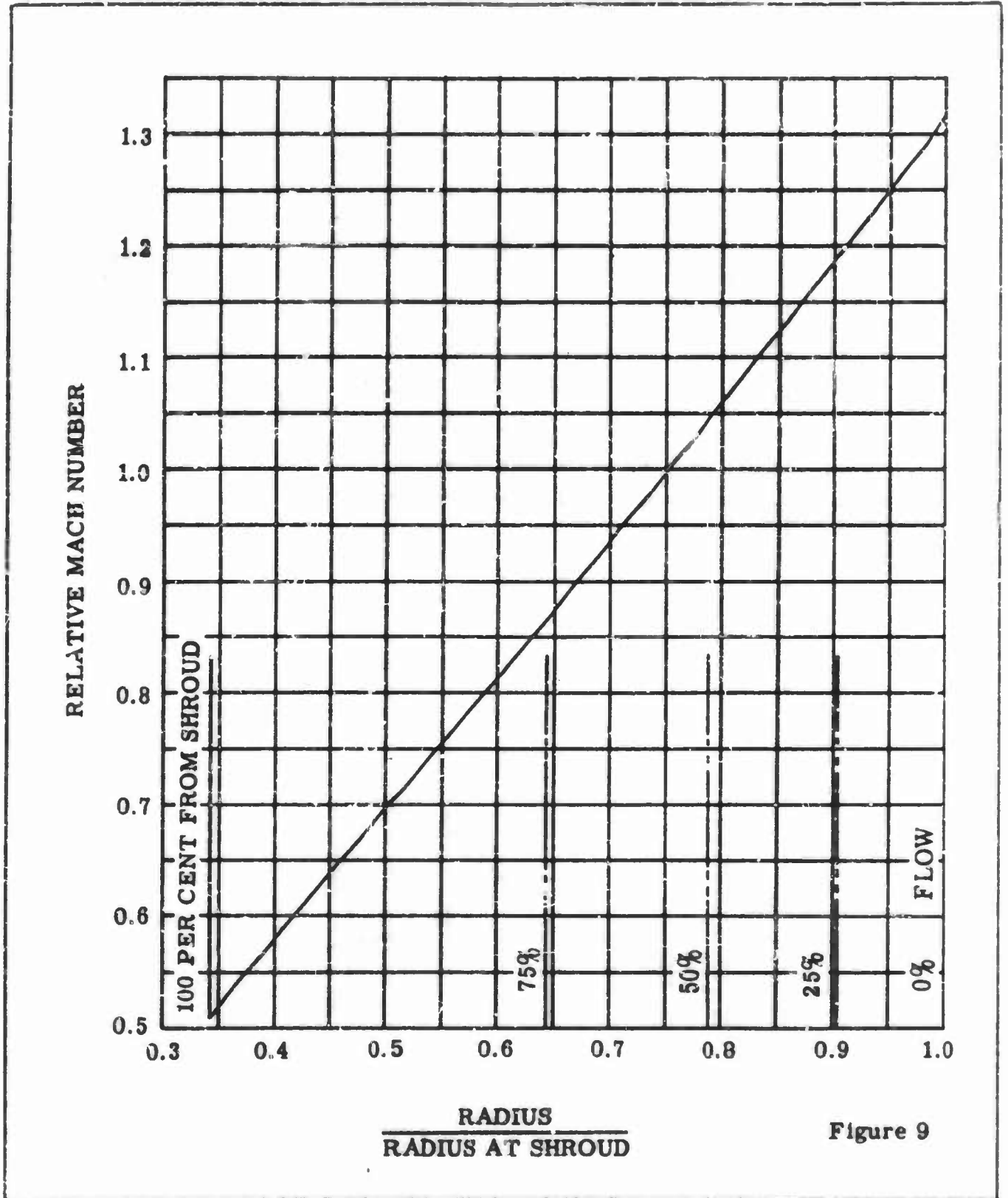


Figure 9

RELATIVE MACH NUMBER ALONG IMPELLER LEADING EDGE

CONFIDENTIAL

CONFIDENTIAL

NOTE: (INCLUDES EFFECTS OF VORTICITY,
VISCOS AND BLADE CLOGGING)

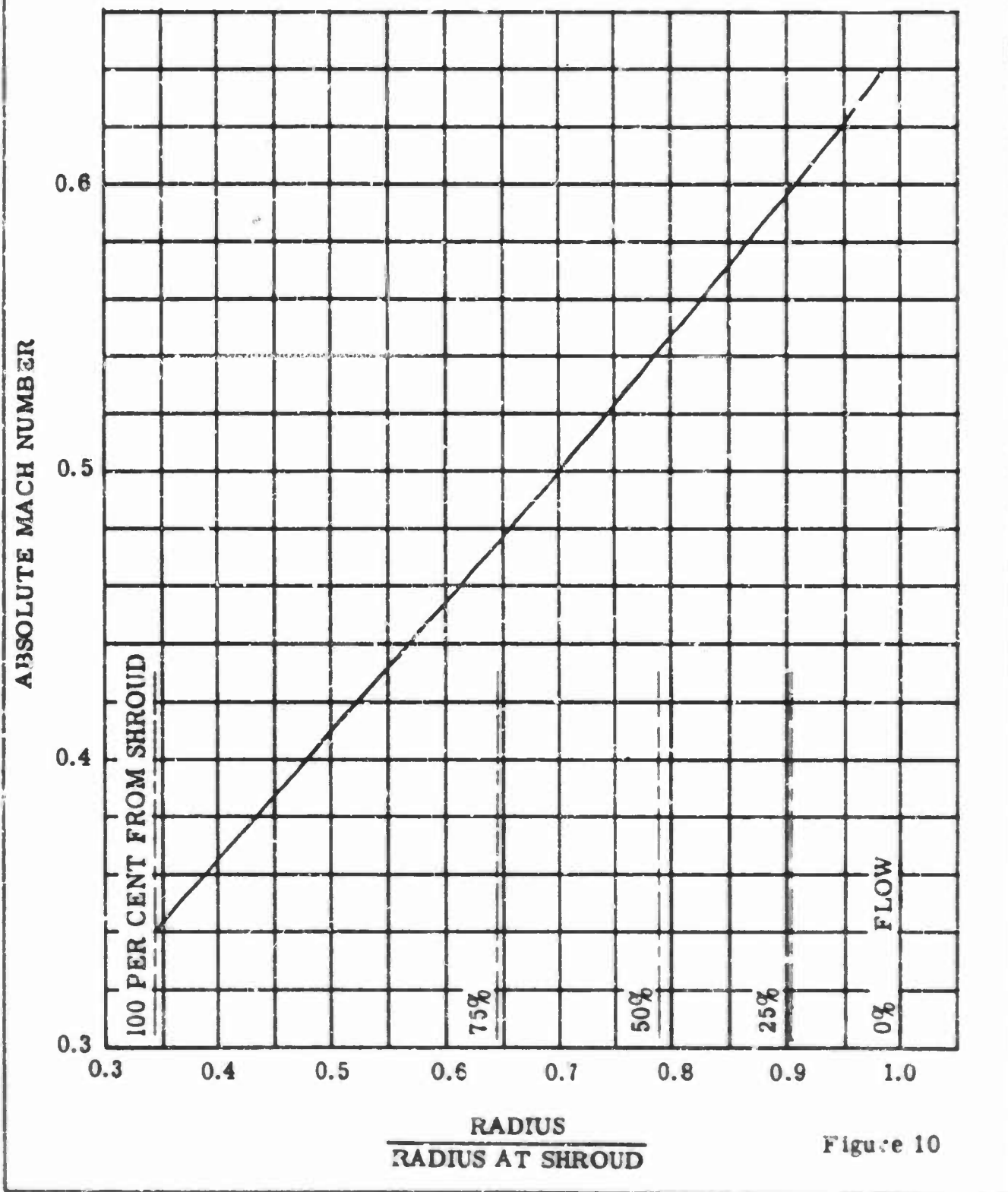


Figure 10

ABSOLUTE MACH NUMBER
ALONG IMPELLER LEADING EDGE

CONFIDENTIAL

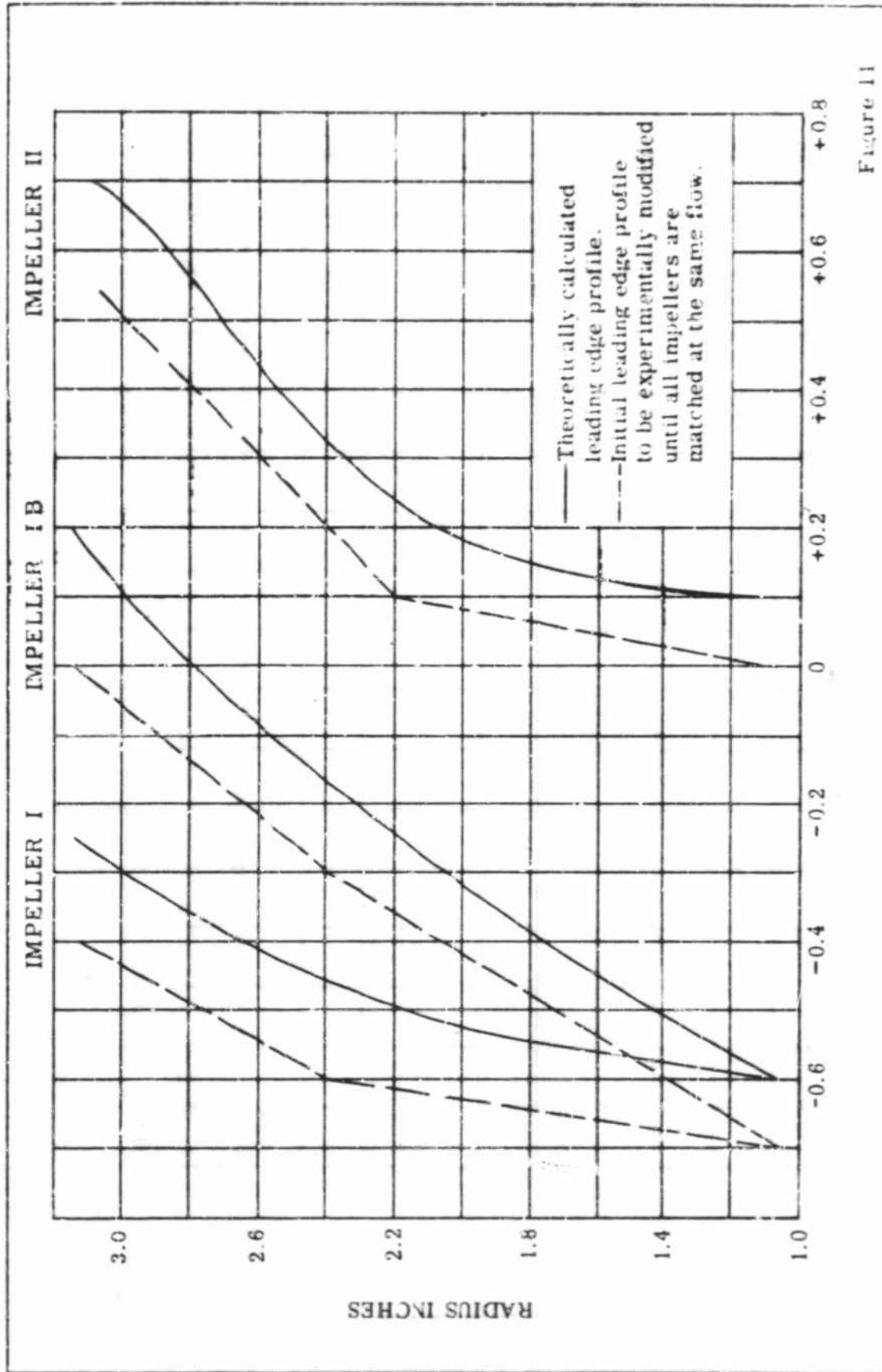


Figure 11

SHAPE OF LEADING EDGES - THEORETICALLY CALCULATED
SHAPE AND FIRST DESIGN SHAPE

CONFIDENTIAL

CONFIDENTIAL

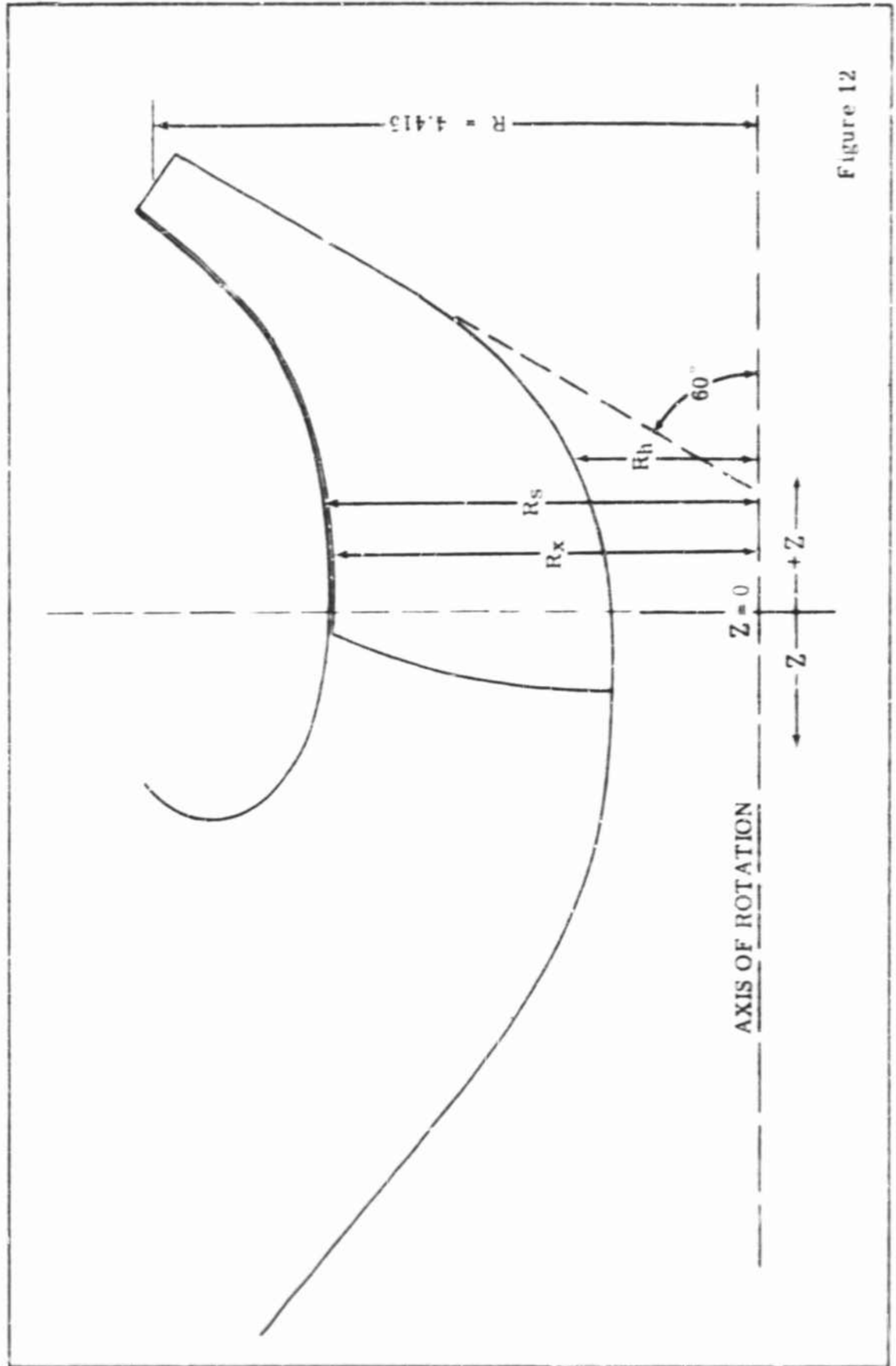


Figure 12

IMPELLER SERIES I

CONFIDENTIAL

CONFIDENTIAL

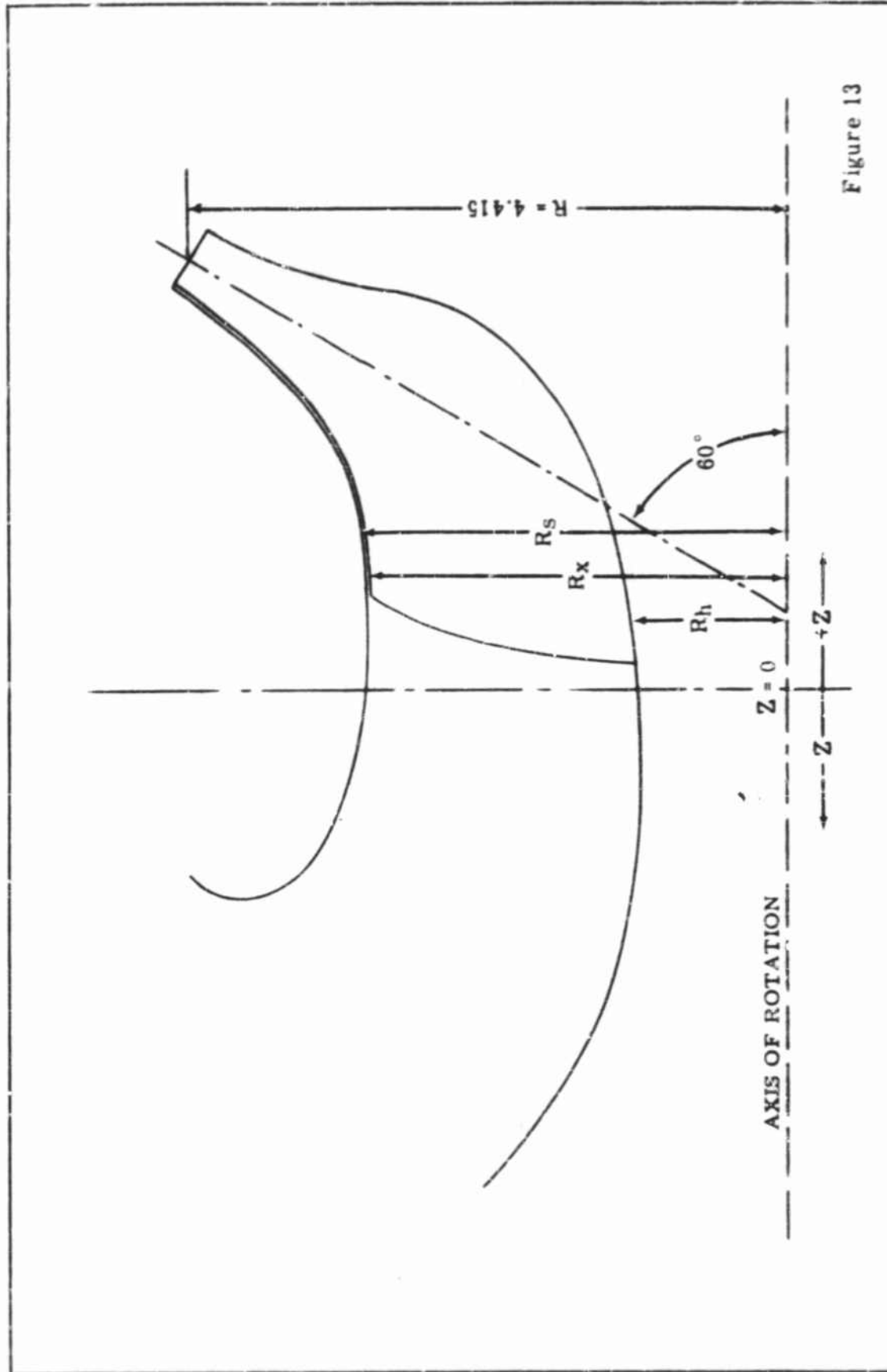
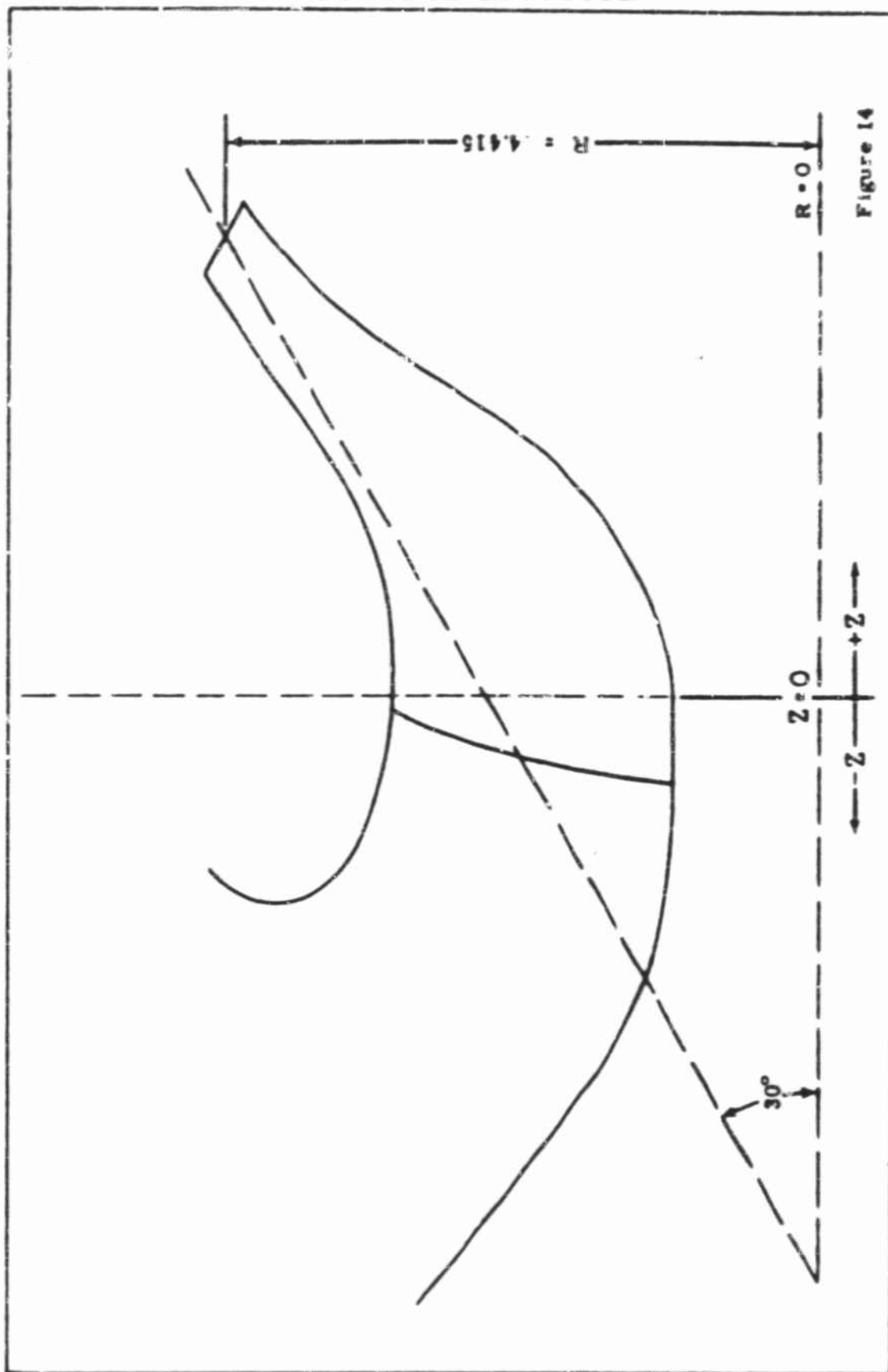


Figure 13

IMPELLER SERIES II

CONFIDENTIAL

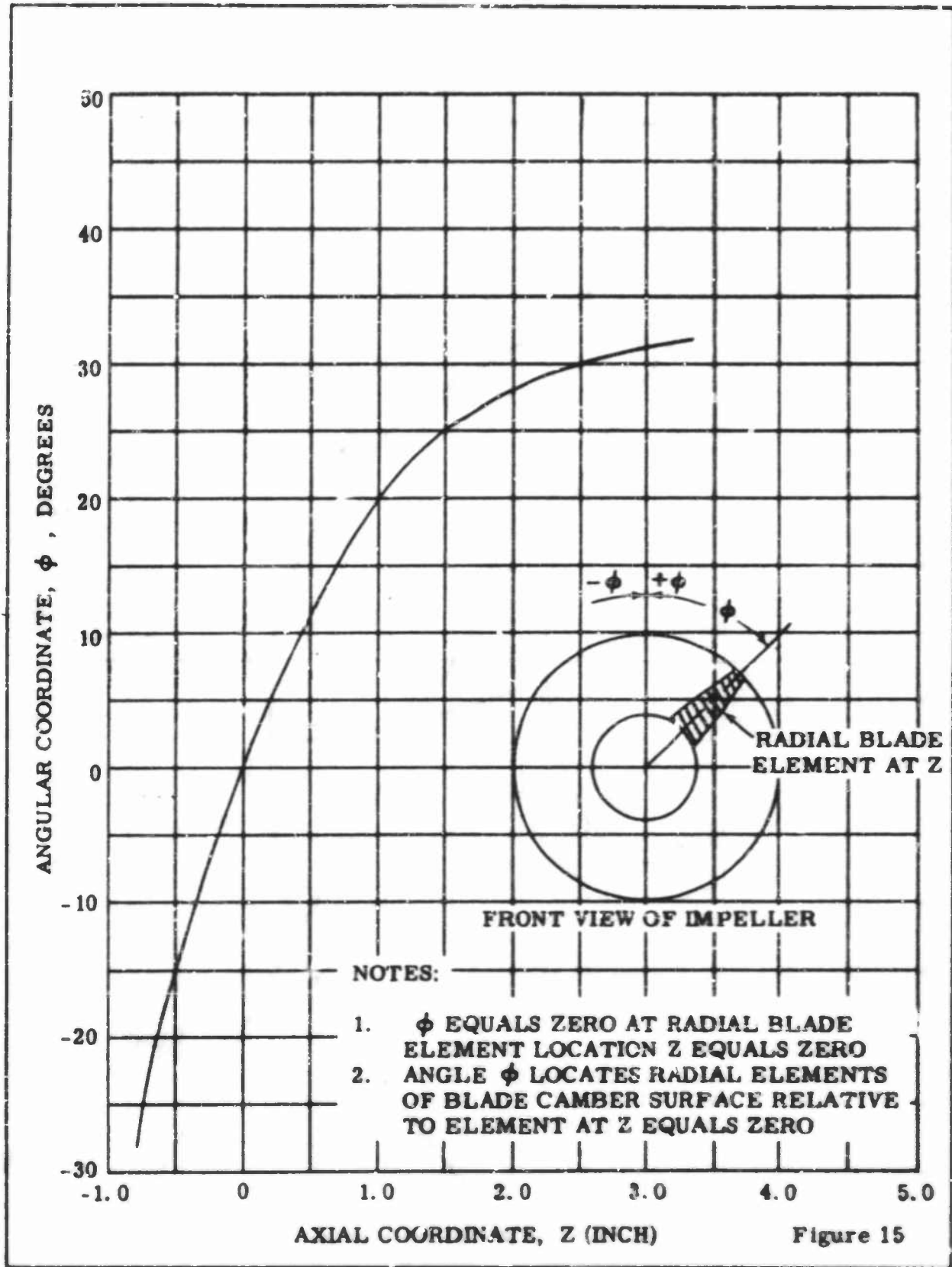
CONFIDENTIAL



IMPELLER SERIES IV

CONFIDENTIAL

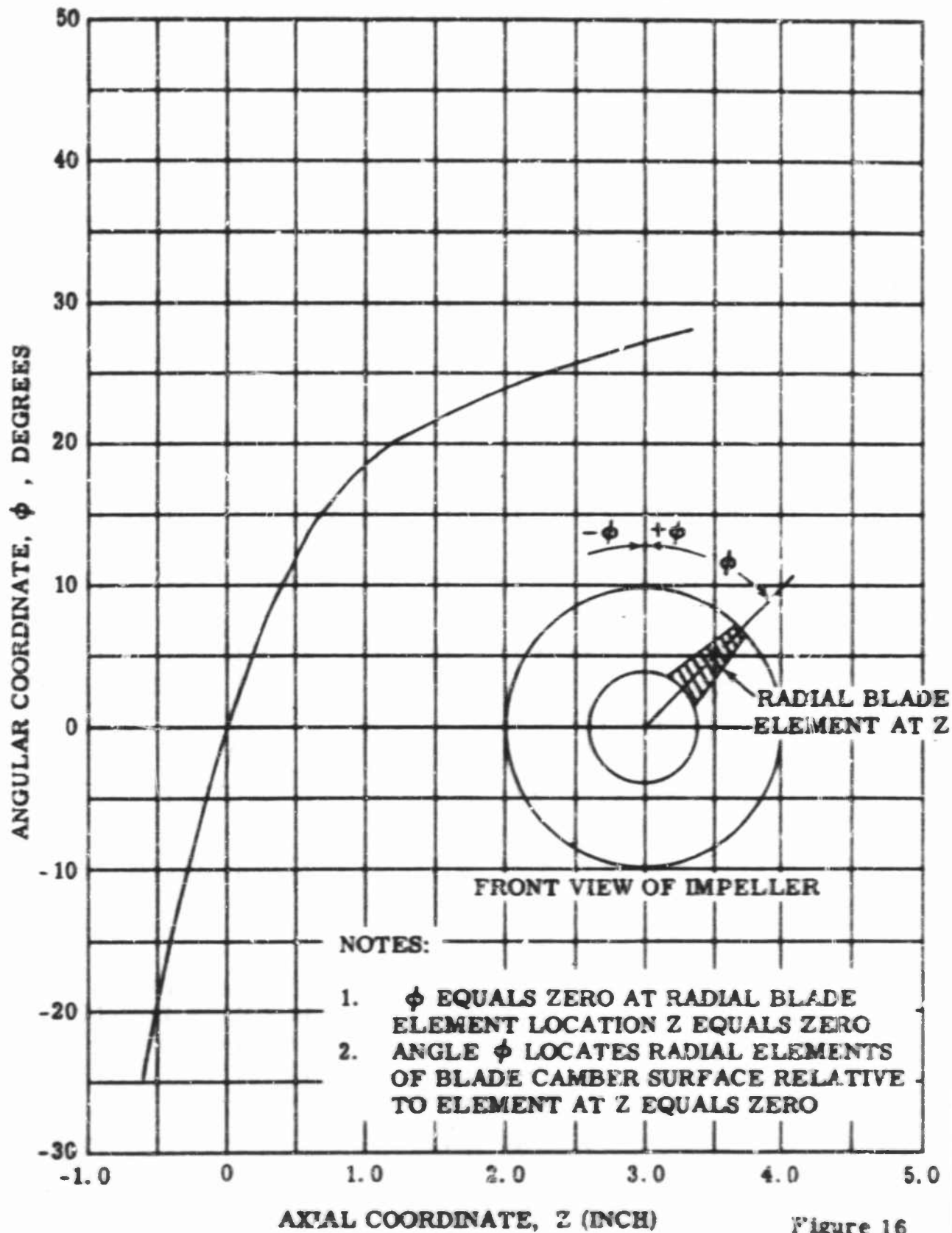
CONFIDENTIAL



IMPELLER I, BLADE ANGULAR COORDINATES

CONFIDENTIAL

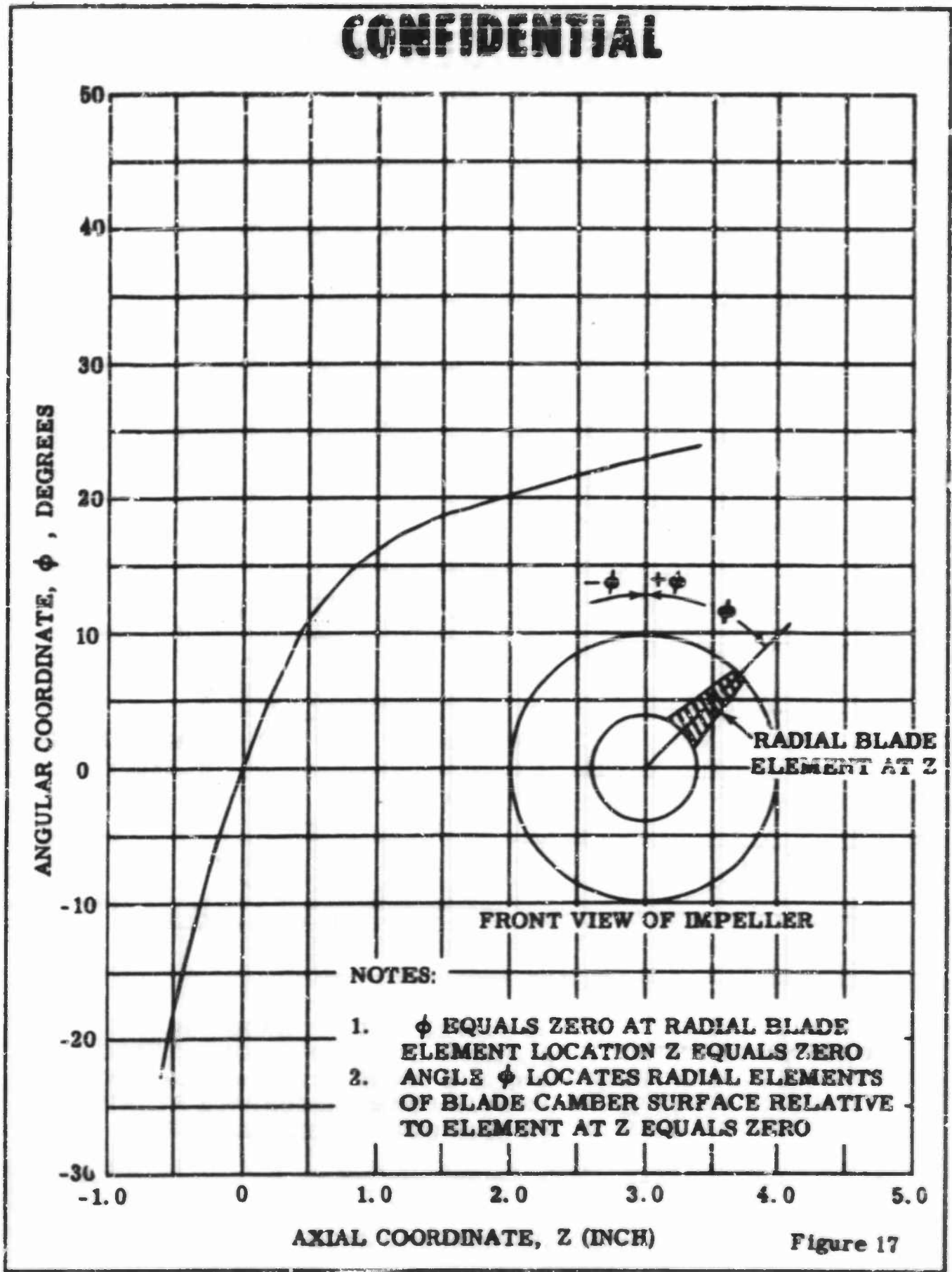
CONFIDENTIAL



IMPELLER IA, BLADE ANGULAR COORDINATES

CONFIDENTIAL

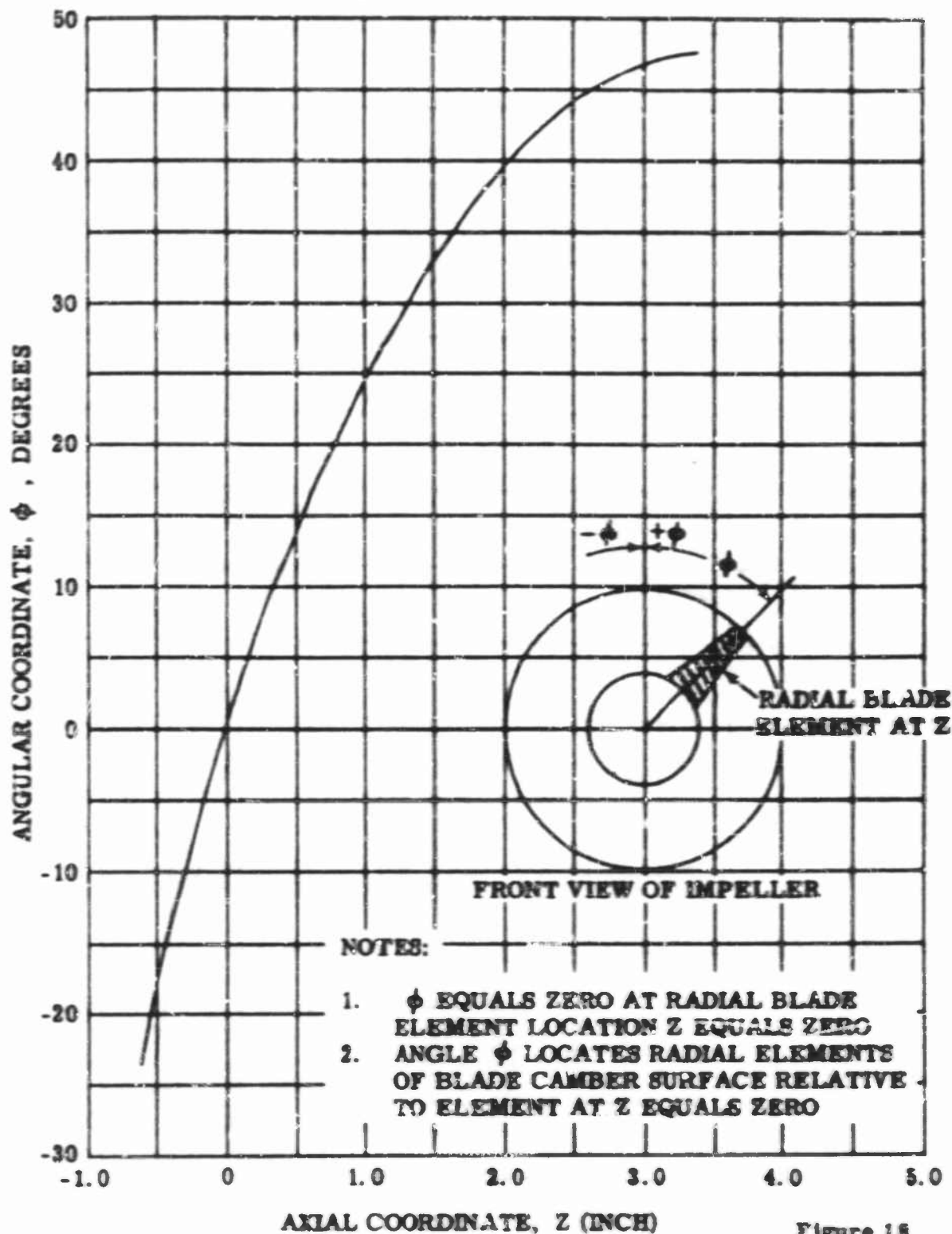
CONFIDENTIAL



IMPELLER IAA, BLADE ANGULAR COORDINATES

CONFIDENTIAL

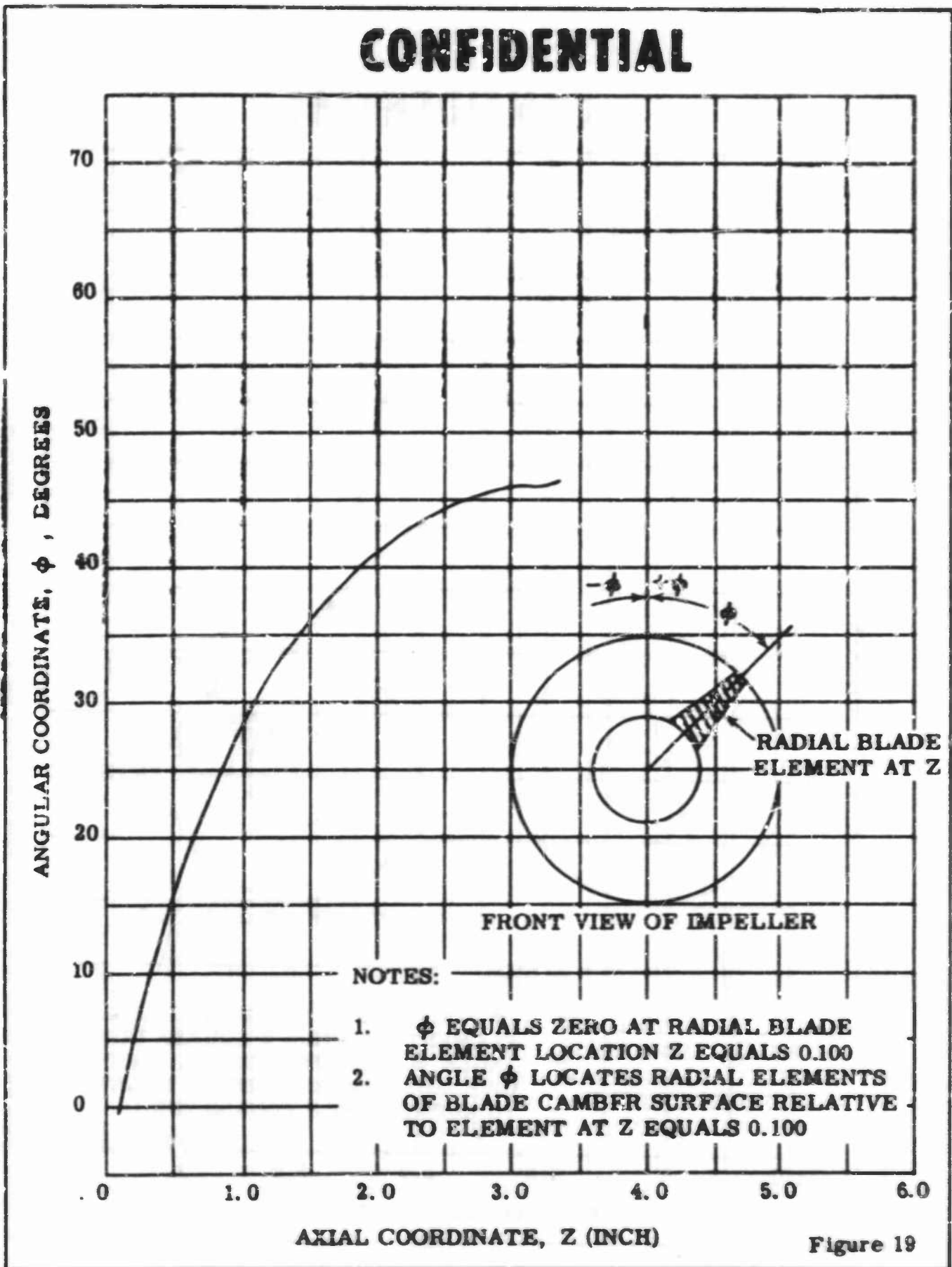
CONFIDENTIAL



IMPELLER IB, BLADE ANGULAR COORDINATES

CONFIDENTIAL

CONFIDENTIAL



IMPELLER II, BLADE ANGULAR COORDINATES

CONFIDENTIAL

CONFIDENTIAL

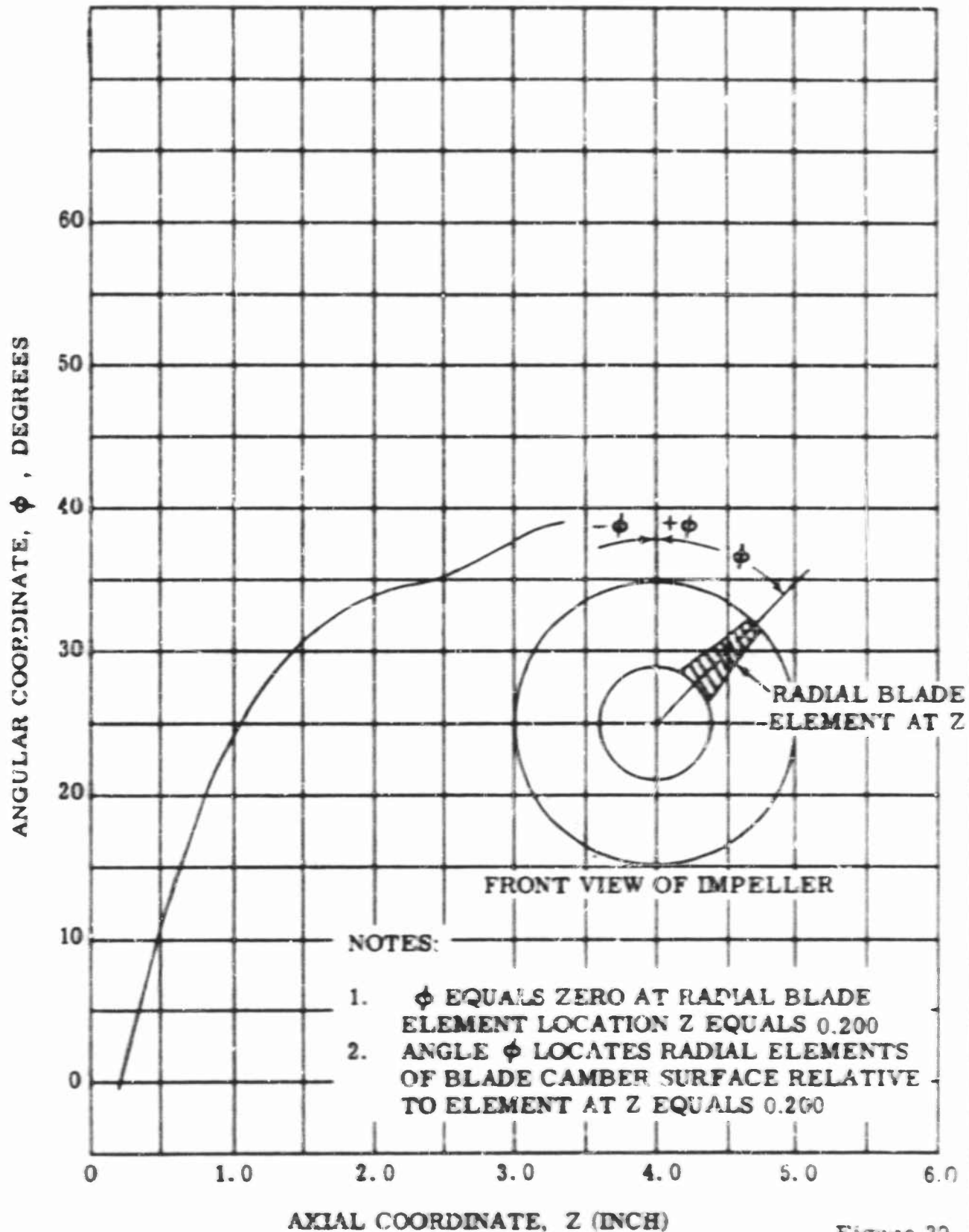
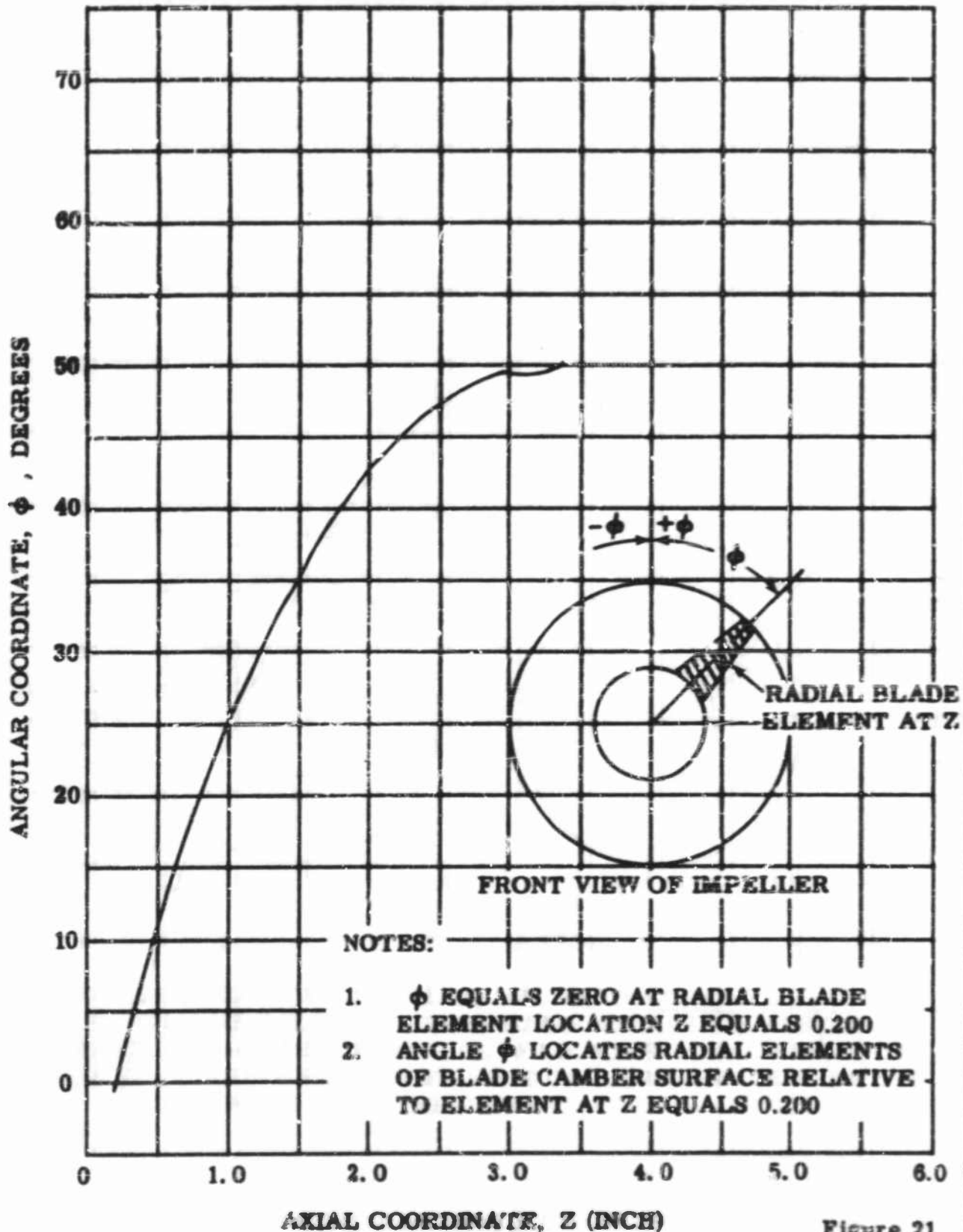


Figure 20

IMPELLER IIA, BLADE ANGULAR COORDINATES

CONFIDENTIAL

CONFIDENTIAL



IMPELLER IIB, BLADE ANGULAR COORDINATES

CONFIDENTIAL

CONFIDENTIAL

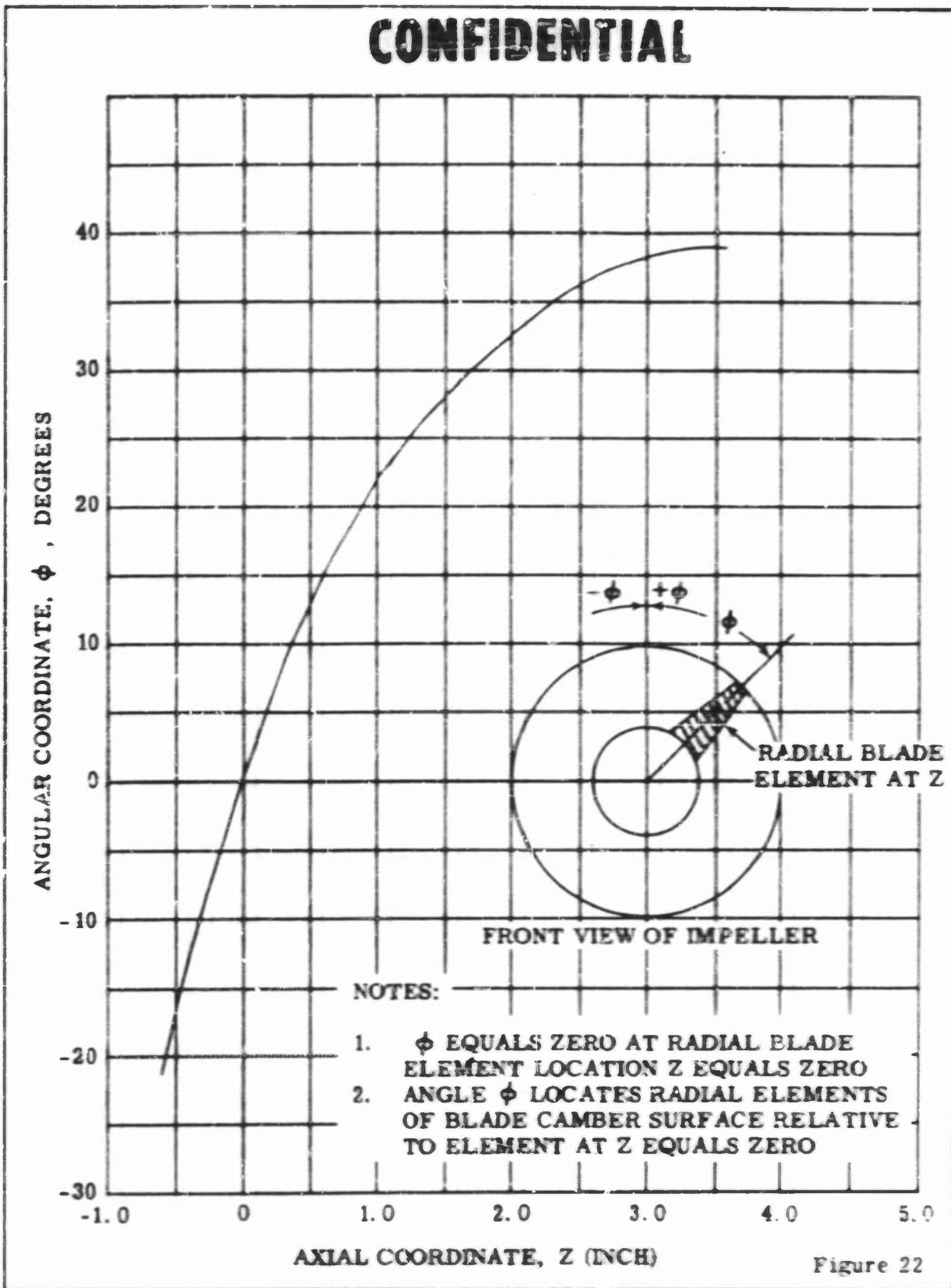


Figure 22

IMPELLER IV, BLADE ANGULAR COORDINATES

CONFIDENTIAL

CONFIDENTIAL

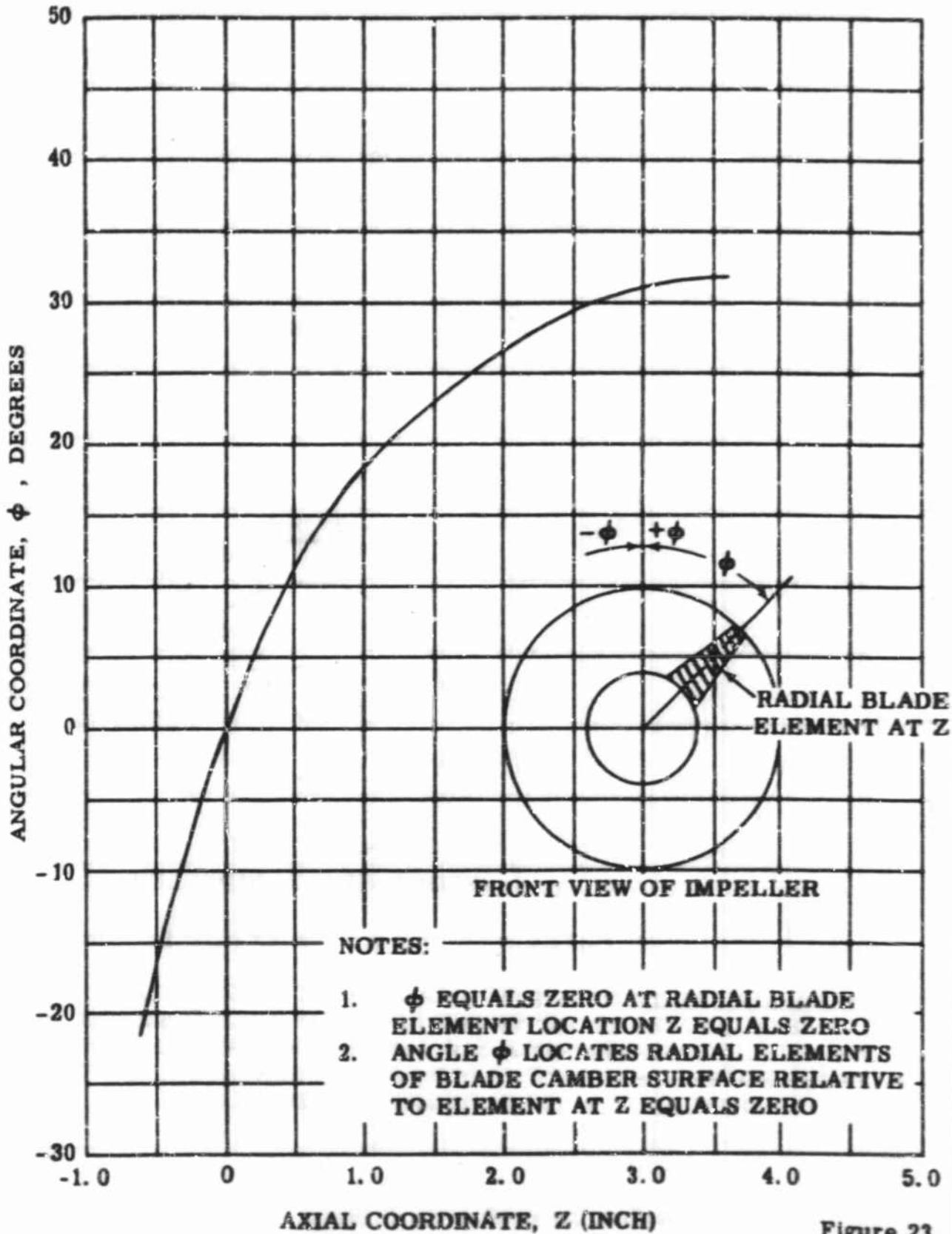
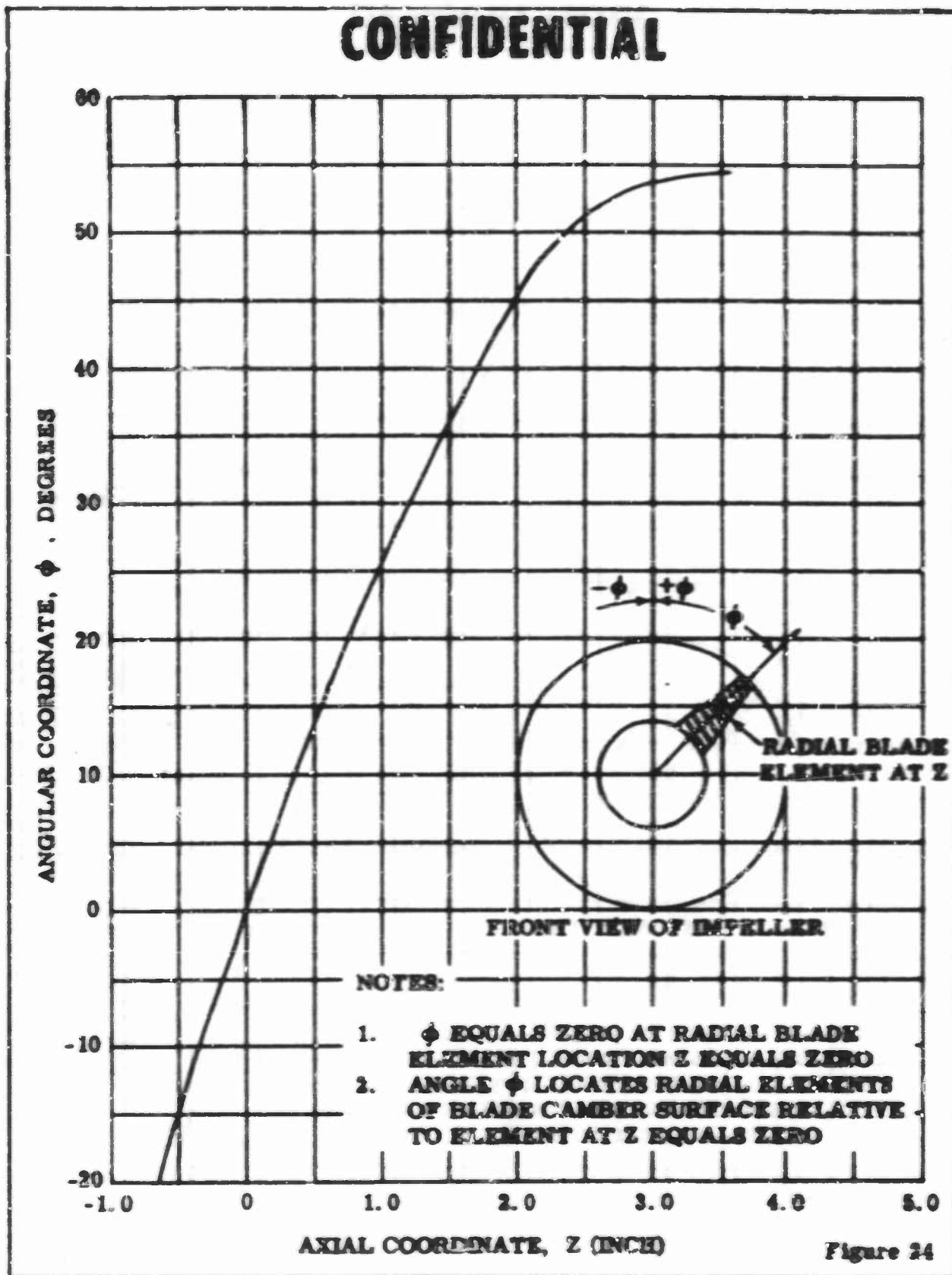


Figure 23

IMPELLER IVA, BLADE ANGULAR COORDINATES

CONFIDENTIAL

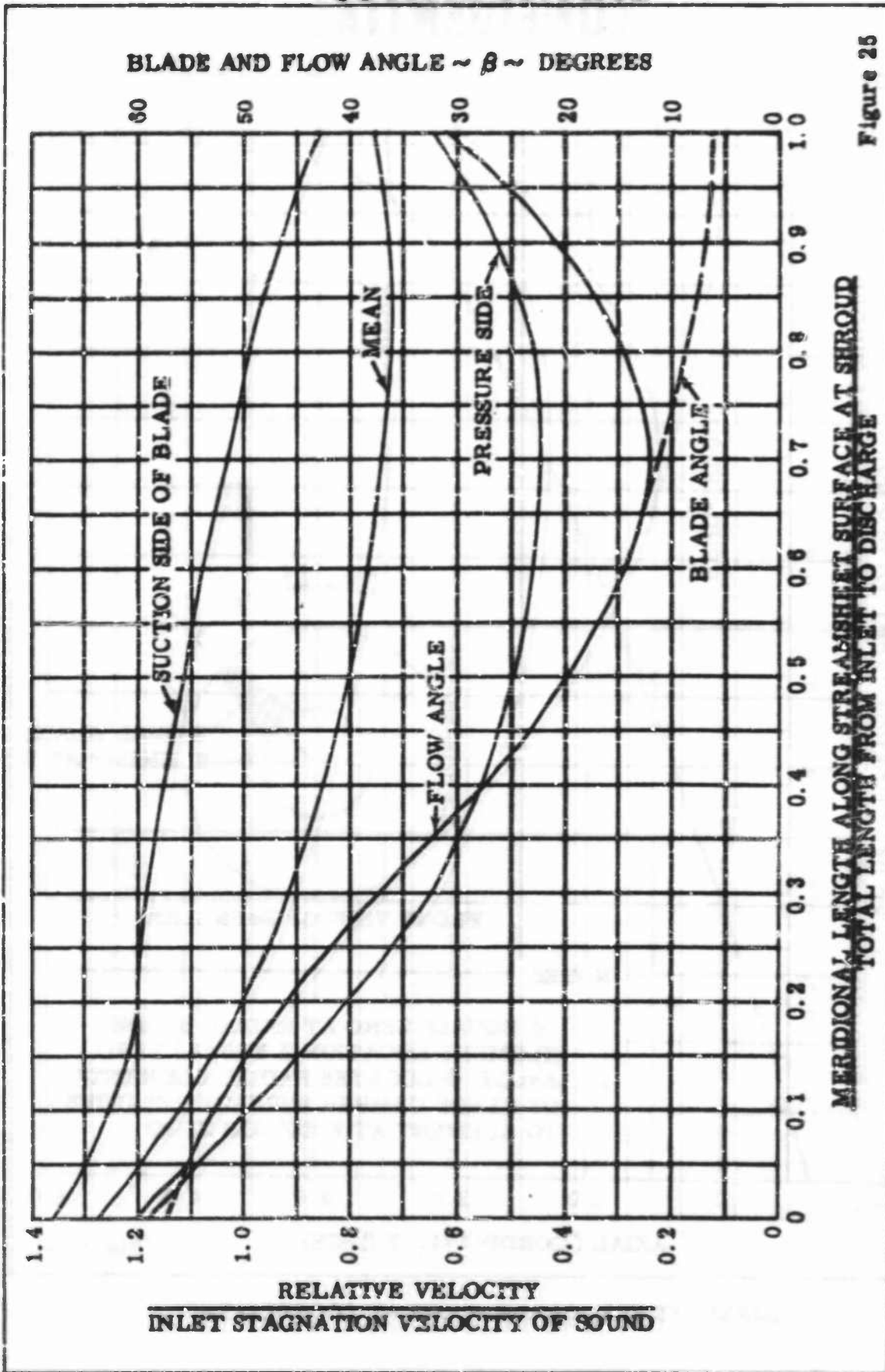
CONFIDENTIAL



IMPELLER IVB, BLADE ANGULAR COORDINATES

CONFIDENTIAL

CONFIDENTIAL



IMPELLER I, RELATIVE VELOCITY DISTRIBUTION, BLADE AND FLOW ANGLE
AT THE SHROUD STREAMSURFACE

CONFIDENTIAL

CONFIDENTIAL

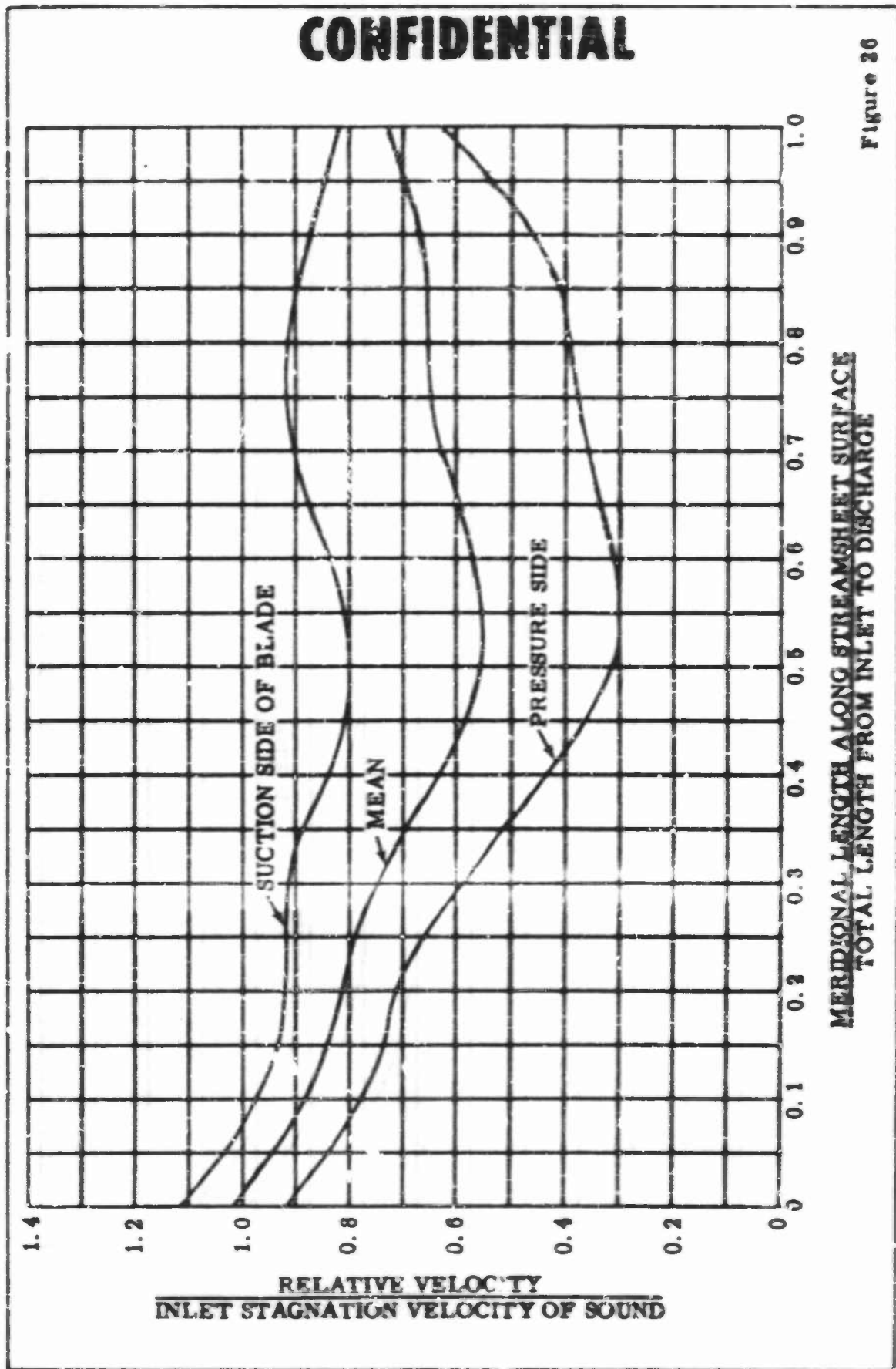


Figure 26

IMPELLER 1. RELATIVE VELOCITY DISTRIBUTION AT THE MEAN STREAMSURFACE

CONFIDENTIAL

CONFIDENTIAL

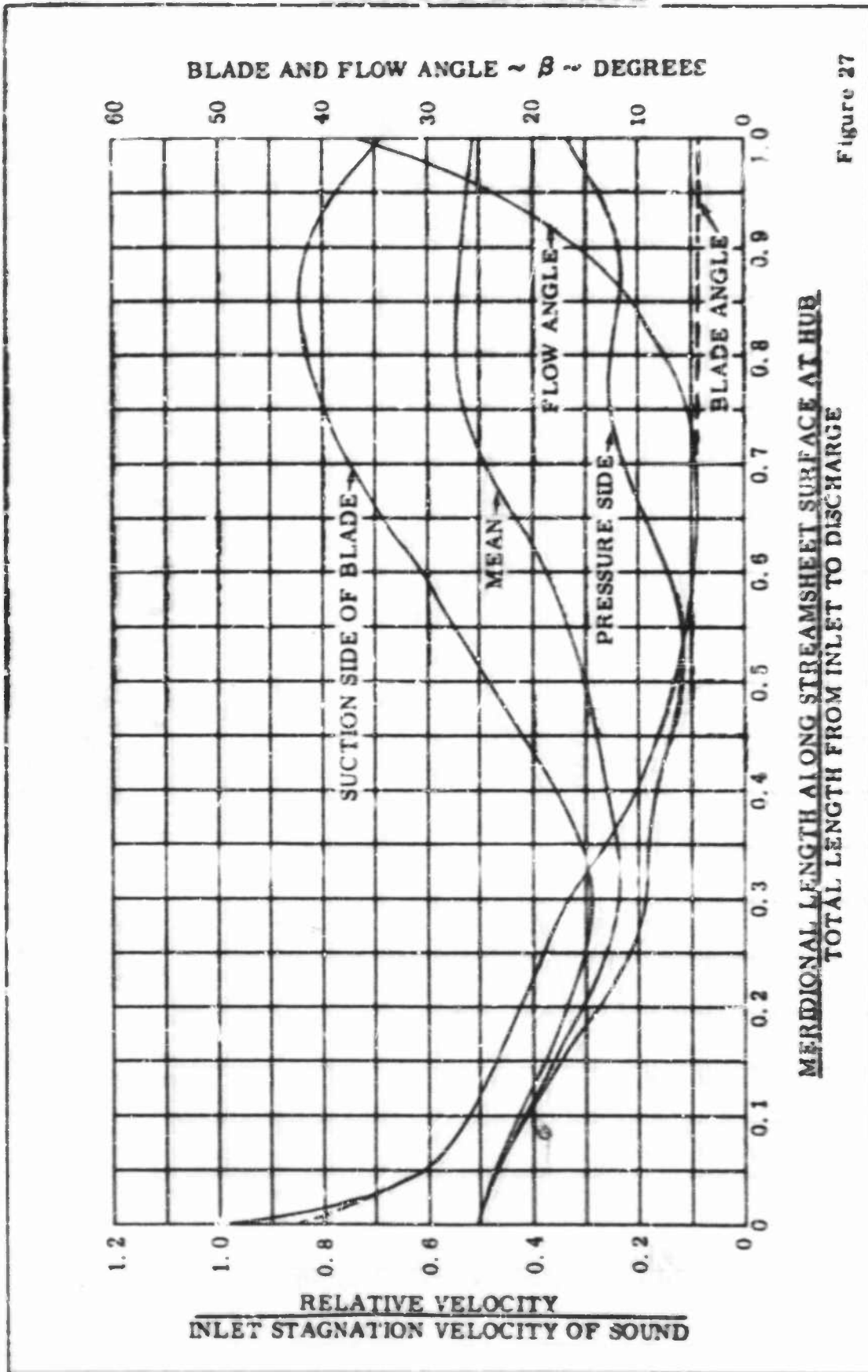


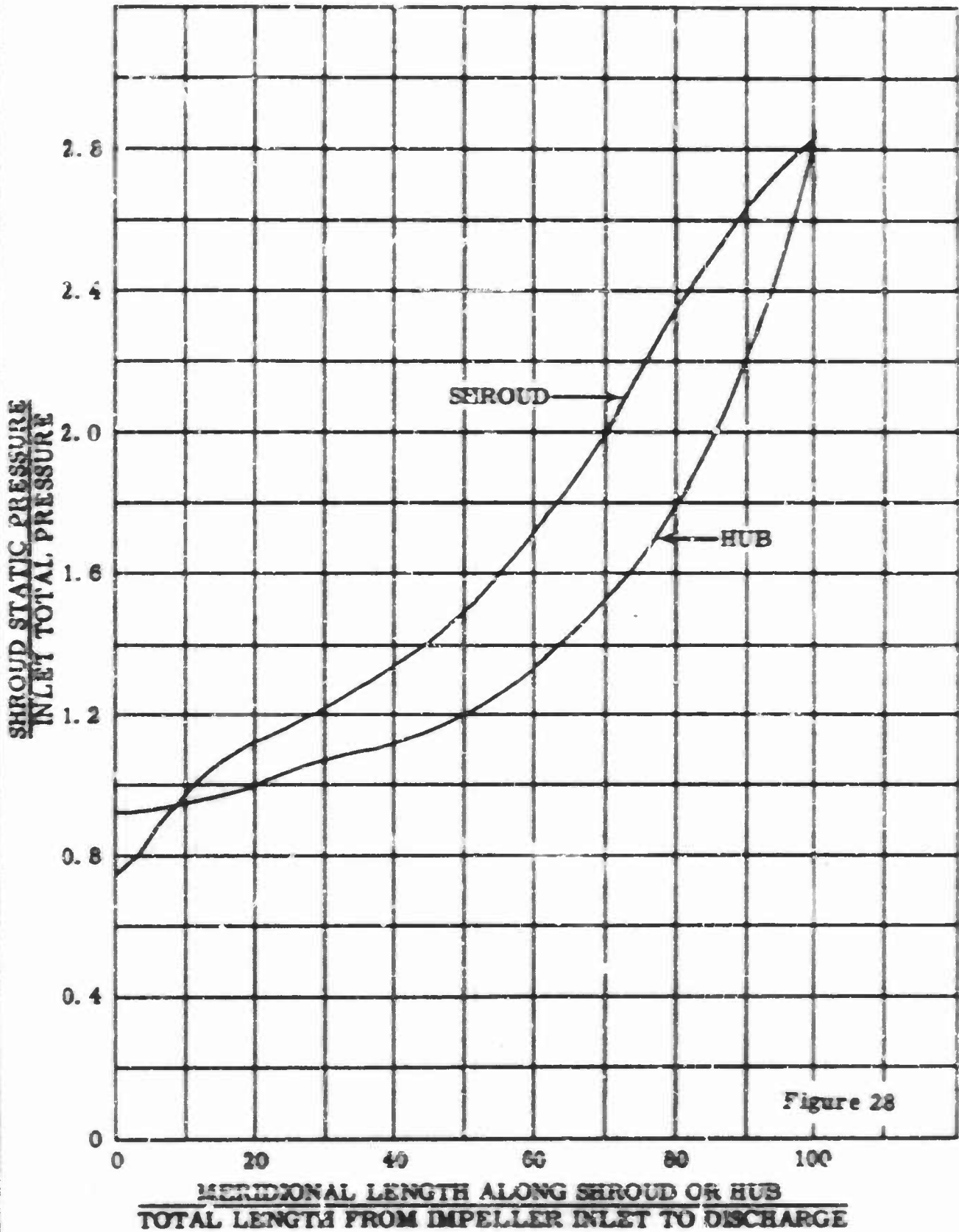
Figure 27

MERIDIONAL LENGTH ALONG STREAMSHEET SURFACE AT HUB
TOTAL LENGTH FROM INLET TO DISCHARGE

IMPELLER I, RELATIVE VELOCITY DISTRIBUTION, BLADE FLOW ANGLE AT THE HUB STREAMSURFACE

CONFIDENTIAL

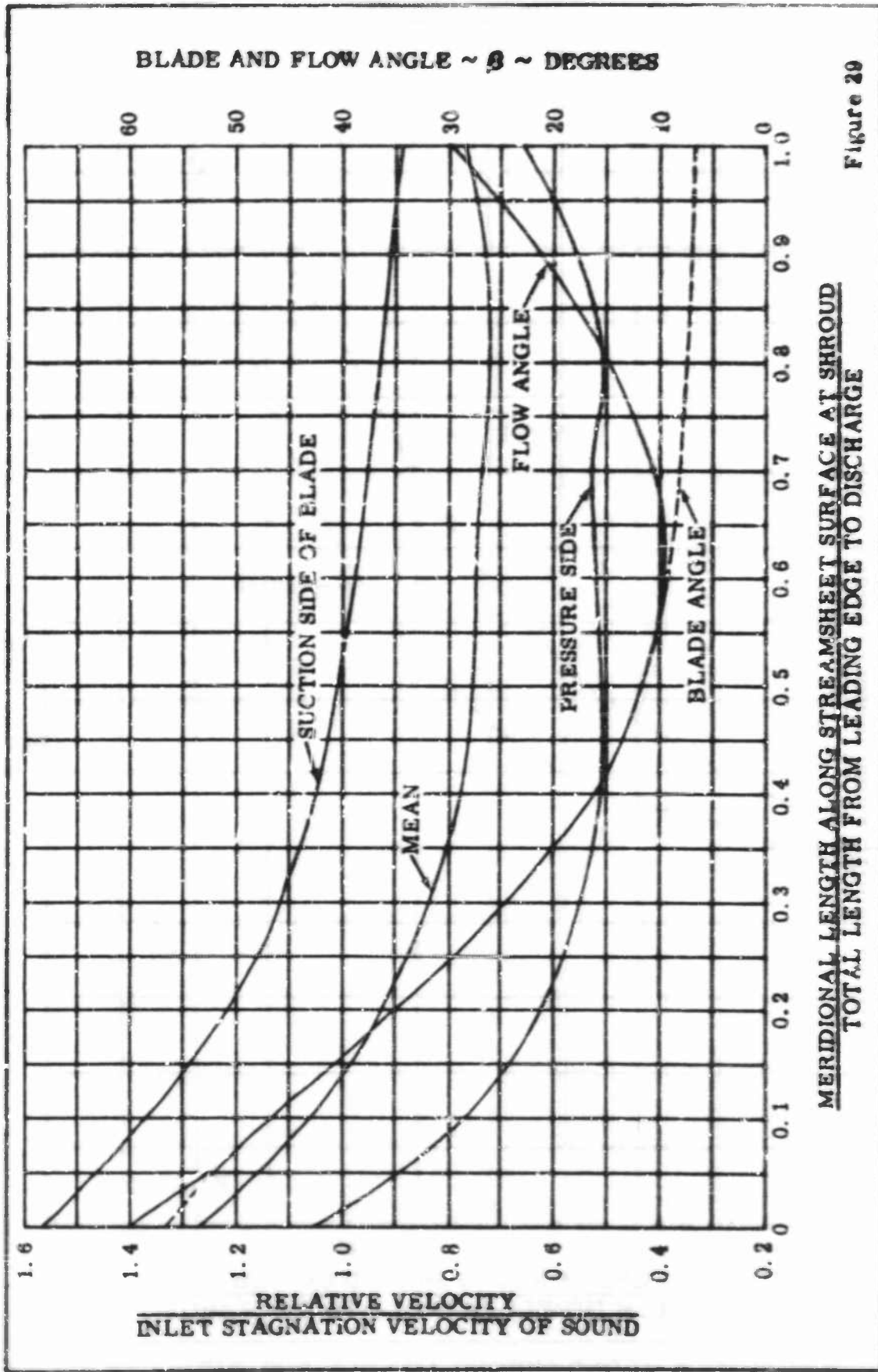
CONFIDENTIAL



PRESSURE DISTRIBUTION ALONG SHROUD AND HUB FOR IMPELLER I

CONFIDENTIAL

CONFIDENTIAL



IMPELLER IA, RELATIVE VELOCITY DISTRIBUTION, BLADE AND FLOW ANGLE
AT THE SHROUD STREAM SURFACE

CONFIDENTIAL

CONFIDENTIAL

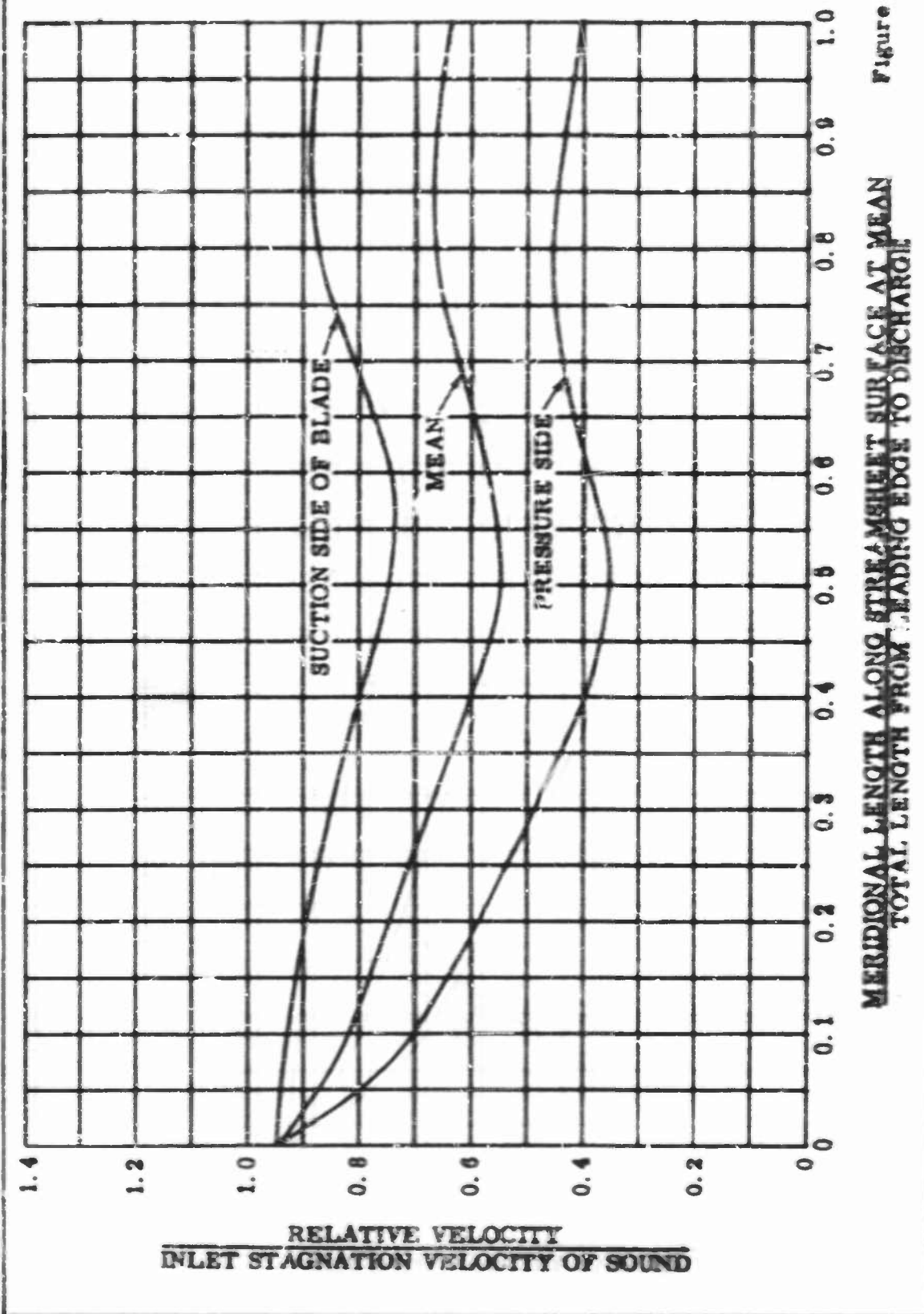


Figure 30

MERIDIONAL LENGTH ALONG STREAMSHEET SURFACE AT MEAN TOTAL LENGTH FROM LEADING EDGE TO DISCHARGE

IMPELLER 1A, RELATIVE VELOCITY DISTRIBUTION AT THE MEAN STREAM SURFACE

CONFIDENTIAL

CONFIDENTIAL

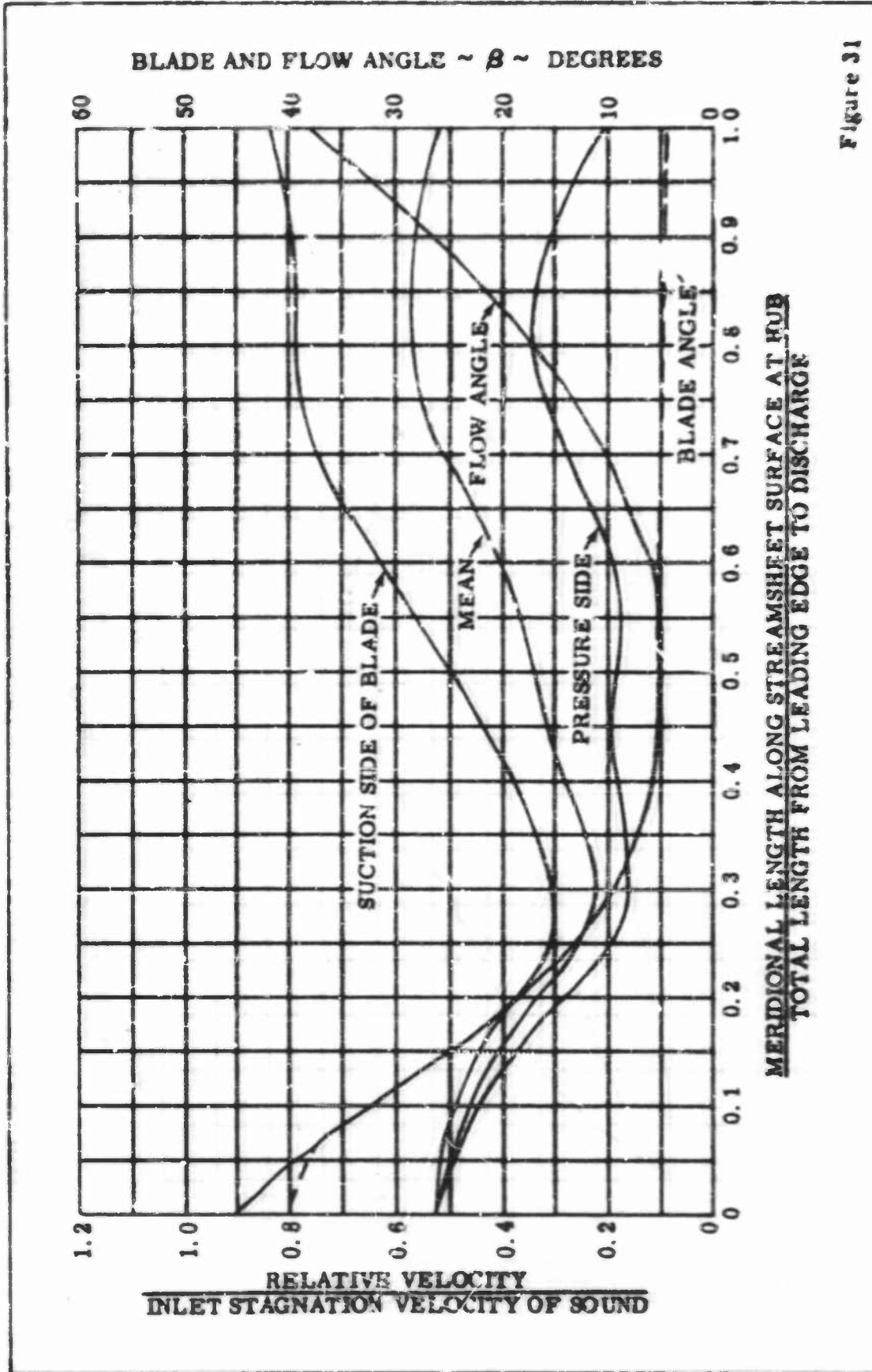
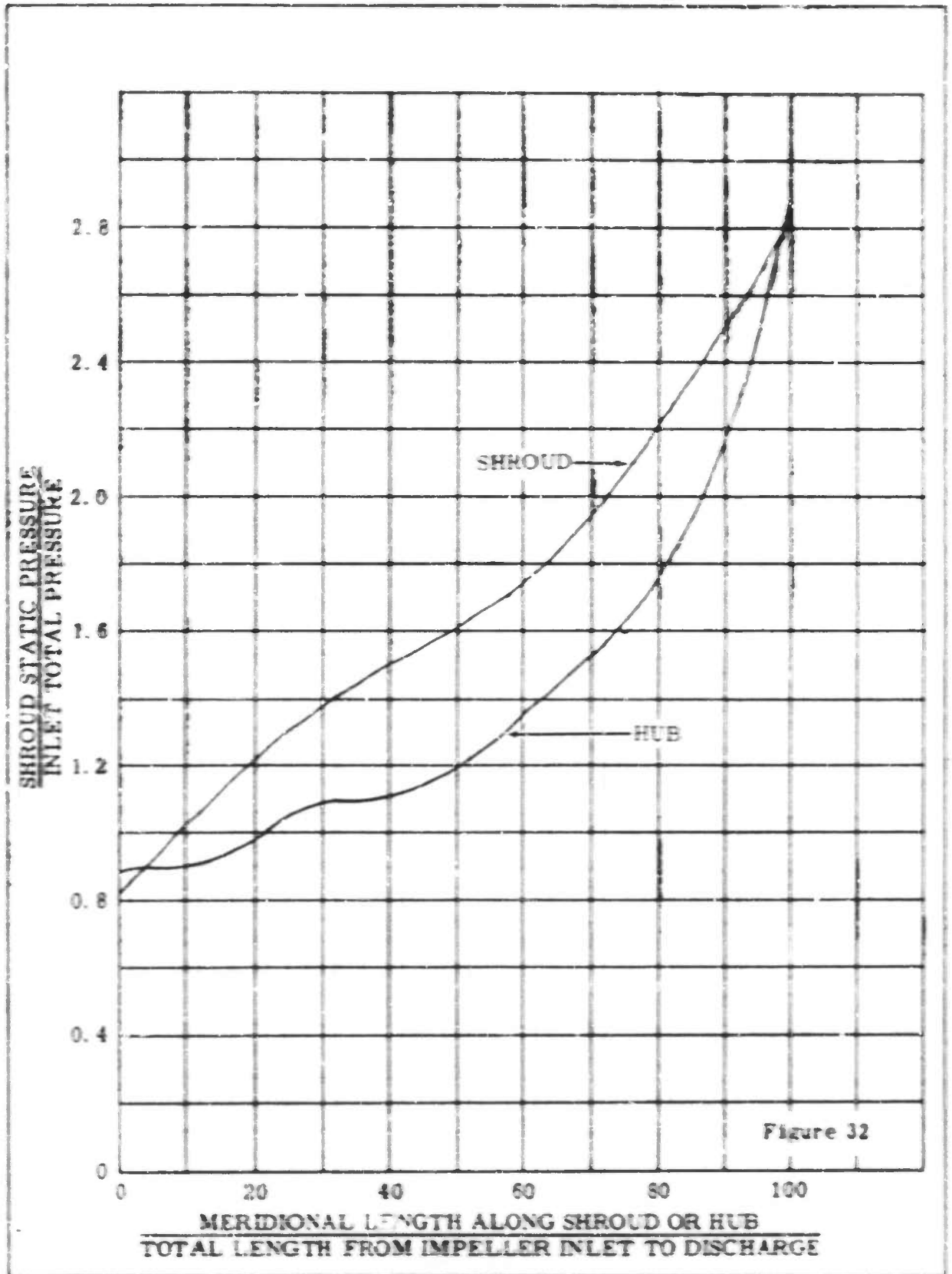


Figure 31

IMPELLER 1A, RELATIVE VELOCITY DISTRIBUTION, BLADE AND FLOW ANGLE
AT THE HUB STREAM SURFACE

CONFIDENTIAL

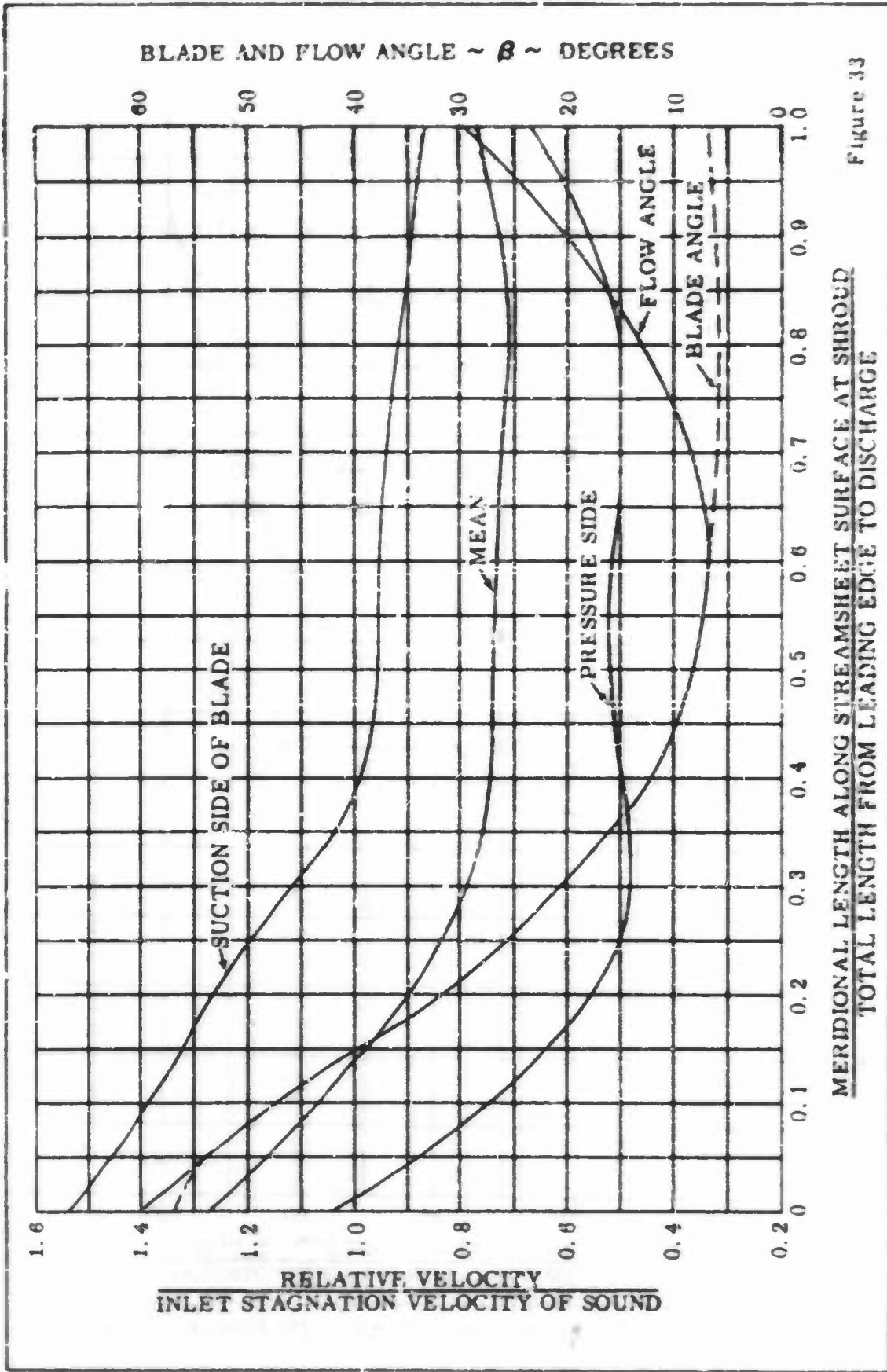
CONFIDENTIAL



PRESSURE DISTRIBUTION ALONG SHROUD AND HUB FOR IMPELLER 1A

CONFIDENTIAL

CONFIDENTIAL



CONFIDENTIAL

CONFIDENTIAL

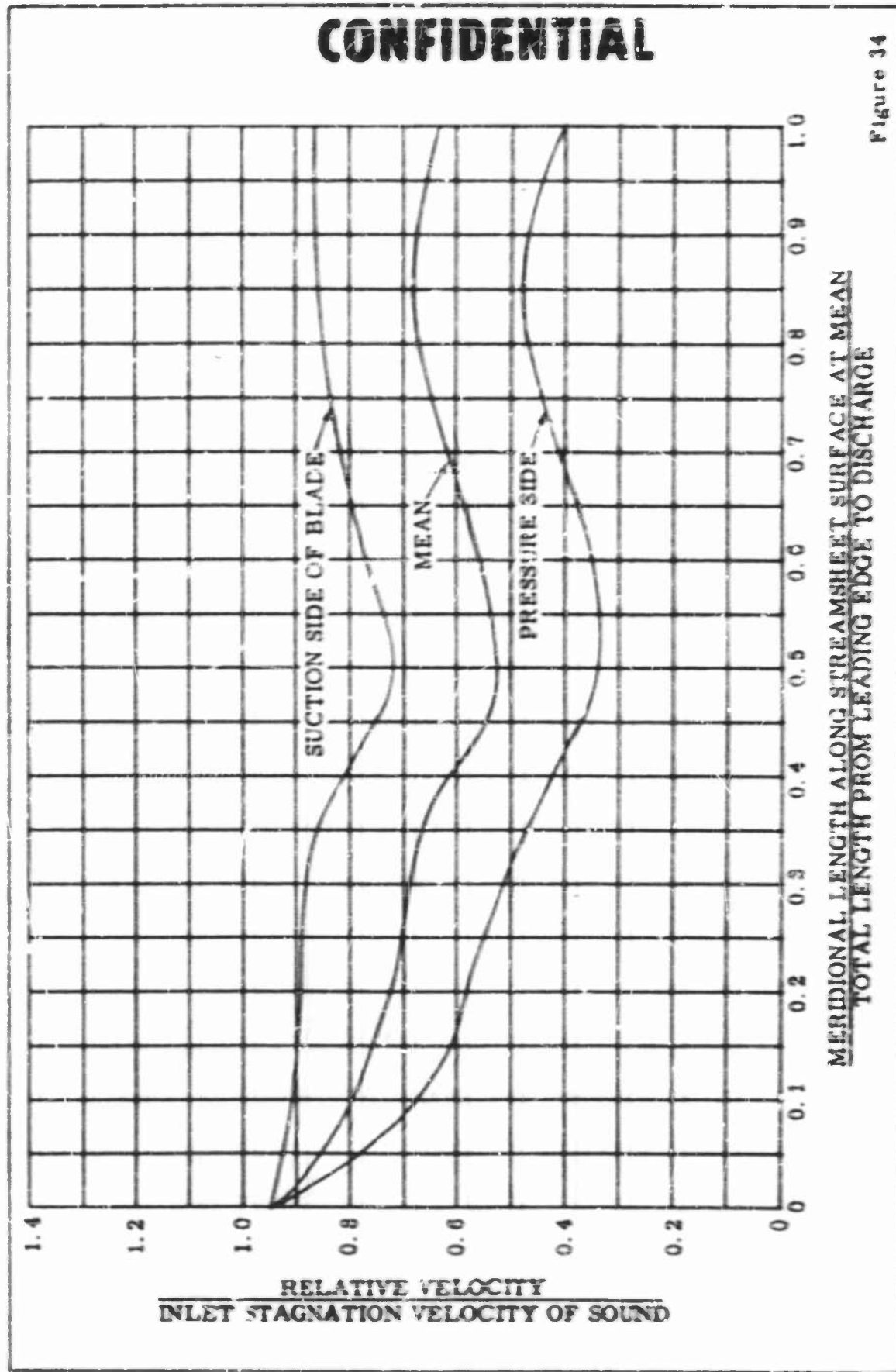


Figure 34

MERIDIONAL LENGTH ALONG STREAMSHEET SURFACE AT MEAN TOTAL LENGTH FROM LEADING EDGE TO DISCHARGE

IMPELLER IAA, RELATIVE VELOCITY DISTRIBUTION AT THE MEAN STREAM SURFACE

CONFIDENTIAL

CONFIDENTIAL

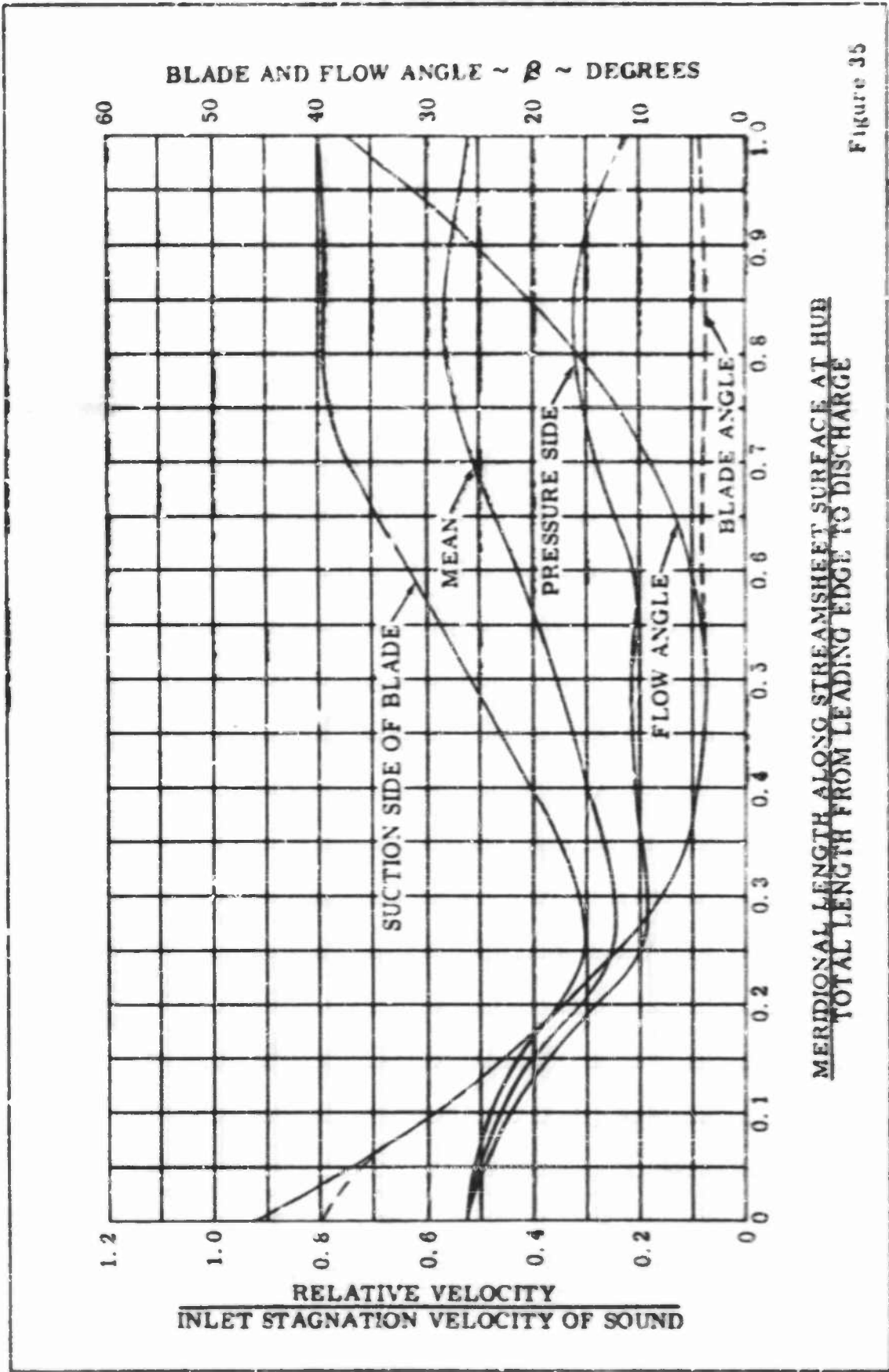


Figure 35

MERIDIONAL LENGTH ALONG STREAMSHEET SURFACE AT HUB
TOTAL LENGTH FROM LEADING EDGE TO DISCHARGE

IMPELLER IAS. RELATIVE VELOCITY DISTRIBUTION, BLADE AND FLOW ANGLE
AT THE HUB STREAM SURFACE

CONFIDENTIAL

CONFIDENTIAL

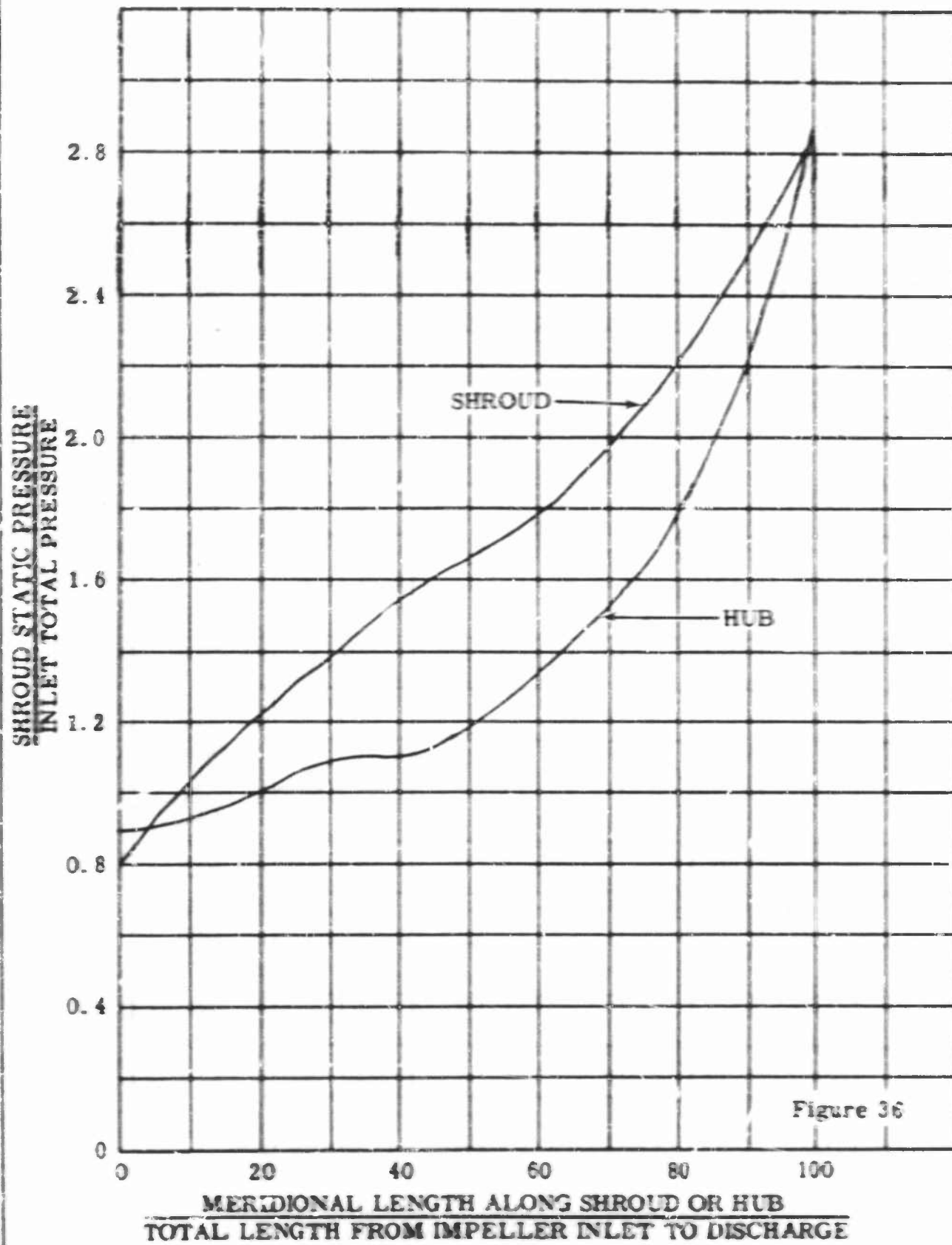
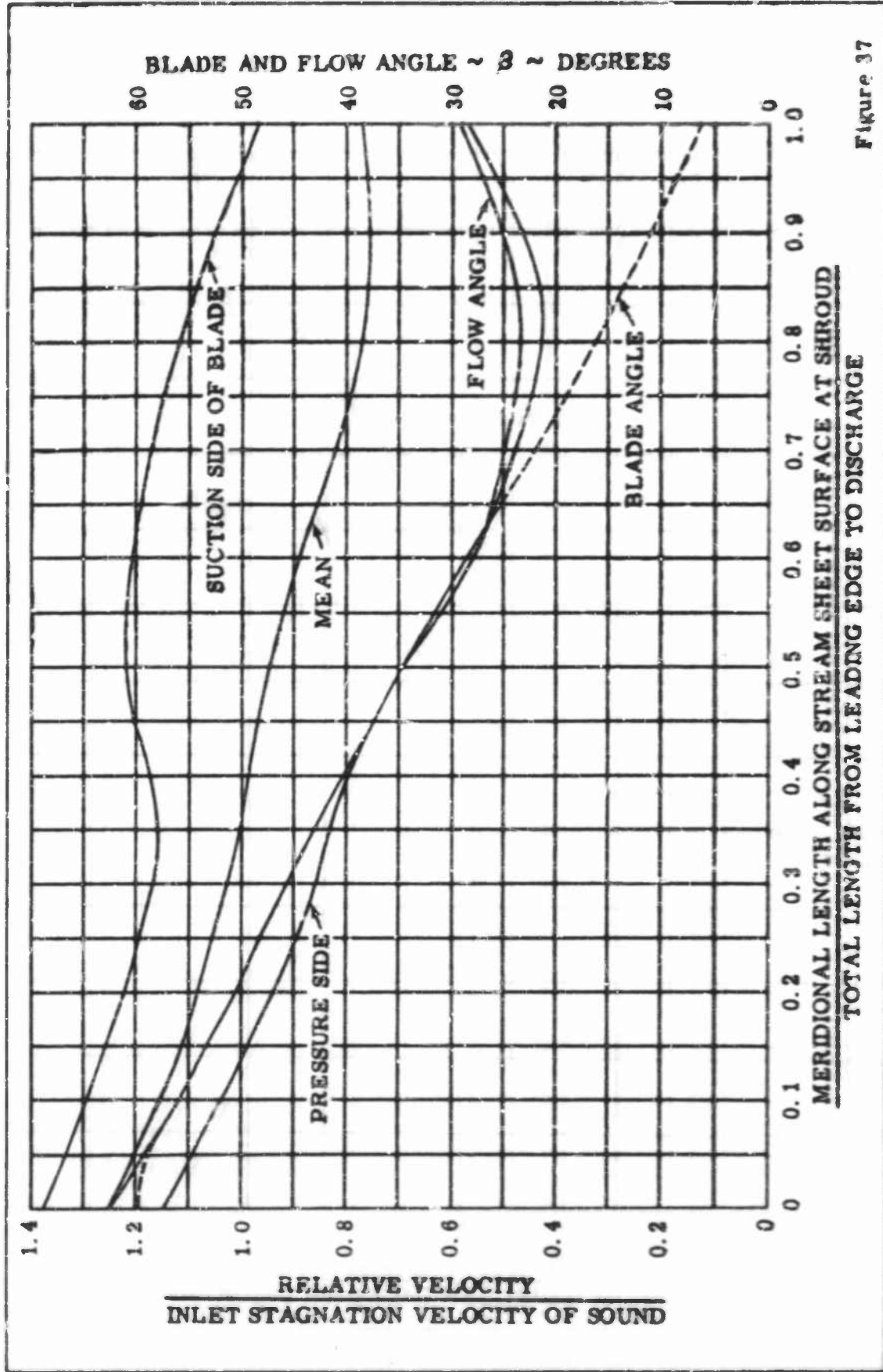


Figure 36

PRESSURE DISTRIBUTION ALONG SHROUD AND HUB FOR IMPELLER IAA

CONFIDENTIAL

CONFIDENTIAL



CONFIDENTIAL

CONFIDENTIAL

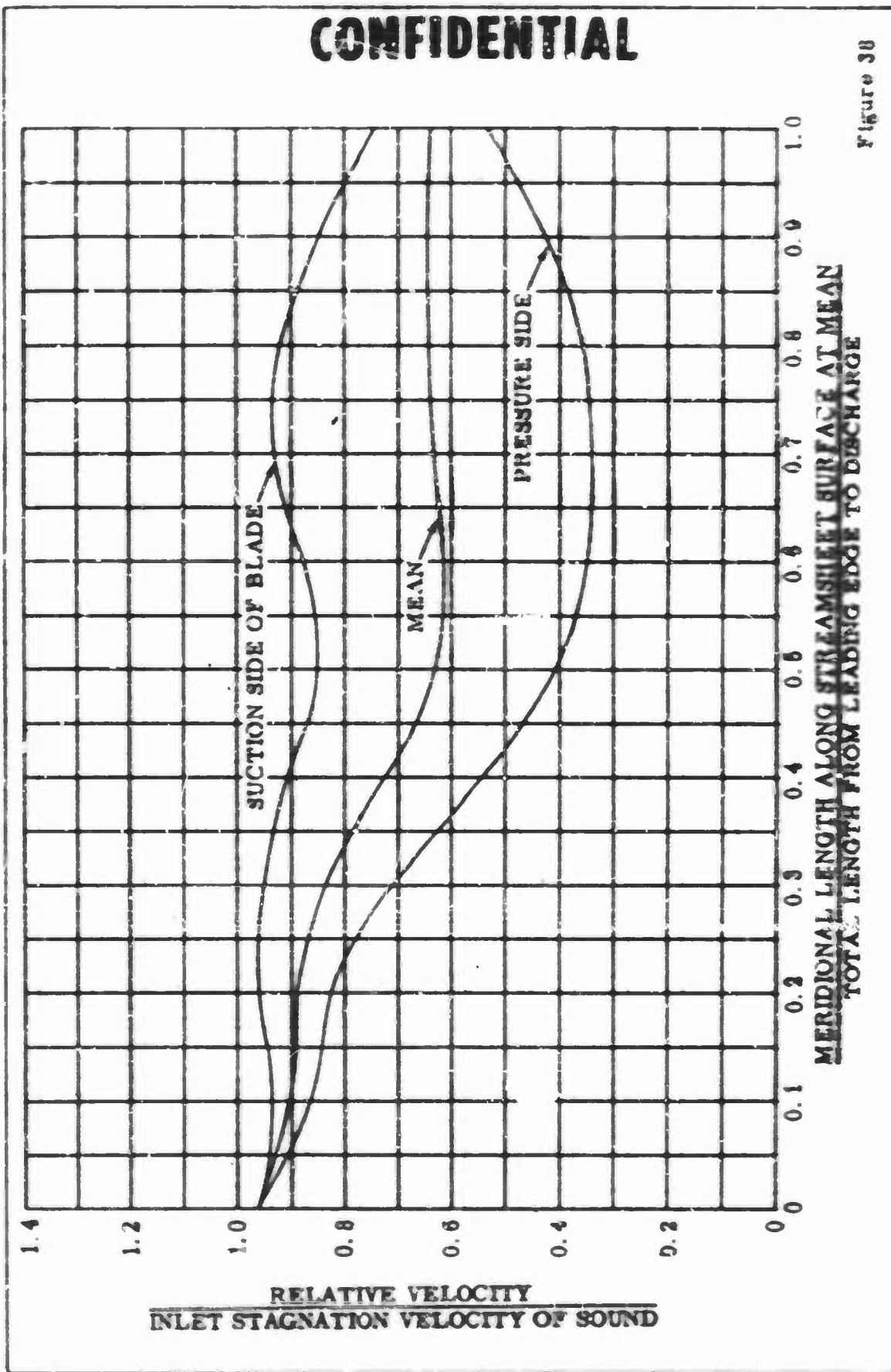


Figure 38

IMPELLER IB, RELATIVE VELOCITY DISTRIBUTION AT THE MEAN STREAM SURFACE

CONFIDENTIAL

CONFIDENTIAL

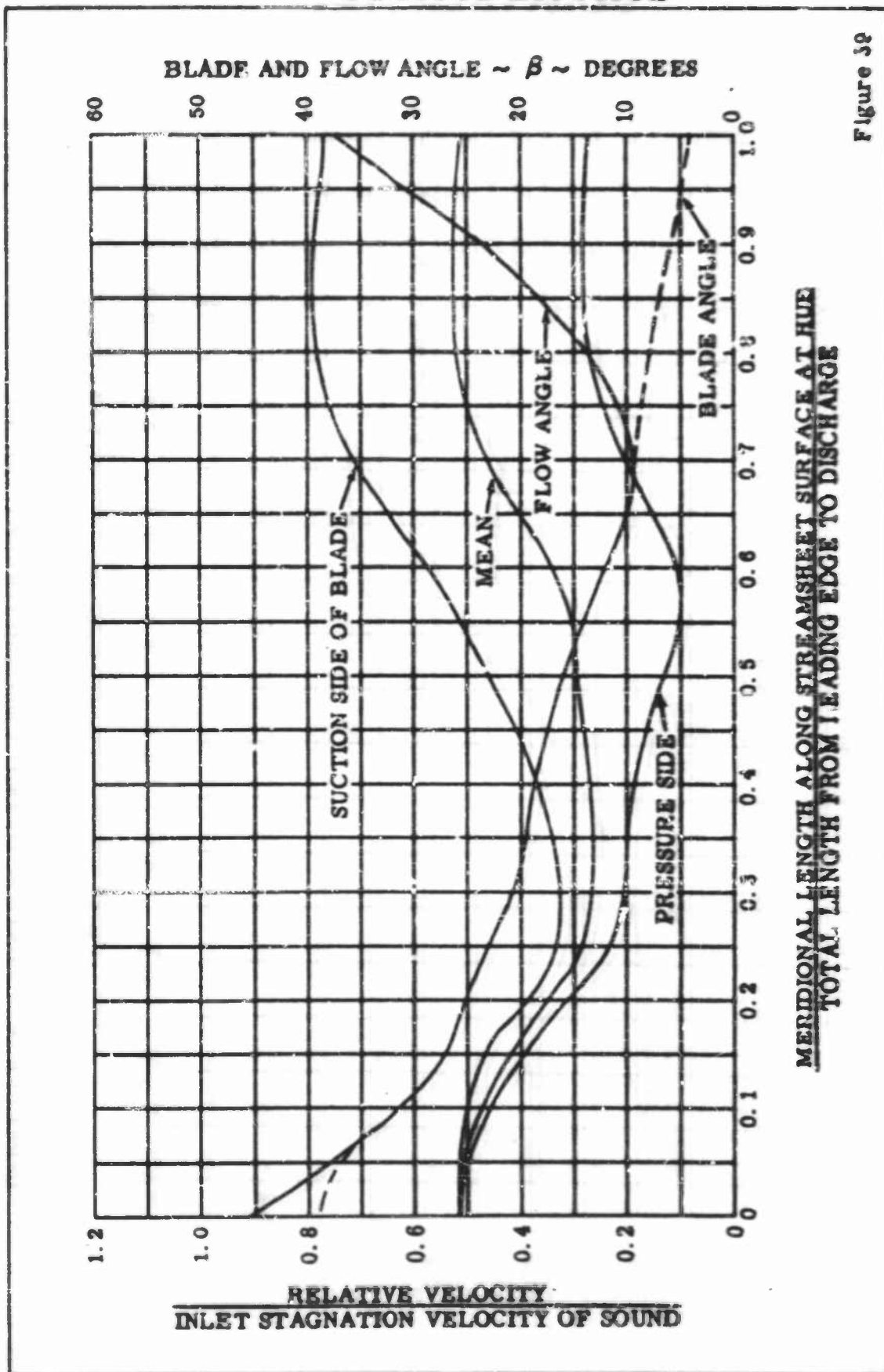


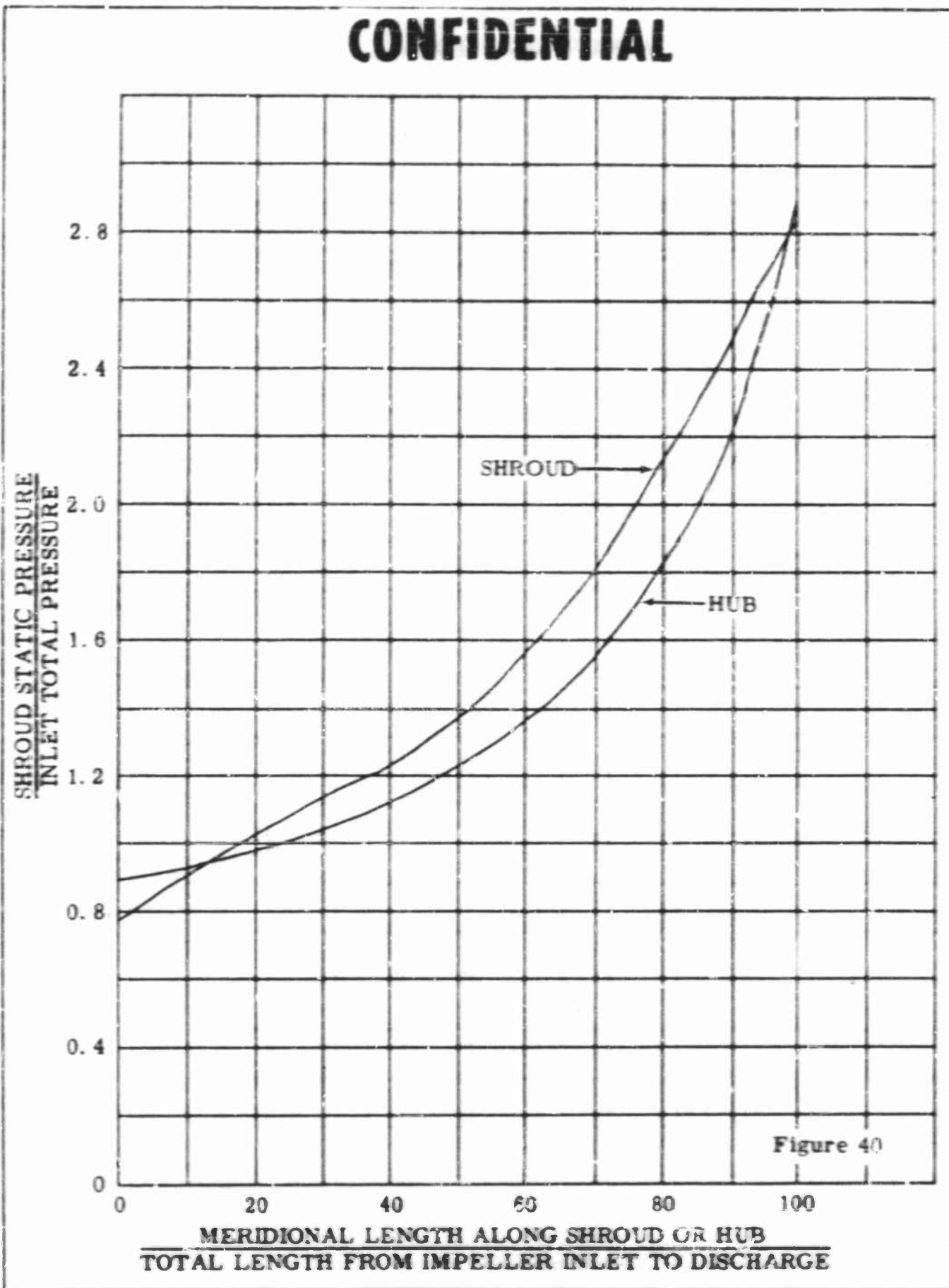
Figure 38

**MERIDIONAL LENGTH ALONG STREAMSHEET SURFACE AT HUB
TOTAL LENGTH FROM LEADING EDGE TO DISCHARGE**

**IMPELLER IB, RELATIVE VELOCITY DISTRIBUTION, BLADE AND FLOW ANGLES
AT THE HUB STREAM SURFACE**

CONFIDENTIAL

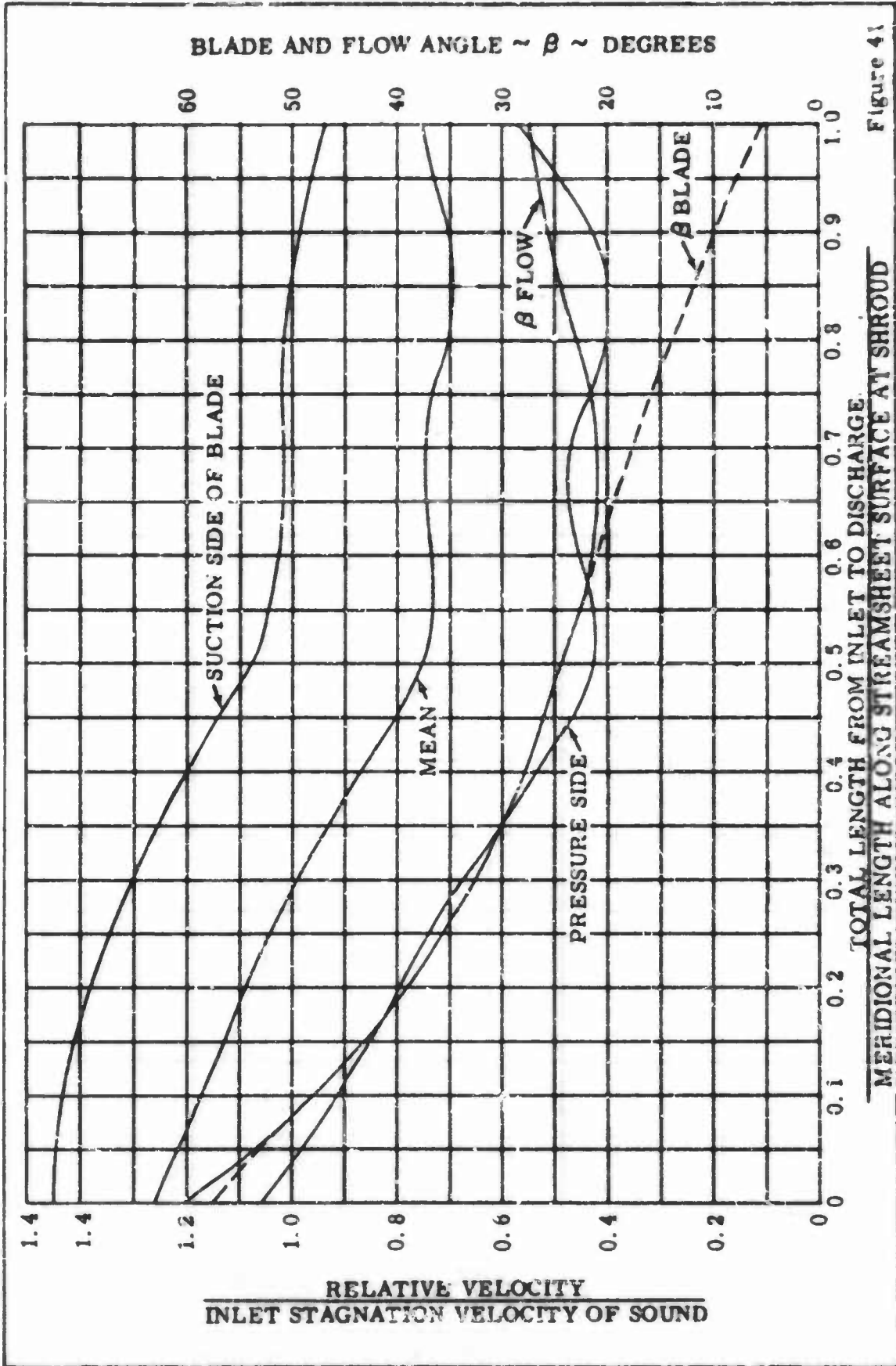
CONFIDENTIAL



PRESSURE DISTRIBUTION ALONG SHROUD AND HUB FOR IMPELLER IB

CONFIDENTIAL

CONFIDENTIAL



CONFIDENTIAL

CONFIDENTIAL

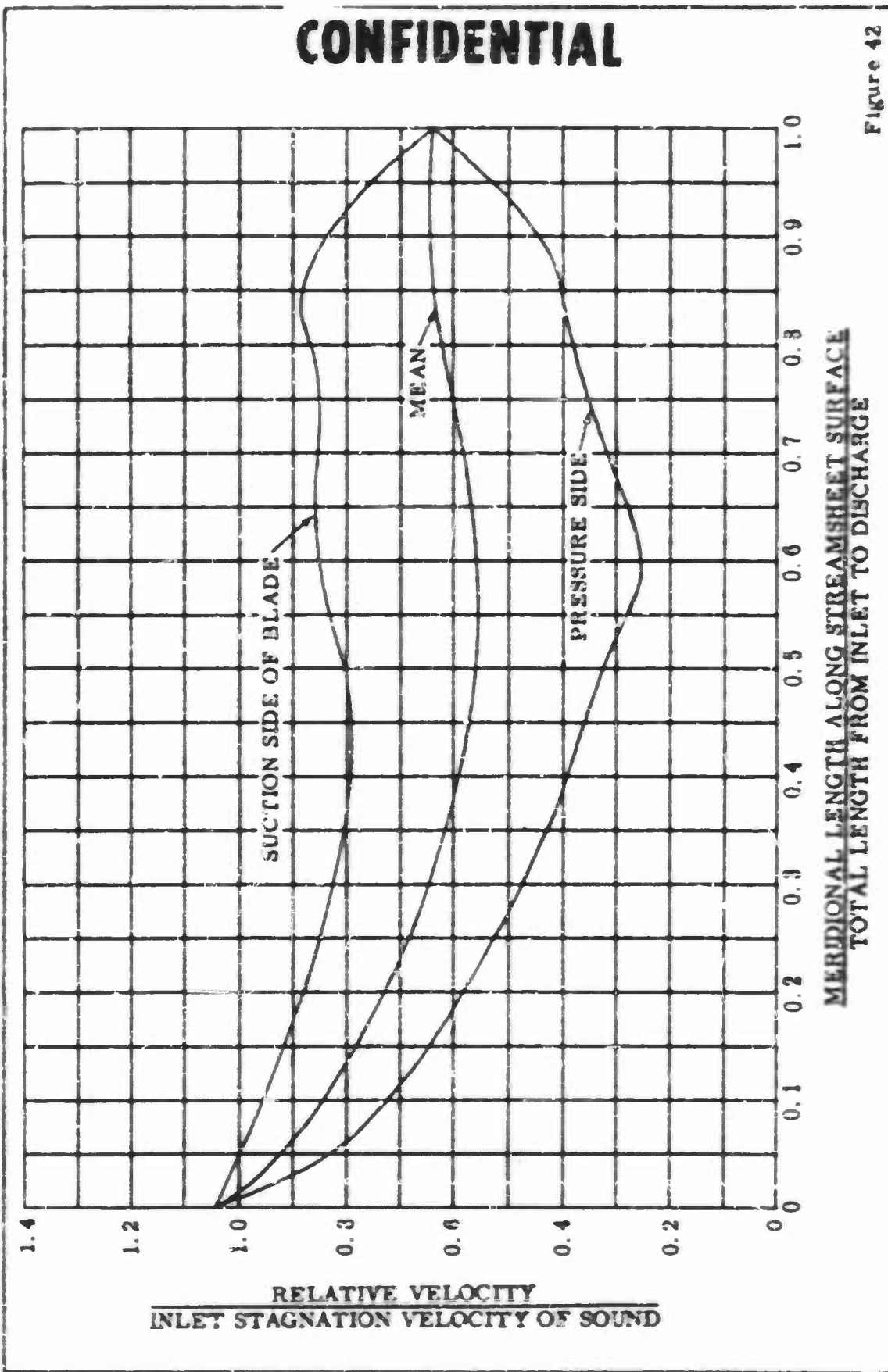
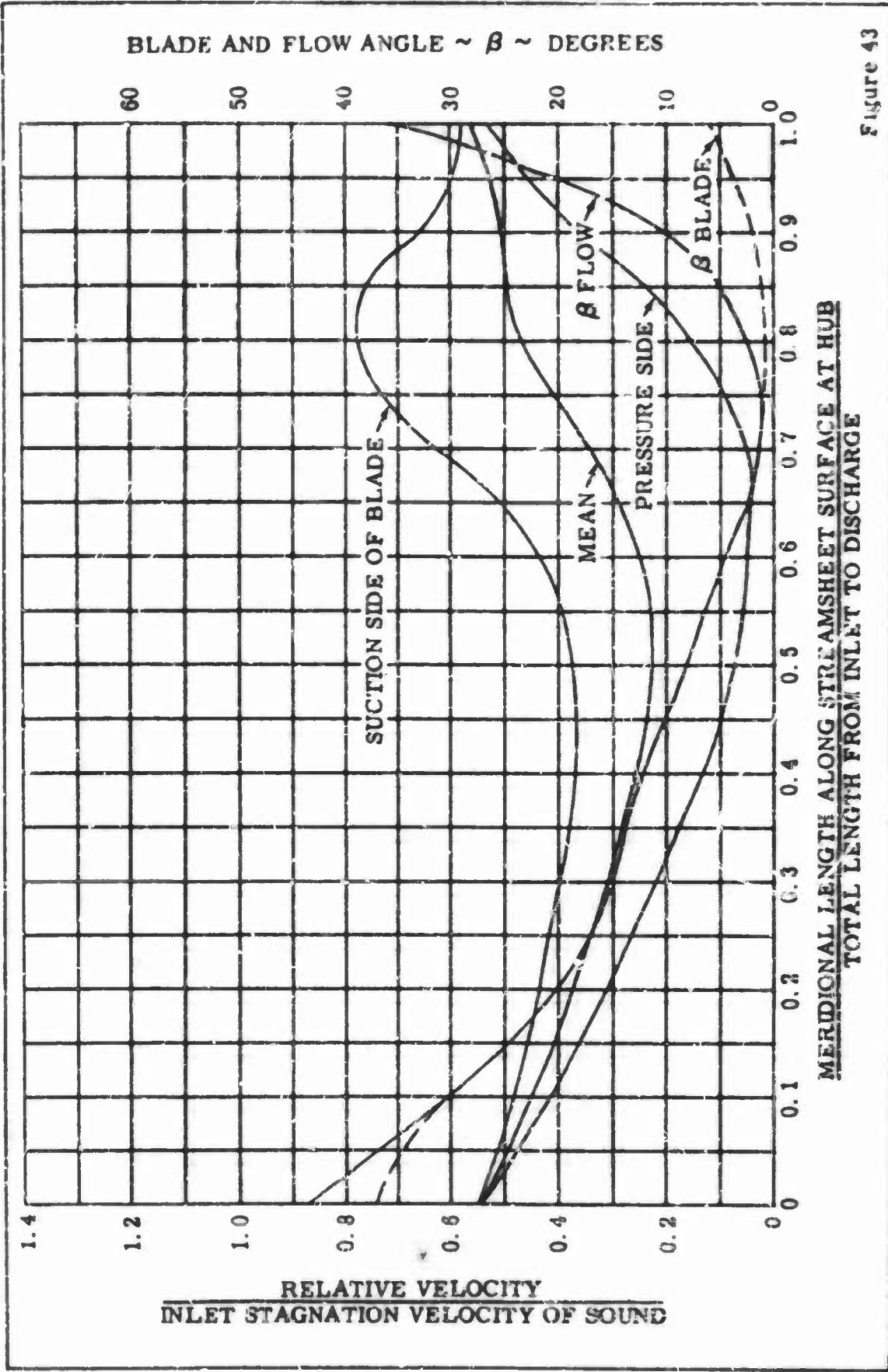


Figure 42

IMPELLER II, RELATIVE VELOCITY DISTRIBUTION AT THE MEAN STREAMSURFACE

CONFIDENTIAL

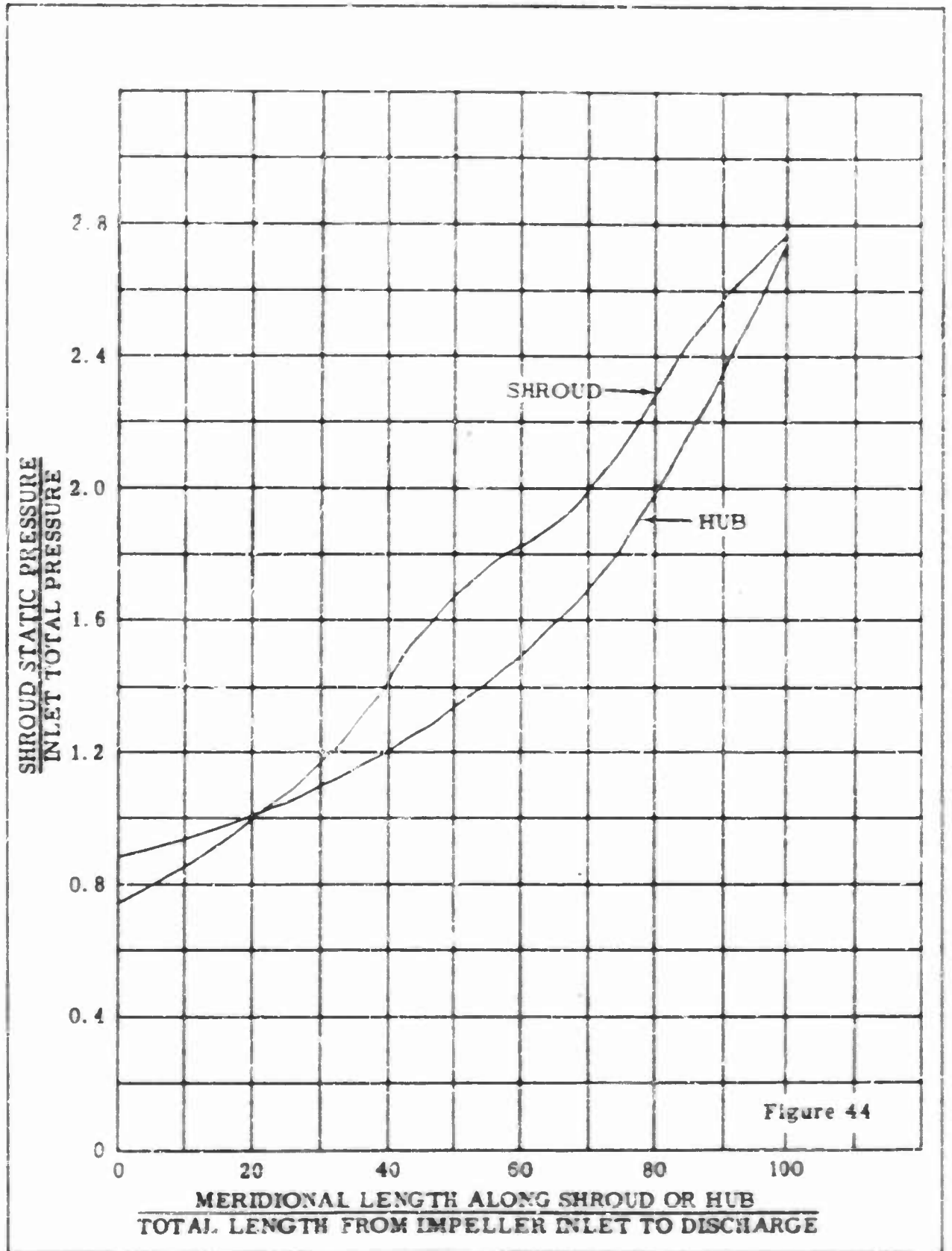
CONFIDENTIAL



IMPELLER II, RELATIVE VELOCITY DISTRIBUTION, BLADE AND FLOW ANGLE AT THE HUB STREAMSURFACE

CONFIDENTIAL

CONFIDENTIAL



PRESSURE DISTRIBUTION ALONG SHROUD AND HUB FOR IMPELLER II

CONFIDENTIAL

CONFIDENTIAL

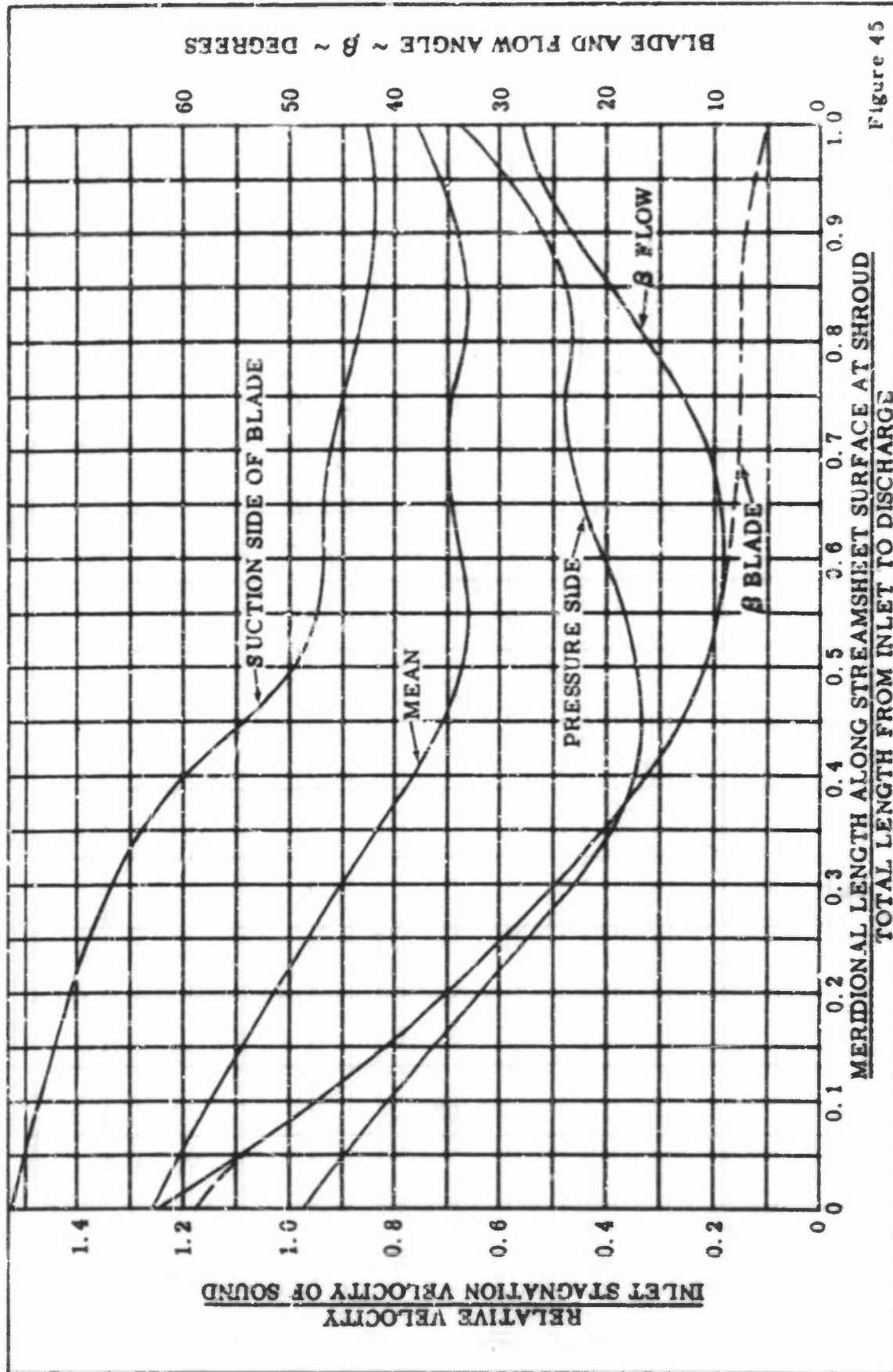
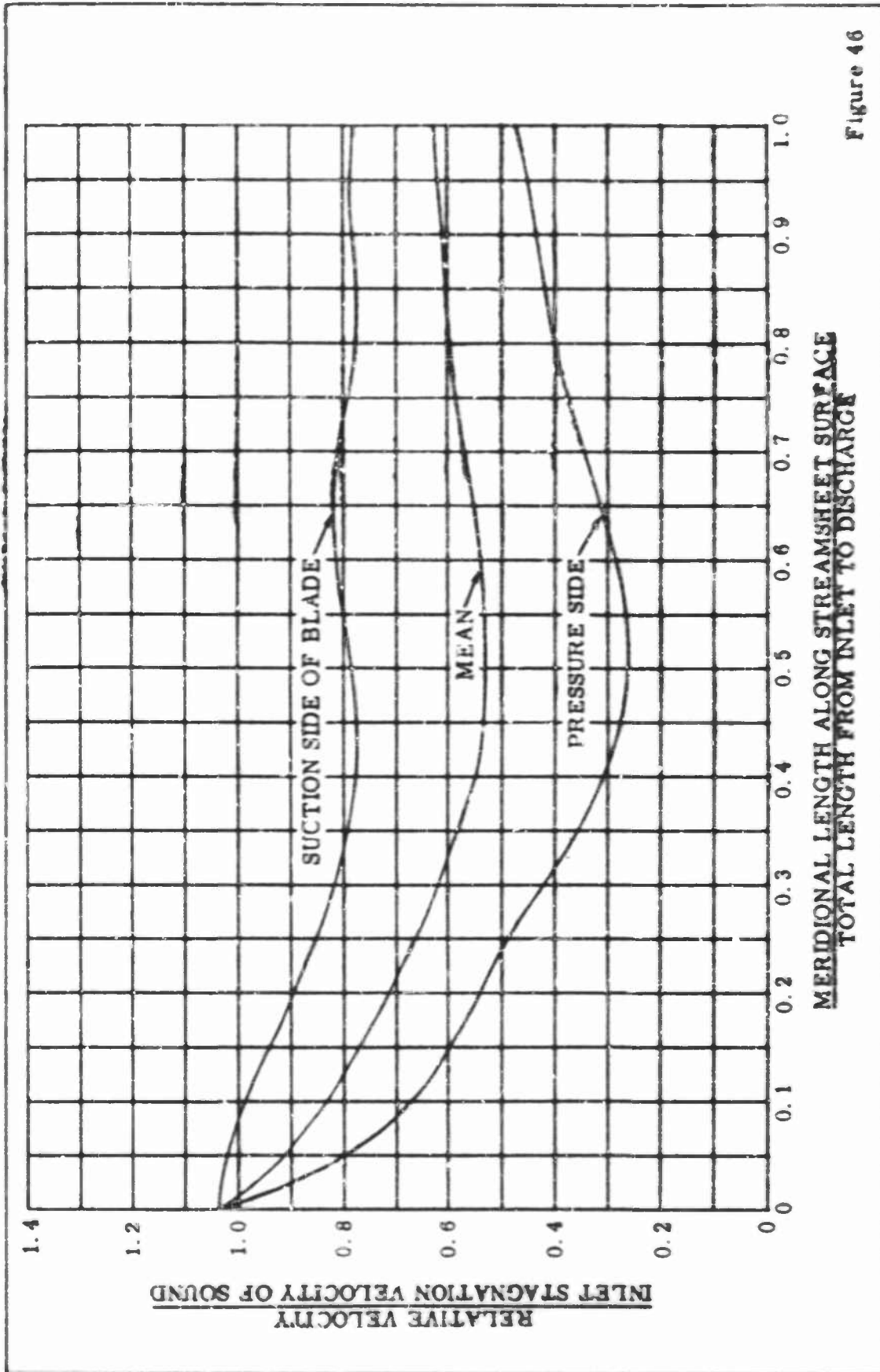


Figure 45

IMPELLER DA, RELATIVE VELOCITY DISTRIBUTION, BLADE AND FLOW ANGLE AT THE SHROUD STREAMSURFACE

CONFIDENTIAL

CONFIDENTIAL



IMPELLER IIA, RELATIVE VELOCITY DISTRIBUTION AT THE MEAN STREAMSURFACE

CONFIDENTIAL

CONFIDENTIAL

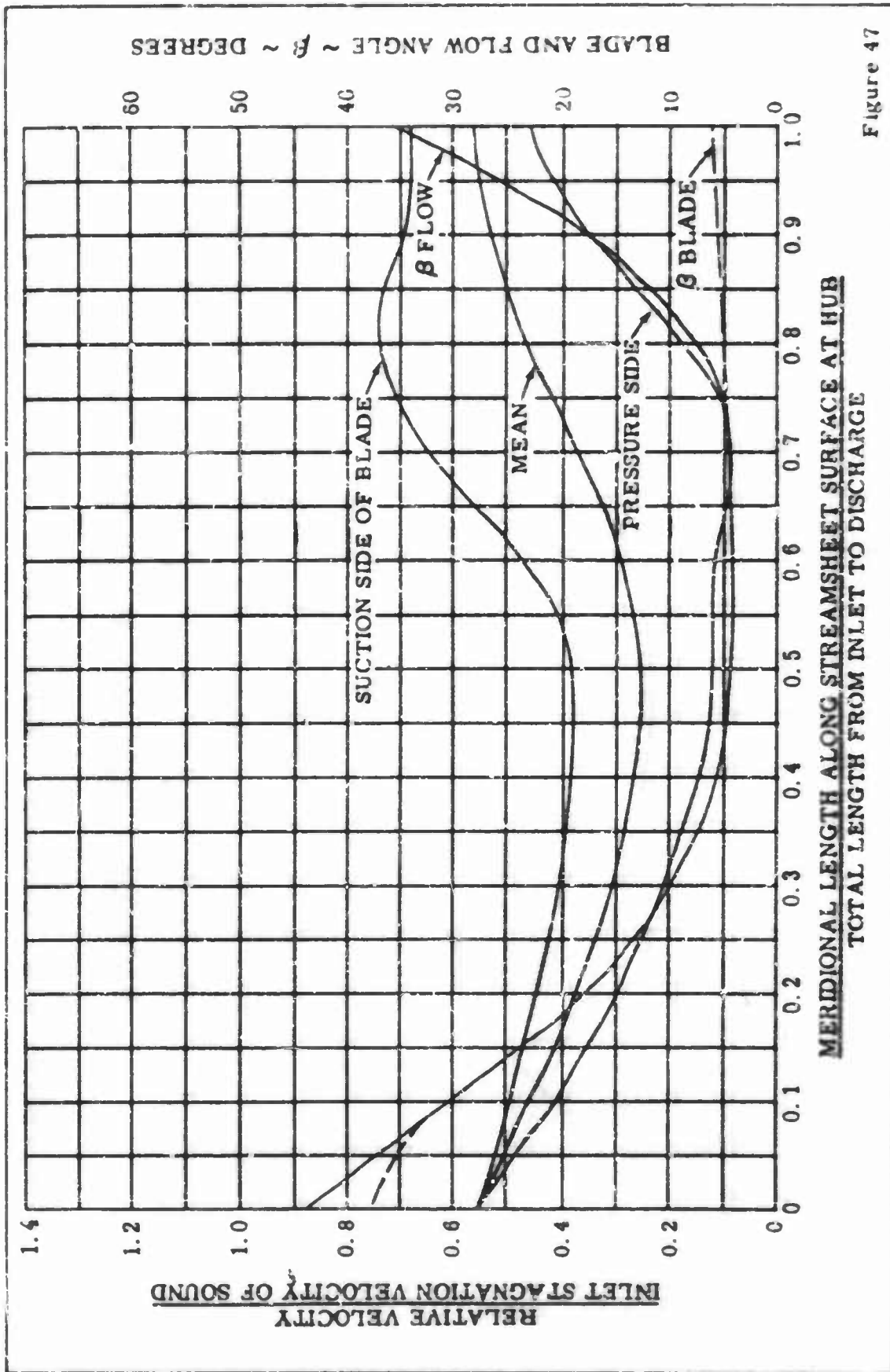
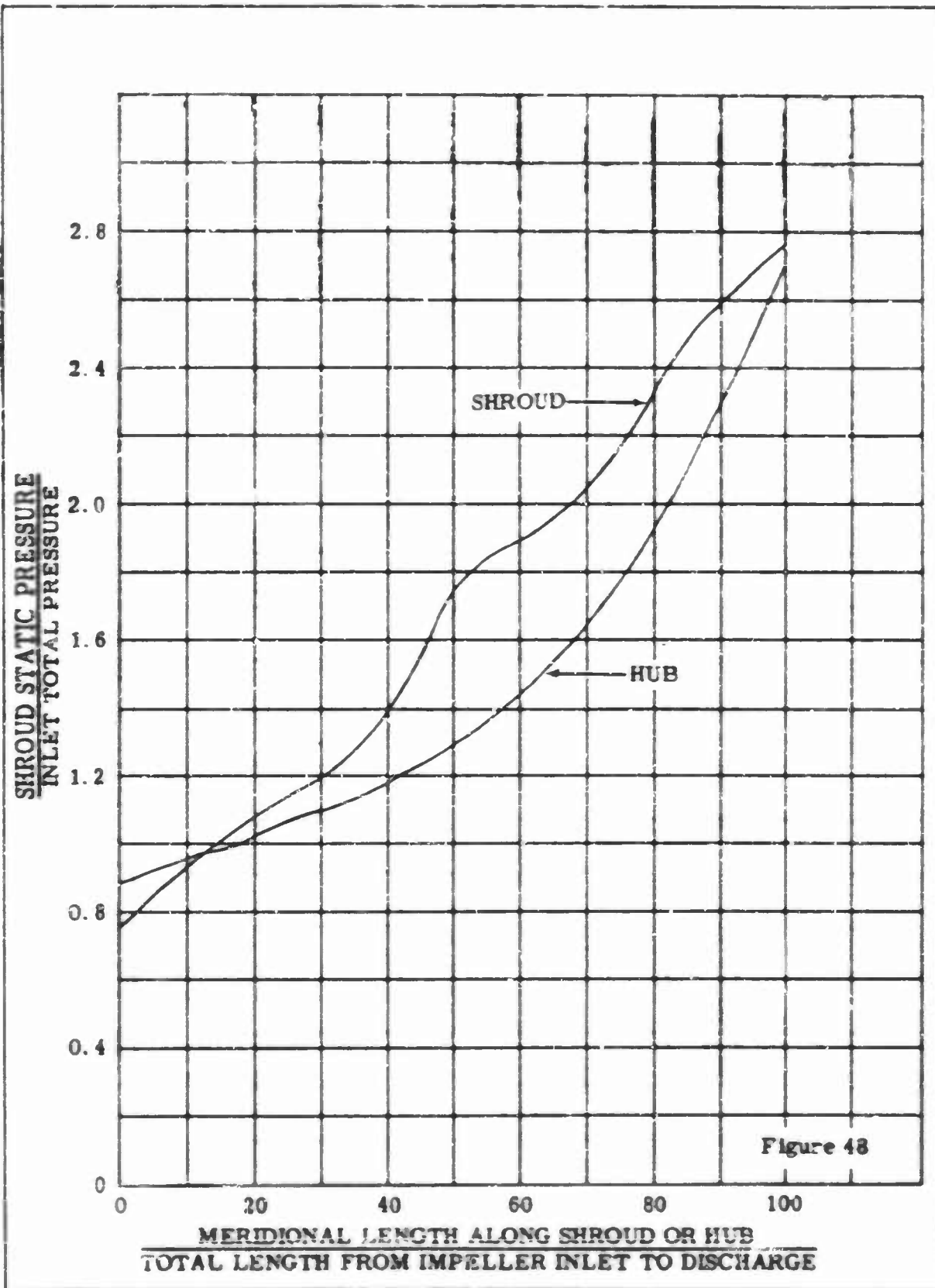


Figure 47

IMPELLER IIA, RELATIVE VELOCITY DISTRIBUTION, BLADE AND FLOW ANGLE AT THE HUB STREAMSURFACE

CONFIDENTIAL

CONFIDENTIAL



PRESSURE DISTRIBUTION ALONG SHROUD AND HUB FOR IMPELLER IIA

WADC TR56-589

89

CONFIDENTIAL

CONFIDENTIAL

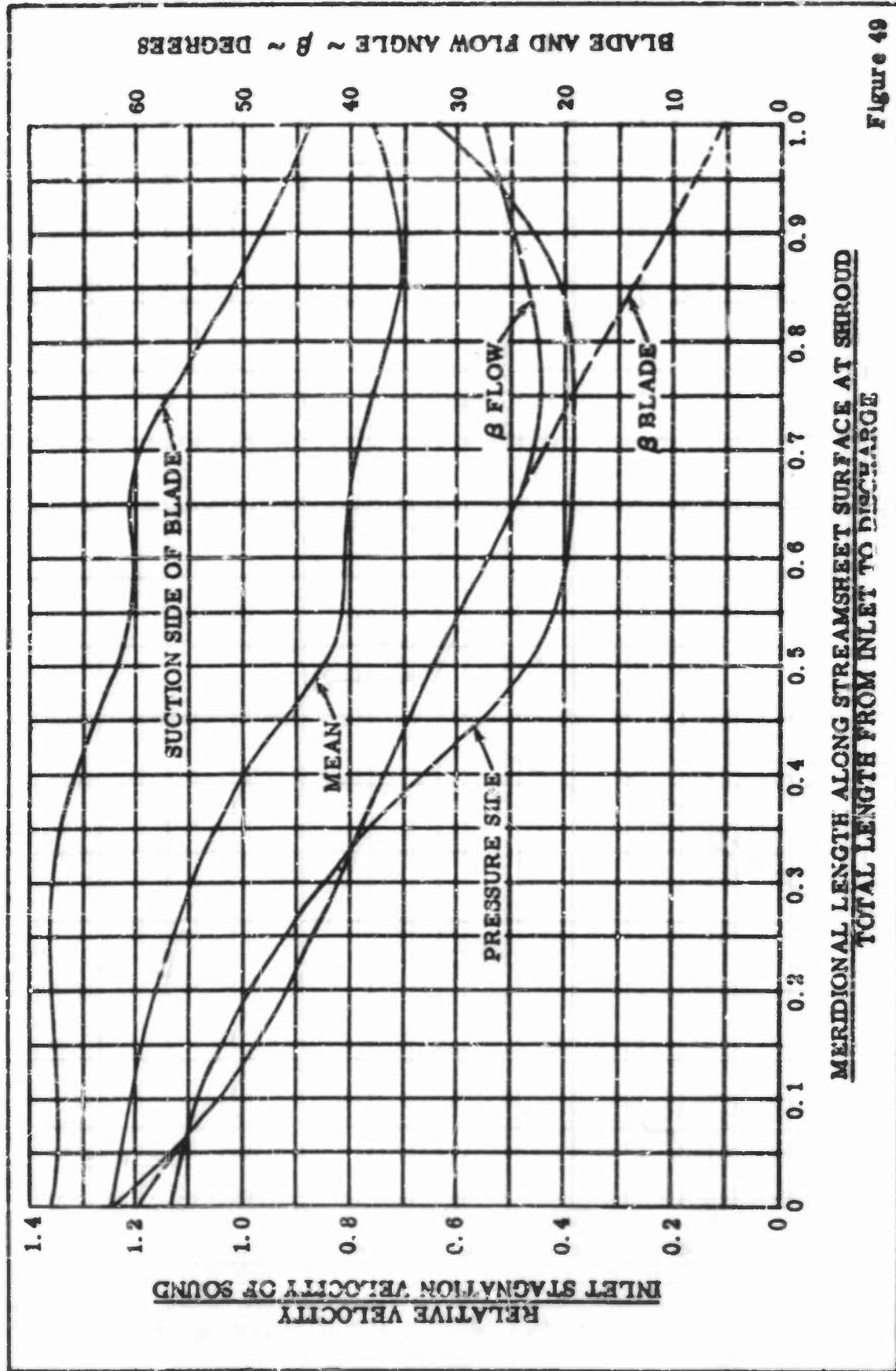


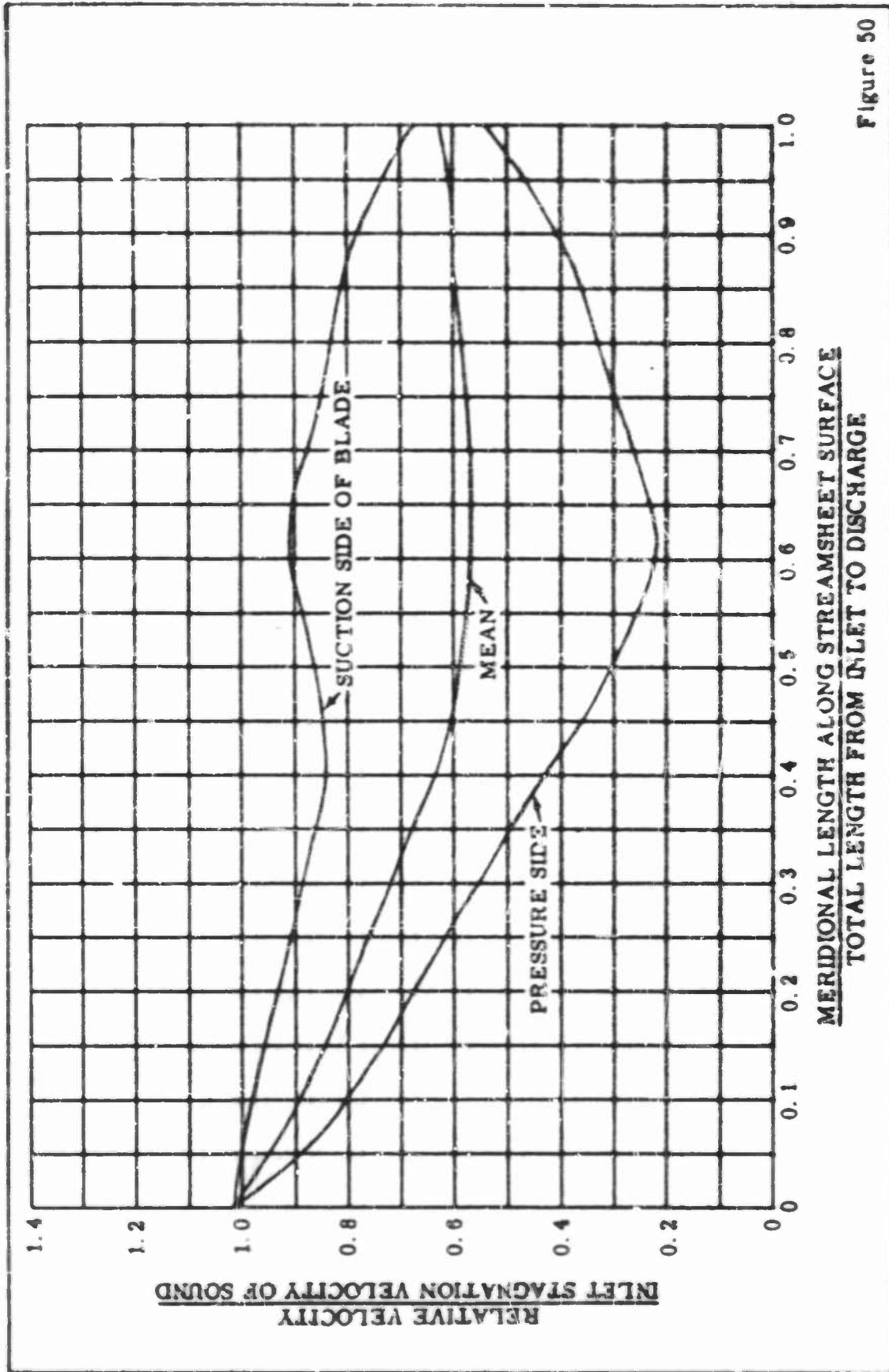
Figure 49

MERIDIONAL LENGTH ALONG STREAMSHEET SURFACE AT SHROUD
TOTAL LENGTH FROM INLET TO DISCHARGE

IMPELLER IIB, RELATIVE VELOCITY DISTRIBUTION, BLADE AND FLOW ANGLE
AT THE SHROUD STREAMSURFACE

CONFIDENTIAL

CONFIDENTIAL



WADC TR56-589

91

CONFIDENTIAL

IMPELLER III, RELATIVE VELOCITY DISTRIBUTION AT THE MEAN STREAMSURFACE

CONFIDENTIAL

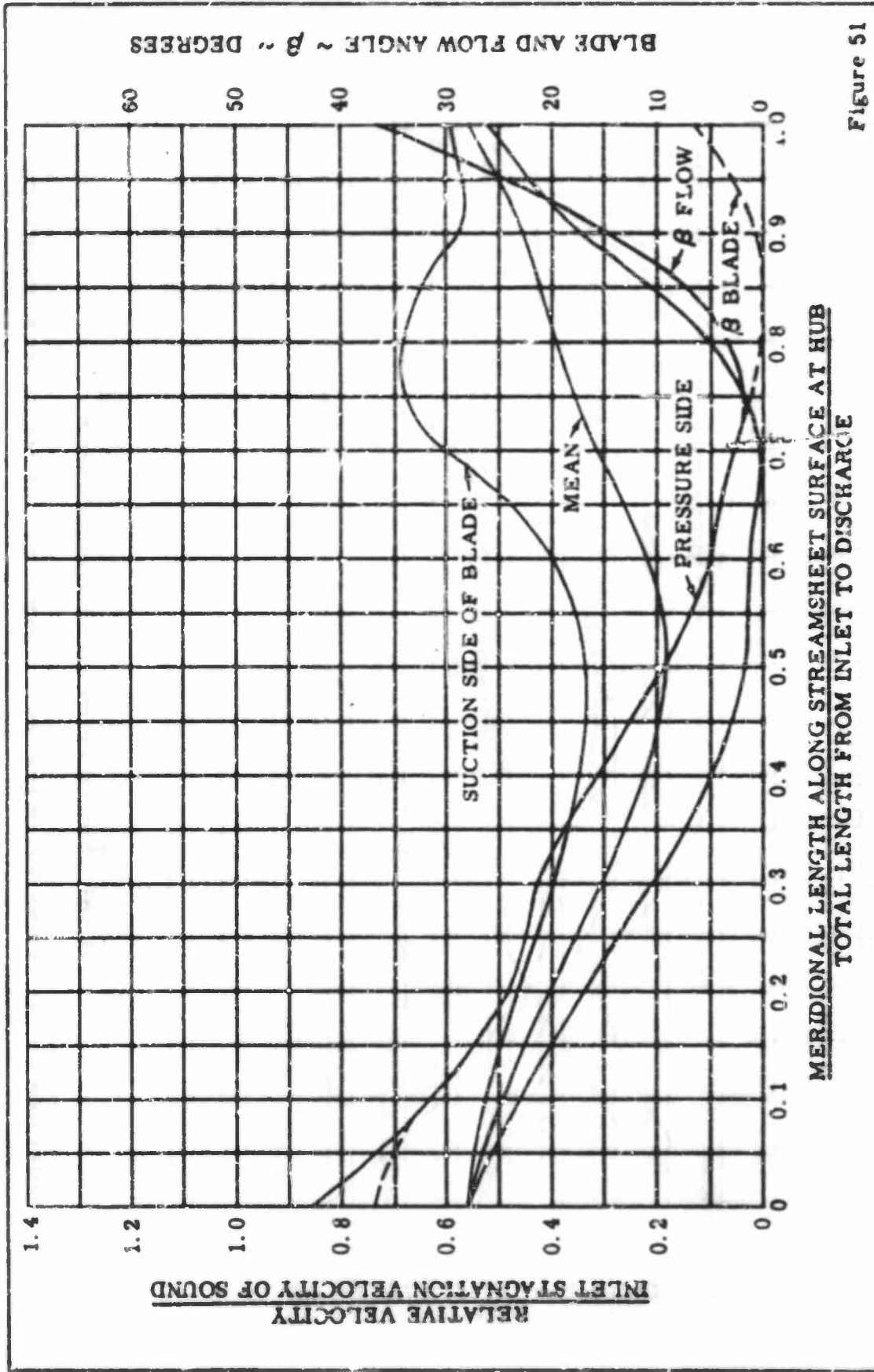
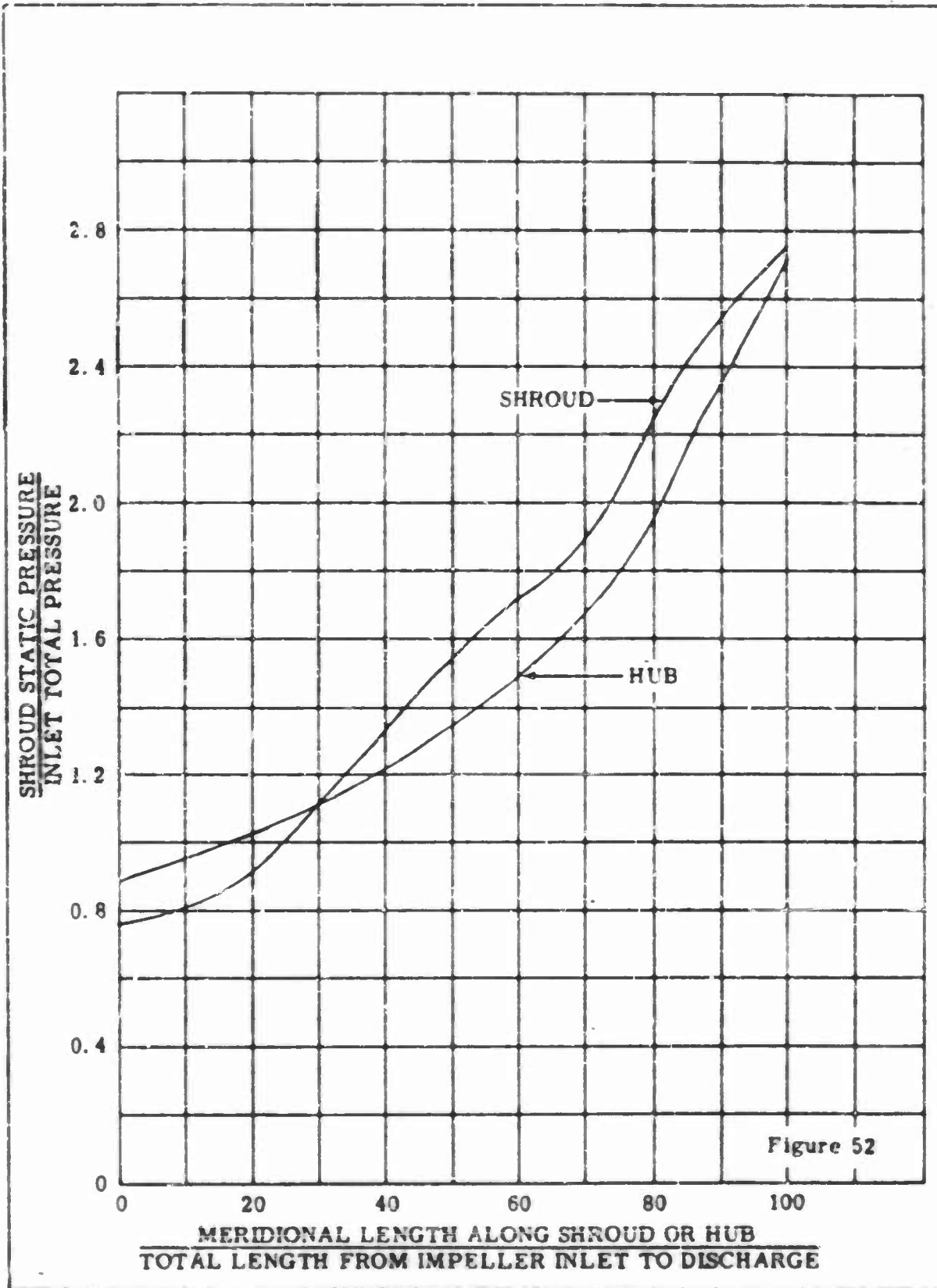


Figure 51

IMPELLER IB, RELATIVE VELOCITY DISTRIBUTION, BLADE AND FLOW ANGLE AT THE HUB STREAMSURFACE

CONFIDENTIAL

CONFIDENTIAL



PRESSURE DISTRIBUTION ALONG SHROUD AND HUB FOR IMPELLER IIB

CONFIDENTIAL

CONFIDENTIAL

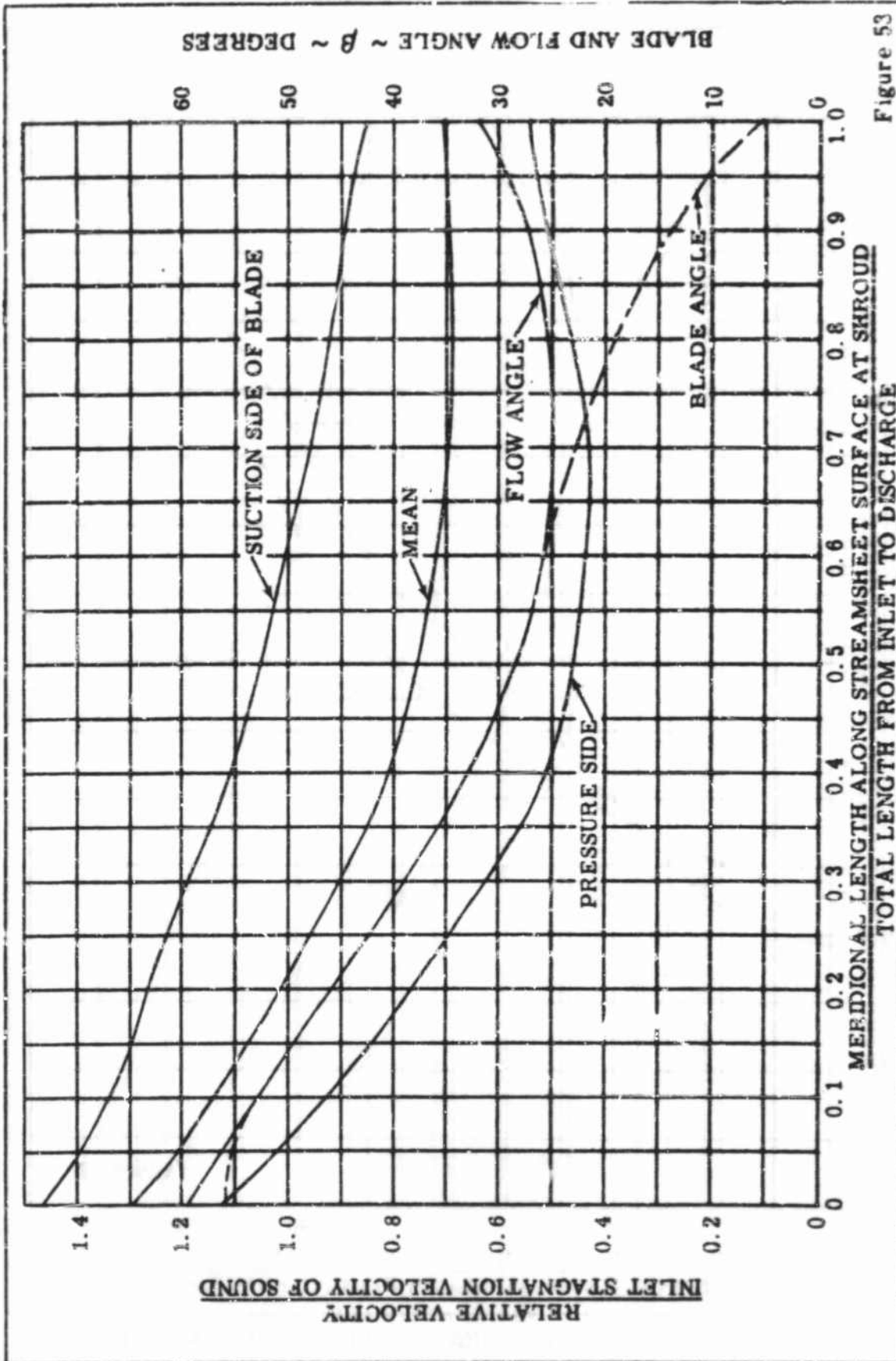


Figure 53

IMPELLER IV, RELATIVE VELOCITY DISTRIBUTION, BLADE AND FLOW ANGLE AT THE SHROUD STREAMSURFACE

CONFIDENTIAL

CONFIDENTIAL

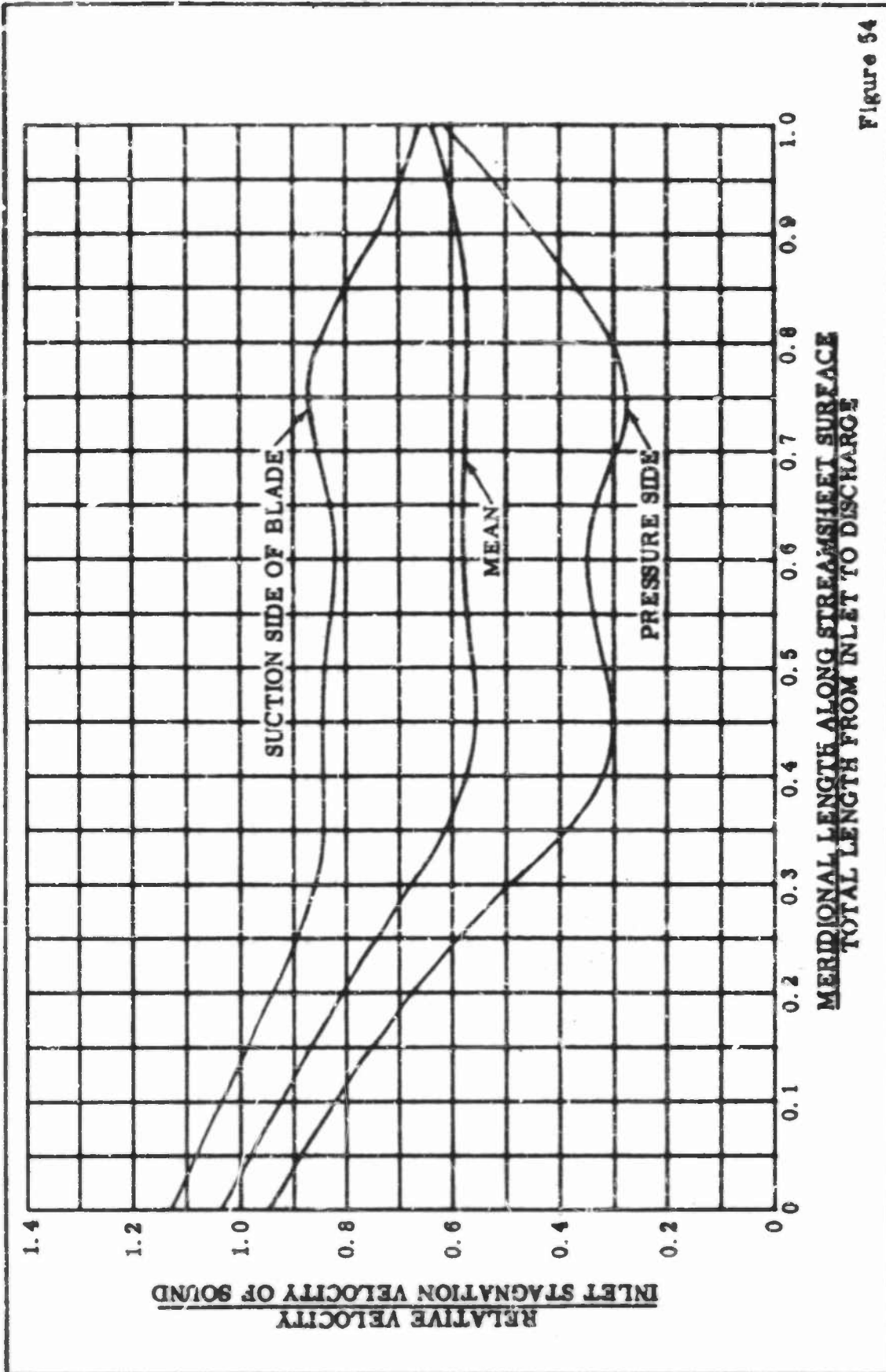


Figure 54

IMPELLER IV, RELATIVE VELOCITY DISTRIBUTION AT THE MEAN STREAMSURFACE

CONFIDENTIAL

CONFIDENTIAL

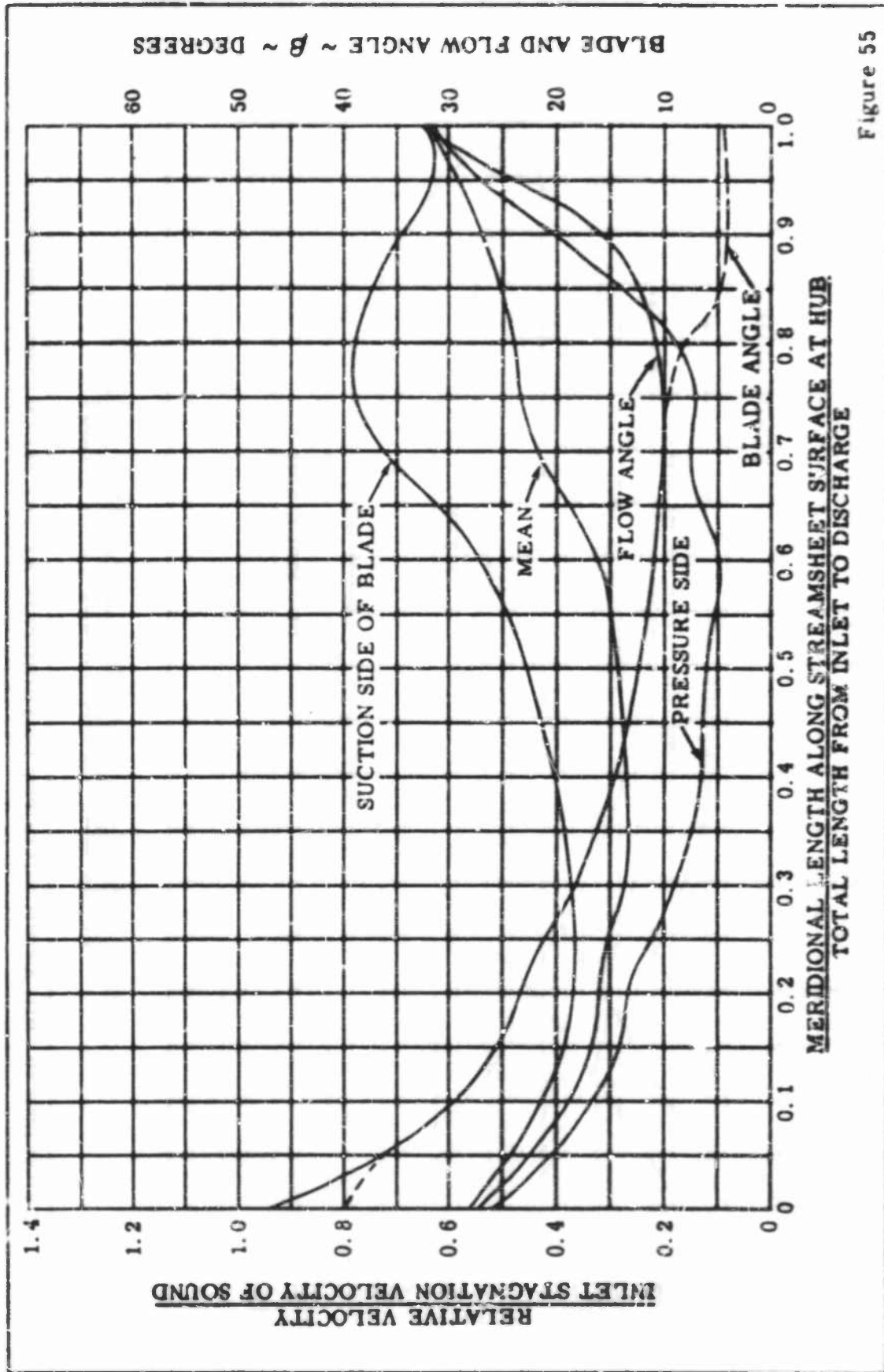
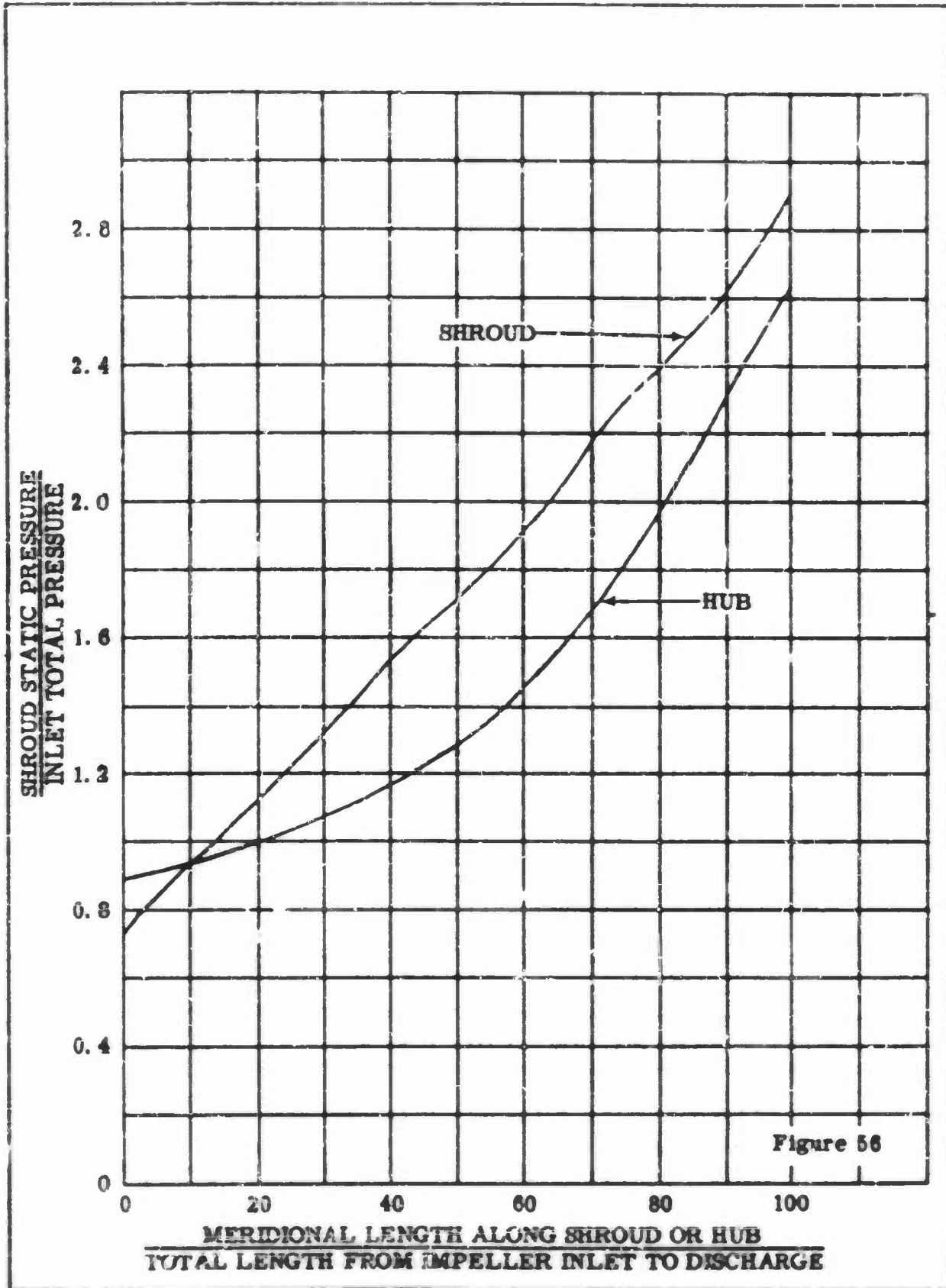


Figure 55

IMPELLER IV. RELATIVE VELOCITY DISTRIBUTION. BLADE AND FLOW ANGLE AT THE HUB STREAMSURFACE

CONFIDENTIAL

CONFIDENTIAL



PRESSURE DISTRIBUTION ALONG SHROUD AND HUB FOR IMPELLER IV

CONFIDENTIAL

CONFIDENTIAL

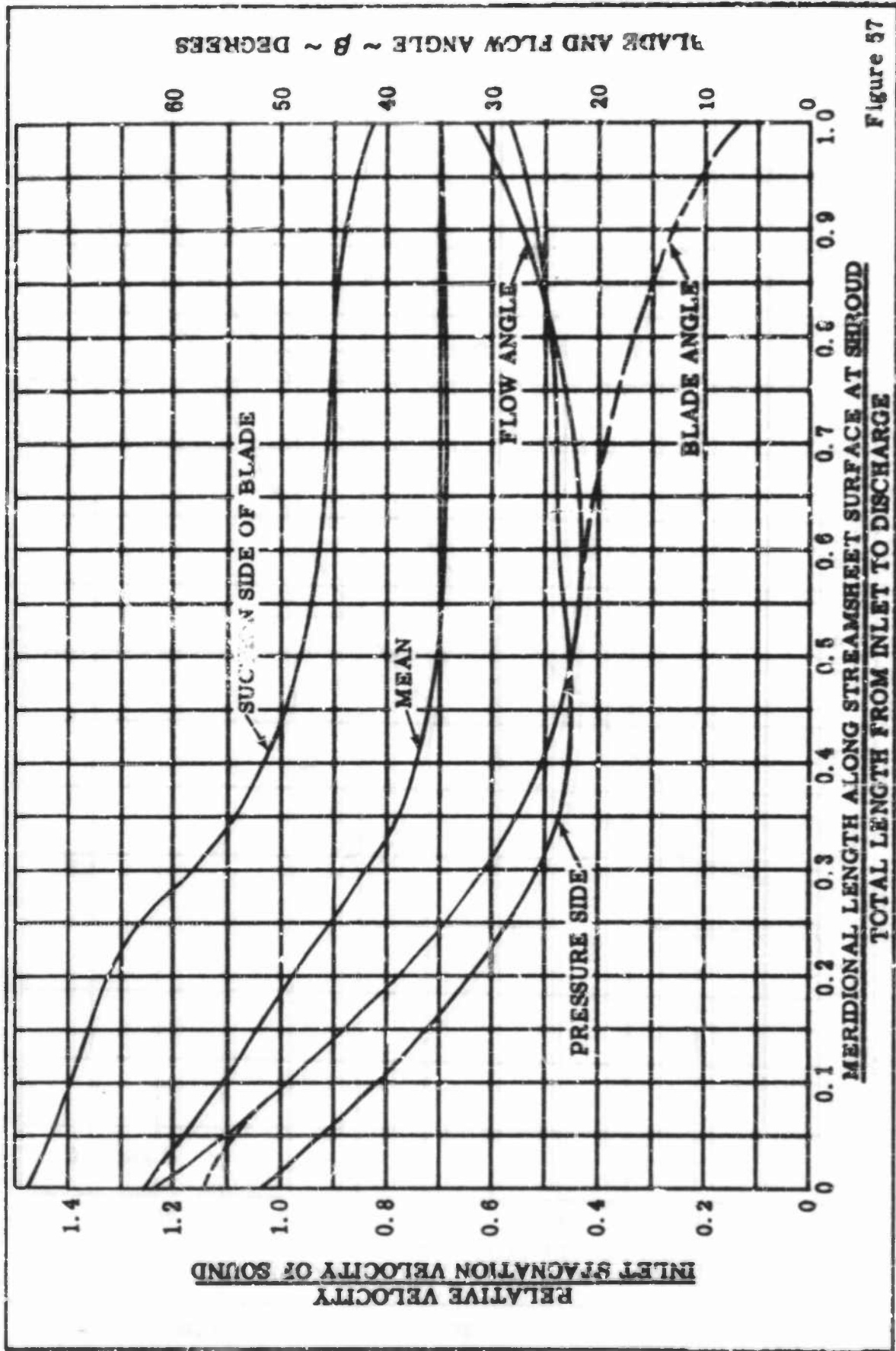


Figure 57

IMPELLER IVA, RELATIVE VELOCITY DISTRIBUTION, BLADE AND FLOW ANGLE AT THE SHROUD STREAMSURFACE

CONFIDENTIAL

CONFIDENTIAL

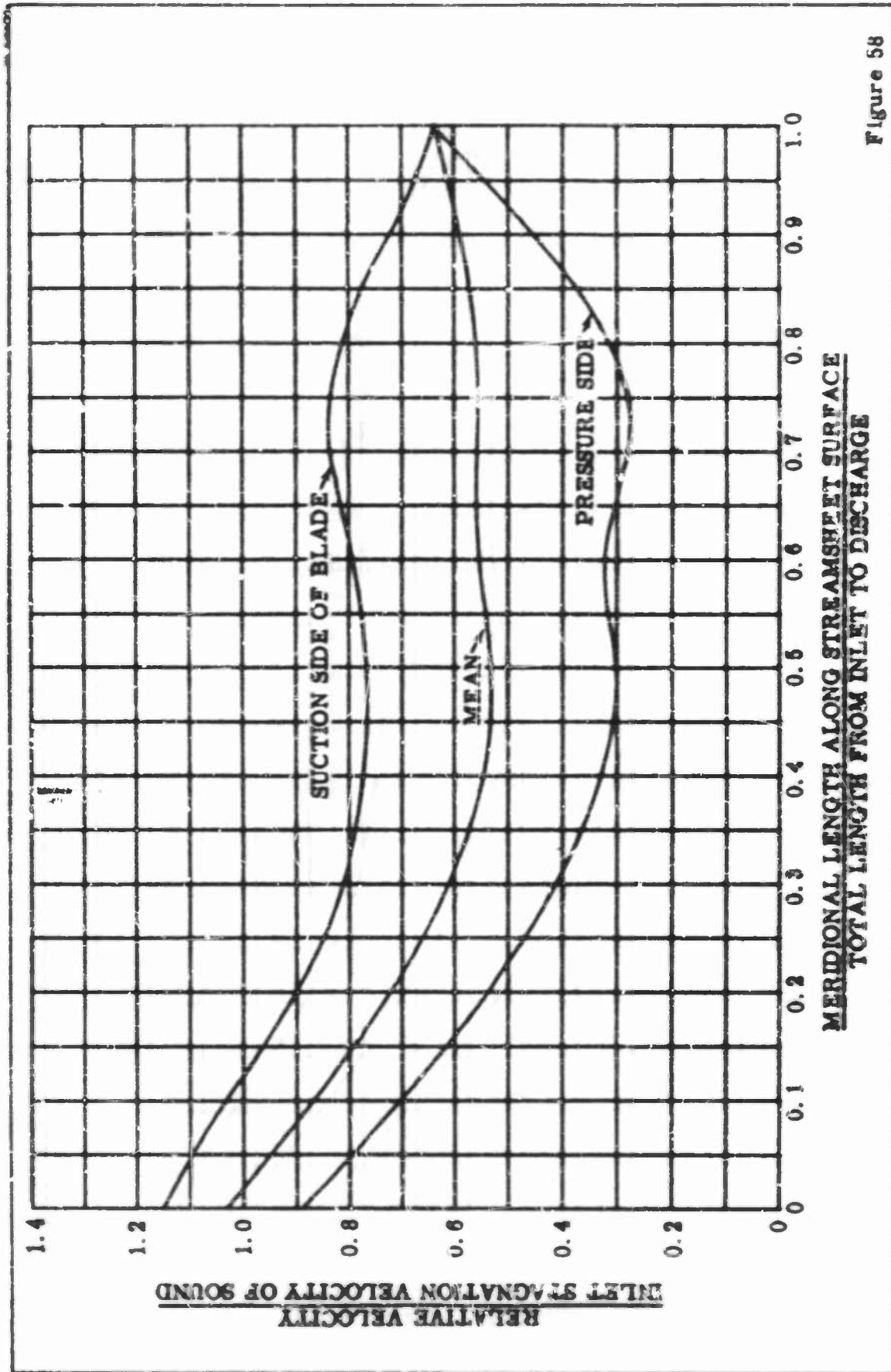


Figure 58

IMPELLER IVA, RELATIVE VELOCITY DISTRIBUTION AT THE MEAN STREAMSURFACE

CONFIDENTIAL

CONFIDENTIAL

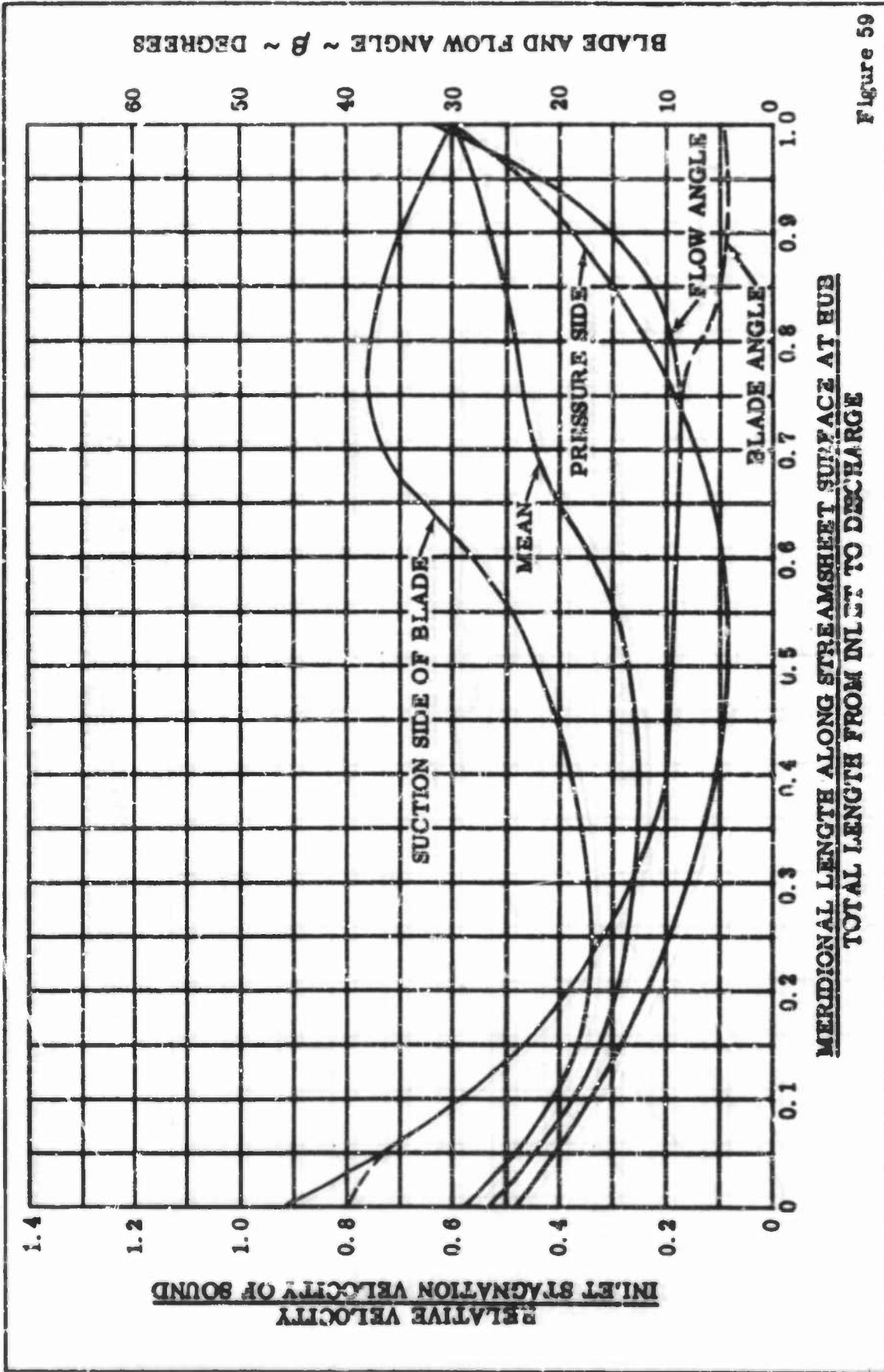


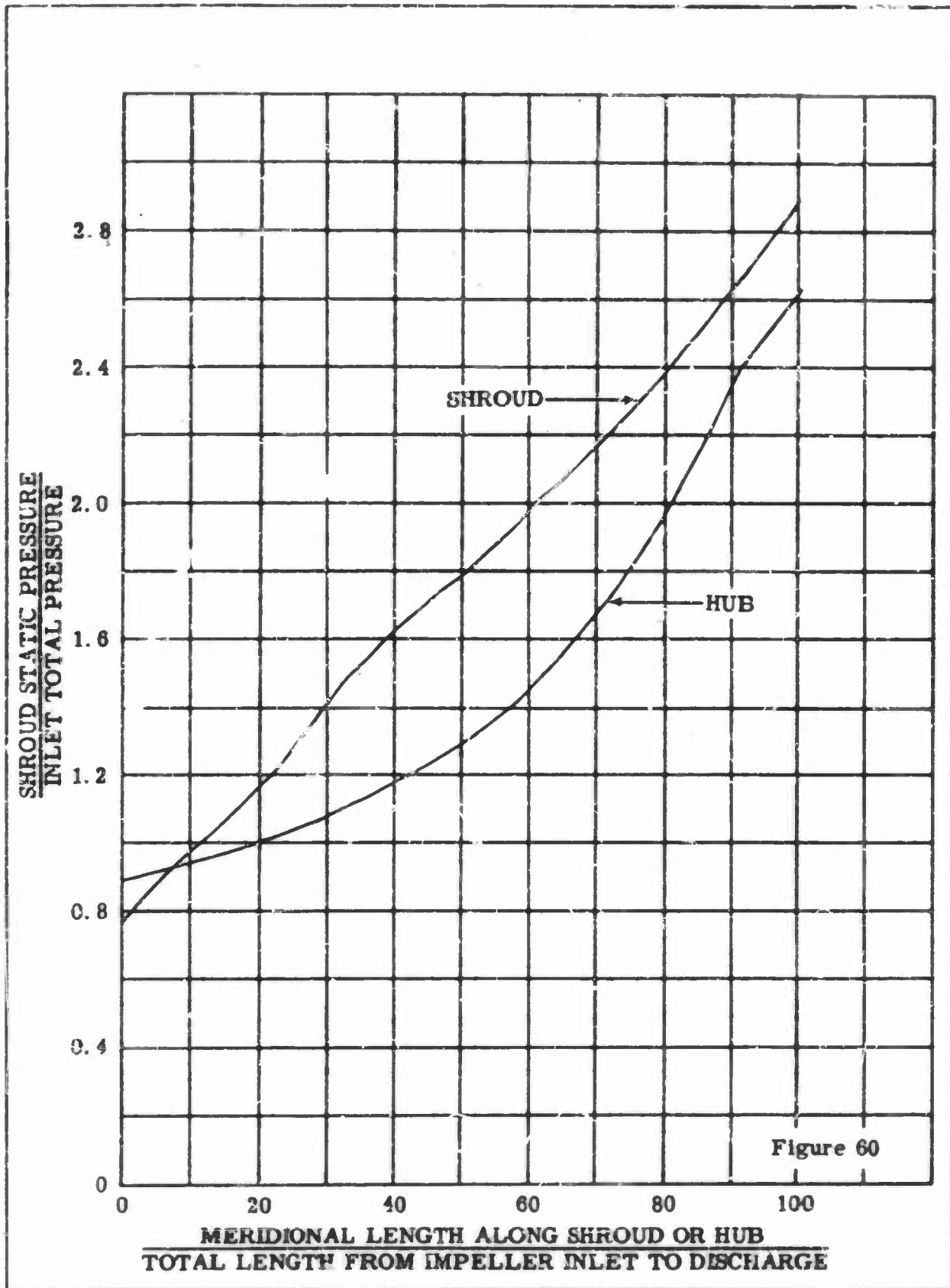
Figure 59

MERIDIONAL LENGTH ALONG STREAMSHEET SURFACE AT HUB
TOTAL LENGTH FROM INLET TO DISCHARGE

IMPELLER IVA, RELATIVE VELOCITY DISTRIBUTION, BLADE AND FLOW ANGLE AT THE HUB STREAMSURFACE

CONFIDENTIAL

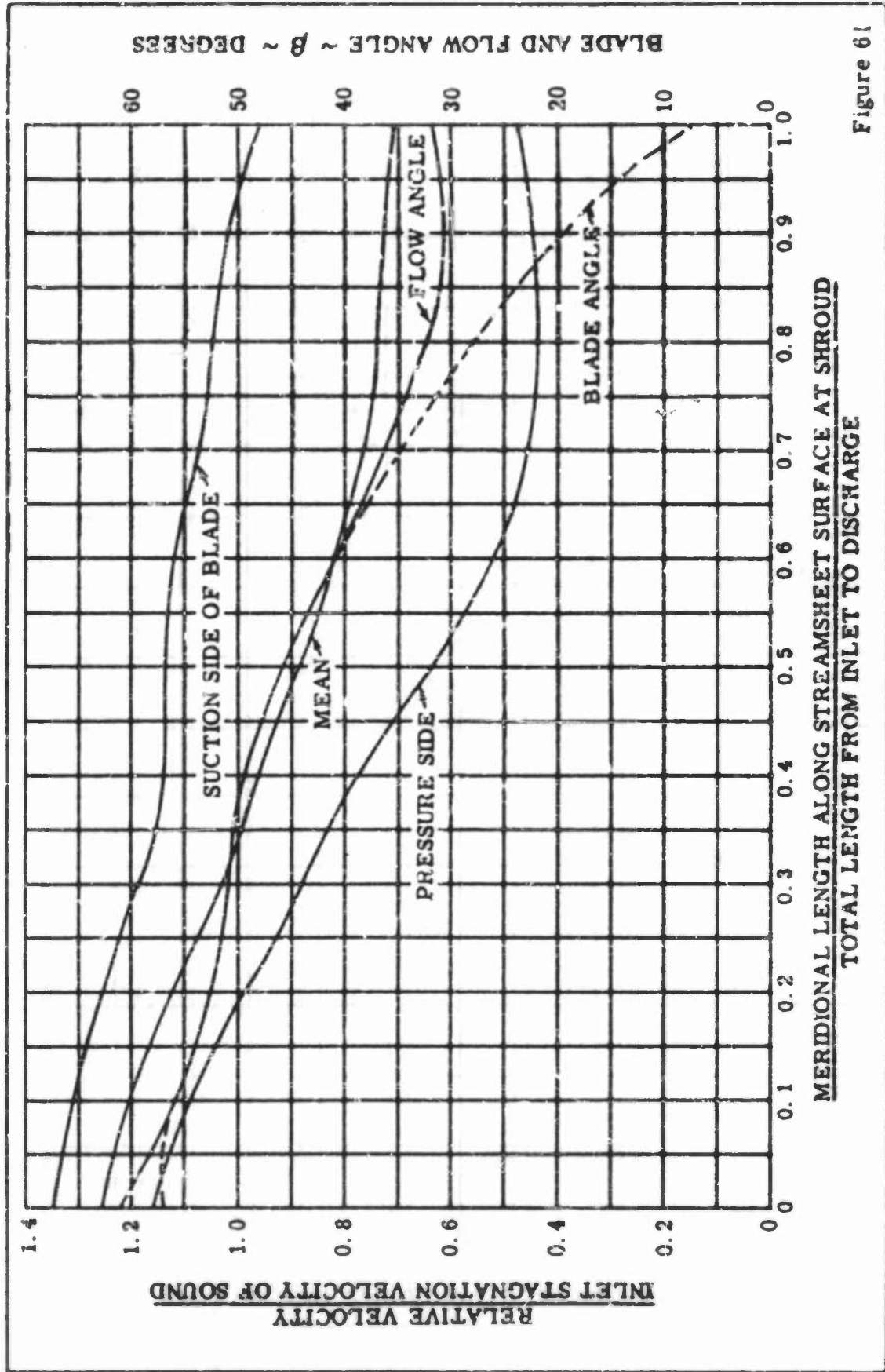
CONFIDENTIAL



PRESSURE DISTRIBUTION ALONG SHROUD AND HUB FOR IMPELLER IVA

CONFIDENTIAL

CONFIDENTIAL



**MERIDIONAL LENGTH ALONG STREAMSHEET SURFACE AT SHROUD
TOTAL LENGTH FROM INLET TO DISCHARGE**

**IMPELLER IVB, RELATIVE VELOCITY DISTRIBUTION, BLADE AND FLOW ANGLE
AT THE SHROUD STREAMSURFACE**

CONFIDENTIAL

CONFIDENTIAL

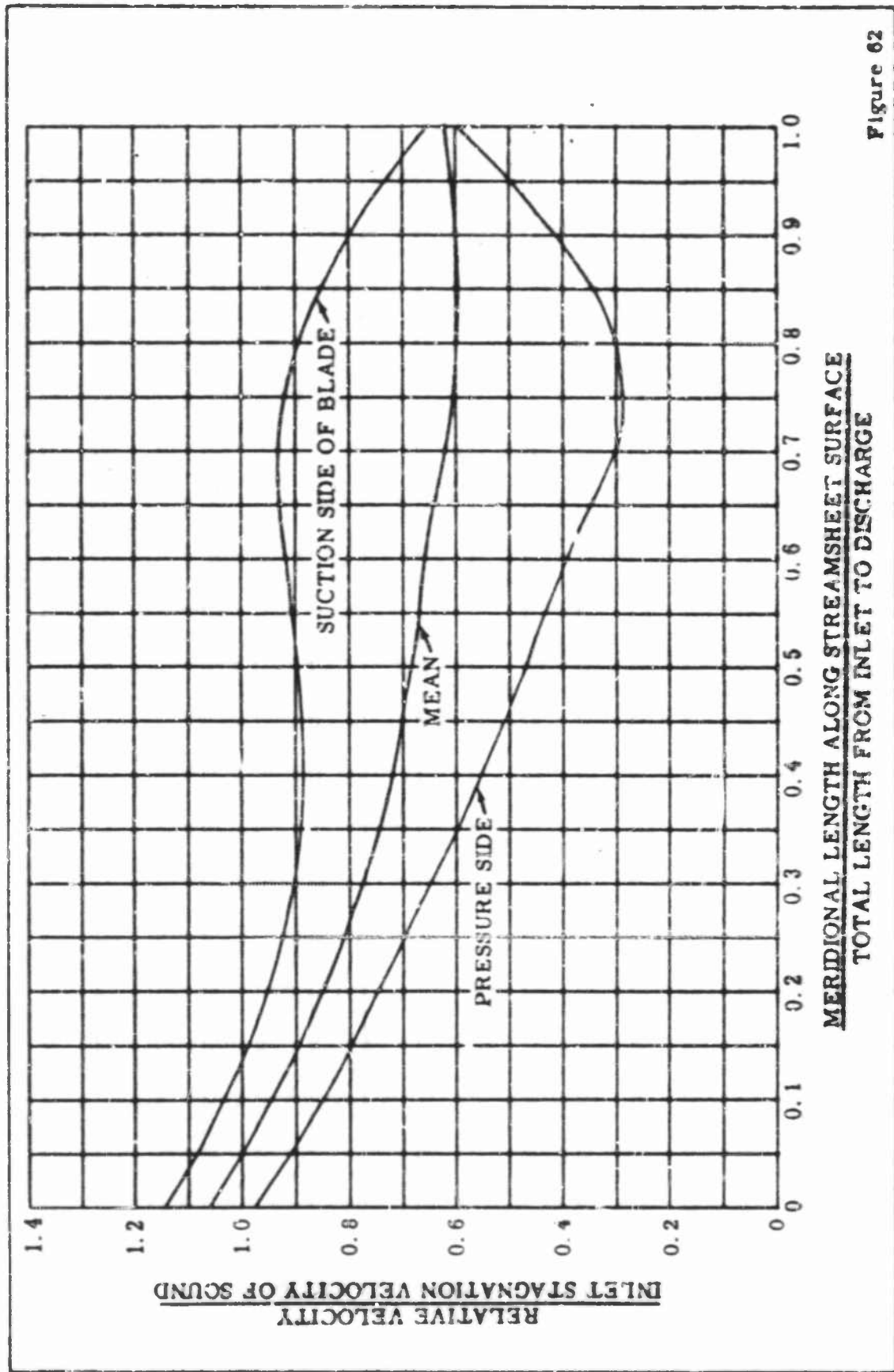


Figure 62

IMPELLER IVB, RELATIVE VELOCITY DISTRIBUTION AT THE MEAN STREAM SURFACE

CONFIDENTIAL

CONFIDENTIAL

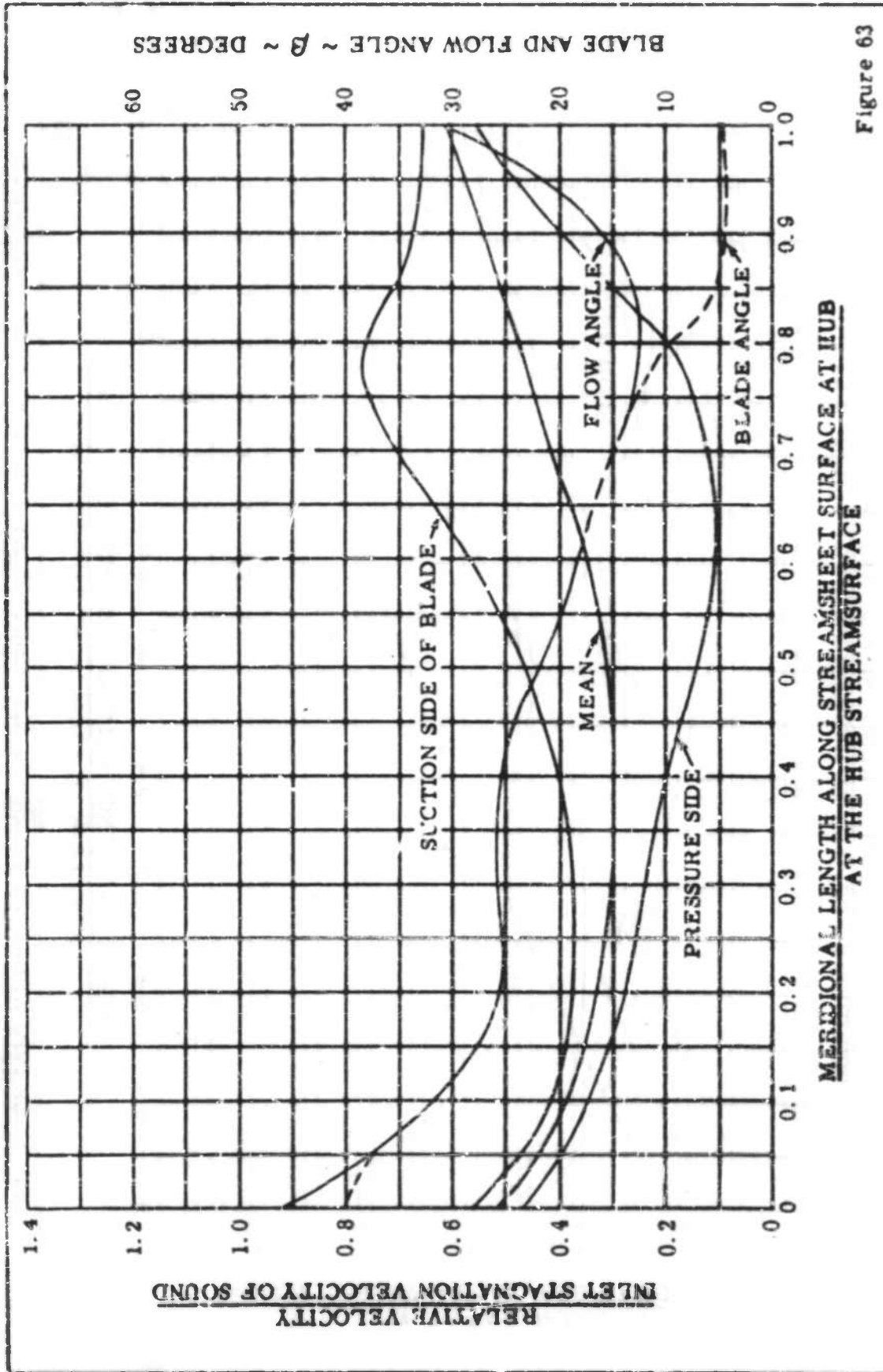
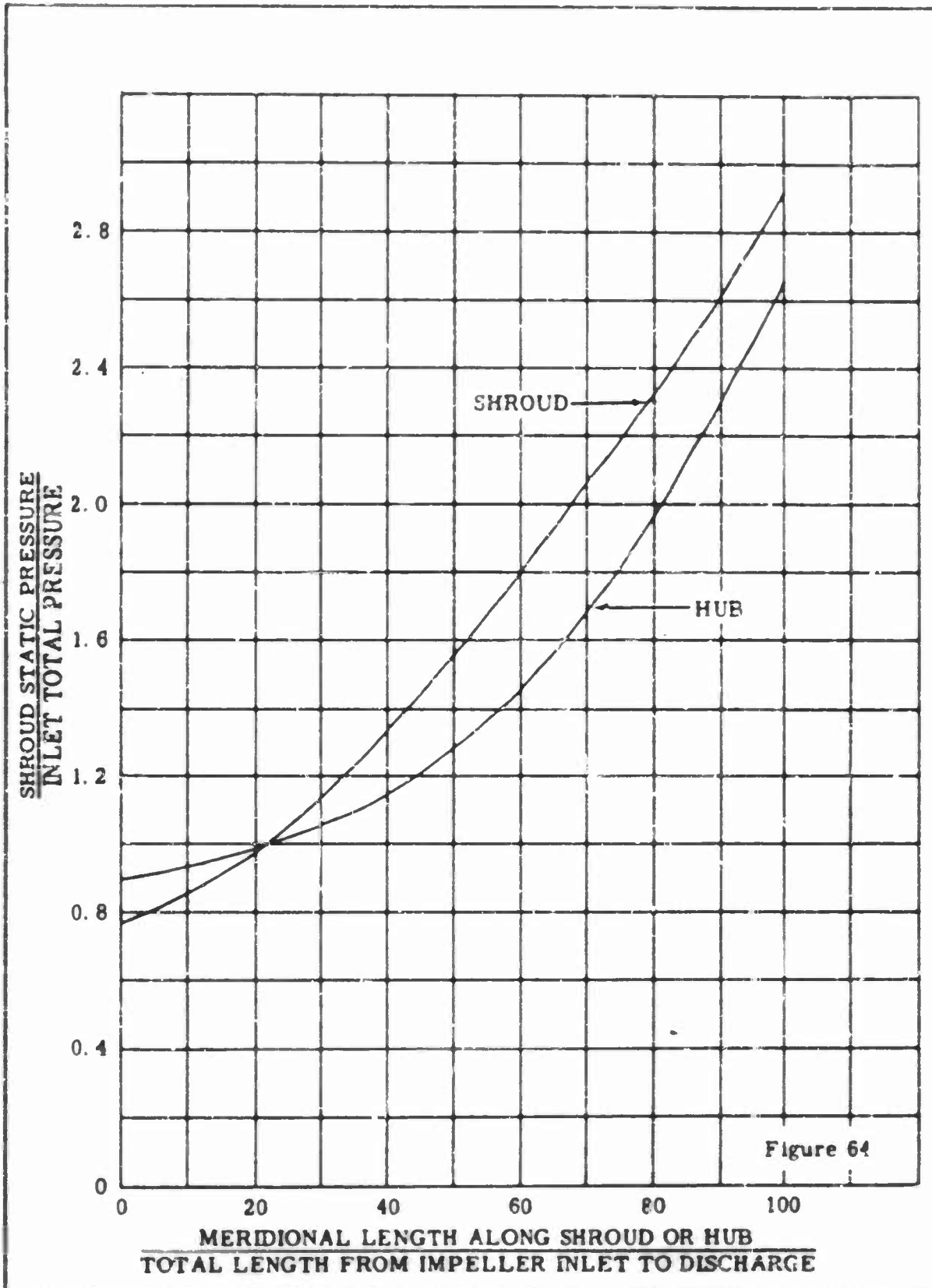


Figure 63

IMPELLER IVB, RELATIVE VELOCITY DISTRIBUTION, BLADE AND FLOW ANGLE AT THE HUB STREAMSURFACE

CONFIDENTIAL

CONFIDENTIAL



PRESSURE DISTRIBUTION ALONG SHROUD AND HUB FOR IMPELLER IVB

CONFIDENTIAL

CONFIDENTIAL

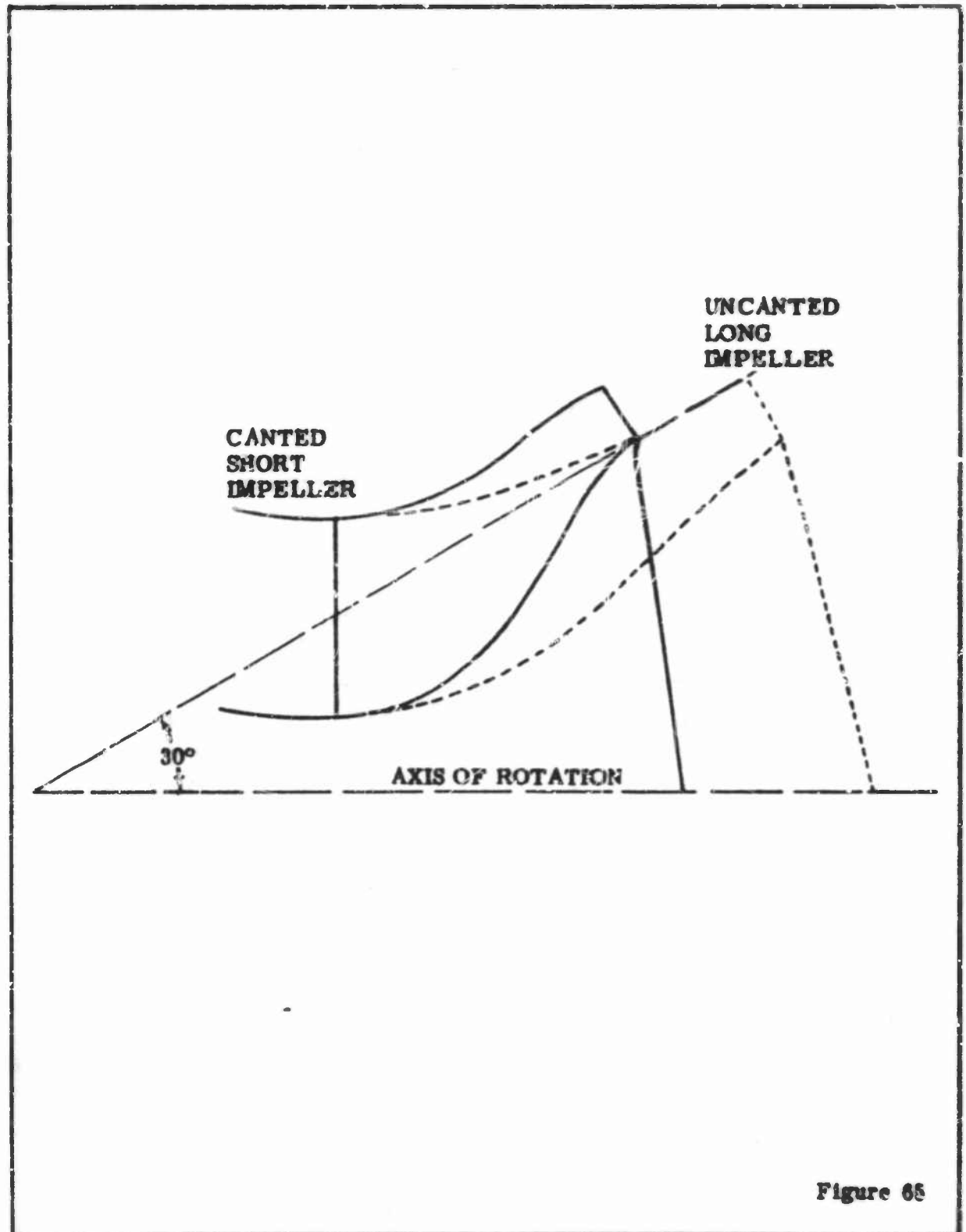
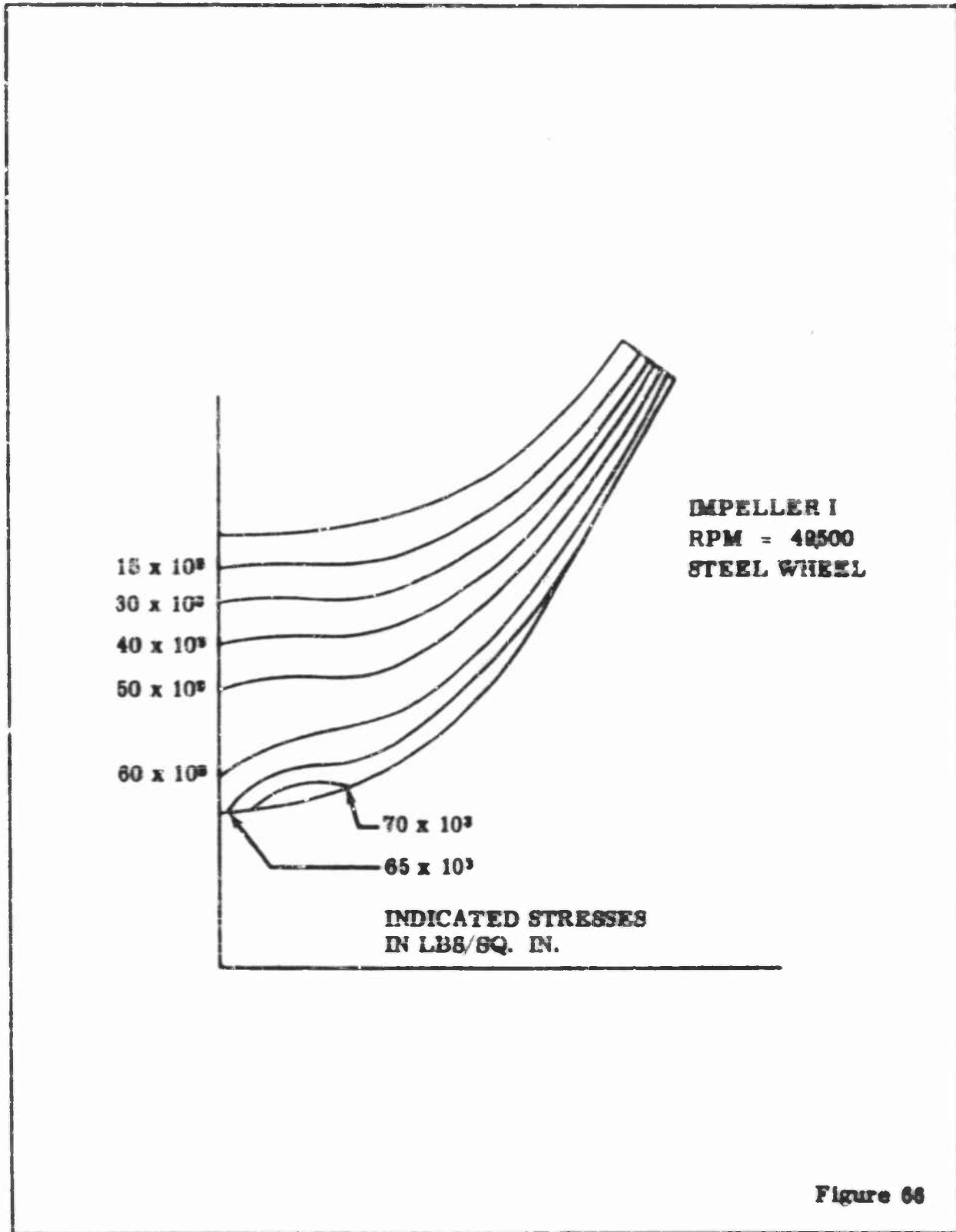


Figure 65

DESIGN OF IMPELLER WITH 30° CONE ANGLE

CONFIDENTIAL

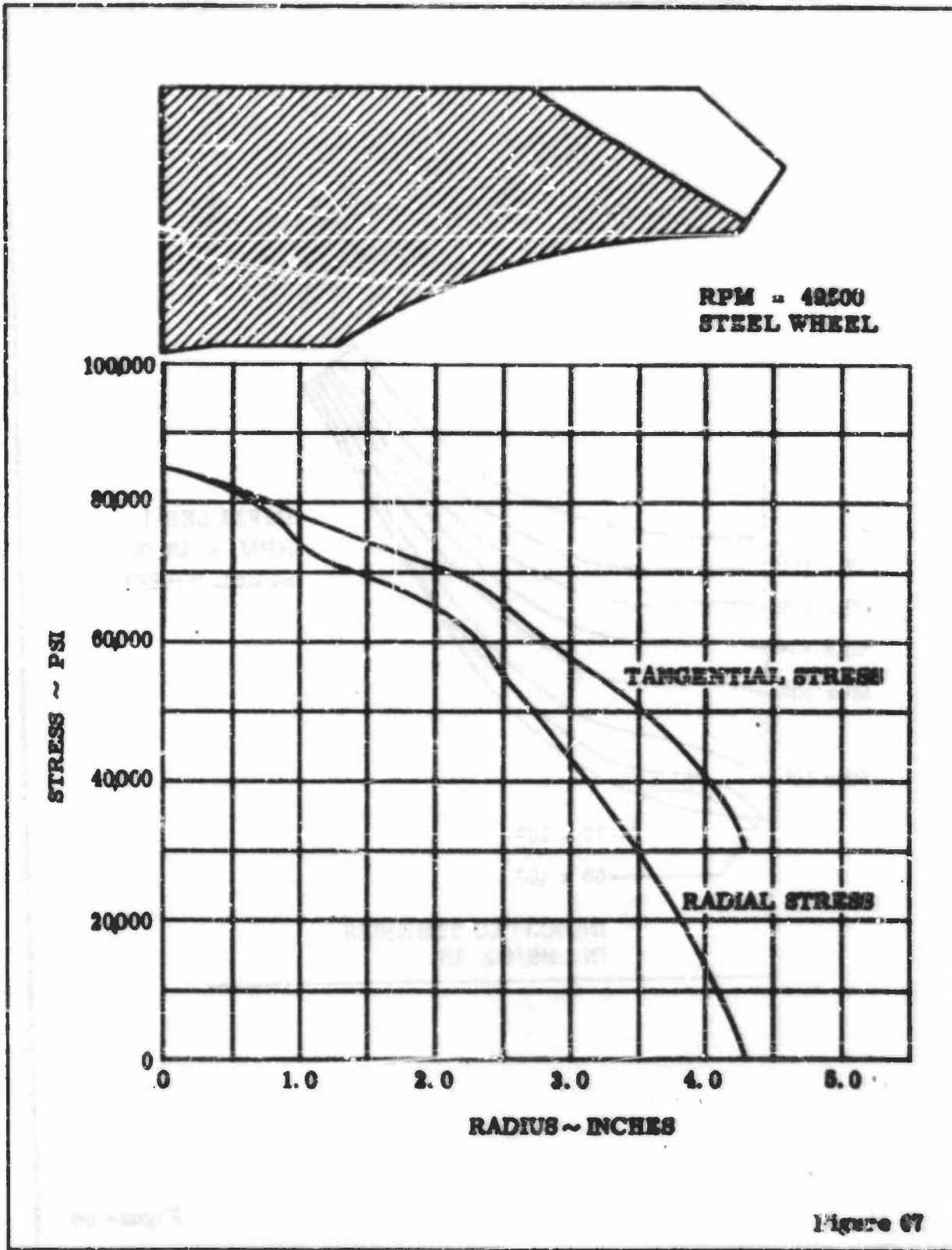
CONFIDENTIAL



CALCULATED BLADE STRESSES IN IMPELLER I

CONFIDENTIAL

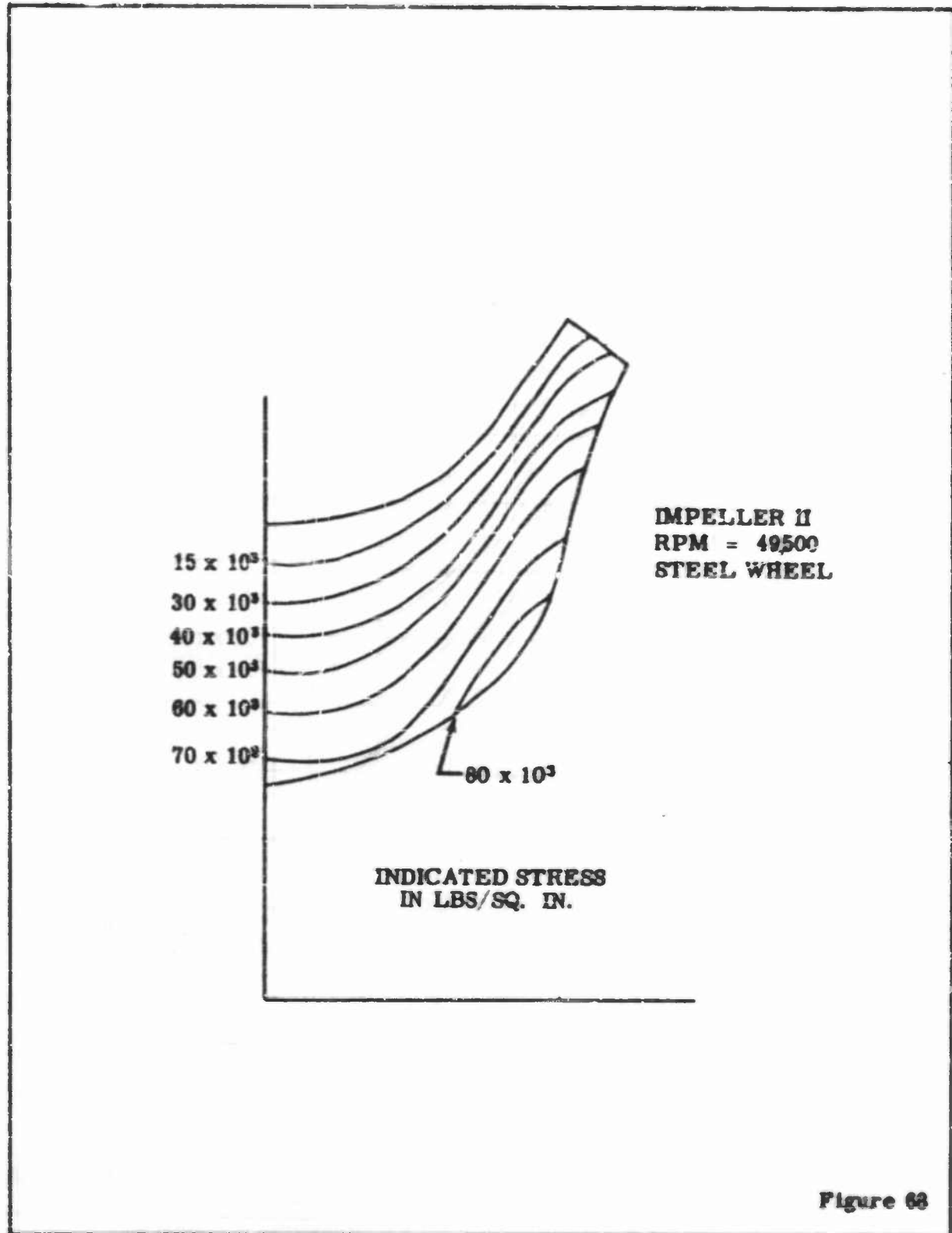
CONFIDENTIAL



HUB STRESSES AT CRITICAL SECTION OF IMPELLER I

CONFIDENTIAL

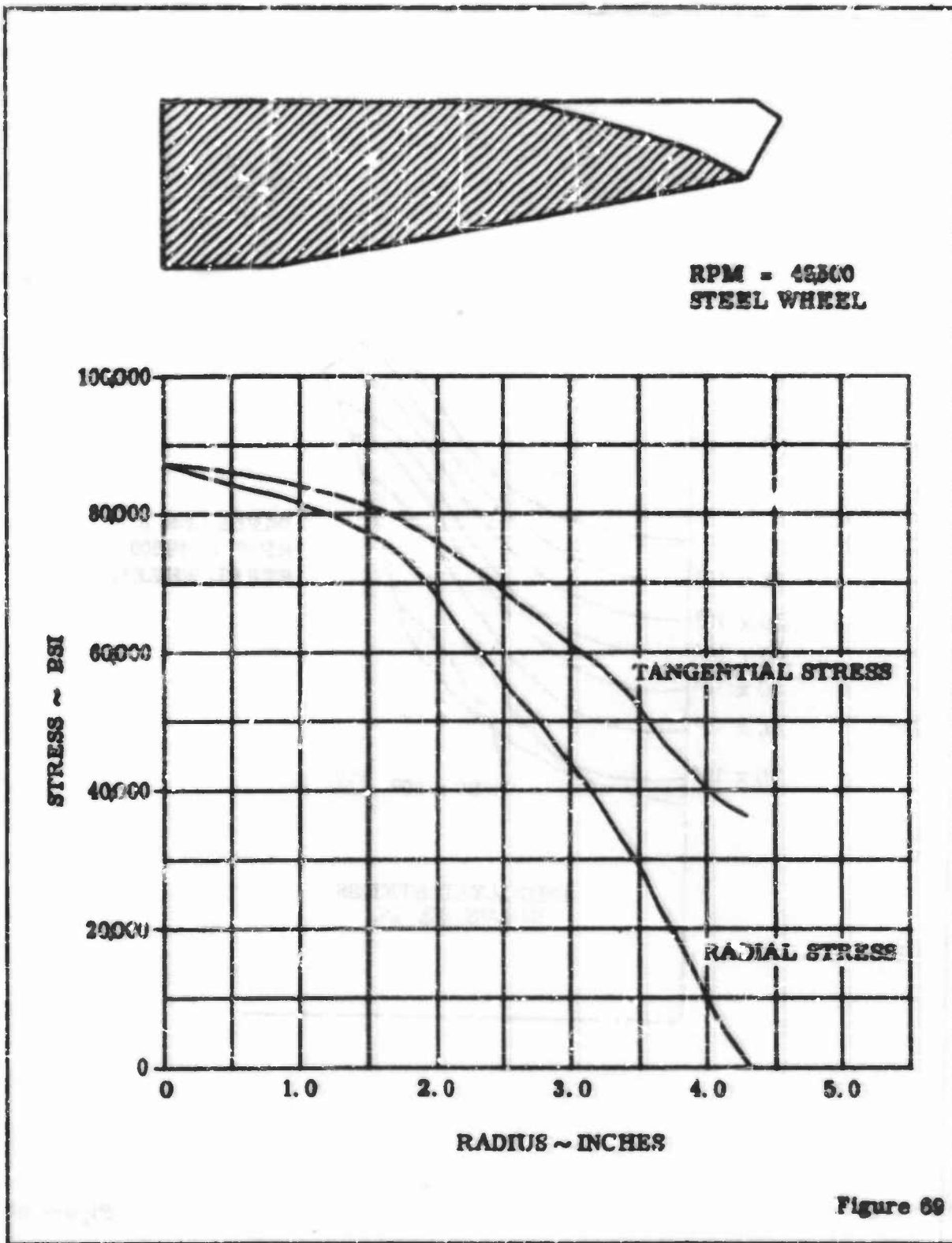
CONFIDENTIAL



CALCULATED BLADE STRESSES IN IMPELLER II

CONFIDENTIAL

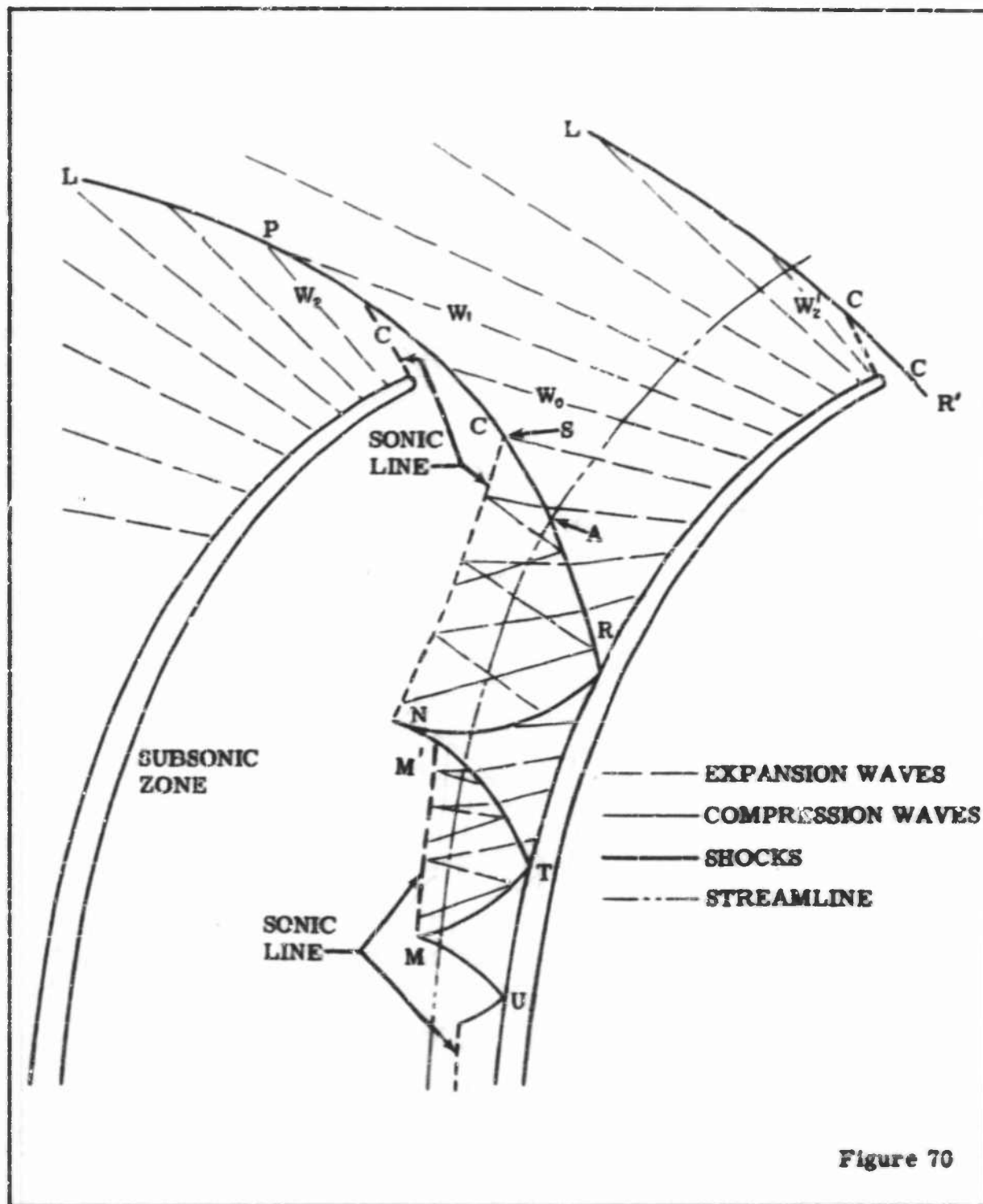
CONFIDENTIAL



HUB STRESSES AT CRITICAL SECTION OF IMPELLER II

CONFIDENTIAL

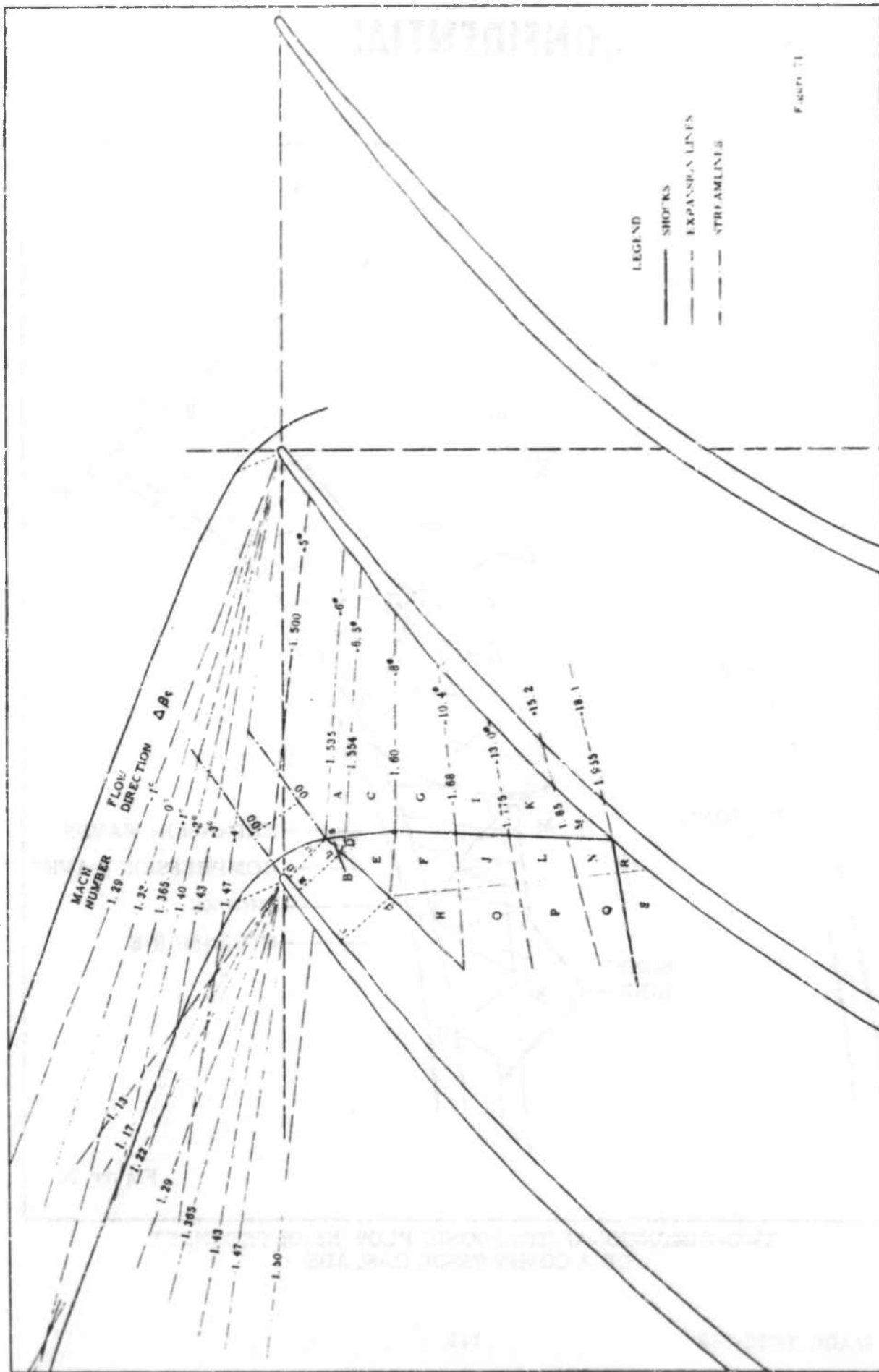
CONFIDENTIAL



TWO-DIMENSIONAL TRANSONIC FLOW NEAR THE INLET OF A COMPRESSOR CASCADE

CONFIDENTIAL

CONFIDENTIAL



TWO-DIMENSIONAL SUPERSONIC FLOW AT INDUCER INLET - IMPELLER I. $\frac{r}{r_{shroud}} = 1.0$

CONFIDENTIAL

CONFIDENTIAL

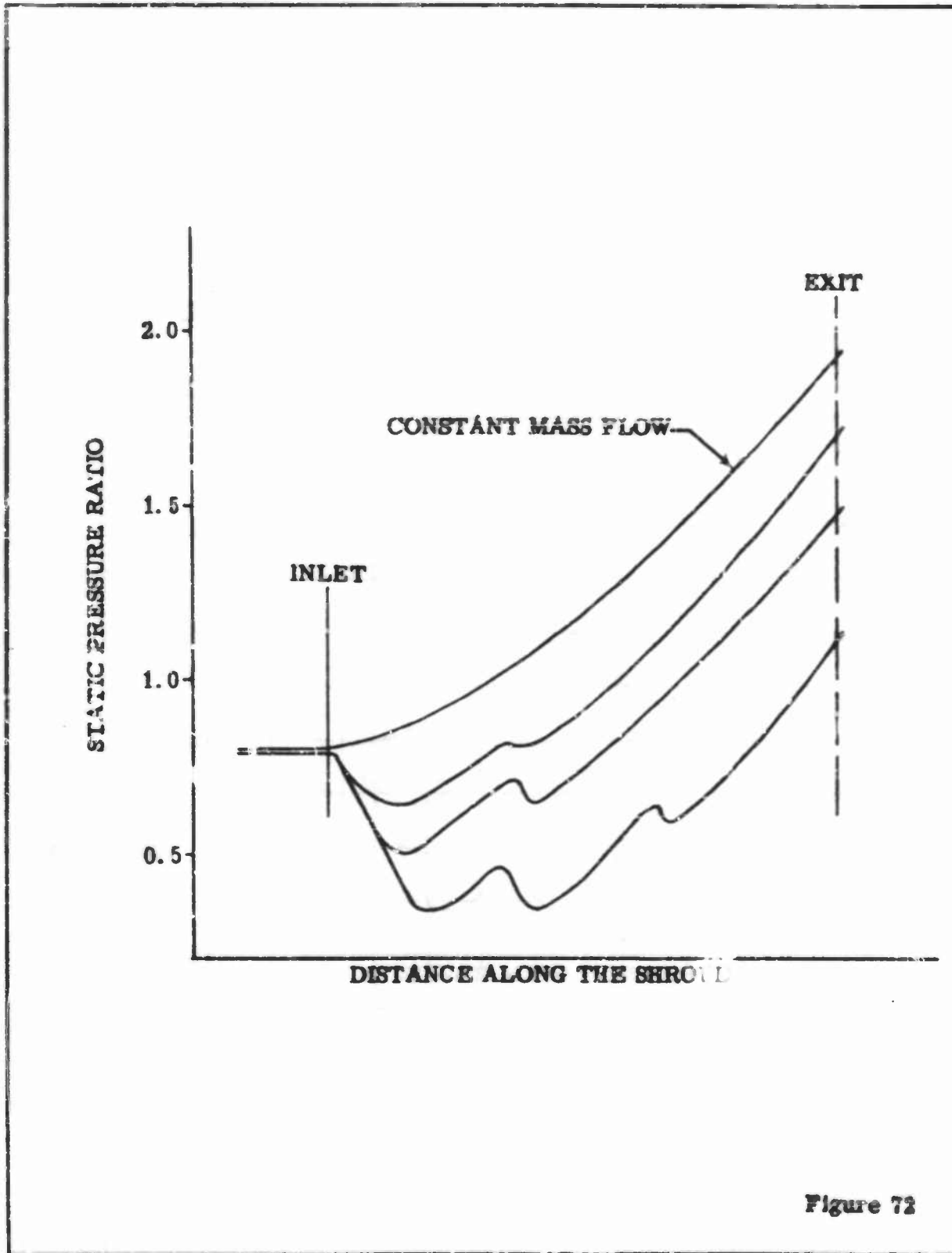
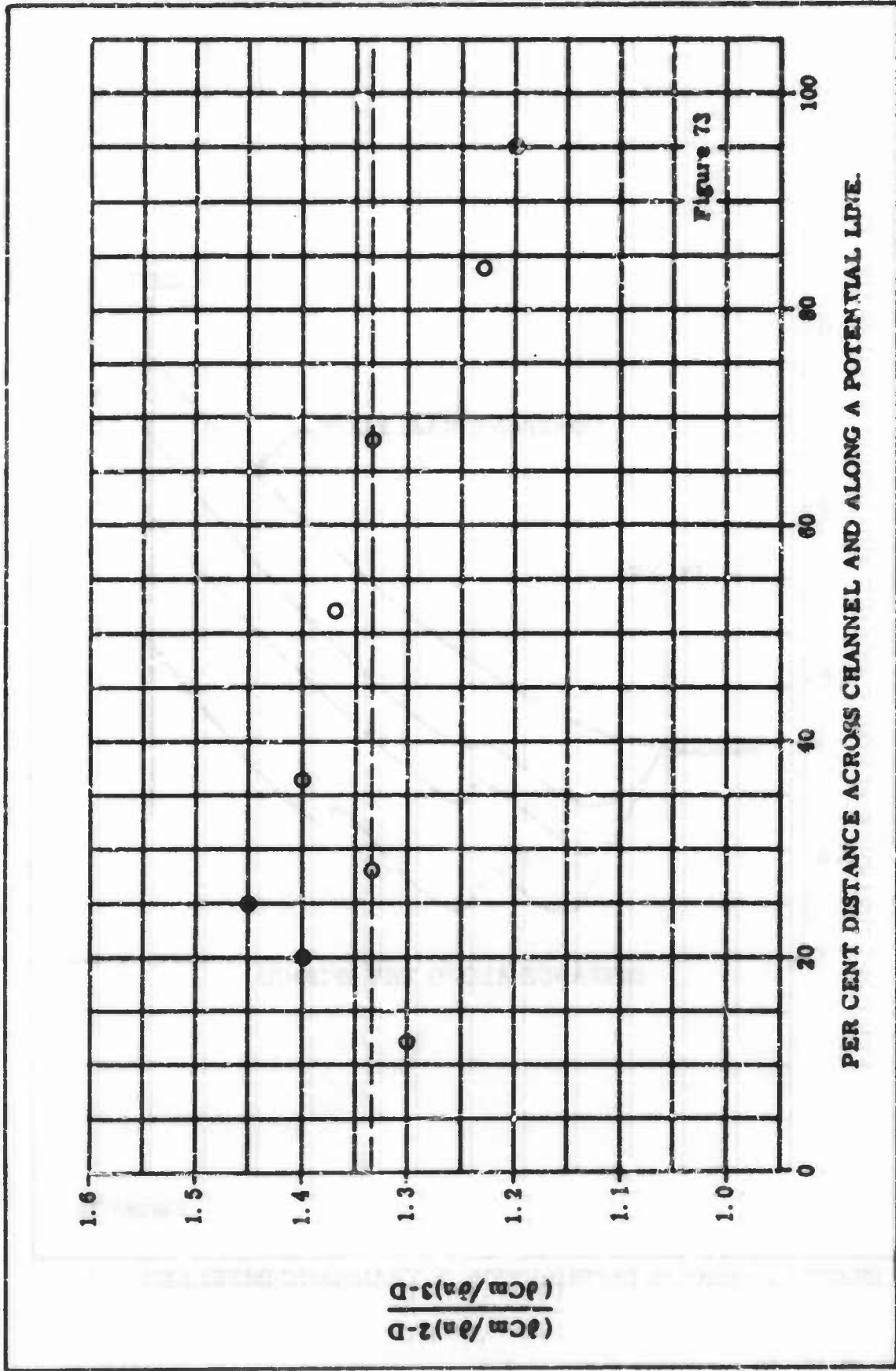


Figure 72

SHROUD PRESSURE DISTRIBUTION IN TRANSONIC IMPELLER

CONFIDENTIAL

CONFIDENTIAL



COMPARISON OF VELOCITY GRADIENTS IN TWO - DIMENSIONAL AND THREE - DIMENSIONAL INLETS
(INCOMPRESSIBLE IRRATIONAL FLOW)

CONFIDENTIAL

CONFIDENTIAL

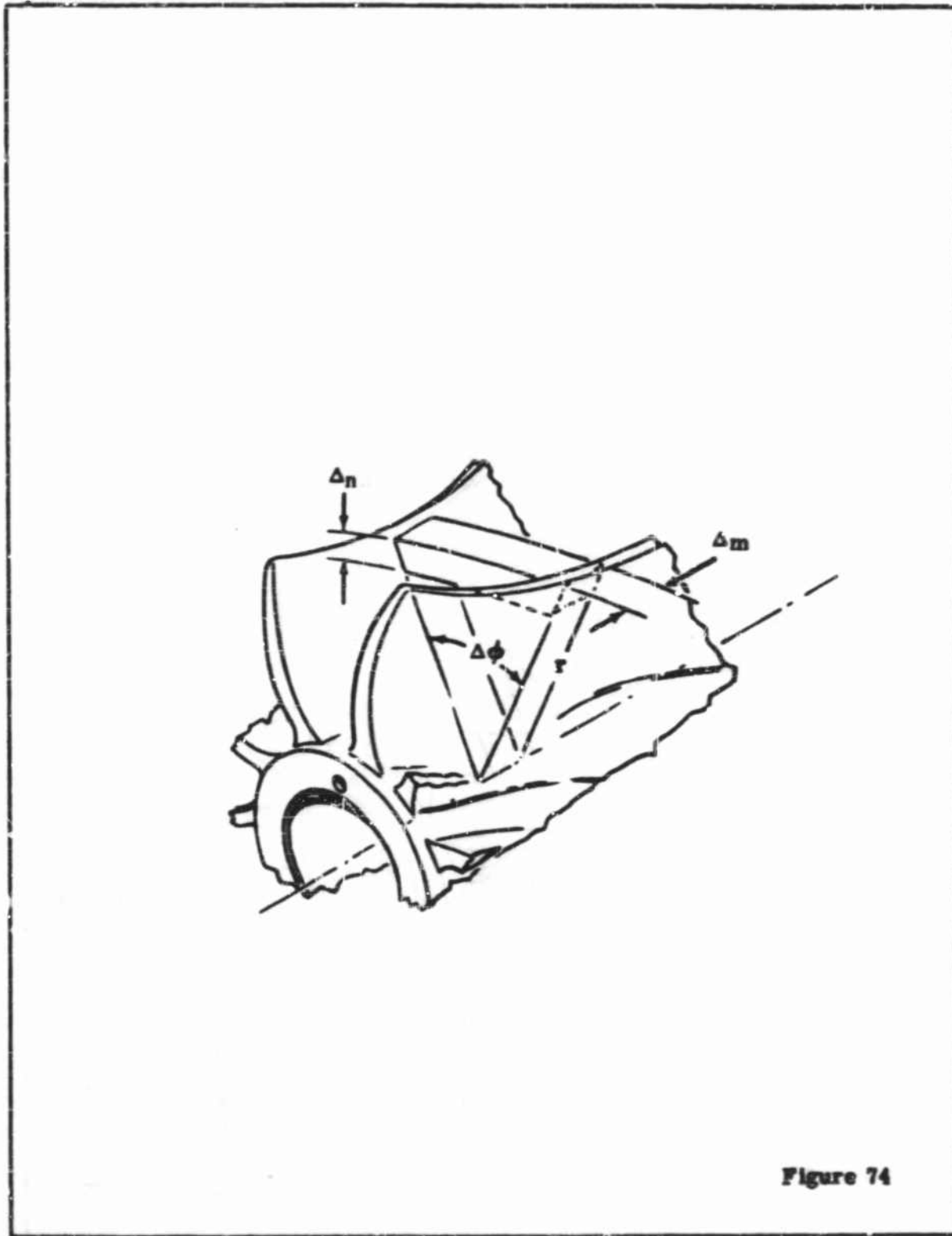


Figure 74

FLUID ELEMENT BETWEEN TWO BLADES FOR
THE CALCULATION OF THE BLADE LOADING

CONFIDENTIAL

CONFIDENTIAL

TABLE I
AERODYNAMIC FEATURES, MIXED-FLOW IMPELLERS

Impeller Designation	Loading Distribution	Impeller Characteristic	Exit Cone Angle	No. of Blades	Impeller Geometry	Velocity Distribution	Pressure Variation
I	Fairly uniform loading with slightly un-loaded inducer				Figure 12 Figure 15 Table VI Table IX	Figure 25 Figure 26 Figure 27	Figure 28
IAA	Heavily loaded Inducer	Long	60°	17	Figure 12 Figure 17	Figure 33 Figure 34 Figure 35	Figure 36
IA	Uniform loading	Impellers			Figure 12 Figure 16	Figure 29 Figure 30 Figure 31	Figure 32
IB	Lightly loaded Inducer				Figure 12 Figure 18 Table VII Table IX	Figure 37 Figure 38 Figure 39	Figure 40
II	Uniform loading				Figure 13 Figure 19 Table VIII Table IX	Figure 41 Figure 42 Figure 43	Figure 44
IIA	Heavily loaded Inducer	Short Impellers	60°	18	Figure 13 Figure 20	Figure 45 Figure 46 Figure 47	Figure 48
IIB	Lightly loaded Inducer				Figure 13 Figure 21	Figure 49 Figure 50 Figure 51	Figure 52

CONFIDENTIAL

TABLE I (Cont'd)

Impeller Designation	Loading Distribution	Impeller Characteristic	Exit Cone Angle	No. of Blades	Impeller Geometry	Velocity Distribution	Pressure Variation
IV	Uniform loading				Figure 14 Figure 22	Figure 53 Figure 54 Figure 55	Figure 56
IVA	Heavily loaded Inducer	Long Impeller	30°	16	Figure 14 Figure 23	Figure 57 Figure 58 Figure 59	Figure 60
IVB	Lightly loaded Inducer				Figure 14 Figure 24	Figure 61 Figure 62 Figure 63	Figure 64

CONFIDENTIAL

TABLE II
IMPELLER DESIGN CONDITIONS

Inlet Conditions	60F and 29.92 in. Hg
Mass Flow $W\sqrt{\theta}/\delta$	401 lb per minute
Impeller efficiency	0.90
Impeller Work Input $\frac{U_2 c_{u2}}{g}$	73,500 ft-lb per lb
Slip Factor	0.81
Flow Factor	See Figure 4
Relative Deceleration Ratio, $\frac{w_2}{w_1}$	0.825
Tip Speed	1740 ft per sec
RPM/ $\sqrt{\theta}$	45,100
Nominal work ratio between shroud and hub, $(U_2 c_{u2})_s / (U_2 c_{u2})_h$	1.06

BASIC GEOMETRY COMMON TO ALL IMPELLERS

Impeller Mean Exit Diameter 8.83 inches
Inducer Tip Diameter to Mean Impeller Exit Diameter Ratio 0.713

COMMON IMPELLER OPERATING CONDITIONS

Total Temperature Rise	390F
Static Temperature Rise	206F
Nominal Maximum Inlet Relative Mach No.	1.32
Mean Discharge Absolute Mach No.	1.14
Impeller Total Pressure Ratio	6.11
Impeller Static Pressure Ratio	2.82
Degree of Reaction	0.535

WADC TR56-589

118

CONFIDENTIAL

CONFIDENTIAL

TABLE III
INLET COORDINATES

<u>Axial Coord. Z(in.)</u>	<u>Radius to Hub R_h(in.)</u>	<u>Radius to Shroud R_s(in.)</u>
-5.800	4.062	
-5.400	3.750	
-5.000	3.418	
-4.600	3.086	
-4.200	2.754	
-4.000	2.588	
-3.800	2.422	
-3.600	2.256	
-3.400	2.090	
-3.300	2.008	
-3.200	1.926	
-3.100	1.848	
-3.000	1.776	
-2.900	1.708	
-2.800	1.645	
-2.700	1.588	
-2.600	1.534	
-2.500	1.482	
-2.400	1.435	
-2.300	1.390	
-2.200	1.348	
-2.100	1.313	
-2.000	1.280	
-1.900	1.249	
-1.800	1.221	
-1.700	1.194	
-1.600	1.170	
-1.500	1.149	
-1.400	1.132	4.360
-1.300	1.116	0.634 (radius)
-1.200	1.105	3.451
-1.100	1.097	3.394
-1.000	1.090	3.344
-0.900	1.084	3.301
-0.800	1.080	3.261

WADC TR56-589

CONFIDENTIAL

TABLE III (Cont'd)

<u>Axial Coord. Z(in.)</u>	<u>Radius to Hub R_h(in.)</u>	<u>Radius to Shroud R_s(in.)</u>
-0.700	1.078	3.229
-0.600	1.078	3.200
-0.500	1.075	3.183
-0.400	1.075	3.168
-0.300	1.075	3.157
-0.200	1.075	3.152
-0.100	1.075	3.150
-0.000	1.075	3.150

CONFIDENTIAL

TABLE IV
IMPELLER SERIES I - HUB AND SHROUD COORDINATES

<u>Axial Coord. Z(in.)</u>	<u>Radius to Hub R_h(in.)</u>	<u>Radius to Shroud R_g(in.)</u>	<u>Radius to Blade Tip R_x(in.)</u>
-0.000	1.075	3.150	3.135
0.100	1.080	3.150	3.135
0.200	1.091	3.150	3.135
0.300	1.103	3.150	3.135
0.400	1.119	3.150	3.135
0.500	1.136	3.151	3.136
0.600	1.158	3.152	3.137
0.700	1.162	3.156	3.141
0.800	1.215	3.165	3.150
0.900	1.251	3.178	3.162
1.000	1.290	3.192	3.176
1.100	1.335	3.213	3.197
1.200	1.384	3.237	3.220
1.300	1.438	3.265	3.248
1.400	1.478	3.297	3.280
1.500	1.561	3.334	3.317
1.600	1.634	3.375	3.356
1.700	1.714	3.420	3.403
1.800	1.804	3.472	3.454
1.900	1.906	3.528	3.510
2.000	2.020	3.589	3.571
2.100	2.148	3.657	3.638
2.200	2.294	3.732	3.712
2.300	2.446	3.816	3.796
2.400	2.611	3.911	3.889
2.500	2.782	4.020	3.998
2.600	2.954	4.128	4.104
2.700	3.125	4.250	4.226

CONFIDENTIAL

CONFIDENTIAL

TABLE IV (Cont'd)

<u>Axial Coord. Z(in.)</u>	<u>Radius to Hub R_h(in.)</u>	<u>Radius to Shroud R_s(in.)</u>	<u>Radius to Blade Tip R_t(in.)</u>
2.800	3.299	4.378	4.352
2.900	3.468	4.517	4.489
2.930		4.560	
2.943			4.548
3.000	3.346		
3.100	3.819		
3.200	4.000		
3.300	4.166		
3.360	4.270		

CONFIDENTIAL

CONFIDENTIAL

TABLE V
IMPELLER SERIES II - HUB AND SHROUD COORDINATES

<u>Axial Coord. Z(in.)</u>	<u>Radius to Hub R_h(in.)</u>	<u>Radius to Shroud R_s(in.)</u>	<u>Radius to Blade Tip R_x(in.)</u>
-1.200	1.105	3.451	
-1.100	1.097	3.394	
-1.000	1.090	3.344	
-0.900	1.087	3.298	
-0.800	1.084	3.257	
-0.700	1.083	3.223	
-0.600	1.083	3.195	
-0.500	1.083	3.169	
-0.400	1.086	3.148	
-0.300	1.090	3.131	
-0.200	1.096	3.117	
-0.100	1.103	3.106	
0.000	1.112	3.096	
0.100	1.120	3.089	
0.200	1.130	3.083	
0.300	1.139	3.080	
0.400	1.149	3.077	
0.500	1.160	3.075	
0.600	1.171	3.075	
0.700	1.184	3.076	3.061
0.800	1.199	3.076	3.063
0.900	1.215	3.083	3.067
1.000	1.234	3.091	3.075
1.100	1.256	3.102	3.086
1.200	1.282	3.119	3.103
1.300	1.315	3.141	3.124
1.400	1.352	3.167	3.150
1.500	1.395	3.198	3.181
1.600	1.440	3.235	3.218
1.700	1.491	3.283	3.264
1.800	1.542	3.337	3.318
1.900	1.597	3.400	3.381

JAIT CONFIDENTIAL

TABLE V (Cont'd)

<u>Axial Coord. Z (in.)</u>	<u>Radius to Hub R_h (in.)</u>	<u>Radius to Shroud R_s (in.)</u>	<u>Radius to Blade Tip R_x (in.)</u>
2.000	1.656	3.473	3.453
2.100	1.718	3.553	3.531
2.200	1.782	3.646	3.624
2.300	1.857	3.749	3.726
2.400	1.940	3.863	3.839
2.500	2.044	3.984	3.959
2.600	2.175	4.115	4.085
2.700	2.345	4.245	4.219
2.800	2.608	4.378	4.352
2.900	3.000	4.518	4.487
2.930		4.560	
2.943			4.548
3.000	3.357		
3.100	3.680		
3.200	3.939		
3.300	4.150		
3.360	4.270		

JAIT CONFIDENTIAL

CONFIDENTIAL

TABLE VI
IMPELLER I --- BLADE COORDINATES

Axial Coord. Z(in.)	Angular Coord. ϕ (deg)	Blade Thicknesses			
		Shroud		Hub	
		Norm.	Tang.	Norm.	Tang.
-0.700	-23.040			0.0280	0.0373
-0.650	-20.970			0.0280	0.0373
-0.600	-18.920			0.0300	0.0400
-0.550	-16.880			0.0360	0.0480
-0.5000	-14.870			0.0440	0.0530
-0.450	-12.926			0.0475	0.0570
-0.400	-11.330	0.0200	0.0368	0.0505	0.0600
-0.350	- 9.671	0.0230	0.0421	0.0540	0.0630
-0.300	- 8.160	0.0255	0.0464	0.0570	0.0655
-0.250	- 6.707	0.0270	0.0486	0.0600	0.0685
-0.200	- 5.285	0.0295	0.0525	0.0625	0.0710
-0.150	- 3.908	0.0320	0.0558	0.0650	0.0735
-0.100	- 2.570	0.0345	0.0600	0.0675	0.0750
-0.050	- 1.273	0.0365	0.0627	0.0700	0.0770
0.000	0.000	0.0385	0.0653	0.0720	0.0795
0.050	1.244	0.0405	0.0668	0.0745	0.0815
0.100	2.460	0.0425	0.0701	0.0760	0.0835
0.150	3.659	0.0445	0.0722	0.0785	0.0855
0.200	4.830	0.0465	0.0738	0.0805	0.0880
0.250	5.982	0.0485	0.0758	0.0825	0.0900
0.300	7.105	0.0505	0.0788	0.0845	0.0915
0.350	8.190	0.0525	0.079 ^o	0.0860	0.0935
0.400	9.250	0.0545	0.0823	0.0880	0.0950
0.450	10.286	0.0565	0.0840	0.0900	0.0970
0.500	11.300	0.0580	0.0855	0.0915	0.0980
0.550	12.294	0.0590	0.0860	0.0930	0.0995
0.600	13.260	0.0595	0.0845	0.0945	0.1005
0.650	14.192	0.0600	0.0835	0.0965	0.1020
0.700	15.100	0.0600	0.0825	0.0980	0.1030
0.750	15.971		0.0810	0.0990	0.1040
0.800	16.820		0.0800	0.1005	0.1050
0.850	17.660		0.0785	0.1015	0.1060
0.900	18.430		0.0770	0.1030	0.1070
0.950	19.175		0.0760	0.1040	0.1080
1.000	19.880	0.0600	0.0750	0.1050	0.1090

WADC TR56-589

CONFIDENTIAL

TABLE VI (Cont'd)

Axial Coord. Z (in.)	Angular Coord. ϕ (deg)	Blade Thicknesses			
		Shroud		Hub	
		Norm.	Tang.	Norm.	Tang.
1.100	21.180	0.0800	0.0725	0.1070	0.1100
1.200	22.350		0.0700	0.1080	0.1105
1.300	23.405		0.0680	0.1085	0.1105
1.400	24.360		0.0665	0.1080	0.1095
1.500	25.220		0.0650	0.1080	0.1075
1.600	25.980		0.0640	0.1025	0.1045
1.700	26.640		0.0635	0.0990	0.1005
1.800	27.210		0.0630	0.0960	0.0970
1.900	27.700		0.0620	0.0935	0.0940
2.000	28.145		0.0620	0.0920	0.0920
2.100	28.585		0.0615	0.0910	0.0910
2.200	29.025		0.0610	0.0900	0.0900
2.300	29.400		0.0610	0.0900	0.0900
2.400	29.760		0.0610	0.0900	0.0900
2.500	30.090		0.0605	0.0900	0.0900
2.600	30.390		0.0600	0.0900	0.0900
2.700	30.670	0.0585	0.0590	0.0900	0.0900
2.800	30.940	0.0560	0.0565	0.0900	0.0900
2.900	31.195	0.0515	0.0515	0.0900	0.0900
2.943		0.0480	0.0480		
3.000	31.470	0.0499	0.0499	0.0880	0.0880
3.100	31.730	0.0534	0.0534	0.0850	0.0850
3.200	31.365	0.0569	0.0569	0.0800	0.0850
3.300	32.175	0.0604	0.0604	0.0710	0.0710
3.360	32.300	0.0625	0.0625	0.0630	0.0650

CONFIDENTIAL

TABLE VII

IMPELLER IB --- BLADE COORDINATES

Axial Coord. Z(in.)	Angular Coord. ϕ (deg)	Blade Thicknesses			
		Shroud		Hub	
		Norm.	Tang.	Norm.	Tang.
-0.700	-27.9138			0.0280	0.0361
-0.650	-25.663			0.0280	0.0361
-0.600	-23.4376			0.0300	0.0386
-0.550	-21.2376			0.0380	0.0487
-0.500	-19.0630			0.0440	0.0563
-0.450	-16.9029			0.0475	0.0605
-0.400	-14.7946			0.0505	0.0641
-0.350	-12.7351			0.0540	0.0683
-0.300	-10.7313			0.0570	0.0713
-0.250	- 8.7856			0.0600	0.0744
-0.200	- 6.9004			0.0625	0.0763
-0.150	- 5.0828			0.0650	0.0783
-0.100	- 3.3301			0.0675	0.0804
-0.050	- 1.6349			0.0700	0.0825
0.000	0.0000	0.0200	0.0410	0.0720	0.0838
0.050	1.5673	0.0245	0.0490	0.0745	0.0860
0.100	3.0847	0.0285	0.0569	0.0760	0.0870
0.150	4.5588	0.0330	0.0648	0.0785	0.0892
0.200	5.9922	0.0370	0.0715	0.0805	0.0908
0.250	7.3868	0.0415	0.0780	0.0825	0.0926
0.300	8.7451	0.0455	0.0831	0.0845	0.0946
0.350	10.0691	0.0500	0.0890	0.0860	0.0959
0.400	11.3502	0.0536	0.0931	0.0880	0.0979
0.450	12.6009	0.0565	0.0959	0.0900	0.0982
0.500	13.8126	0.0580	0.0964	0.0915	0.1012
0.550	14.9926	0.0590	0.0962	0.0930	0.1025
0.600	16.1420	0.0595	0.0957	0.0945	0.1040
0.650	17.2627	0.0600	0.0950	0.0965	0.1059
0.700	18.3565		0.0934	0.0980	0.1071
0.750	19.4247		0.0924	0.0990	0.1080
0.800	20.4634		0.0912	0.1005	0.1091
0.850	21.4845		0.0897	0.1015	0.1099
0.900	22.4943		0.0884	0.1030	0.1112
0.950	23.4889		0.0875	0.1040	0.1120
1.000	24.4593	0.0600	0.0853	0.1050	0.1129

CONFIDENTIAL

TABLE VII (Cont'd)

Axial Coord. Z(in.)	Angular Coord. ϕ (deg)	Blade Thicknesses				
		Shroud		Hub		
		Norm.	Tang.	Norm.	Tang.	
1.100	26.3367	0.0600	0.0839	0.1070	0.1144	
1.200	28.1197	↑ ↓	0.0818	0.1080	0.1150	
1.300	29.8185		0.0797	0.1085	0.1152	
1.400	31.4891		0.0776	0.1080	0.1144	
1.500	32.9869		0.0760	0.1060	0.1121	
1.600	34.4760		0.0741	0.1025	0.1081	
1.700	35.9002		0.0724	0.0990	0.1040	
1.800	37.2565		0.0709	0.0960	0.1002	
1.900	38.5461		0.0694	0.0935	0.0973	
2.000	39.7540		0.0600	0.0680	0.0920	0.0952

CONFIDENTIAL

TABLE VIII
IMPELLER II --- BLADE COORDINATES

Axial Coord. Z(in.)	Angular Coord. ϕ (degr)	Blade Thicknesses			
		Shroud		Hub	
		Norm.	Tang.	Norm.	Tang.
0.100	0.000			0.0280	0.0371
0.200	4.134			0.0305	0.0383
0.250	6.031			0.0343	0.0428
0.300	7.903			0.0367	0.0455
0.350	9.739			0.0382	0.0470
0.400	11.532			0.0394	0.0483
0.450	13.278			0.0407	0.0496
0.500	14.975			0.0420	0.0507
0.550	16.622	0.0206	0.0412	0.0431	0.0517
0.600	18.209	0.0202	0.0395	0.0442	0.0525
0.650	19.721	0.0201	0.0382	0.0454	0.0532
0.700	21.155	0.0203	0.0376	0.0467	0.0539
0.750	22.499	0.0214	0.0381	0.0479	0.0545
0.800	23.774	0.0230	0.0392	0.0490	0.0552
0.850	24.984	0.0248	0.0410	0.0502	0.0559
0.900	26.124	0.0270	0.0425	0.0513	0.0565
0.950	27.204	0.0291	0.0442	0.0525	0.0574
1.000	28.224	0.0311	0.0457	0.0538	0.0584
1.100	30.134	0.0346	0.0480	0.0560	0.0601
1.200	31.868	0.0374	0.0495	0.0584	0.0620
1.300	33.457	0.0393	0.0500	0.0607	0.0640
1.400	34.922	0.0407	0.0502	0.0628	0.0658
1.500	36.264	0.0420	0.0505	0.0648	0.0675
1.600	37.494	0.0435	0.0510	0.0668	0.0693
1.700	38.622	0.0450	0.0517	0.0687	0.0710
1.800	39.649	0.0466	0.0526	0.0704	0.0726
1.900	40.575	0.0483	0.0537	0.0722	0.0743
2.000	41.414	0.0500	0.0550	0.0744	0.0764
2.100	42.164	0.0517	0.0561	0.0780	0.0798
2.200	42.837	0.0534	0.0572	0.0832	0.0848
2.300	43.448	0.0552	0.0586	0.0907	0.0921
2.400	44.004	0.0569	0.0598	0.1000	0.1012

CONFIDENTIAL

TABLE VIII (Cont'd)

IMPELLER II --- BLADE COORDINATES

Axial Coord. Z(in.)	Angular Coord. ϕ (degr)	Blade Thicknesses			
		Shroud		Hub	
		Norm.	Tang.	Norm.	Tang.
2.500	44.489	0.0584	0.0607	0.1121	0.1131
2.600	44.944	0.0597	0.0615	0.1251	0.1260
2.700	45.339	0.0597	0.0610	0.1328	0.1332
2.800	45.674	0.0577	0.0585	0.1356	0.1360
2.900	45.924	0.0485	0.0488	0.1335	0.1335
3.000	46.049	0.0463	0.0465	0.1286	0.1286
3.100	46.164	0.0500	0.0502	0.1203	0.1203
3.200	46.312	0.0525	0.0538	0.1060	0.1061
3.300	46.504	0.052	0.0575	0.0838	0.0840
3.360	46.661	0.0525	0.0598	0.0595	0.0598

CONFIDENTIAL

CONFIDENTIAL

TABLE IX
LEADING EDGES FOR IMPELLERS I, IB, II

Shape of initial leading edge profile

Axial Coordinates Z in.	Radius to point on leading edge		
	<u>Impeller I</u>	<u>Impeller IB</u>	<u>Impeller II</u>
-0.70	1.075	1.075	
-0.65	1.740	1.235	
-0.60	2.400	1.400	
-0.55	2.575	1.570	
-0.50	2.765	1.750	
-0.45	2.95	1.895	
-0.40	3.135	2.060	
-0.35		2.230	
-0.30		2.400	
-0.25		2.520	
-0.20		2.640	
-0.15		2.765	
-0.10		2.885	
-0.05		3.01	
-0.0		3.135	1.120
+0.05			1.650
+0.10			2.200
+0.15			2.295
+0.20			2.390
+0.25			2.490
+0.30			2.580
+0.35			2.675
+0.40			2.770
+0.45			2.870
+0.50			2.965
+0.55			3.060

CONFIDENTIAL

CONFIDENTIAL

NOMENCLATURE

a	Sonic velocity at temperature - T
A	Area
a	Radius of sphere and cylinder
c	Absolute velocity of fluid
c_p	Specific heat at constant pressure
d	Inducer diameter
D	Impeller mean exit diameter
F_r	Blade force upon fluid, in radial direction
f	$1 - \left(\frac{d_h}{d_t}\right)^2$
g	Gravitational constant
ΔH	Change in total head
h	Enthalpy
J	Mechanical equivalent of heat
k	Ratio of specific heats
K	$c_{m_1, \text{aver}} / c_{m_1, s}$
N	Rotative speed, revolutions per sec
m, n	System of coordinates relative to the streamlines in the meridional plane; m is along the streamline, increasing from impeller inlet to exit; n is normal to the streamline, increasing from shroud to hub

CONFIDENTIAL

n	Polytropic exponent
p	Pressure
Q	Impeller volume flow under inlet conditions
r	Radial coordinate measured from axis of rotation
\bar{R}	Perfect gas constant for air
R	Streamline radius of curvature in the meridional plane
s	Entropy
T	Temperature R
t	Tangential blade thickness
u	impeller tangential velocity = $r\omega$
U	Impeller mean exit tip speed
U	Uniform flow at $\pm\infty$ for a cylinder or a sphere
w	Impeller relative velocity
W_c	Compressor mass rate of flow
z	Axial coordinate, increasing from the impeller inlet to the impeller exit
Z	Number of blades

CONFIDENTIAL

SUBSCRIPTS

- () **aver** **Average**
- () **B** **Blade**
- () **C** **Compressor**
- () **H** **Hub**
- () **I** **Impeller**
- () **is** **Isentropic**
- () **m** **Refers to the meridional component**
- () **n** **Refers to a component normal to the streamline in the meridional plane**
- () **p** **Potential flow**
- () **pr** **Applies to the blade pressure surface**
- () **r** **Radial component**
- () **ϕ** **Along a streamline**
- () **s** **Shroud**
- () **suct** **Supplies to the blade suction surface**
- () **u** **Tangential component**
- () **x** **Impeller blade tip**
- () **z** **Axial component**

CONFIDENTIAL

CONFIDENTIAL

GREEK SYMBOLS

α	Angle between the axis of rotation and an tangent to a stream-line in the meridional plane
β	Angle between the relative flow direction and the meridional plane
δ	Pressure/14.7
η	Efficiency
ϵ	Viscous clogging coefficient
λ	Temperature coefficient
ν	Specific Speed
ϕ	Flow parameter
ϕ	Angular coordinate in a plane normal to the impeller axis of rotation
ψ	Stream function, such that
	$\frac{\partial \psi}{\partial r} = r \frac{\rho}{\rho_0} w_z$
ρ	Mass density
σ	Geometrical parameter $\frac{2n}{Z} \sin a$
θ	Temperature/520, Polar coordinate for cylinder and sphere
ω	Rotational speed, rad per sec
ζ	Vorticity

CONFIDENTIAL

BIBLIOGRAPHY

- 1) J. E. Coppage, F. Dallenbach, H. P. Eichenberger, G. H. Hlavka, E. M. Knoernschild, N. Van Le - "Study of Supersonic Radial Compressors for Refrigeration and Pressurization Systems". AiResearch Manufacturing Co., Feb., 1956.
- 2) Walter M. Osborn and Joseph T. Hamrick - "Design and Test of Mixed-Flow Impellers, I - Aerodynamic Design Procedure". NACA - RM E52E05 Sept., 19, 1952, Classification cancelled.
- 3) Joseph R. Withee, Jr., and William L. Beede - "Design and Test of Mixed-Flow Impellers, II - Experimental Results, Impeller Model MFI-1A". NACA - RM E52E22 Sept., 19, 1952, Confidential.
- 4) Joseph T. Hamrick, Walter M. Osborn, and William L. Beede - "Design and Test of Mixed-Flow Impellers, III - Design and Experimental Results for Impeller Model MFI-2A and Comparison with Impeller Model MFI-1A". NACA - RM E52L22a March 10, 1953, Confidential.
- 5) Joseph T. Hamrick, William L. Beede, and Joseph R. Withee, Jr., "Design and Test of Mixed-Flow Impellers, IV - Experimental Results for Impeller Models MFI-1 and MFI-2 with Changes in Blade Height". NACA - RM E53L02 February 11, 1954, Confidential.
- 6) Walter M. Osborn - "Performance of Mixed-Flow Impeller, Model MFI-1B, with Diffuser Vanes at Equivalent Impeller Speeds from 1100 to 1700 Feet per Second". NACA - RM E54D23 June 16, 1954, Confidential.
- 7) Joseph T. Hamrick and Walter M. Osborn - "Design and Test of Mixed-Flow Impellers, V - Design Procedure and Performance Results for Two-Vaned Diffusers Tested with Impeller Model MFI-1B". NACA - RM E55E13 July 7, 1955, Confidential.

CONFIDENTIAL

- 8) A. Busemann, Das Förderhöhenverhältnis Radialer Kreiselpumpen mit Logarithmisch - Spiraligen Schaufeln". Z. Agnew Math. Mech. Vol. 8, Page 372, 1928.
- 9) A. Stodola - "Steam and Gas Turbines". McGraw-Hill Book Co., N.Y. 1927.
- 10) B. Eckert - "Axialkompressoren und Radial-Kompressoren". Springer Verlag, Berlin - 1953.
- 11) Bruno Eck - "Ventilatoren" Springer Verlag Berlin, 1950.
- 12) Wislicenus - "Fluid Mechanics of Turbomachinery". McGraw-Hill Book Co., N.Y., 1947.
- 13) Joseph T. Hamrick, Ambrose Ginsburg and Walter M. Osborn - "Method of Analysis for Compressible Flow Through Mixed-Flow Centrifugal Impellers of Arbitrary Design" NACA Report 1082.
- 14) C. H. Wu - "Three-Dimensional Flow in Turbomachinery". NACA TN2604.
- 15) G. O. Ellis, J. D. Stanitz - "Comparison of Two- and Three-Dimensional Potential Flow Solutions in a Rotating Impeller Passage". NACA TN2806.
- 16) J. T. Hamrick, A. Ginsburg, W. M. Osborn - "Method of Analysis for Compressible Flow Through Mixed-Flow Impellers of Arbitrary Design". NACA TN2165.
- 17) J. D. Stanitz, G. O. Ellis - "Two-Dimensional Flow on General Surfaces of Revolution in Turbomachines". NACA TN2654.
- 18) General Electric Publication - Cat. No. 112L152 g1, g2, - Instructions Analog Field Plotter.
- 19) P. Ruden - "Investigation of Single-Stage Axial Fans". NACA TN1604.

CONFIDENTIAL

- 20) J. D. Stanitz, G. O. Ellis - "Two-Dimensional Compressible Flow in Centrifugal Compressors with Straight Blades". NACA - Report 954.
- 20a) A. J. Stepanoff - "Centrifugal and Axial-Flow Pumps". John Wiley and Sons, 1948.
- 21) Walter M. Osborn - "Design and Test of Mixed-Flow Impellers, VII-Experimental Results for Parabolic-Bladed Impeller with Alternate Blades Cut Back to Form Splitter Vanes". NACA RM E55L15, March 16, 1956, Confidential.
- 22) Kenneth J. Smith and Walter M. Osborn - "Design and Test of Mixed-Flow Impellers, VI - Performance of Parabolic-Bladed Impeller with Shroud Redesigned by Rapid Approximate Method". NACA RM E55F23, Sept. 7, 1955, Confidential.
- 23) Ward W. Wilcox - "Design and Performance of Experimental Axial-Discharge Mixed-Flow Compressor, II - Performance of Impeller". NACA RM E8F07, August 12, 1948, Classification cancelled.
- 23a) Arthur W. Goldstein - "Design and Performance of Experimental Axial-Discharge Mixed-Flow Compressor, I-Impeller Design Theory". NACA RM E8F04 August 12, 1948, Restricted.
- 24) Ward W. Wilcox and William H. Robbins - "Design and Performance of an Experimental Axial-Discharge Mixed-Flow Compressor, III-Over-all Performance of Impeller and Supersonic-Diffuser Combination". NACA RM E51A02, April 30, 1951, Confidential.
- 25) John F. Klapproth, John J. Jacklitch, Jr., and Edward R. Tysi - "Design and Performance of a 1400-Foot-Per-Second-Tip-Speed Supersonic Compressor Rotor". NACA RM E55A27, April 11, 1955, Confidential.
- 26) Francis C. Schwenk, Seymour Lieblein, and Geo. W. Lewis, Jr. - "Experimental Investigation of an Axial-Flow Compressor Inlet Stage Operating at Transonic Relative Inlet Mach Numbers, III-Blade-Row Performance of Stage with Transonic Rotor and Subsonic Stator at Corrected Tip Speeds of 800 and 1000 Feet per Second". NACA RM E53G17, September 16, 1953, Confidential.

CONFIDENTIAL

- 27) Edward R. Tysl, Francis C. Schwenk, and Thomas B. Watkins - "Experimental Investigation of a Transonic Compressor Rotor with a 1.5-Inch Chord Length and an Aspect Ratio of 3.0, I-Design, Over-all Performance, and Rotating-Stall Characteristics". NACA RM E54L31, March 28, 1955, Confidential.
- 28) Seymour Lieblein, Geo. W. Lewis, Jr., and Donald M. Sandercock - "Experimental Investigation of an Axial-Flow Compressor Inlet Stage Operating at Transonic Relative Inlet Mach Numbers, I-Overall Performance of Stage with Transonic Rotor and Subsonic Stators up to Rotor Relative Inlet Mach Number of 1.1". NACA RM E52A24, March 10, 1952, Confidential.
- 29) Melvyn Savage and A. Richard Felix - "Investigation of a High-Performance Axial-Flow Compressor Transonic Inlet Rotor Designed for 37.5 Pounds per Second per Square Foot of Frontal Area - Aerodynamic Design and Over-all Performance". NACA RM L55A05, March 24, 1955, Confidential.
- 30) Ward W. Wilcox and Linwood C. Wright - "Investigation of Two-Stage Counter-rotating Compressor, I-Design and Over-all Performance of Transonic First Compressor Stage". NACA RME56C15, May 22, 1956, Confidential.
- 31) Ward W. Wilcox - "Investigation of Impulse-Type Supersonic Compressor with Hub-Tip Ratio of 0.6 and Turning to Axial Direction, II-Stage Performance with Three Different Sets of Stators". NACA RM E55F28, August 16, 1955, Confidential.
- 32) Ward W. Wilcox - Investigation of Impulse-Type Supersonic Compressor with Hub-Tip Ratio of 0.6 and Turning to Axial Direction, I-Performance of Rotor Alone". NACA RM E54B25, May 6, 1954, Confidential.

CONFIDENTIAL

CONFIDENTIAL

- 33) John F. Klapproth - "General Considerations of Mach Number Effects on Compressor-Blade Design". NACA RM E53L22a, April 7, 1954, Confidential.
- 34) A. D. Prian, D. J. Michel - "An Analysis of the Flow in the Rotating Passage of Large Radial Inlet Centrifugal Compressors at a Tip Speed of 700 ft/sec.". NACA TN2548.
- 35) D. J. Michel, A. Ginsburg, J. Mizisin - "Experimental Investigation of Flow in the Rotating Passages of a 48 in. Impeller at Low Tip Speeds". NACA RM E51D20.
- 36) D. J. Michel, J. Mizisin, V. D. Prian - "Effect of Changing Passage Configuration on Internal Flow Characteristics of a 48 in. Centrifugal Compressor - Part I Change in Blade Shape". NACA TN2706.
- 37) J. Mizisin, D. J. Michel - "Effect of Changing Passage Configuration on Internal Flow Characteristics of a 48 in. Centrifugal Compressor - Part II, Change in Hub Shape". NACA TN2835.
- 37a) A. Kantrowitz - "The Supersonic Axial Compressor". NACA Report No. 974.
- 38) Goldstein and Schacht - "Performance of a Supersonic Compressor with Swept and Tilted Diffuser Blades". NACA RME54L29.
- 39) Geo. W. Lewis, Jr. - "Experimental Investigation of Axial-Flow Compressor Inlet Stage Operating at Transonic Relative Inlet Mach Numbers, II - Blade Coordinate Data". NACA E52C77.
- 40) Goldberg - "Experimental Investigation of an Axial-Flow Supersonic Compressor Having Sharp Leading Edges, with Mean $l/c = 0.08$ and of the Effect of Leading Edge Radius". NACA RM L54K16.
- 41) C. H. Wu and E. L. Costilow - "A Method of Solving the Direct and Inverse Problem of Supersonic Flow Along Arbitrary Stream Filaments of Revolution in Turbomachines". NACA TN2492.

CONFIDENTIAL

CONFIDENTIAL

- 42) E. L. Costilow - "Application of Characteristic Blade-to-Blade Solution to Flow in a Supersonic Rotor with Varying Stream Filament Thickness". NACA TN2992.
- 43) C. H. Wu - "A General Theory of Three-Dimensional Flow with Subsonic and Supersonic Velocity in Turbomachines having Arbitrary Hub and Casing Shapes - Part I and II. ASME Paper No. 50-A-79.
- 44) E. Beder and R. D. Buhler - "A Study of a Cascade System for Supersonic Flow Diffusion". WADC Technical Report 54-261, May, 1954.
- 45) J. Todd - "An Experimental Study of Three-Dimensional High-Speed Air Conditions in a Cascade of Axial Flow Compressor Blades". Aeronautical Research Council - R and M 2792 ARC Technical Report.
- 46) E. M. Knoernschild - "Proposed Study of Radial and Mixed-Flow Compressors". AIResearch Report No. AAC-1844, Rev. 1 Nov. 12, 1954.
- 47) H. P. Eichenberger - "First Quarterly Progress Report Research on Mixed-Flow Compressors". AIResearch Report No. GT-1298, Rev. 1, July 15, 1955.
- 48) J. L. Dussourd - "Second Quarterly Progress Report, Research on Mixed-Flow Compressors". AIResearch Report No. GT-5138-R, October 15, 1955.
- 49) J. L. Dussourd - "Third Quarterly Progress Report, Research on Mixed-Flow Compressors" - AIResearch Report No. GT-5215-R, January 15, 1956.
- 50) J. L. Dussourd - "Fourth Quarterly Progress Report, Research on Mixed-Flow Compressors". -AIResearch Report No. GT-5346-R, July 15, 1956.
- 51) H. P. Eichenberger - "Proposal for the Fabrication, Testing and Analysis of Mixed-Flow Impellers". AIResearch Report No. GT-5194-R, Rev. 1, Feb. 29, 1956.
- 52) C. H. Wu - "A General Through-Flow Theory of Fluid Flow with Subsonic or Supersonic Velocity in Turbomachines of Arbitrary Hub and Casing Shapes". NACA TN2302.

CONFIDENTIAL

APPENDIX A

**DERIVATION OF RELATIONS CONTROLLING
THE IMPELLER EXTERNAL OVER-ALL GEOMETRY**

(1) IMPELLER INLET TO EXIT DIAMETER RATIO

(a) Relation between specific speed and inlet to exit diameter ratio

$$v = \frac{N\sqrt{Q}}{(g\Delta H)^{3/4}}$$

Allowing

$$N = \frac{U}{\pi D}$$

$$Q = \frac{\pi}{4} c_{m1} d_s^2 f$$

$$g\Delta H = \eta_1 \lambda U^2$$

$$(c_{m1})_{aver} = K c_{m1s}$$

$$\left(\frac{U}{D}\right) \frac{1}{c_{m1s}} = \tan \beta_s$$

There follows

$$v = 0.282 \frac{\sqrt{Kf}}{(\eta_1 \lambda)^{3/4}} \frac{1}{\sqrt{\tan \beta_s}} \left(\frac{d_s}{D}\right)^{3/2}$$

In this equation:

(1) $\tan \beta_s$ can be evaluated for the condition of minimum inducer tip relative Mach Number
(See part B below.)

(2) For conventional impellers the ratio $\frac{\sqrt{Kf}}{(\eta_1 \lambda)^{3/4}}$ is never very far from 1.0.

(3) Impeller specific speed is then directly related to the ratio of impeller inlet to exit diameters.

CONFIDENTIAL

(b) Value of β_{s1} for minimum inlet relative velocity

This condition is very nearly that of minimum inducer tip relative Mach Number. It will be worked out for constant rpm and constant mass rate of flow

$$w_{s1}^2 = (N\pi)^2 d_s^2 + \frac{(W_c/g\rho_1)^2}{(Kf\frac{\pi}{4})^2} \frac{1}{d_s^4}$$

Introducing $A^* = \frac{A^*}{A} \frac{\pi d_s^2}{4} f$

and differentiating with respect to d_s^2 , $\frac{d(w_{s1}^2)}{d(d_s^2)} = (N\pi)^2$

$$-2\left(\frac{W_c}{\frac{P}{\rho_{01}} Kf \frac{\pi}{4} d_s^3 g\rho_{01}}\right)^2 + \frac{W_c^2}{d_s^5 \left(\frac{\pi}{4}\right)^2 f^2 \frac{A^*}{A} K^2 (g\rho_{01})^2} \frac{d(P_{01}/P)^2}{d(A/A^*)}$$

Equating the right-hand side to zero and solving for d_s

$$d_s = \left(\frac{W_c}{N\frac{\pi}{4} Kf g\rho_{01}}\right)^{1/3} \left[2\left(\frac{P_{01}}{P}\right)^2 - \frac{A}{A^*} \frac{d(P_{01}/P)^2}{d(A/A^*)}\right]^{1/6}$$

This relation may now be introduced into an expression for $\tan \beta_{s1}$

$$\tan \beta_{s1} = \frac{N\pi d_s}{W_c/g\rho \frac{\pi}{4} d_s^2 Kf}$$

$$= \frac{P}{P_{01}} \sqrt{\left[2\left(\frac{P_{01}}{P}\right)^2 - \frac{A}{A^*} \frac{d(P_{01}/P)^2}{d(A/A^*)}\right]} \quad (A-2)$$

The right-hand side is a function of the average inlet Mach Number only. It is so plotted on figure 2.

CONFIDENTIAL

(c) Expression for specific speed in terms of conventional compressor coordinates.

It is convenient to express dimensionless specific speed in terms of more conventional compressor coordinates

$$v = \frac{N\sqrt{Q}}{(g\Delta H)^{3/4}} \quad \text{where}$$

$$N = \text{RPM}/60$$

$$Q = \frac{W_c}{60g\rho_{o1}} = 0.2185 \frac{W_c \theta_{o1}}{\delta_{o1}}$$

where W_c is in lbs/min.

$$\begin{aligned} g\Delta H &= Jg c_p (\Delta T_o)_{is} \\ &= 6060 T_{o1} \left[\frac{(T_{o2})_{is} - T_{o1}}{T_{o1}} \right] \\ &= 3\,150\,000 \theta_{o1} \left[\left(\frac{P_{o2}}{P_{o1}} \right)_{is}^{\frac{k-1}{k}} - 1 \right] \end{aligned}$$

Combining all this

$$v = \frac{1}{0.913 \times 10^7} \frac{\text{RPM}}{\sqrt{\theta_{o1}}} \left(\frac{W_c \sqrt{\theta_{o1}}}{\delta_{o1}} \right)^{1/2} \frac{1}{\left[\left(\frac{P_{o2}}{P_{o1}} \right)_{is}^{\frac{k-1}{k}} - 1 \right]^{3/4}} \quad (\text{A-4})$$

$$= \frac{2.095}{10^4} \left(\frac{U}{\sqrt{\theta_{o1}}} \right) \left(\frac{W_c \sqrt{\theta_{o1}}}{D^2 \delta_{o1}} \right)^{1/2} \frac{1}{\left[\left(\frac{P_{o2}}{P_{o1}} \right)_{is}^{\frac{k-1}{k}} - 1 \right]^{3/4}} \quad (\text{A-5})$$

CONFIDENTIAL

- (d) Expression for the ratio of inducer tip diameter to impeller tip diameter.

In equation A-5, we may replace $\left[\left(\frac{\rho_{02}}{\rho_{01}} \right)^{\frac{k-1}{k}} - 1 \right]$

$$\text{by } \frac{1}{3.15 \times 10^6} \lambda \eta_I \frac{U^2}{\theta_{01}}$$

Equation A-1 and A-5 in this form.

$$0.282 \frac{\sqrt{Kf}}{(\eta_I \lambda)^{3/4}} \frac{1}{\sqrt{\tan \beta_s}} \left(\frac{d_s}{D} \right)^{3/2} = \frac{2.095}{10^6} \left(\frac{U}{\sqrt{\theta_{01}}} \frac{1}{D} \right) \times$$

$$\left(\frac{Wc \sqrt{\theta_{01}}}{\delta_{01}} \right)^{1/2} \frac{1}{\left(\frac{1}{3.15 \times 10^6} \lambda \eta_I \frac{U^2}{\theta_{01}} \right)^{3/4}}$$

and after simplification.

$$\left[\frac{U}{\sqrt{\theta_{01}}} \frac{Kf}{\frac{Wc \sqrt{\theta_{01}}}{\delta_{01}}} \right]^{1/2} \frac{1}{\sqrt{\tan \beta_s}} D_{\text{inches}} = 6.69 \sqrt{\left(\frac{D}{d_s} \right)^3} \quad (\text{A-6})$$

This equation conveys essentially the same information as equation A-1. Its form is, however, more convenient and it is plotted on Figure 3.

CONFIDENTIAL

(2) IMPELLER EXIT WIDTH

(a) State of fluid at impeller exit. The state of the fluid anywhere in the impeller can be expressed in terms of the impeller tangential velocity and the fluid relative velocity from the first law.

$$\frac{kR}{k-1} T_{01} + \frac{uc_u}{g} = \frac{kR}{k-1} T + \frac{c^2}{2g}$$

From the geometry

$$w^2 = c^2 + u^2 - 2uc_u$$

Combining

$$2g \frac{kR}{k-1} (T_{01} - T) = w^2 - u^2$$

$$\frac{T}{T_{01}} = 1 + \frac{k-1}{2} \left(\frac{u^2}{a_{01}^2} - \frac{w^2}{a_{01}^2} \right) \quad (A-7)$$

which is useful in calculating impeller temperatures. Impeller pressures and densities are computed by assuming isentropic relations to hold in the inlet, upstream of the leading edge and adiabatic flow with losses to exist within the impeller. On this basis the density ratio follows as

$$\begin{aligned} \rho/\rho_{01} &= (\rho_{1av}/\rho_{01}) (\rho/\rho_{1av}) \\ &= (\rho_{1av}/\rho_{01}) \left(\frac{T}{T_{01}} \cdot \frac{T_{01}}{T_{1av}} \right)^{1/n-1} \\ &= (\rho_{1av}/\rho_{01}) \left\{ \frac{T_{01}}{T_{1av}} \left[1 + \frac{k-1}{2} \left(\frac{u^2}{a_{01}^2} - \frac{w^2}{a_{01}^2} \right) \right] \right\}^{1/n-1} \quad (A-8) \end{aligned}$$

CONFIDENTIAL

Similarly for pressure

$$\frac{p_2}{p_{01}} = \left(\frac{\rho_{1av}}{\rho_{01}} \right) \left\{ \frac{T_{02}}{T_{1av}} \left[1 + \frac{k-1}{2} \left(\frac{u^2}{a_{01}^2} - \frac{w^2}{a_{01}^2} \right) \right] \right\}^{\frac{n}{n-1}} \quad (A-9)$$

In this equation $\frac{T_{02}}{T_{1av}}$, $\frac{\rho_{02}}{\rho_{1av}}$, $\frac{p_{02}}{p_{1av}}$

are functions of the average inlet Mach Number. The quantity n is a polytropic exponent, which differs from k in that it makes allowance for estimated impeller losses. It is related to the impeller efficiency in the following manner.

$$\frac{(T_{02})_S}{T_{01}} - 1 = \eta_I \left(\frac{T_{02}}{T_{01}} - 1 \right)$$

but

$$\frac{(T_{02})_S}{T_{01}} = \frac{(T_2)_S}{T_1} \frac{T_1}{T_{01}} \left(\frac{T_{02}}{T_2} \right)_S$$

$$\frac{T_{02}}{T_{01}} = \frac{T_2}{T_1} \frac{T_1}{T_{01}} \frac{T_{02}}{T_2}$$

Here $\left(\frac{T_{02}}{T_2} \right)_S = \frac{T_{02}}{T_{01}}$ and $\frac{p_2}{p_1} = \frac{(p_2)_S}{p_1}$

combining

$$\frac{T_1}{T_{01}} \frac{T_{02}}{T_2} \left[\left(\frac{p_2}{p_1} \right)^{\frac{k-1}{k}} - \left(\frac{p_2}{p_1} \right)^{\frac{n-1}{n}} \eta_I \right] = 1 - \eta_I \quad (A-10)$$

For design purposes, the value of n may be computed from this equation for desired values of wheel reaction and wheel inlet velocities, and for estimated impeller efficiencies.

CONFIDENTIAL

(b) Impeller Viscous flow coefficient

(1) Original definition

In the design procedure of this report, the viscous flow coefficient may be defined as the ratio of the impeller exit width to the theoretical width that would satisfy mass flow impeller efficient and the exit velocity triangle. The velocity triangle takes into consideration all the impeller losses without separating impeller windage and internal losses which thus affect both the leaving total pressure and the leaving tangential velocity component. Thus the viscous flow coefficient is more or less a catch-all term seeking to account all at once for the impeller external losses and boundary layer development as well.

Recent experimental work at AIResearch shows that this coefficient, as defined above, can be either smaller or greater than 1.0. That this is possible is made clear if one realizes that consistency must be had between the impeller efficiency and the flow factor. A flow factor is necessary only insofar as it relates the energy profile and the mass flow profile at the exit. This factor is necessarily close to unity, except for grossly distorted velocity distributions. The introduction of the windage loss into this definition can only be justified from the standpoint of simplification of the design procedure.

(2) Exact definition

Two rigorous definitions of an exit flow coefficient can be formulated. Only the second one however is really useful for design purposes.

CONFIDENTIAL

The exit flow coefficient may be defined as the ratio of the actual to the theoretical flow. Theoretical flow may be visualized as that calculated from a theoretical isentropic impeller of the same aerodynamic work input and the same degree of reaction. Such a definition is however quite trivial. Little usefulness can be made of the resulting flow coefficient which further has the disadvantage of having the rather low numerical value of 0.6-0.7.

A useful definition of flow coefficient is that which is prescribed by the necessary consistency which must exist between flow and energy if an averaged two-dimensional profile, as is present at the impeller discharge, is to be represented by a single velocity triangle. In simple language, it is a factor required by the fact that the meridional component of the integrated exit absolute velocity is different from the integrated value of the meridional component of this velocity. The resulting flow coefficient is obviously a function of the shape of the velocity profile. For a good exit profile at the discharge of an impeller of this type, it is about 0.96. This coefficient is the only one that needs to be taken into account in fixing the impeller discharge width.

CONFIDENTIAL

APPENDIX B

EQUATIONS FOR THE AXI-SYMMETRIC FLOW IN IMPELLER PASSAGES - EQUATIONS FOR DESIGN PROCEDURE

Below are given the equations controlling the motion of the fluid inside the impeller. They are derived for the axi-symmetric case corresponding to an infinite number of blades, and for inviscid, incompressible fluid.

I GENERAL CASE

Derivation of the particular form of the general equation used in the design procedure will be made using as a starting point the vorticity component in the meridional plane.

$$\frac{\partial w_m}{\partial n} + \frac{w_m}{R} = - \frac{\tan \beta}{r \cos \alpha} \left[\frac{\partial(r c_u)}{\partial r} \right] \quad Z = \text{constant} \quad (\text{B-1})$$

The vector representing the total vorticity is a vector directed along the blade and along a line of constant angular momentum in the meridional plane. The axial component of this vorticity is

$$\xi_z = - \frac{1}{r} \frac{\partial(r c_u)}{\partial r}$$

which is nothing more than the definition of vorticity in radial coordinates (ref. 12). The tangential component is

$$- \frac{\tan \beta}{r \cos \alpha} \left[\frac{\partial(r c_u)}{\partial r} \right]$$

Equation (B-1) may also be derived directly from the Lorenz equations.

Now returning to equation (B-1)

$$r c_u = r^2 \omega - r w_m \tan \beta$$

$$\left[\frac{\partial(r c_u)}{\partial r} \right]_{Z = \text{constant}} = 2 r \omega - r w_m \frac{1}{\cos^2 \beta} \frac{\partial \beta}{\partial r} - r \tan \beta \frac{\partial w_m}{\partial r} - w_m \tan \beta \quad (\text{B-2})$$

CONFIDENTIAL

The condition of radial blade elements is introduced in the form

$$\left[\frac{\tan \beta}{r \cos \alpha} \right]_{Z = \text{constant}} = \text{constant}$$

or

$$\frac{\partial \beta}{\partial r} = -\tan \beta \cos^2 \beta \tan \alpha \frac{d\alpha}{dr} + \frac{\cos^2 \beta}{r} \tan \beta \quad (B-3)$$

In addition

$$\frac{dw_m}{dr} = \frac{\partial w_m}{\partial m} \sin \alpha - \frac{\partial w_m}{\partial n} \cos \alpha \quad (B-4)$$

$$\frac{d\alpha}{dr} = \frac{\partial \alpha}{\partial m} \sin \alpha - \frac{\partial \alpha}{\partial n} \cos \alpha \quad (B-5)$$

Combining equations (B-1, -2, -3, -4, -5)

$$\begin{aligned} \frac{\partial w_m}{\partial n} + \frac{w_m}{R} = & -\frac{\tan \beta}{r \cos \alpha} \left\{ 2r\omega - \frac{r w_m}{\cos^2 \beta} \left[-\sin \beta \cos \beta \tan \alpha \right. \right. \\ & \left. \left. \left(\frac{\partial \alpha}{\partial m} \sin \alpha - \frac{\partial \alpha}{\partial n} \cos \alpha \right) + \frac{\cos \beta}{r} \sin \beta \right] - r \tan \beta \left[\frac{\partial w_m}{\partial m} \sin \alpha \right. \right. \\ & \left. \left. - \frac{\partial w_m}{\partial n} \cos \alpha \right] - w_m \tan \beta \right\} \end{aligned}$$

which simplifies to

$$\begin{aligned} \frac{\partial w_m}{\partial n} (1 + \tan^2 \beta) + w_m \left[\frac{1}{R} (1 + \tan^2 \beta \tan^2 \alpha) - \tan^2 \beta \tan \alpha \frac{\partial \alpha}{\partial n} \right. \\ \left. - \frac{2 \tan^2 \beta}{r \cos \alpha} \right] = \tan^2 \beta \tan \alpha \frac{\partial w_m}{\partial m} - \frac{\tan \beta}{\cos \alpha} 2\omega \end{aligned}$$

CONFIDENTIAL

II SPECIFIC LOCAL REGIONS

In specific regions of the impeller, the general equation can be expressed in simplified forms suitable for hand computation.

(a) Inducer portion of impeller.

Starting with equation B-1 and introducing the condition of radial blade elements in terms of the shroud conditions

$$\frac{\tan \beta}{r \cos \alpha} = \frac{\tan \beta_s}{r_s \cos \alpha_s}$$

$$\frac{\partial w_m}{\partial n} + \frac{w_m}{R} = - \frac{\tan \beta_s}{r_s \cos \alpha_s} \left[\frac{\partial (rc_u)}{\partial r} \right]_{Z = \text{constant}} \quad (\text{B-100})$$

Now $rc_u = r^2 \omega - r w_m \tan \beta$ as before

$$= r^2 \omega - \frac{r^2 w_m}{r_s} \tan \beta_s \frac{\cos \alpha}{\cos \alpha_s}$$

In the inducer $\frac{\cos \alpha}{\cos \alpha_s} \cong 1.0$

$$\frac{\partial (rc_u)}{\partial r} = 2r\omega - \frac{\tan \beta_s}{r_s} \left[r^2 \frac{\partial w_m}{\partial r} + 2r w_m \right]$$

Eq (B-100) becomes

$$\frac{\partial w_m}{\partial n} + \frac{w_m}{R} = - \frac{\tan \beta_s}{\cos \alpha_s} \left\{ 2\omega \frac{r}{r_s} - \tan \beta_s \left[\frac{r^2}{r_s^2} \frac{\partial w_m}{\partial r} + 2w_m \frac{r}{r_s} \right] \right\}$$

As a further simplifying assumption,

$$\frac{\partial w_m}{\partial r} \cong \frac{\partial w_m}{\partial n}$$

in the inducer section and the final equation becomes

$$\frac{\partial w_m}{\partial n} \left[1 + \frac{1}{\cos \alpha_s} \left(\tan \beta_s \frac{r}{r_s} \right)^2 \right] + w_m \left[\frac{1}{R} - 2 \frac{\tan^2 \beta_s}{\cos \alpha_s} \frac{r}{r_s^2} \right] = - 2\omega \frac{\tan \beta_s}{\cos \alpha_s} \frac{r}{r_s} \quad (\text{B-102})$$

CONFIDENTIAL

This equation is linear and may be solved with the help of an integrating factor.

$$\text{Letting } 1 + \frac{1}{\cos \alpha_s} \left(\tan \beta_s \frac{r}{r_s} \right)^2 = f_1$$

$$\frac{1}{R} - 2 \frac{\tan^2 \beta_s}{\cos \alpha_s} \frac{r}{r_s^2} = f_2$$

$$- 2 w \frac{\tan^2 \beta_s}{\cos \alpha_s} \frac{r}{r_s} = f_3$$

$$f_2 / f_1 = f_4 \quad f_3 / f_1 = f_5$$

the equation reduces to

$$\frac{\partial w_m}{\partial n} + f_4 w_m = f_5$$

$e^{\int f_4 dn}$ is the integrating factor and

$$w_m = \frac{1}{e^{\int f_4 dn}} \int e^{\int f_4 dn} f_5 dn + \frac{K}{e^{\int f_4 dn}}$$

were the constant. K must be such that continuity is satisfied in the impeller passage.

$$K = \frac{\frac{W_c}{\epsilon} - \int_{\text{shroud}}^{\text{hub}} \left[g \rho (2 \pi r - Z) \frac{1}{e^{\int_0^n f_4 dn}} \int_0^n e^{\int_0^n f_4 dn} f_5 dn \right] dn}{\int_{\text{shroud}}^{\text{hub}} \frac{1}{e^{\int_0^n f_4 dn}} g \rho (2 \pi r - Z) dn}$$

CONFIDENTIAL

(b) Downstream portion of impeller

In the downstream portions of the impeller, simplifying assumptions other than those in the inducer portion may be made for easier handling of the equation. In view of the fact that little distortion of the meridional streamlines occurs in the down-stream portion, it is pertinent to assume that their radii of curvature will remain nearly equal to the radii of curvature of the potential flow through the corresponding bladeless passage. Starting from equation (B-101)

$$\frac{\partial w_m}{\partial n} + \frac{w_m}{R} = - \frac{\tan \beta_2}{\cos \alpha_2} \left[2 \omega \frac{r}{r_2} - \tan \beta_2 \left(\frac{r^2}{r_2^2} \frac{\partial w_m}{\partial r} + 2 w_m \frac{r}{r_2} \right) \right] \quad (\text{B-101})$$

Here, we express the meridional velocity in terms of meridional velocity for zero vorticity $(w_m)_p$ and a correction quantity

Δw_m

$$w_m = (w_m)_p + \Delta w_m$$

For the potential flow

$$\frac{\partial (w_m)_p}{\partial n} + \frac{(w_m)_p}{R} = 0 \quad (\text{B-103})$$

CONFIDENTIAL

Further

$$\begin{aligned} \left(\frac{\partial w_m}{\partial r} \right) &= \left(\frac{\partial w_m}{\partial n} \right) \frac{\partial n}{\partial r} + \left(\frac{\partial w_m}{\partial m} \right) \frac{\partial m}{\partial r} \\ &= - \frac{\partial w_m}{\partial n} \cos \alpha + \frac{\partial w_m}{\partial m} \sin \alpha \end{aligned} \quad (B-101)$$

Introducing all this into equation (B-101)

$$\begin{aligned} \frac{\partial \Delta w_m}{\partial n} + \frac{\Delta w_m}{R} &= - \frac{\tan \beta_s}{\cos \alpha_s} \left\{ 2 \omega \frac{r}{r_s} \right. \\ &- \tan \beta_s \left[\frac{r^2}{r_s^2} \left(\sin \alpha \frac{\partial (\Delta w_m)_p}{\partial m} + \sin \alpha \frac{\partial \Delta w_m}{\partial m} \right. \right. \\ &- \cos \alpha \frac{\partial (w_m)_p}{\partial n} - \cos \alpha \frac{\partial \Delta w_m}{\partial n} \left. \right) + 2 \frac{r}{r_s^2} (w_m)_p \\ &\left. \left. + 2 \frac{r}{r_s^2} \Delta w_m \right] \right\} \end{aligned}$$

CONFIDENTIAL

In this equation we replace $\frac{\partial(w_m)}{\partial n} \rho$ by $-\frac{(w_m)}{R} \rho$.

In a mixed flow impeller, it happens that the angle α at any point is very nearly equal to the angle α_s taken at the same Z value. Therefore

$$\frac{\cos \alpha}{\cos \alpha_s} \approx \frac{\sin \alpha}{\sin \alpha_s} \approx 1.0$$

$$\begin{aligned} & \frac{\partial \Delta w_m}{\partial n} \left(1 + \tan^2 \beta_s \frac{r^2}{r_s^2}\right) + \Delta w_m \left[\frac{1}{R}\right. \\ & \left. - 2 \frac{\tan^2 \beta_s}{\cos \beta_s} \frac{r}{r_s^2} = - 2 \omega \frac{r}{r_s} \frac{\tan \beta_s}{\cos \alpha_s} \right] \end{aligned} \quad (B-105)$$

$$+ \tan^2 \beta_s \tan \alpha_s \frac{r^2}{r_s^2} \frac{\partial(w_m)}{\partial m} \rho + \tan^2 \beta_s \frac{r^2}{r_s^2} \frac{(w_m)}{R} \rho$$

$$+ 2 \frac{\tan^2 \beta_s}{\cos \alpha_s} \frac{r}{r_s^2} (w_m) \rho + \tan^2 \beta_s \tan \alpha_s \frac{\partial \Delta w_m}{\partial m}$$

This equation is linear, except for the presence of the last term. The solution is carried out by an iterative process. The last term is omitted and the remainder of the equation solved for each potential line. This permits the evaluation of the term in $\frac{\partial(\Delta w_m)}{\partial m} \rho$.

The potential line solution is then repeated with all terms included, until convergence is met. The solution of the linear equation is carried out as outlined under part A above, except for the evaluation of the constant of integration which now has the form

$$K = - \frac{\int_{shr}^{hub} \frac{\int_0^n f_0 dn}{e \int_0^n f_0 dn} g \rho (2\pi r - Zt) dn}{\int_{shr}^{hub} \frac{g \rho (2\pi r - Zt) dn}{\int_0^n f_0 dn}}$$

CONFIDENTIAL

APPENDIX C

EQUATIONS FOR THE AXI-SYMMETRIC FLOW IN IMPELLER PASSAGES - EQUATIONS FOR THE NUMERICAL SOLUTION OF THE DIRECT PROBLEM

The basic equation for the numerical solution of the flow in impeller I was taken as equation 53 of ref. 52.

$$\begin{aligned} & \left(1 + \frac{\tan^2 \beta}{\cos^2 \alpha}\right) \frac{\partial^2 \psi}{\partial r^2} - \frac{1}{r} \left(1 - \frac{\tan^2 \beta}{\cos^2 \alpha}\right) \frac{\partial \psi}{\partial r} + \frac{\partial^2 \psi}{\partial z^2} \\ & - \frac{1}{\rho} \left[\left(1 + \frac{\tan^2 \beta}{\cos^2 \alpha}\right) \frac{\partial \psi}{\partial r} \frac{\partial \rho}{\partial r} + \frac{\partial \psi}{\partial z} \frac{\partial \rho}{\partial z} \right] + 2\omega r \frac{\tan \beta}{\cos \alpha} \frac{\rho}{\rho_m} \\ & + \frac{r^2 \rho^2}{\psi \left(\frac{\partial \psi}{\partial r}\right) \rho_{02}} \left[- \frac{\partial}{\partial r} \left(h + \frac{w^2}{2} - \frac{r^2 \omega^2}{2}\right) + \frac{T \partial s}{\partial r} + Fr \right] = 0 \end{aligned} \quad (C-1)$$

Three particular variations of this equation are of interest: (1) In the particular case of compressible flow in the inlet, C-1 reduces to:

$$\frac{\partial^2 \psi}{\partial r^2} - \frac{1}{r} \frac{\partial \psi}{\partial r} + \frac{\partial^2 \psi}{\partial z^2} + \frac{1}{\rho} \frac{\partial \psi}{\partial r} \frac{\partial \rho}{\partial r} + \frac{1}{\rho} \frac{\partial \psi}{\partial z} \frac{\partial \rho}{\partial z} = 0 \quad (C-3)$$

(2) In the case of incompressible inviscid flow in an impeller with radial elements and no pre-whirl (in which case comparison can be made with equation B-6):

$$\left(1 + \frac{\tan^2 \beta}{\cos^2 \alpha}\right) \frac{\partial^2 \psi}{\partial r^2} - \frac{1}{r} \left(1 - \frac{\tan^2 \beta}{\cos^2 \alpha}\right) \frac{\partial \psi}{\partial r} + \frac{\partial^2 \psi}{\partial z^2} + 2\omega r \frac{\tan \beta}{\cos \alpha} = 0 \quad (C-4)$$

CONFIDENTIAL

If the following relations are introduced, equation C-4 reduces to B-6

$$\cos \alpha = \frac{dr}{dn} = \frac{\partial \psi / \partial r}{\sqrt{(\partial \psi / \partial r)^2 + (\partial \psi / \partial z)^2}}$$

$$\tan \alpha = (dr/dz)_{\psi} = -\frac{\partial \psi / \partial z}{\partial \psi / \partial r}$$

$$w_m = \frac{1}{r} \sqrt{\left(\frac{\partial \psi}{\partial r}\right)^2 - \left(\frac{\partial \psi}{\partial z}\right)^2}$$

$$R = \frac{-\left[\left(\frac{\partial \psi}{\partial z}\right)^2 + \left(\frac{\partial \psi}{\partial r}\right)^2\right]^{3/2}}{\frac{\partial^2 \psi}{\partial z^2} \left(\frac{\partial \psi}{\partial r}\right)^2 - 2 \frac{\partial^2 \psi}{\partial r \partial z} \frac{\partial \psi}{\partial z} \frac{\partial \psi}{\partial r} + \frac{\partial^2 \psi}{\partial r^2} \left(\frac{\partial \psi}{\partial z}\right)^2}$$

$$\frac{\partial w_m}{\partial n} = \frac{1}{r} \left\{ \frac{\left(\frac{\partial \psi}{\partial z}\right)^2 \frac{\partial^2 \psi}{\partial z^2} + 2 \frac{\partial \psi}{\partial r} \frac{\partial \psi}{\partial z} \frac{\partial^2 \psi}{\partial r \partial z} + \left(\frac{\partial \psi}{\partial r}\right)^2 \frac{\partial^2 \psi}{\partial r^2}}{\left(\frac{\partial \psi}{\partial z}\right)^2 + \left(\frac{\partial \psi}{\partial r}\right)^2} - \frac{1}{r} \frac{\partial \psi}{\partial r} \right\}$$

$$\frac{\partial w_m}{\partial m} = \frac{1}{r} \left\{ \frac{\frac{\partial \psi}{\partial r} \frac{\partial \psi}{\partial z} \left(\frac{\partial^2 \psi}{\partial z^2} - \frac{\partial^2 \psi}{\partial r^2}\right) - \left[\left(\frac{\partial \psi}{\partial z}\right)^2 - \left(\frac{\partial \psi}{\partial r}\right)^2\right] \frac{\partial^2 \psi}{\partial r \partial z}}{\left(\frac{\partial \psi}{\partial z}\right)^2 + \left(\frac{\partial \psi}{\partial r}\right)^2} + \frac{\partial \psi / \partial z}{r} \right\}$$

$$\frac{\partial \alpha}{\partial n} = \frac{\frac{\partial \psi}{\partial z} \frac{\partial \psi}{\partial r} \left(\frac{\partial^2 \psi}{\partial r^2} - \frac{\partial^2 \psi}{\partial z^2}\right) + \frac{\partial \psi}{\partial r \partial z} \left[\left(\frac{\partial \psi}{\partial z}\right)^2 - \left(\frac{\partial \psi}{\partial r}\right)^2\right]}{\left[\left(\frac{\partial \psi}{\partial z}\right)^2 + \left(\frac{\partial \psi}{\partial r}\right)^2\right]^{3/2}}$$

Equation C-4 is of interest in that its solution, carried out simultaneously with an exact expression for the density, yields a solution directly comparable to the quasi-compressible procedure as used in the general design procedure.

(3) The form of equation C-1, presently coded for numerical solution, makes full allowance for compressibility, but is restricted to impellers with radial elements and no pre-whirl. The effect of losses is included to the degree that it affects the magnitude of the local densities; but the effect of the losses on the radial entropy gradient is neglected. The clogging effects due to both the presence of the blades and the viscous effects are included.

CONFIDENTIAL

With these conditions, equation C-1 becomes:

$$\begin{aligned} & \left(1 + \frac{\tan^2 \beta}{\cos^2 \alpha}\right) \frac{\partial^2 \psi}{\partial r^2} - \frac{1}{r} \left(1 - \frac{\tan^2 \beta}{\cos^2 \alpha}\right) \frac{\partial \psi}{\partial r} + \frac{\partial^2 \psi}{\partial z^2} \\ & - \frac{1}{\rho} \left[\left(1 + \frac{\tan^2 \beta}{\cos^2 \alpha}\right) \frac{\partial \psi}{\partial r} \frac{\partial \rho}{\partial r} + \frac{\partial \psi}{\partial z} \frac{\partial \rho}{\partial z} \right] + 2 \omega r \frac{\tan \beta}{\cos \alpha} \frac{\rho}{\rho_0} = 0 \end{aligned} \quad (C-5)$$

This equation (C-5) must be solved simultaneously with the polytropic density relationship

$$\rho/\rho_0 = \left[1 + \frac{k-1}{2} \left(\frac{u^2}{a_0^2} - \frac{w^2}{a_0^2} \right) \right]^{\frac{1}{n-1}} \quad (C-6)$$

For purposes of numerical computations, equations C-5 and C-6 were expressed on a dimensionless basis, using barred symbols for dimensionless quantities which are defined as follows:

$$\begin{aligned} \bar{\psi} &= \psi / W_c \quad 2\pi r \rho_0 \\ \bar{\rho} &= \rho / \rho_0 \\ \bar{r} &= r/h \quad \text{where } h \text{ is the grid mesh size of the flow net.} \\ \bar{z} &= z/h \\ \bar{w} &= \frac{w}{W_c / 2\pi h^2 \rho_0} \end{aligned}$$

CONFIDENTIAL

Further, the following definition is made of the over-all clogging factor e_f

$$e_f = e \times \text{Blades}$$

e is viscous coefficient and is prescribed ;

$$\text{Blades} = 1 - \frac{Z t_f}{2\pi r}$$

We may replace the ratio $\frac{\tan \beta}{\cos \alpha}$ by its equivalent $\bar{r} \frac{\partial \phi}{\partial \bar{z}}$

Writing partial derivatives with the conventional subscript notation,

($\partial \psi / \partial z = \psi_z$ etc.) equation C-5 becomes:

$$\begin{aligned} \bar{\psi}_{rr} - \frac{1}{\bar{r}} \bar{\psi}_{r\bar{r}} + \bar{\psi}_{z\bar{z}} - \left(\frac{\bar{\rho}_{\bar{z}}}{\bar{\rho}} + \frac{e \bar{z}}{e} \right) \bar{\psi}_{z\bar{z}} - \left(\frac{\bar{\rho}_{\bar{r}}}{\bar{\rho}} + \frac{e \bar{r}}{e} \right) \bar{\psi}_{r\bar{r}} \\ - \left(\frac{\bar{\rho}_{\bar{r}}}{\bar{\rho}} + \frac{e \bar{r}}{e} \right) \bar{r}^2 \phi_z^2 \bar{\psi}_{r\bar{r}} + \left(\bar{\psi}_{r\bar{r}} + \frac{\bar{\psi}_{\bar{r}}}{\bar{r}} \right) \bar{r}^2 \phi_z^2 \\ = - 2 \bar{\omega} \bar{r}^2 \phi_z e \bar{\rho} \end{aligned} \tag{C-7}$$

Likewise in equation C-6

$$w = \frac{w_m}{\cos \beta} \tag{C-8}$$

where

$$\begin{aligned} w_m &= \sqrt{w_r^2 + w_z^2} \\ &= \frac{W_c}{2\pi e \bar{r} h \bar{\rho} \rho_{01}} \sqrt{\left(\frac{\partial \bar{\psi}}{\partial \bar{z}} \right)^2 + \left(\frac{\partial \bar{\psi}}{\partial \bar{r}} \right)^2} \end{aligned} \tag{C-9}$$

CONFIDENTIAL

and where

$$\begin{aligned} \cos \beta &= \frac{1}{\sqrt{1 + (\bar{r} \cos \alpha \frac{\partial \phi}{\partial \bar{z}})^2}} \\ &= \frac{1}{\sqrt{1 + \bar{r}^2 (\frac{\partial \phi}{\partial \bar{z}})^2}} \frac{(\partial \psi / \partial r)^2}{(\partial \bar{\psi} / \partial \bar{z})^2 + (\partial \bar{\psi} / \partial \bar{r})^2} \end{aligned} \quad (C-10)$$

Introducing this into equation C-6, there follows, after simplification:

$$\bar{\rho} = \left\{ 1 + \frac{k-1}{2} \left(\frac{W_c}{2 \pi \rho_{01} a_{01} h^2} \right)^2 \left[\bar{r}^2 \bar{\omega}^2 - \frac{\bar{\psi} \bar{z}^2 + \bar{\psi}_r^2 (1 + \bar{r}^2 \phi \bar{z}^2)}{(\epsilon \bar{\rho} \bar{r})^2} \right] \right\}^{\frac{1}{n-1}} \quad (C-11)$$

Solution of the flow in the impeller is then reduced to the simultaneous solution of equation C-7 and C-11.

It may be recalled that from equation C-1, the term involving the radial entropy gradient was omitted, somewhat arbitrarily, but mainly to avoid the extra complicating features that it introduces. Thus, for a polytropic process:

$$T ds = \left(\frac{1}{k-1} - \frac{1}{n-1} \right) R dT$$

and since

$$\frac{T}{T_{0r}} = 1 + \frac{k-1}{2} \left(\frac{u^2}{a_{01}^2} - \frac{w^2}{a_{01}^2} \right)$$

$$\frac{T \partial s}{\partial r} = \frac{n-k}{(n-1)kg} \left(r \omega^2 - w \frac{\partial w}{\partial r} \right)$$

CONFIDENTIAL

An idea of the added complication may be had by noting that the relative velocity w must be obtained from relations C-8, C-9 and C-10, which themselves involve the density.

CONFIDENTIAL

CONFIDENTIAL

APPENDIX D

EQUATIONS FOR THE CORRECTION FROM THE TWO-DIMENSIONAL TO THE AXI-SYMMETRIC FLOW UPSTREAM OF IMPELLER

i Approximate correction to convert the velocity distribution of an incompressible 2-dimensional flow to that of an incompressible axi-symmetrical flow.

Comparison is made here of the velocity gradients along a potential line for a two-dimensional flow passage and an axi-symmetric flow passage of identical meridional section. The standard correction is taken from the well known flows around a sphere and a cylinder, at the point of maximum velocity for a sphere.

$$c_m = \left[\frac{U a^3}{2r^3} \sin \theta + U \sin \theta \right]$$

using standard classical notation.

At any angle θ

$$\frac{\partial c_m}{\partial r} = - \frac{3}{2} U \frac{a^3}{r^4} \sin \theta$$

For a cylinder

$$c_m = U \left(1 + \frac{a^2}{r^2} \right) \sin \theta$$

$$\frac{\partial c_m}{\partial r} = - 2 U \frac{a^2}{r^3} \sin \theta$$

$$\text{And } \frac{(\partial c_m / \partial r)_{2\text{-Dim}}}{(\partial c_m / \partial r)_{3\text{-Dim}}} = \frac{4}{3} \frac{r}{a}$$

CONFIDENTIAL

$$\text{Near the periphery } \frac{\partial c_m}{\partial r} = \frac{\partial c_m}{\partial n} \text{ and } r = a$$

$$\frac{(\partial c_m / \partial n)_{2\text{-Dim}}}{(\partial c_m / \partial n)_{3\text{-Dim}}} = \frac{4}{3}$$

We may now extend the application of this ratio to axi-symmetrical shapes for which the meridional view is other than a circle, as for example both to the hub and shroud of a compressor inlet. And by interpolation, it may be safely assumed that this same ratio is applicable to any point along its potential line, between hub and shroud.

A check of this principle was made for a given inlet for which both the two-dimensional and the axi-symmetrical solution were available. The results shown on fig. 73 indicates the quantity 4/3 to be representative of the average.



APPENDIX E

BLADE TO BLADE SOLUTION

I Direct Problem: Calculation of the blade loading for a given geometry.

An expression for the blade loading can be obtained by application of the laws of angular momentum to the fluid element of figure 74

$$\Delta p \, dm \, dn \, r = w \cos \beta \, g \rho : \Delta \phi \, dn \, d(rc_u)$$

$$\frac{\Delta p}{\Delta \phi} = \bar{\rho} \, \bar{w} \, c \, \bar{\beta} \, \frac{d(r\bar{c}_u)}{dm}$$

where the barred quantities denote mean quantities between the containing blade surface. It is clear that these mean quantities could be taken as the corresponding quantities of the axi-symmetric solution.

Now at a given radius the total pressure is constant

$$\Delta p = \bar{\rho}_2 (w_{suct}^2 - w_{pr}^2)$$

Assuming that

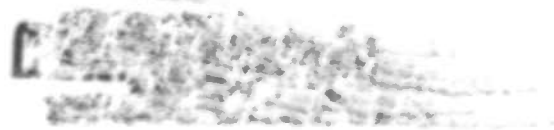
$$\bar{\rho} \, \bar{w} = \frac{1}{2} \bar{\rho} (w_{suct} + w_{pr})$$

$$\Delta p = \bar{\rho} \, \bar{w} (w_{suct} - w_{pr}) = \bar{\rho} \, \bar{w} \, \Delta w$$

and

$$\frac{\Delta w}{\Delta \phi} = \cos \bar{\beta} \, \frac{d(r\bar{c}_u)}{dm}$$

(D-1)



In view of the simplifying assumptions introduced in this derivation, particularly in the handling of the average quantities, the resulting must be regarded as an index of the blade loading, rather than a true velocity difference. This fact does not detract from its usefulness. The relative velocities on the pressure and suction sides are taken as

$$w_{\text{suct}} = w_{\text{mean}} + \frac{\Delta w}{2}$$

$$w_{\text{pr}} = w_{\text{mean}} - \frac{\Delta w}{2}$$

II Inverse problem: required blade angle to produce a given loading

$$r c_u = r(r\omega - w_m \tan \beta)$$

$$\frac{d(r c_u)}{dm} = 2 r \omega \frac{dr}{dm} - w_m \frac{d(\tan \beta)}{dm}$$

$$- r \tan \beta \frac{dw_m}{dm} - w_m \tan \beta \frac{dr}{dm}$$

Substituting into equation D-1 and rearranging terms, yields

$$\frac{d(\tan \beta)}{dm} = \left(\frac{2r\omega - w_m \tan \beta}{r w_m} \right) \frac{dr}{dm}$$

$$- \frac{\Delta w}{\Delta \phi \cos \beta r w_m} - \frac{\tan \beta}{w_m} \frac{dw_m}{dm} \quad (D-2)$$

If a tentative meridional velocity distribution has been calculated and a desired loading distribution established, the blade shape can be obtained. The equation is non-linear and can best be solved by proceeding in a step by step fashion from impeller inlet to exit. For each limit step, $\frac{\Delta \tan \beta}{\Delta m}$ can be computed since the mean value of β can be anticipated.

